NGU Report 2001.029

The Rogaland Intrusive Massifs
- an excursion guide

Geological Survey of Norway
N-7441 Trondheim, Norway
Tel.: 47 73 90 40 00
Telefax 47 73 92 16 20

REPORT

Report no.: 2001.029 | ISSN 0800-3416 | Grading: Open

Title:
The Rogaland Intrusive Massifs - an excursion guide

Authors:
Jean-Clair Duchesne (editor)

Client:
NGU and ESF

County:
Rogaland

Commune:
Sokndal, Lund, Eigersund

Map-sheet name (M=1:250.000)
Stavanger, Mandal

Map-sheet no. and -name (M=1:50.000)

Deposit name and grid-reference:

Number of pages: 139 Price (NOK): 428
Map enclosures:

Fieldwork carried out:	Date of report:	Project no.:	Person responsible:
	20 June 2001	286501	

Summary:

The Rogaland Anorthosite Province comprises three major massif-type anorthosites, two smaller-sized anorthositic-leuconoritic bodies, as well as a large layered, dominantly noritic intrusion. A mangero-noritic intrusion is found in the northeastern part of the province and major acidic intrusions are located to the far southeast. The Rogaland Anorthosite Province was emplaced into the Sveconorwegian orogenic belt of southwest Scandinavia at 931±3 Ma. Emplacement took place at around 5.5 kbar producing a thermal aureole with osumilite and pigeonite isograds and evidence for dehydration melting. The early history of the hosting terrane most likely dates back to Gothian or late Pre-Gothian times and contain evidence for numerous episodes of folding and deformation. Contact metamorphism was superimposed on a crustal volume, which had been exposed to Sveconorwegian granulite facies metamorphism between 1024 and 970 Ma.

Deformation patterns, mineral compositional considerations and geothermobarometry imply that the Rogaland anorthosites crystallized along a P-T trajectory starting at 10-13 kbar, and were emplaced in a mushy state. The possibility that primitive jotunites may be parental to the andesine anorthosites have recently been substantiated, and experimental data show that these jotunites most likely formed by melting of gabbronoritic sources in the lower crust. The 230 km^2 Bjerkreim-Sokndal Layered Intrusion also derive from jotunitic parents, and jotunites form a continuous liquid line of descent filling the gap between basic and acidic rocks in Rogaland. This intrusion contains a >7000 m thick layered cumulate sequence, consisting of virtually all the rock types belonging to the anorthosite kindred. The intrusion morphology, layering and compositional variation result from a variety of magma chamber processes, which are discussed in detail. The Rogaland Anorthosite Province also hosts numerous Fe-Ti oxide deposits of variable size, grade and composition. The oxide deposits have been divided into three basic types based on their oxide-phosphate association; type 1: ilmenite-only, type 2: ilmenite + magnetite and type 3: ilmenite + magnetite + apatite.

This excursion guide provides detailed itineraries to most parts of the Rogaland Anorthosite Province, with in-depth descriptions of more than 40 key localities, The itineraries cover the various anorthosites, the Bjerkreim-Sokndal Layered Intrusion, jotunitic and acidic intrusions, the hosting metamorphic complex, as well as Fe-Ti oxide and sulfide deposits.

Keywords: Fagrapport	Titanium	Ilmenite
Anorthosite	Proterozoicum	

Field workshop 8-12th July 2001 on

Ilmenite Deposits in the Rogaland Anorthosite Province

The Rogaland Intrusive Massifs

- an excursion guide

Jean-Clair DUCHESNE

(editor)

A revised and enlarged version of parts of «*Geology of Southermost Norway: an excursion guide*» (C. Maijer and P. Padget, editors) Norges geologiske undersøkelse, Special publication n°1, 1987, 109 p.

Bibliographic reference:
Duchesne, J-C (ed.). 2001: *The Rogaland Intrusive Massifs, an excursion guide*. NGU report 2001.29. Geological survey of Norway. 137pp.

CONTENTS

Figures

Photos

Tables

List of contributors

Jean-Clair DUCHESNE (University of Liège, Belgium)
Bernard BINGEN (Norsk Geologiske Undersøkelse, Trondheim, Norway)
Olivier BOLLE (University of Liège, Belgium)
Daniel DEMAIFFE (Free University of Brussels, Belgium)
Hervé DIOT (University of La Rochelle, France)
Robert MAQUIL (Geological Survey of Luxembourg, G.D. Luxembourg)
Brian ROBINS (University of Bergen, Norway)
Henrik SCHIELLERUP (NTNU, Trondheim, Norway)
Jacqueline VANDER AUWERA (University of Liège, Belgium)
Edith WILMART (University of Liège, Belgium, now at CEPT, CNRS, France)
J. Richard WILSON (University of Aarhus, Denmark)

Foreword

(by J.C. Duchesne)

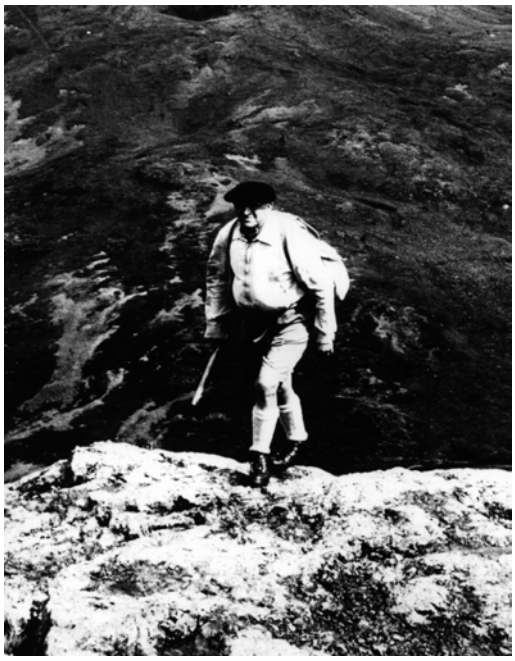

In Memoriam Paul MICHOT (1902-1999).
A life-long scrutinizer of Rogaland rocks

Paul Michot began studying the Egersund anorthositic Province in 1937. He defined the various massifs, provided the first geological map, and elaborated a sophisticated model for the geological and petrological evolution of the Rogaland igneous masses and metamorphic envelope, which is a masterpiece of complexity, consistency and strictness. In 1960, he published a guidebook (Michot 1960) and later, his major ideas on anorthosites, formerly developed in many papers, were condensed in cooperation with his son Jean in the Plattsburg symposium (Michot & Michot 1969). Under his impulse, many petrological and geochemical studies were initiated in the massifs he had defined and in the southern part of the Province, where he had not worked. New data - which mean new constraints, but also new questions - were added to the anorthosite problem. Basically however Michot's map still remains essentially unaltered.

In 1984, a NATO Advanced Science Institute was held in Moi on the topic "The deep Proterozoic crust in the North Atlantic Provinces". This was an opportunity to visit the Rogaland anorthosites and to bring up to date Michot's guidebook by focusing on some aspects which were re-investigated more thoroughly (the Egersund-Ogna massif, the jotunite dyke system, the Bjerkreim-Sokndal mineralogy and geochemistry) or were unknown to P. Michot (the Hidra massif). This guidebook was published as part of "The Geology of Southernmost Norway: an excursion guide" by Maijer & Padget (1987). After 1984, new data were acquired, especially on the Bjerkreim-Sokndal massif, by groups from various universities: Århus (led by J.R. Wilson), Bergen (B. Robbins) and Liège (J.C. Duchesne). In 1992, a meeting was held in Rogaland on "Magma chambers and processes in anorthosite formation" as part of the IGCP programme 290 on "Anorthosite and related rocks". It was a good opportunity to revise and update the preceding guidebook. The present revised and enlarged third version of this guidebook is written for the workshop on "Ilmenite Deposits in the Rogaland Anorthosite Province" held at Moi, Norway, July 8-12, 2001, under the ESF's GEODE-project "The Fennoscandian Shield Precambrian Province".

In nearly two decades, a significant volume of new data have been acquired on the various geological units of the province, and some of the ideas have been deeply modified. The basic structure of the guidebook is however preserved: thematic papers summarise the state of the art on the various units, and itineraries show salient localities, most of them with easy access. Two themes have been added: the first one is devoted to the acidic rocks of the Bjerkreim-Sokndal intrusion and its south-eastern Apophysis as well as to the jotunitic dyke system. The second addition deals with the Fe-Ti deposits and particularly with the world-class Tellnes ilmenite deposit, their genesis and their evolution. The introductory chapter, initially written by Jean Michot and myself, has been revised by myself only.

I wish to acknowledge all contributors to this guide (J. Richard Wilson, Brian Robins, Daniel Demaiffe, Robert Maquil, Edith Wilmart) and particularly newcomers: Jacqueline Vander Auwera and Olivier Bolle from the University of Liège (Belgium), Henrik Schiellerup from the Norwegian University of Science and Technology and NGU (Trondheim, Norway), Bernard Bingen from NGU (Trondheim, Norway), and Hervé Diot from the University of La Rochelle (France). I am also very grateful to Are Korneliussen, Project Leader of the GEODE sub-project “Ilmenite Deposits in the Rogaland Anorthosite Province”.

Jean-Clair Duchesne
(February 2001)

***

Part I

Photo 0.1. In the Åna-Sira anorthosite massif

Chapter 1

THE ROGALAND ANORTHOSITE PROVINCE: AN INTRODUCTION

(by J.C. Duchesne and B. Bingen)

The Sveconorwegian orogenic belt

The Rogaland Igneous Province is situated at the southwestern end of the exposed Sveconorwegian orogenic belt in Rogaland – Vest Agder. The Sveconorwegian belt of Fennoscandia is generally correlated with the Grenvillian belt of Laurentia. Both belts formed during a polyphase orogenic event between 1.25 and 0.90 Ga, at the transition between the Mesoproterozoic and Neoproterozoic (Berthelsen 1980; Falkum 1985; Rivers et al. 1989; Gorbatschev & Bogdanova 1993; Davidson 1995; Rivers & Corrigan 2000). They are generally depicted as the product of the collision between an unknown plate and the margin of the Fennoscandian and Laurentian shields respectively.

The Sveconorwegian orogen (Fig. 1.1) is situated to the west of the 1.9–1.8 Ga Svecofennian domain and the 1.85–1.65 Ga Transcandinavian Igneous Belt. It is made up of a number of Palaeo- to Mesoproterozoic lithotectonic domains separated by major shear zones, and cut obliquely by the Palaeozoic Oslo rift (Berthelsen 1980; Gorbatschev & Bogdanova 1993; Åhäll & Gower 1997). No consensus exists today regarding the nomenclature of the lithotectonic domains; in the following text, crustal domains are divided into major domains called segments or terranes and smaller domains called sectors. The easternmost domain of the orogen, the Eastern Segment, is parautochthonous, and mainly consists of reworked granitoids of the Transcandinavian Igneous Belt foreland (Christoffel et al. 1999; Söderlund et al. 1999). The other domains, to the west of the Mylonite Zone, are Sveconorwegian allochthons (Park et al. 1991; Stephens et al. 1996; Möller 1998; Andersson et al. submitted). Three major terranes, bounded by orogen-parallel shear zones, can be defined (Fig. 1.1.). These are, from east to west, the Idefjorden terrane (Åhäll et al. 1998), the Telemark – Bamble terrane and the Rogaland – Hardangervidda terrane. In this subdivision, the Idefjorden terrane extends on both sides of the Oslo rift (Bingen et al. in press) and the Telemark – Bamble terrane includes the Telemark, Bamble and Kongsberg sectors, although the link between the Telemark sector and the Bamble and Kongsberg sectors is a matter of debate. To the west of the Mandal – Ustaoset Line, the Hardangervidda and the Rogaland – Vest Agder sectors are considered as a parts of one single terrane.

In the Sveconorwegian orogen, Sveconorwegian magmatic rocks increase in volume westwards. 1.3–1.2 Ga pre- to early-Sveconorwegian magmatic rocks of variable type are distributed all over the orogen. The volume of this magmatism is poorly assessed in S Norway. It comprises, among others, 1.20 Ga syenite plutons along the Sveconorwegian Frontal Deformation Zone (Jarl 1992), 1.20 Ga low-K diorite – tonalite plutons in the Bamble sector (Knudsen & Andersen 1999), the 1.28 Ga Iveland–Gautestad metagabbroic complex of low- to medium-K tholeiitic to calc-alkaline signature in the Telemark sector (Pedersen & Konnerup-Madsen 2000) and 1.27–1.25 Ga acid volcanic rocks (Breive Group) of undefined geochemical signature in the Hardangervidda sector (Sigmond 1978; Bingen unpublished data). 1.19–1.15 Ga magmatic rocks form a well-defined magmatic suite in the western part of the orogen in the Telemark – Bamble and Rogaland – Hardangervidda terranes. This suite includes (deformed) charnockite to granite plutons, the volcanic rocks of the Bandak Group and minor (meta)gabbro bodies (Dons 1960; Dahlgren et al. 1990; Kullerud & Machado 1991; Heaman & Smalley 1994; Nordgulen et al. 1997; Zhou et al. 1995 ; Bingen & van Breemen 1998a). Granitoids in this suite display an A-type geochemical signature. As opposed to the Grenvillian orogen, no coeval anorthosite massifs are reported in the Sveconorwegian orogen. A short-lived suite of high-K calc-alkaline porphyritic granodiorite

plutons (Feda suite) intruded at 1.05 Ga in (and only in) the westernmost Rogaland–Hardangervidda terrane (Bingen et al. 1993; Bingen & van Breemen 1998a). Voluminous 1.00–0.90 Ga late- to post-tectonic plutonism occurs in the Idefjorden terrane and westwards (compilation in Andersson et al. 1996). The largest of these complexes are the 0.93–0.92 Ga Flå, Iddefjorden and Bohus granite plutons in the Idefjorden terrane (Eliasson & Schöberg 1991; Nordgulen et al. 1997) and the anorthosite massifs and related rocks in Rogaland–Vest Agder that are the subject of this guidebook. The emplacement of the Rogaland anorthosite complex is estimated at 931 ± 3 Ma (Schärer et al. 1996), and represents a surprisingly short magmatic event (<10 m.y.).

Sveconorwegian metamorphism varies in intensity from greenschist to granulite facies, and is not coeval in the different sectors. The Eastern Segment displays an amphibolite facies domain and a high-pressure granulite facies domain in the southern part with local occurrence of eclogite-facies rocks (Johansson et al. 1991; Möller 1998; 1999). The timing of high-grade metamorphism including eclogite-facies overprint is well constrained between 0.98 and 0.96 Ga (Connelly et al. 1996; Söderlund 1996; Andersson et al. 1999; Söderlund et al. 1999; Johansson et al. in press). In the Idefjorden terrane, the intensity and timing of Sveconorwegian metamorphism is not well constrained. It is older than 1.04 Ga (Romer & Smeds 1996). In the centre of the Telemark sector, metamorphism is generally of low grade and deposition of the impure clastic sediments of the Bandak and Heddal Groups (cover to the volcanic rocks) took place in an intraorogenic basin between 1.12 and 1.05 Ga and later (Bingen et al. 1999; de Haas et al. 1999). In the coastal regions of the Bamble sector, early-Sveconorwegian medium-pressure (c. 7.5 kbar) granulite facies metamorphism (Touret 1971; Lamb et al. 1986; Nijland & Maijer 1993; Knudsen 1996) is bracketed between 1.15 and 1.10 Ga (Kullerud & Machado 1991; Knudsen et al. 1997; Cosca et al. 1998). In the Rogaland–Vest Agder sector three phases of Sveconorwegian metamorphism are reported (Tobi et al. 1985, Maijer 1987). The timing of the main phase of regional metamorphism (M1, see hereafter) is estimated at 1.02–0.97 Ga (Bingen and van Breemen 1998b).

All major shear zones in the Sveconorwegian orogen were active during the Sveconorwegian orogeny, but possibly formed initially during older events (Sigmond 1985; Heaman & Smalley 1994; Page et al. 1996). To the east of the Oslo rift, major shear zones display a sinistral shear component (Hageskov 1985; Park et al. 1991; Stephens et al. 1996). From the age of deformed intrusive rocks, ductile deformation in amphibolite facies conditions is constrained to be younger than 1.13 Ga along the Kristiansand-Posrgrunn shear zone (separating the Bamble and Telemark sectors, Fig. 1.1) and younger that 1.04 Ga along the Mandal–Ustaoset Line (separating the Rogaland – Hardangervidda from the Telemark – Bamble terrane). Direct zircon dating of amphibolite facies metamorphism and associated ductile deformation yield ages of 0.98–0.97 Ga along the Mylonite zone (separating the Eastern Segment from the Idefjorden terrane) (Larson et al. 1999; Andersson et al. submitted) and 1.01 Ga along the Åmot – Vardefjell shear zone (separating the Idefjorden and Telemark terranes) (Bingen, unpublished data).

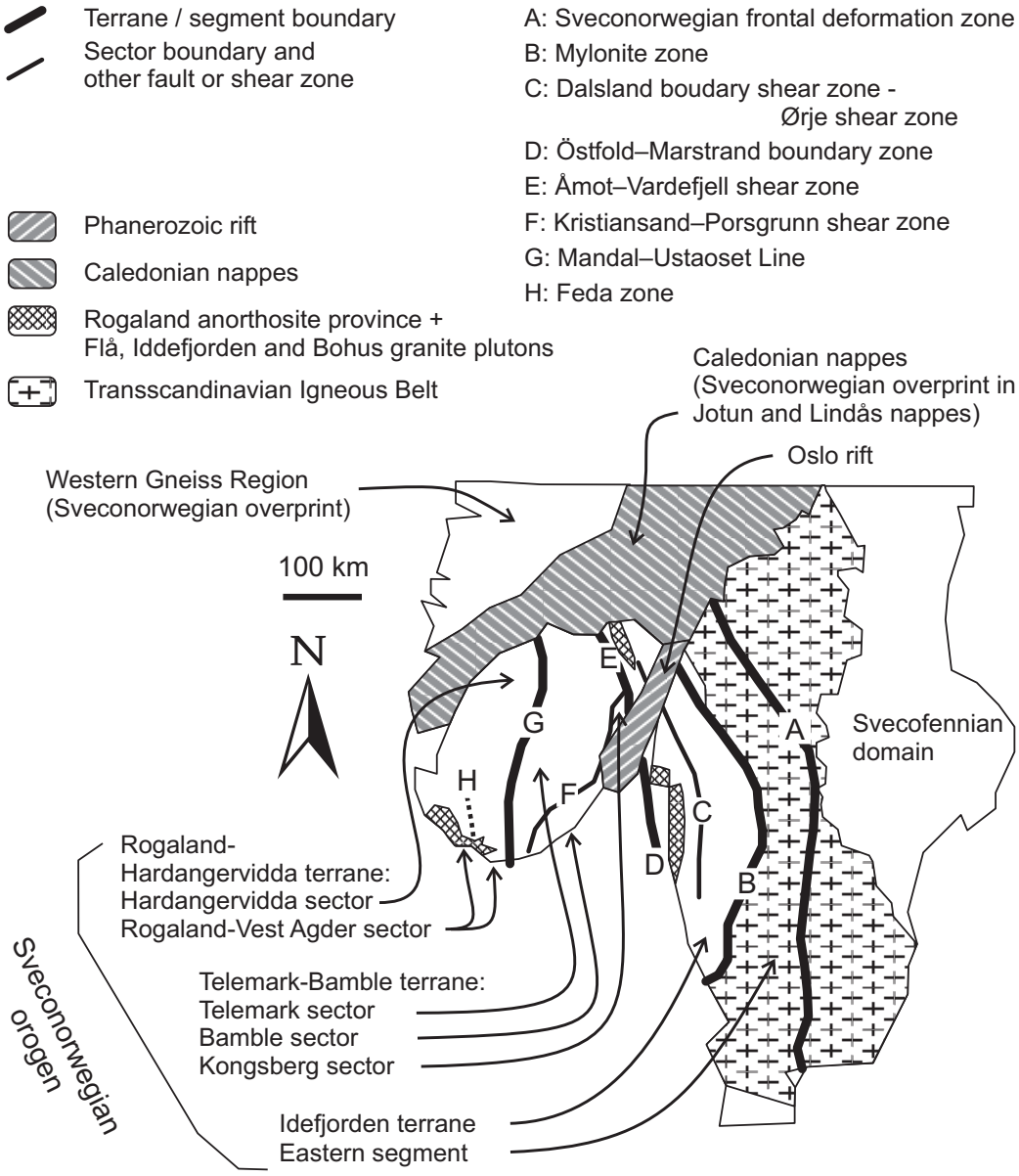

Fig. 1.1. Sketch map of SW Scandinavia showing the major lithotectonic domains of the Sveconorwegian orogen. The largest post-tectonic 0.93–0.92 Ga magmatic complexes are shown.

Understanding of the Sveconorwegian orogenic evolution at continent scale is speculative today. Compilation of the ages of regional metamorphism indicates that the main orogenic phase took place between 1.02 and 0.96 Ga, with maximum shortening of the orogen at 0.97 Ga (age of eclogite facies metamorphism in the parautochthonous Eastern Segment). The age of metamorphism tends to decrease eastwards, suggesting that this phase propagated towards the foreland. This phase included large (sinistral transpressive ?) displacement of terranes and thrusting of allochthon terranes on the parautochthonous Eastern Segment, and was followed by relaxation. The high-K calc-alkaline signature of 1.05 Ga granodiorite plutons (Feda suite in the west of the orogen) led Bingen et al. (1993) to suggest that a subduction regime prevailed at 1.05 Ga and thus that the 1.02–0.97 Ga orogenic phase marked the end of subduction. The existence of a subduction regime is nevertheless not the only possible interpretation of geochemical data, as melting of a juvenile component of the lower crust in a distinct geotectonic environment is a possible alternative to generate this type of magmatism (Roberts & Clemens 1993; Liégeois et al. 1998). So far, no satisfactory geotectonic interpretation has been proposed for the early-Sveconorwegian 1.19–1.15 Ga magmatism and

the shortly following 1.15–1.10 Ga high-grade metamorphism preserved in the Bamble sector. Although the 1.19–1.15 Ga granitoids display an A-type geochemical signature, they cannot be considered as anorogenic. This early-Sveconorwegian magmatism and subsequent metamorphism possibly correspond to (1) docking of the allochthonous terranes, some of which would be exotic to the Fennoscandian shield before colliding, (2) closure of a back arc basin as represented by the Stora Le Marstrand belt in the Idefjorden terrane, or (3) large scale stike-slip motion of terranes of Fennoscandian affinity at the margin of the Fennoscandian shield.

Geological setting in Rogaland – Vest Agder

Following Falkum (1985; 1998), the amphibolite to granulite facies basement complex in the Rogaland – Vest Agder sector includes three main lithological units (Fig. 1.2): banded gneiss, granitic "pink" gneiss and augen gneiss (Feda suite). The banded gneisses are strongly migmatic and consist of alternating mafic and felsic layers ranging in thickness from less than a centimetre to several metres. Mafic rocks are amphibolite to norite and felsic rocks are leuco-granitoids. Intercalation of kinzigitic (garnet-cordierite-sillimanite-biotite) gneiss, metaquartzite, and marble are evidence of a supracrustal origin for at least part of the banded gneiss units. They have poorly defined Palaeo- to Mesoproterozoic ages (Versteeve 1975; Menuge 1988). Granitic pink (ortho-) gneiss intruded the banded gneiss and form monotonous domains. Augen gneiss with large alkali feldspar phenocrysts (cm to dm size) form elongate bodies parallel to the regional structure. Intrusion of the porphyritic granodiorite plutons deformed to augen gneiss is estimated at 1050 +2/-8 Ma (Bingen and van Breemen 1998a). Other major components of the Rogaland – Vest Agder sector are large c. 1.19–1.15 Ga meta-granite to charnockitic plutons of A-type geochemical affinity (Gloppurdi, Botnevatn and Hidderskog bodies) (Versteeve 1975; Wielens et al. 1980; Zhou et al. 1995), c. 0.98–0.90 Ga post-tectonic granites (Falkum 1966; Wilson et al. 1977; Pasteels et al. 1979) and the 0.93 Ga anorthosite massifs and related rocks (Schärer et al. 1996).

The Rogaland – Vest Agder sector is limited to the east by the Mandal–Ustaoset Line, a lithospheric scale deformation zone (Sigmond 1985). In the region of Mandal, the Mandal–Ustaoset line is made up of a N–S trending amphibolite facies banded gneiss unit bordered to the west by an elongate augen gneiss body, the 1049 +2/-8 Ma Mandal augen gneiss. Post-tectonic granites straddle the Mandal–Ustaoset Line (Sigmond 1985; Andersson et al. 1996). They are especially voluminous directly to the west of the Line. This distribution suggests that the Mandal–Ustaoset Line channelled emplacement of post-tectonic granitoids. The Mandal–Ustaoset Line is clearly a Sveconorwegian tectonic zone as deformation affected 1.05 and 1.035 Ga granitoids situated along the zone (Bingen and van Breemen 1998a). Nevertheless, along the northern part of the Line, evidence of deformation as old as 1.5 Ga is reported (Sigmond 1985; 1997), which implies that the tectonic zone was possibly active over a long time interval. Offshore geophysics indicate large offsets of the Moho south of the Mandal–Ustaoset Line and of the Feda zone (in Fig. 9 of Andersson et al. 1996), which suggests discontinuities of lithospheric scale. The Feda augen gneiss, which outcrops some 12 km east of the anorthosite massif (Fig. 1.2), might have intruded in a zone of weakness, in a similar way as the Mandal augen gneiss. Duchesne et al. (1999) have proposed that it could represent the zone along which the anorthosite bodies were emplaced. These basement rocks in Rogaland – Vest Agder underwent a long and complex tectonic and metamorphic evolution that includes several phases of folding and of interaction with plutonic rocks. North of the anorthosite province, Michot (1956b; 1960) recognized two phases of isoclinal folding with large recumbent folds (Storefjell nappe), followed by a vertical axial plane folding phase (Lakksvelefjeld syncline), which he extended in the Bjerkreim-Sokndal synform. North-east and east of the anorthosite province, Hermans et al. (1975) have identified four deformation phases and south-east of the province, in the Flekkefjord area, Falkum (1966; 1998) defined

six folding phases. Detailed correlation between the deformation phases as defined by the various authors is still unclear, though the two phases of isoclinal folding that have been identified at regional scale presumably resulted from the same events.

The grade of Sveconorwegian metamorphism increases from E to W and can be described in a succession of four isograds (Fig. 1.2) (Tobi et al. 1985; Maijer 1987; Bingen et al. 1990): (1) clinopyroxene-in (Cpx-in) isograd, defined in the Feda augen gneiss suite, which marks the appearance of Cpx joining the amphibolite facies biotite + amphibole paragenesis; (2) orthopyroxene-in (Opx-in) in rocks of leucocratic composition; (3) osumilite-in (Osum-in) in supracrustal gneiss; (4) (inverted) pigeonite-in (Pig-in) in mafic rocks. The last two isograds wrap around the igneous intrusions. The other two are parallel to the igneous contact southeast of the complex, but diverge from it in the north.

The isograd pattern results from the superposition of three major metamorphic phases, M1, M2 and M3 (Tobi et al. 1985; Maijer 1987). To account for some old age measurements, Priem & Verschure (1982) postulated another older M0 phase, but the existence of this phase has not been substantiated by petrological data. A Caledonian M4 phase, in prehnite-pumpelliyite to lower greenschist facies, has been documented (Hermans et al. 1975). The intensity of M4 increases to the north and a green biotite-in isograd can be defined parallel to the Caledonian front to the north of the anorthosite province (Fig. 1.2). The M2 metamorphism is the most intense one and did erase most of the M1 parageneses. It was not associated with pervasive deformation (as indicated by the preservation of corona-like textures and non-oriented mineral assemblages) and most likely corresponds to a thermal aureole around the igneous intrusions. Geothermobarometric methods provide temperatures for the M2 phase as high as 800–900 °C in various lithologies, including osumilite + spinel + orthopyroxene and quartz + spinel parageneses in pelitic protoliths (Jansen et al. 1985; Wilmart & Duchesne 1987). The pressure conditions of crystallization of the Bjerkreim-Sokndal intrusion were experimentally determined to be less or equal than 5 kbar (Vander Auwera & Longhi 1994), providing a good estimate for the pressure of the M2 contact metamorphism. This estimate is equivalent to the 5.5 kbar determined by thermodymamic modelling of osumilite-bearing mineral assemblages in the granulite-facies gneisses (Holland et al 1996) and is narrower than the previously estimated range, extending from 3–4 kbar (Jansen et al. 1985) to 6–7 kbar (Wilmart & Duchesne 1987), estimated by geothermobarometric methods in various gneisses and in acidic charnockitic igneous rocks. Between the Opx-in and the Osum-in isograds, a hornblende + quartz out isograd (not shown on Fig. 1.2) has been documented (Maijer 1987).

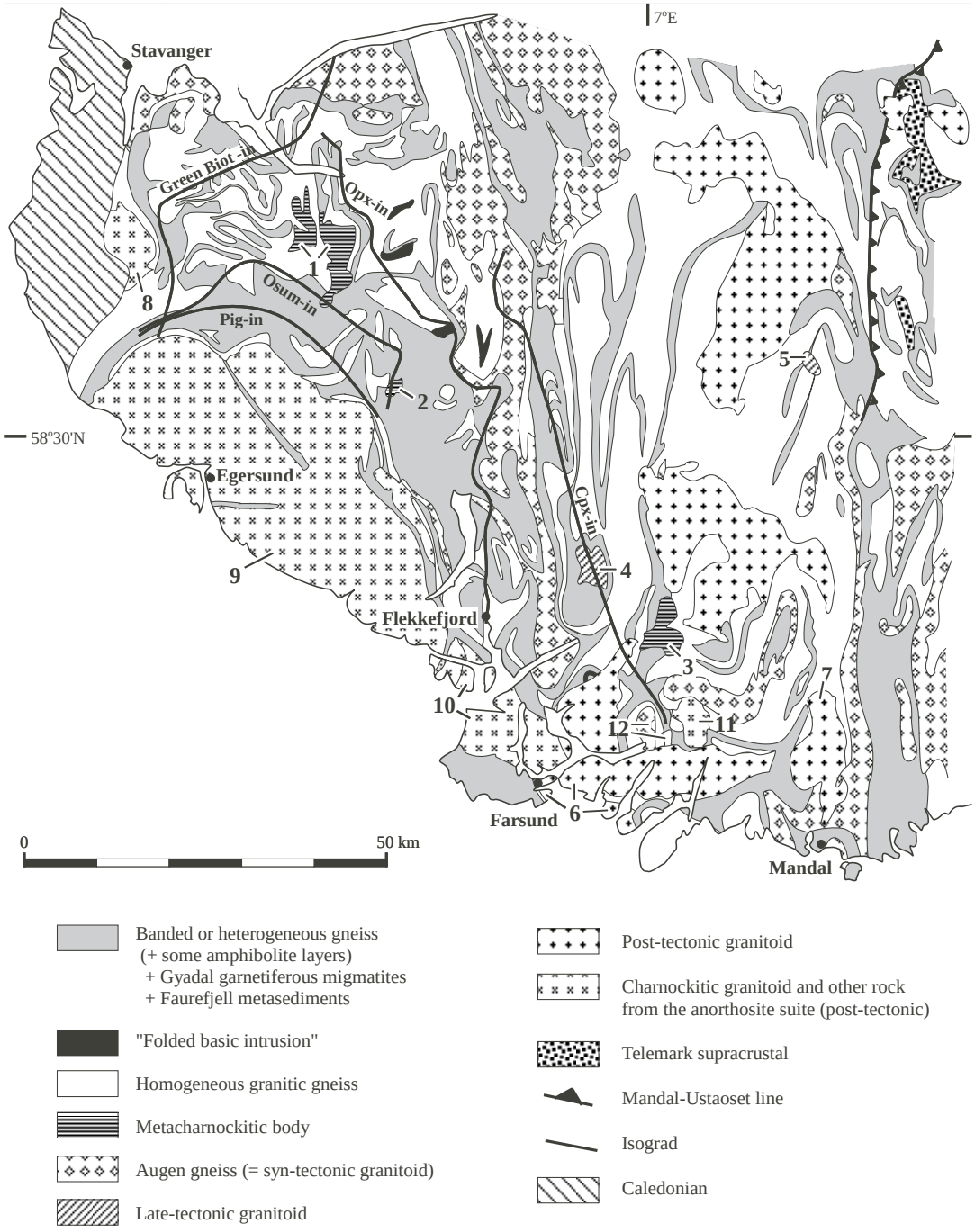

Fig. 1.2. Geological map of the southern part of the Rogaland – Vest Agder segment (Sigmond 1985). Isograds Pig-in (= pigeonite in), Osum-in (= osumulilite in) and Green Biot-in (= green biotite) have been plotted after Tobi et al. (1985), isograd Opx-in (= ortopyroxene in) after Falkum (1982) and isograd Cpx-in (= ortopyroxene in) after Bingen et al. (1996). 1: Gloppurdi meta-charnokite; 2: Botnevatnet meta-charnokite; 3: Hidderskog meta-charnokite; 4: Homme granite; 5: Åseral granite; 6: Lyngdal granodiorite; 7: Holum granite; 8: Sjelset acidic rocks; 9: Rogaland anorthosite province; 10: Farsund charnokite; 11 Klevan granite; 12: Lyngdal hyperite.

To the west of this isograd, towards the contact of the anorthosite massif, 1–2 cm-thick "dehydration rims" of noritic composition are observed whenever amphibolite are in contact with quartzo-feldspathic rocks, i.e. in the banded gneiss or around mafic inclusions in acidic igneous rocks. They result from a metasomatic SiO_2 diffusion mechanism (Vander Auwera 1993). The constant rim thickness suggests static (atectonic) conditions during formation. The M3 phase, only very locally associated with a late deformation, is a phase of retrograde metamorphism producing a variety of corona textures, symplectites and exsolutions. A range of P–T conditions (500–700°C and 3–4 kbar) have been reported (Jansen et al. 1985; Wilmart & Duchesne 1987). The composition of metamorphic fluids changed from CO_2-rich fluids during the M2 phase to CH_4 and N_2 during the M3 phase (Van den Kerkhof et al. 1991). Relicts of M1 mineral assemblages occur in metapelitic rocks (biotite + garnet + sillimanite), in mafic rocks (green hornblende + biotite + Cpx) and in rocks with granitic composition (biotite + green hornblende). Sapphirine locally occurs in Mg-rich compositions (Hermans et al. 1975; Tobi et al. 1985; Maijer 1987).

The origin of the Opx-in isograd has long been debated. When it was originally mapped, it was interpreted as a product of the same contact metamorphism that produced the Osum-in and Pig-in isograds, though it is not strictly parallel with them (Tobi et al. 1985; Maijer 1987). Tobi and Jansen (cited in Maijer, 1987) were however not completely convinced by that interpretation because they suspected that granulite facies conditions were reached during the M1 phase in the western part of the area. For them, the Opx-in isograd is reflecting the transition from regional amphibolite facies in the east to granulite facies to the west, and therefore is older than the M2 phase. Later Bingen et al. (1990) mapped the Cpx-in isograd grossly parallel to the Opx-in isograd and showed that both isograds are cutting across the well-dated (1050 +2/-8 Ma) Feda augen gneiss suite. The emplacement age of the whole anorthosite complex was then measured by the U–Pb method on zircon and baddeleyite at 931 ± 3 Ma (Schärer et al. 1996). Recently Bingen & van Breemen (1998b) measured the age of a prograde breakdown reaction of monazite in the Feda suite, which they correlate with the Opx-in reaction, at 1024-970 Ma. This supports the hypothesis that the M2 phase and the Opx-in reaction can be decoupled, that the climax of metamorphism affecting the whole area is younger than 1050 Ma and that the phase of regional metamorphism M1 reached granulite facies condition around 1.02–0.97 Ga. A cluster of monazite U–Pb ages in the range 930–925 Ma probably reflects the timing of M2 metamorphism. Titanite sampled at regional scale provides a well-grouped U–Pb average age of 918 ± 2 Ma reflecting regional cooling below ca. 610 °C (Bingen and van Breemen 1998b).

The intrusive units in the Rogaland anorthosite province

The Rogaland anorthosite province comprises three large massif-type anorthositic bodies (Egersund, Håland-Helleren and Åna-Sira), a layered intrusion (Bjerkreim-Sokndal), two smaller bodies of leuconorite (Hidra and Garsaknatt) and to the south three acidic intrusions: the Farsund charnockite, the Lyngdal and the Kleivan granites (fig. 1.3). They are emplaced in an envelope of granulite facies gneisses with which most massifs show broadly concordant contacts.

The Egersund-Ogna body is made of monotonous anorthositic rocks. It is characterized by a central part somewhat enriched in aggregates of giant orthopyroxene and plagioclase crystals and by a marginal zone, leuconoritic and strongly foliated. The contact with the envelope is generally concordant. The overall structure is that of a mantled dome (Michot 1957b). The petrology of the Egersund-Ogna body is summarized and discussed later in this guidebook.

The Håland-Helleren body has been divided into two different units by Michot (1961a; 1961b). The Håland massif is made up of folded foliated anorthosite and leuconorite in

various proportions, with granoblastic structure, locally grading into an igneous-like association between anorthosite and (leuco)-norite. The progressive transition between metamorphic and igneous textures has been interpreted by P. Michot (1955b) and J. Michot (1957a) as due to a leuconoritic anatexis of pre-existing anorthosito-noritic gneisses.

The Helleren massif (formerly also called the Amdal-Helleren-Rödland massif) cuts across the Håland and the Egersund-Ogna massifs. It is dominated by a coarse-grained anorthosite but also comprises leuconoritic parts and anorthosito-leuconoritic complexes similar to those described in Egersund-Ogna. It has other similarities with Egersund-Ogna, namely the presence of giant Al-rich orthopyroxene crystals and of blocky inclusions of foliated anorthosito-noritic rocks. However, it lacks the continuous foliated inner margin characteristic of the Egersund-Ogna body. The massif has been studied by Michot (1961a; 1961b) and interpreted as the result of a regional leuconoritic anatexis (basic palingenesis) of an anorthosito-noritic gneissic basement, similar to the Håland massif. The occurrence of Al-rich Opx megacrysts however indicates a polybaric evolution (Longhi et al. 1993) and precludes the formation of melts at the level of emplacement. An alternative explanation is to consider the anorthositic-noritic gneiss not as an old basement but as the margin of the intrusion, similar to the margin of the Egersund-Ogna body, and produced by syn-emplacement deformation. The Håland massif could thus represent the cap of a diapir and the Helleren body its more central part, capable to cut through its roof.

The Åna-Sira body has many features in common with the Helleren massif and possibly was emplaced in a similar way, though somewhat earlier in the igneous evolution. A detailed mapping has been carried out by geologists from Clausthal Technical University. Universiteit under the leadership of H. Krause (Krause & Pedall 1980). The massif contains two large ilmenite-ore deposits, the Storgangen vein and the Tellnes ilmenite-norite lens, the latter still in active production and yielding a substantial amount of the ilmenite world production. Krause and co-workers have produced detailed studies of the various ore-deposits of the massif (Krause & Zeino-Mahmalat 1970; Gierth & Krause 1973; Krause & Pape 1975; Knorn & Krause 1977). The Bjerkreim-Sokndal layered intrusion associates the whole anorthosite-mangerite suite of rocks and thus remains a key-point in the understanding of the " anorthosite problem ". Since the 1960 guidebook (Michot 1960), more data were made available by Michot (1965) and by various authors. They are summarized later in this guidebook. The SW flank of the intrusion, at the contact with the neighbouring anorthositic Helleren massif is intruded by the Eia-Rekefjord jotunitic body which is related to an extended dyke-system, cutting across all massif-type anorthosite bodies and the lower part of the Bjerkreim-Sokndal intrusion. The Hidra and Garsaknatt leuconoritic bodies, of smaller size, intruded into the metamorphic envelope at a late stage of the igneous evolution (Michot & Michot 1969; Demaiffe et al. 1973). Their most typical features are, for the former, the occurrence of a conspicuous fine-grained jotunitic margin - the sole occurrence in all massifs of a continuous " chilled margin " -, and for the latter, numerous massive or foliated anorthositic and leuconoritic inclusions. In contrast with the other massifs, the plagioclase is not granulated and the subophitic character of the texture, typical of atectonic conditions, is well preserved.

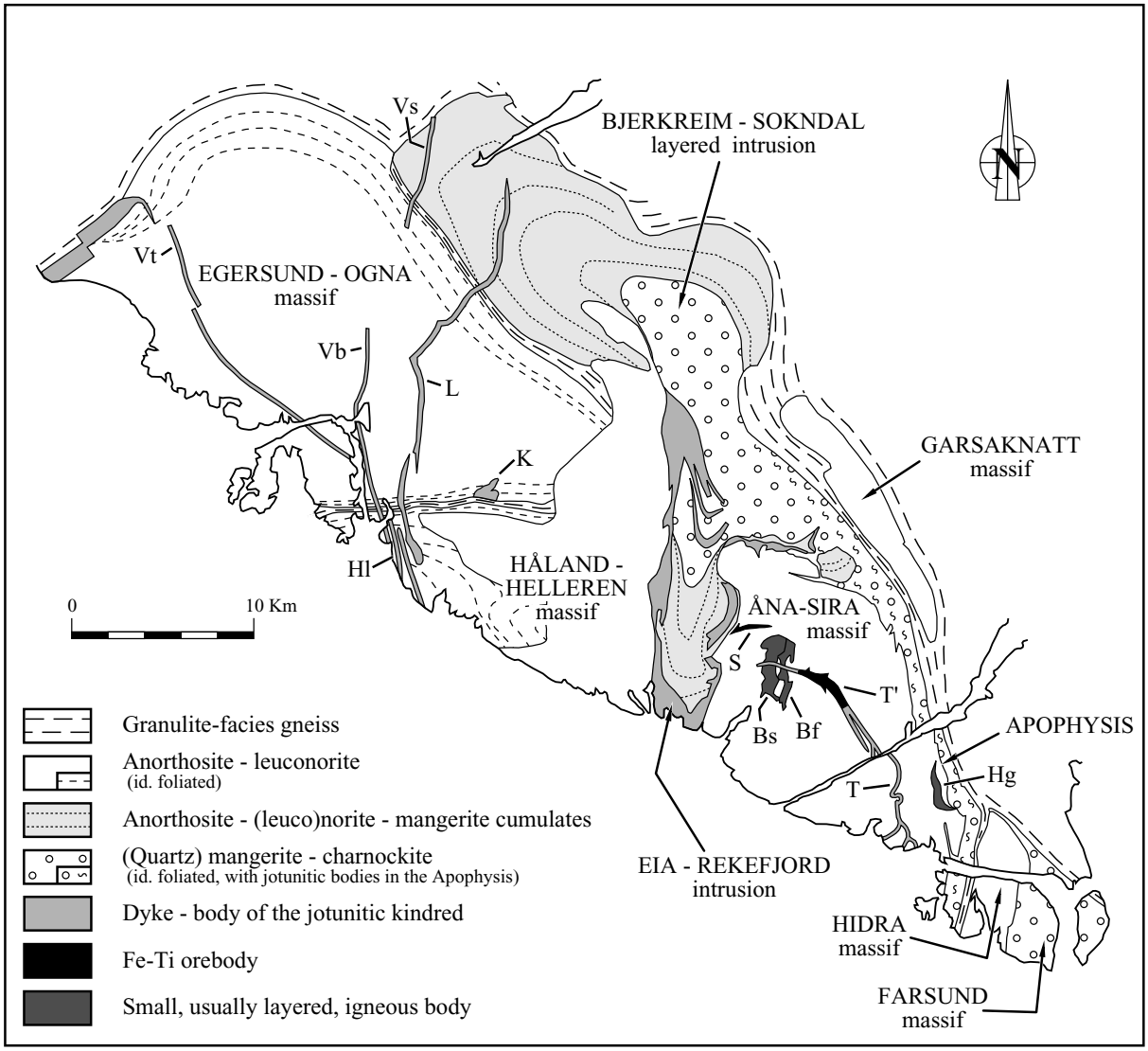

Fig. 1.3. The Rogaland anorthosite province (after Michot 1960, Michot & Michot 1969, Rietmeijer 1979, Wilmart 1982, Duchesne et al. 1985a; Krause et al. 1985; Duchesne 1987b; Duchesne 1987a; Wilson et al. 1996; Bolle 1998). Bs: Bøstølen intrusion; Bf: Pegmatite norite of the Blåfjell deposit; Hg: Hogstad layered intrusion; Hl: Håland dyke; K: Koldal intrusion; L: Lomland dyke; S: Storgangen deposit; T: Tellnes dyke; T': Tellnes deposit; Vb: Varberg dyke; Vt: Vettaland dyke; Vs: Vaersland dyke. *Note that the Egersund dolerite dyke swarm has not been figured*.

A mangero-noritic body is located in southwards prolongation of the Mydland lobe of the Bjerkreim-Sokndal intrusion (Michot & Michot 1969; Demaiffe 1972; Bolle 1996; Bolle et al. 1997). Because of his location, it is called the Apophysis. It is intruding the eastern contact between the Åna-Sira body and the metamorphic envelope.

The Puntavoll-Lien norito-granitic zone (Michot 1955a) and the septum that separate the Egersund-Ogna body from the Håland massif and from the Bjerkreim-Sokndal intrusion, respectively, are of complex origin. Michot (1956a) concluded that a norite intrusive in the contact zone was transformed into norito-granitic banded gneiss by metasomatic fluids that leached out the mafic minerals and redeposited them into Fe-Ti oxide bodies (mafic front) leaving behind an anorthositic residue. The occurrence of garnet-cordierite-sillimanite gneiss within the norito-granitic banded gneiss - thus indicating a pelitic protolith - and the overall similarity of these gneiss with banded gneiss formation commonly found in the metamorphic envelope, however, strongly suggest that the norito-granitic zone of Michot is in fact a septum

of highly deformed metamorphic supracrustal rocks wedged in between the anorthosite massifs.

The Farsund charnockite and the Lyngdal and Kleivan granites are fully described in the Maijer and Padget (1987) guidebook, to which the reader is referred.

A system of Neoproterozoic WNW-ESE dolerite dykes – the so-called Egersund dyke swarm – with aphanitic chilled borders, intrudes the whole igneous complex and the metamorphic envelope (Bingen et al. 1998b).

Geophysical data

Geophysical data on the Rogaland anorthositic province have been synthesized by (Smithson & Ramberg 1979). The Mohorovicic discontinuity is presently about 28 km deep near Egersund (Sellevoll & Aalstad 1971), and the heat flow through the anorthositic bodies is 0.4 to 0.5 HFU (Swanberg et al. 1974). Gravity measurements have led to an overall confirmation of the geological interpretation. A positive gravity anomaly, ranging from 10 to 30 mgal, is centred on the Bjerkreim-Sokndal intrusion, which has been modelled as a syncline containing 4 km-thick noritic material. A seismic image of the basal portion has been recently acquired (Deemer & Hurich 1997). No anomaly can be detected under the massif-type anorthosites, indicating that no complementary mafic material is present beneath the anorthosite. The Åna-Sira body has been inferred to be 4 km thick, which, combined to the heat flow measurement, suggests that the crust below is made up of low-heat producing deep-crustal rocks.

The deep seismic profile ILP-11, has been collected offshore of Rogaland. It has been interpreted by Andersson et al. (1996). Similarly, the undersea extension of the Rogaland anorthosite complex has been drawn after aeromagnetic data (Smethurst et al. 1994). The relationships with the onshore geology are still to be worked out.

Tentative reconstruction of the geological evolution in Rogaland–Vest Agder

In view of the recent age determinations and structural reconstruction, we suggest the following sequence of tectono-metamorphic and plutonic events in the Rogaland – Vest Agder sector. We are still in doubt however with the exact relationship between the M1 metamorphism and the two major isoclinal recumbent fold phases (F2 and F3 phases of Falkum (1998) and D2 and D3 of Hermans et al. (1975) and the two phases of Michot (1956b; 1960). Pervasive deformation on such large scale must have been associated with a (high-grade) metamorphism event older than the intrusion of the Feda porphyritic granite suite. We have chosen to push the first isoclinal recumbent fold phase (F2) into Gothian times, before the emplacement of early-Sveconorwegian charnockitic bodies at c. 1.19–1.15 Ga. The age constraints for F2, F3 and F4 are nevertheless very poor and, for example, these phases could as well result from a continuous deformation in a relatively short time interval. The F3 phase must have started before the intrusion of the porphyritic Feda granodiorite suite and the latter is folded by the F4 phase. We therefore propose the following sequence of events in the Rogaland – Vest Agder sector.

Pre-Sveconorwegian and Gothian times (>1.25 Ga)

Extraction of the crustal material from the mantle (island arc material) given by Nd depleted mantle model ages (T_{DM}) at 1.5–1.9 Ga (Menuge 1988).

Detrital zircon in metaquartzite of the Faurefjell metasediments clustering around 1.65 Ga (de Haas et al. 1999).

F1 and possibly F2 folding phases of Falkum (1998) coeval with M0 phase of metamorphism and or plutonism (Versteeve 1975, Pasteels & Michot 1975; Priem & Verschure 1982).

Intrusion of various granitoids with U–Pb ages between 1.6 and 1.4 Ga (Pasteels & Michot 1975; Priem & Verschure 1982).

Old inherited components in zircon from Tellnes deposit (1.69 Ga) and Helleren anorthosite (1.45 Ga) (Schärer et al. 1996).

Sveconorwegian orogeny (1.25 – 0.98 Ga)

Intrusion of A-type granite to charnockite plutons: Gloppurdi and Botnevatn bodies at 1180 ± 70 Ma (WR Rb–Sr age) (Versteeve 1975; Wielens et al. 1981), and Hidderskog body at 1159 ± 5 Ma (U–Pb zircon age) (Zhou et al. 1995).

Inherited component in zircon from the margin of the Egersund-Ogna body (1.24 Ga) (Schärer et al. 1996).

Beginning of the M1 upper amphibolite facies metamorphism and F2–F3 isoclinal recumbent folds of Falkum (1998). These episodes probably started before the intrusion of the Feda porphyritic granodiorite suite at 1050 +2/-8 Ma.

Intrusion of the Feda porphyritic high-K calc-alkaline granodiorite suite at 1051 +2/-8 Ma (U–Pb zircon age)(Bingen & van Breemen 1998a).

Climax of the M1 upper amphibolite (E) facies and granulite (W) facies metamorphism, separated by an Opx-in isograd at 1024 – 970 Ma (monazite U–Pb ages) (Bingen & van Breemen 1998b); F4 tight to isoclinal fold phase (Falkum 1998)

Intrusion of the Homme granite at 998 Ma ± 14 Ma (WR Rb–Sr age) (Falkum & Pedersen 1979)

F5 tight to close amphibolite facies deformation

F6 open to gentle (non-penetrative) deformation (Falkum 1998).

End of the regional deformation regime between 998 Ma and 980 Ma.

Post-collisional regime (0.98 - 0.90 Ga)

Intrusion of the Holum granite, which is the first post-orogenic granite situated on the western side of the Mandal–Ustaoset Line at 980 ± 34 Ma (WR Rb-Sr age) (Wilson et al. 1977).

Intrusion of the massif-type anorthosite bodies and related rocks at 931 ± 3 Ma (U–Pb zircon ages) (Schärer et al. 1996).

M-2 thermal metamorphism at 930-925 Ma (monazite U–Pb ages) (Bingen & van Breemen 1998b).

Intrusion of the Tellnes ilmenite norite at 920 ± 3 Ma (U–Pb zircon age) (Schärer et al. 1996).

Granitic plutonism straddling the Mandal–Ustaoset line between c. 0.98 and 0.90 Ga, ending with the intrusion of the Bessefjell granite at 904 ± 16 Ma (WR Rb–Sr age) (compilation in Andersson et al. 1996).

Regional cooling through closure temperature for Pb diffusion in titanite (c. 610 °C) at 918 ± 2 Ma (titanite U–Pb ages) (Bingen & van Breemen 1998b) and cooling through closure temperature for Ar diffusion in hornblende (c. 550 °C) at

916 +12/-14 Ma ($^{40}Ar/^{39}Ar$ ages on amphibole in pyroxene-rich samples) (Bingen et al. 1998a).

Intrusion of mineralized pegmatites, namely the Rymteland pegmatite at 916 ± 6 Ma (U–Pb uraninite age) (Pasteels et al. 1979).

Crystallization of low-U (hydrothermal?) monazites in the Feda augen gneiss suite at 912–904 Ma (monazite U–Pb ages) (Bingen & van Breemen 1998b).

Closure of the Rb–Sr isotopic system at mineral scale in biotite and feldspar between 895–853 Ma (Verschure et al. 1980; Bingen et al. 1990).

Intrusion of the WSW–ENE trending undeformed Hunnedalen dyke swarm at 855 ± 59 or 835 ± 47 Ma (Sm–Nd mineral ages) or 848 ± 27 Ma ($^{40}Ar/^{39}Ar$ age on biotite) (Maijer & Verschure 1998; Walderhaug et al. 1999).

Pre-Caledonian rifting and Caledonian period (0.61 - 0.4 Ga)

Intrusion of the WNW–ESE trending Egersund basaltic dyke swarm at 616 ± 3 Ma (U–Pb baddeleyite age) (Bingen et al. 1998b).

M-4 pumpellyite-prehnite facies and greenschist facies metamorphism (c. 400 Ma based on lower intercepts zircon U–Pb discordia lines and secondary K-Ar ages on green biotite (Verschure et al. 1980; Priem & Verschure 1982).

Chapter 2

THE EGERSUND-OGNA MASSIF

(by J.C. Duchesne and R. Maquil)

The Egersund-Ogna massif (EGOG) is an anorthositic dome, approximately 20 km in diameter, emplaced in granulite facies terranes. Petrographically and chemically, the anorthosite is monotonous at large and made up of granulated, equal-sized (1-3 cm), homogeneous plagioclase (An_{40-45}) with locally some megacrysts of orthopyroxene and plagioclase. The marginal zone of the massif (1-3 km thick) is leuconoritic on the average and presents a pronounced gneissic texture. The foliation in the leuconoritic margin and in the envelope is generally concordant. This overall concordance, also recognized by P. Michot (1957, p.28) has local exceptions. For example, P. Michot has described, on the NW contact (Roligheden), a recumbent fold whose inverse flank is cross-cut by the foliated leuconorite. This fact was taken by him as evidence of the contemporaneity of the intrusion with a first phase of isoclinal folding affecting the region. For the present authors, local discordant contacts are not inconsistent with the model of intrusion developed below.

Field relations

Detailed mapping by Maquil (1980) (Fig. 2.1) has led to distinguish several varieties of anorthosites and leuconorites, forming a more or less concentric structure. In the most central part of the massif (along the coast, near Hellvik), the concentration of phenocrysts of plagioclase (5-20 cm) and of megacrysts of orthopyroxene (opx) are higher than elsewhere. The latter form metre-sized subophitic agglomerates with megacrysts of plagioclase. Medium-grained norite or leuconorite also occurs as patches or lenses (usually oriented) in the anorthosite, this structure frequently merges into its inverse - norite or leuconorite with lenses of medium-grained to coarse-grained anorthosite (agglomerates of plagioclases) - and forms what is called the anorthositic-noritic complex. It can thus be viewed as made up of metre-sized lens-shaped agglomerates or megacrysts of plagioclases and orthopyroxenes, embedded in a finer-grained matrix, grading from pure anorthosite to norite. The noritic material characteristically varies in grain size. It can pass over short distances from a pegmatite to a fine-grained rock. The relation with the anorthosite shows all gradations between diffuse, anastomosed contacts and sharp, abrupt, dyke-like contacts. These various characters are not restricted to the core of the massif but can be observed at several places in the anorthosite. Small hemo-ilmenite veinlets occur exclusively in the core of the massif.

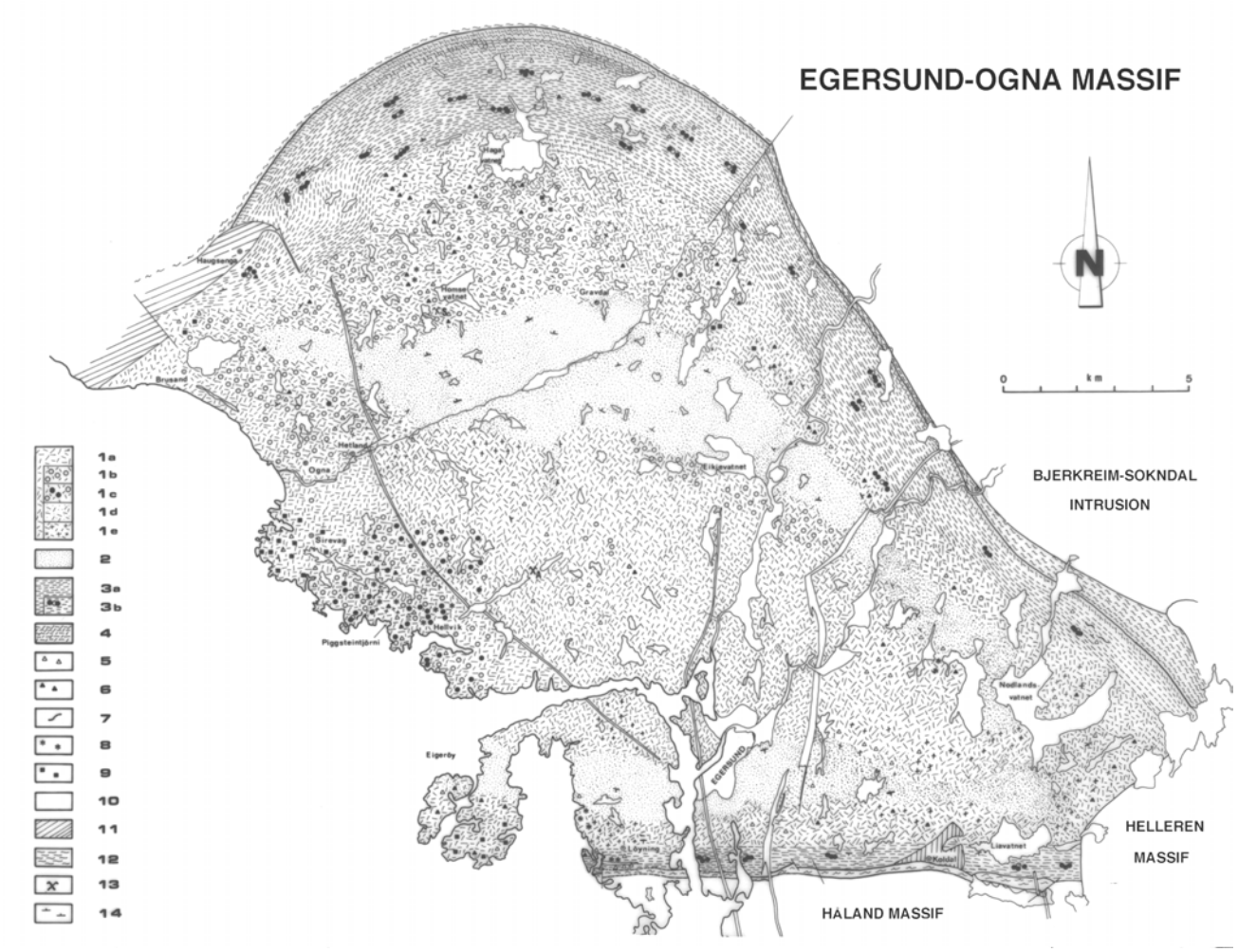

Fig. 2.1. Geological map of the Egersund-Ogna massif-type anorthositic body.
Legend:

1. Medium-grained anorthosite
1A. Anorthosite with phenocrysts and aggregates of plagioclase (5-30 cm)
1B. Anorthosite with aggregates of megacrysts of ortopyroxenes and plagioclases
1C. Homogeneous leuconoritic anorthosite
1D. Association of interfingered anorthosite and norite with sharp or diffuse contacts
2. Homogeneous leuconorite, faintly foliated
3. Foliated anorthosite and leuconorite
3B. Stretched aggregates of megacrysts (opx and/or plagioclase)
4. Foliated anorthosite
5. Noritic dykes (without Fe-Ti oxide minerals) (variable grain-size)
6. Ibid (with Fe-Ti oxide mineral)
7. Fe-Ti oxide veins and veinlets
8. Layered norite-pyroxenite intrusion
9. Zone of anorthositic and leuconoritic foliated inclusions
10. Monzonoritic and noritic dyke
11. Layered noritic to monzonoritic intrusion
12. Charnockitic and migmatitic gneisses
13. Mine: A: Kaolinitized anorthosite
    Exploration site: S: Fe-Ni sulfide
14. Strike and dip

Note: the dolerite dyke swarm is not represented.

The marginal zone of the massif can be considered as being formed by rock types and associations similar to those of the core of the massif but in various stages of deformation, producing a variety of textures from a simple magmatic orientation to a completely recrystallized granoblastic texture.

The mega-opx are kinked, granulated and stretched over several metres along the foliation. The aggregates of phenocrysts of plagioclases give rise to layers, bands or lenses of meta-anorthosite; the norite, to noritic gneisses, etc. The foliation always coincides with the layering. Rapid variation in grain-size of the foliated rocks can be attributed to differing deformation rates and/or to variation in grain size of the original rock. Dykes of noritic material can be found cutting across the foliation: a single unfoliated dyke can be sheared (and foliated) in place, faulted and displaced a few metres away along strike. This indicates that deformation in the margin has taken place in several episodes and has become less and less pervasive and progressively restricted to discrete surfaces. This is good evidence of continuous deformation.

Photo 2.1 High-alumina orthopyroxene megacrysts in anorthosite. The hammer handle is 1 m long.

A homogeneous, faintly foliated leuconorite constitutes a third important petrographic unit. It is grossly concentric with the core and at equal distance to the margin (Fig. 2.1). A system of Fe-Ti oxide-rich noritic dykes, with variable grain size though commonly pegmatitic (Michot 1960), cuts across the anorthosite and Bjerkreim-Sokndal (BKSK) intrusion. The dykes occur everywhere in the anorthosite but are more concentrated towards the margin. Petrographically, they contrast with the noritic material of the anorthosito-noritic complex by the presence of Fe-Ti oxide minerals.

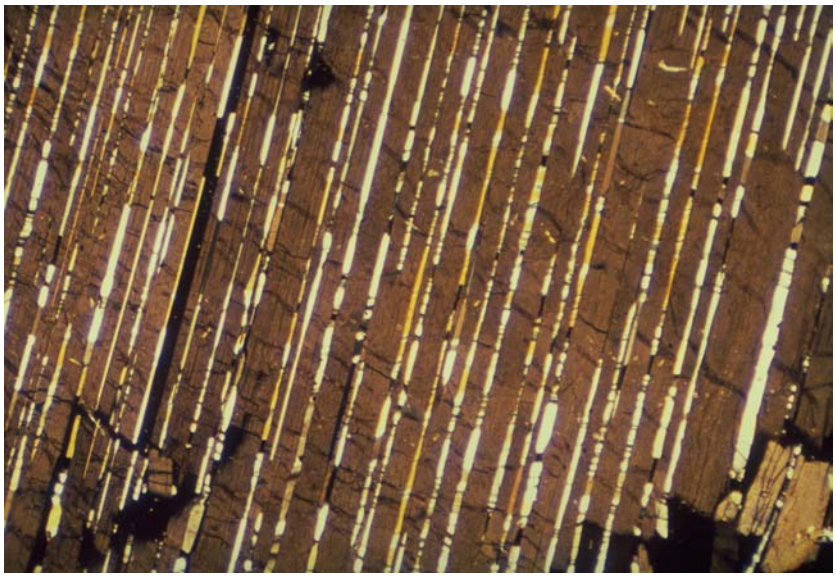

Photo 2.2 Plagioclase and Fe-Ti oxide exsolutions in opx megacryst (sample 66-119) (see Table 2.1. for the bulk composition).

Numerous blocky fragments of meta-anorthosites and meta-leuconorites occur as inclusions in the central anorthosite (mentioned by Michot 1960, on Ystebröd Island).

Mineral geochemistry

The anorthosite and related leuconorites and norites from the central part of the massif contain a plagioclase of monotonous composition: the anorthite content is between 40 and 45 wt.%, Sr 800-1000 ppm; Ba 100-250 ppm; K_2O 0.5-0.8%. The plagioclase phenocrysts are usually different from the matrix plagioclase. Nevertheless some of them, namely those associated with megacrysts of orthopyroxene in sub-ophitic texture, are more calcic (An_{55}), but with similar Sr contents, lesser K_2O (<0.4%) and Ba (<100 ppm) contents. They typically show labradorescence (Bøggild intergrowths).

The megacrysts of orthopyroxenes contain numerous exsolution lamellae of plagioclase (Emslie 1975 ; Maquil & Duchesne 1984)), a peculiarity which is common to all anorthositic massifs in the Egersund Province as well as in most anorthosite massifs elsewhere in the world. Their bulk chemical compositions are given in Table 2.1. Little variation in Fe/Mg ratio is to be reported (Fig. 2.2). Experimental data indicate that Ca-tschermakitic opx are stable only at high pressure and temperature. For an Al_2O_3 content of about 7-9% - which characterizes the opx from the central part of the massif - estimates of pressures between 10 and 12 kb were suggested by Maquil (1979) and later confirmed by the experiments of Fram & Longhi (1992).

Exsolution of plagioclase takes place by decreasing pressure and oxidizing conditions when it is coupled with the exsolution of oxide mineral (Emslie 1975). By contrast the opx of the norite which encloses agglomerates of megacrysts has an Al-content around 2-3% Al_2O_3, a value also shared by cumulate opx from the neighbouring BKSK intrusion and by granoblastic leuconoritic gneisses from the margin. The Cr content of the mega-opx from the central part comprises between 600-950 ppm, values definitely higher than those of the norite opx (less than 200 ppm) (see Fig. 2.3).

Table 2.1. Bulk chemical composition of aluminous mega-orthopyroxenes from the Egersund-Ogna massif (central part and margin), the Helleren massif and the Åna-Sira massif (Analysts: G. Bologne - wet chemical analysis of major elements; R. Maquil - trace elements by XRF).

	1	2	3	4	5	6	7	8	9	10	11	12	13
SiO_2	50.05	50.59	50.32	50.97	51.54	51.08	52.88	48.69	49.23	48.99	49.56	49.53	48.46
TiO_2	0.40	0.38	0.47	0.55	0.35	0.47	0.20	0.61	0.89	0.62	0.66	0.83	0.64
Al_2O_3	8.35	7.02	8.86	3.50	5.69	5.69	3.50	8.41	7.31	7.57	7.35	7.82	8.72
Fe_2O_3	3.38	2.98	3.17	5.31	4.00	3.59	3.60	5.33	4.51	3.68	5.96	5.20	5.19
FeO	10.55	11.45	10.52	18.41	10.30	12.90	13.34	12.63	13.53	13.43	12.11	12.70	11.27
MnO	0.18	0.23	0.13	0.33	0.27	0.28	0.25	0.25	0.28	0.26	0.27	0.23	0.23
MgO	25.74	24.88	23.11	18.55	26.00	23.71	25.35	22.70	22.02	23.04	22.53	22.95	23.91
CaO	1.44	1.33	1.27	1.37	1.39	1.57	0.60	1.54	2.07	1.66	1.71	1.20	1.47
Na_2O	0.22	0.17	0.35	0.17	0.25	0.28	0.24	0.31	0.31	0.20	0.14	0.24	0.25
K_2O	0.04	0.06	0.12	0.08	0.22	0.25	0.12	0.07	0.09	<0.04	0.05	0.09	<0.04
P_2O_5	0.07	0.06	0.09	0.02	0.01	0.01	0.13	0.06	0.03	0.03	0.03	0.04	0.01
Total	100.42	99.15	98.40	99.27	100.17	99.84	100.22	100.60	100.28	99.52	100.38	100.83	100.18
Trace elements (ppm)													
Cr	730	639	784	280	996	1321*	1209*	595	595	578	565	728*	891
Ni	245	323	206	155	283	193*	345*	219	258	235	218	222*	321
Co	112	100	106	120	95	110*	112*	122	118	124	121	122*	114
V	192	156	178	399	172	205*	170*	215	214	209	201	206*	196
Zn	89	59	75	222	60	83*	150*	104	104	96	106	105*	82
Structural formula													
Si	1.7816	1.8271	1.8198	1.9114	1.8440	1.8518	1.9035	1.7608	1.7922	1.7893	1.7930	1.7826	1.7488
Al IV	0.2184	0.1729	0.1802	0.0886	0.1560	0.1482	0.0965	0.2392	0.2078	0.2107	0.2070	0.2174	0.2512
Al VI	0.1319	0.1257	0.1974	0.0660	0.0840	0.0949	0.0519	0.1193	0.1059	0.1150	0.1065	0.1143	0.1196
Ti	0.0107	0.0104	0.0128	0.0155	0.0095	0.0129	0.0054	0.0165	0.0243	0.0171	0.0180	0.0225	0.0173
Fe^{3+}	0.0907	0.0812	0.0865	0.1501	0.1075	0.0980	0.0973	0.1451	0.1234	0.1010	0.1622	0.1410	0.1409
Fe^{2+}	0.3140	0.3459	0.3181	0.5773	0.3084	0.3912	0.4016	0.3820	0.4119	0.4102	0.3665	0.3823	0.3402
Mn	0.0053	0.0069	0.0039	0.0106	0.0032	0.0085	0.0076	0.0076	0.0085	0.0081	0.0083	0.0069	0.0069
Mg	1.3658	1.3395	1.2459	1.0372	1.3873	1.2815	1.3604	1.2237	1.1950	1.2547	1.2152	1.2314	1.2863
Ca	0.0550	0.0514	0.0491	0.0550	0.0533	0.0610	0.0231	0.0598	0.0807	0.0650	0.0663	0.0463	0.0568
Na	0.0150	0.0117	0.0243	0.0122	0.0172	0.0196	0.0169	0.0217	0.0219	0.01400	0.0100	0.0169	0.0173
K	0.0017	0.0026	0.0056	0.0036	0.0099	0.0118	0.0056	0.0030	0.0044	0.0000	0.0022	0.0043	0.0000
P	0.0021	0.0017	0.0026	0.0005	0.0004	0.0004	0.0039	0.0017	0.0009	0.0009	0.0009	0.0013	0.0004
cat	3.9911	3.9749	3.9414	3.9244	3.9759	3.9682	3.9690	3.9779	3.9726	3.9862	3.9540	3.9632	3.9861
En	74.81	73.69	73.34	57.01	74.77	69.96	72.26	67.59	65.99	68.54	67.16	68.39	70.50
Fs	22.18	23.5	23.78	39.97	22.37	26.71	26.51	29.10	29.54	27.91	29.19	29.06	26.37
Wo	3.01	2.8	2.88	3.02	2.86	3.33	1.22	3.31	4.47	3.55	3.65	2.56	3.13

(*) duplicate analyses

Sample location: 1. JCD66.119.2B – Egersund-Ogna massif - Kalvshagen (LK156.872) Agglomerate of the central anorthosite (see stop 1.3); 2. JCD75.23.1A - id. - Rubben (LK174-881) id; 3. JCD75.24 - id. Skansefjellet (LK167-887) id; 4. JCD75.39 - id - N. Soltuva (LK228-925) - Foliated noritic pegmatite; 5. JCD75.32B - id. - W. Haugsenga (LK128-971) - Undeformed core of an enormous megacryst from the gneissic margin (see stop 1.4); 6. JCD75.63.1 - id. - Road E18 near Eikenstein (LK301-918) - Undeformed part of a megacryst from the gneissic margin; 7. JCD64.02 - id. - Road E18 near Krossmoen (LK315-904) – id; 8. JCD75.65 - Amdal-Helleren-Rödland massif - Stemmetjörna (LK360-744) - Aggregate of megacrysts (plagioclase and green spine exsolutions); 9,10,11. B1,B2,B3 - id (same location as JCD75.65) (collection J.Bellière); 12. JCD75.74A - Åna-Sira massif - E. Allestad (LK550-654) - Aggregate of megacrysts (plagioclase and green spinel exsolutions); 13. JCD75.75 - id - W. Stavvatnet (LK5395-614) - id.

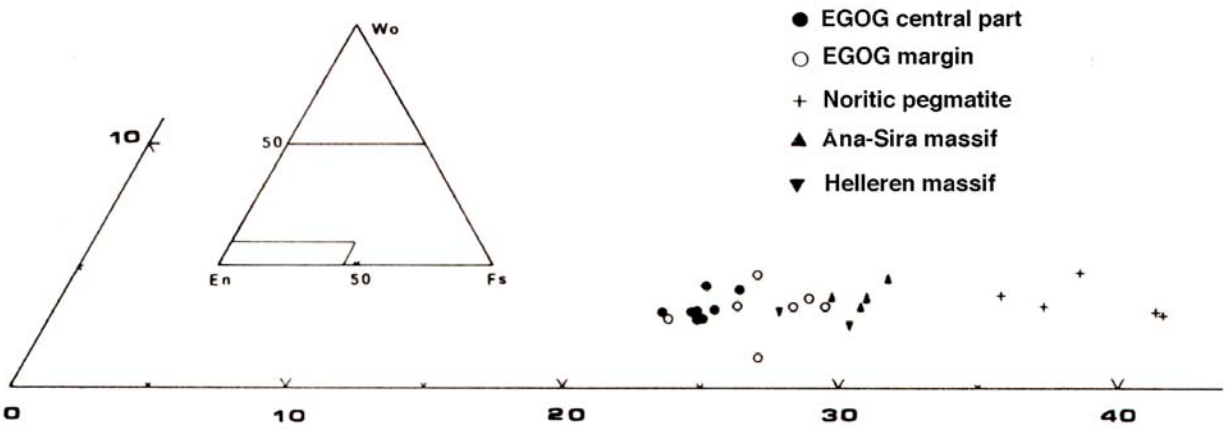

Fig. 2.2. Plot of chemical compositions of mega-orthopyroxenes (see Table 2.1.) in the pyroxene diagram. The opx from the pegmatitic noritic dykes are distinctly Fe-richer than the other types, which show relatively little scattering.

Notable differences exist in the geochemistry of mega-opx and plagioclase from the central part and from the marginal zone of the massif. Undeformed mega-opx from the margin contain 3.5-6% Al_2O_3 with Cr between 600 and 1500 ppm (Fig.2.3). Plagioclases in the margin vary from An_{45} up to An_{75} and have an uniformly low Sr content (350-450 ppm) and low Ba content (< 100 ppm), as was noted by Duchesne (1966) and by Duchesne & Demaiffe (1978) (Fig. 2.5).

Compared to Cr, the other trace elements in mega-opx show little variation (Fig.2.4): V = 289± 29 ppm; Ni = 276 ± 45 ppm; Zn = 133± 22 ppm; Co = 103 ± 7 ppm; MnO = 0.24 ± 0.02 ppm. This indicates that during mineral melt equilibrium the bulk partition coefficients of the various elements remain close to unity, which in turn implies cotectic crystallization of plagioclase and orthopyroxene and precludes olivine and Fe-Ti oxides at the liquidus (Maquil et al. 1980).

Plagioclases from blocky inclusions of leuconoritic and anorthositic gneiss are geochemically similar to those from the foliated margin of the massif (Fig. 2.5). Since these geochemical characters are restricted to plagioclase from the margin and the inclusions are texturally similar to the gneisses of the margin, it can be concluded that they represent fragments broken from the margin of the massif.

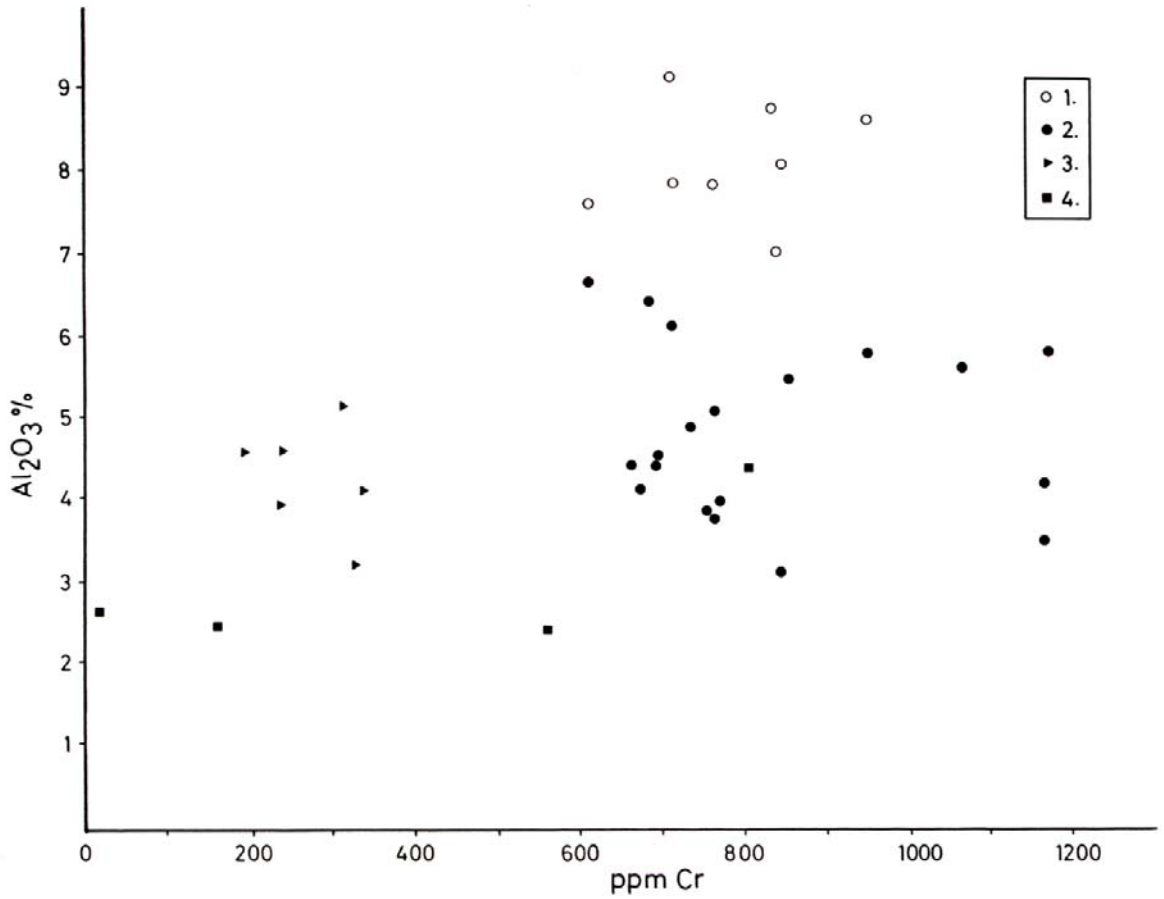

Fig. 2.3. Cr (ppm) vs Al_2O_s (%) variations in mega-opx from EGOG massif (Table 2.1). Legend: 1: central anorthosite; 2: foliated margin; 3: noritic pegmatite; 4: cuspate opx separated from medium grained leuconorite in the anorthosite-norite complex.

Geothermometry

Though clinopyroxene is relatively rare in the EGOG body, Maquil and Duchesne (1984) have selected cpx-bearing samples in various geological occurrences and measured opx-cpx compositions. Application of Wells' (1977) geothermometer and consideration on the Al-content of the pyroxenes give the following main results:

1. Equilibrium temperatures in stretched and recrystallized mega-opx from the margin (granoblastic texture) are on the average higher than in metabasites of the granulitic envelope, some samples from the margin indicating temperatures in excess of 100°C over that of the envelope;
2. The maximum temperatures measured in the margin are also higher than solidus temperatures in the norites from the centre;
3. Exsolution in mega-opx have started at higher temperatures and pressures than those that prevailed at completion of crystallization or during recrystallization.

Petrogenesis

Generation of huge and monotonous masses of anorthosite has been long debated. It is the central question of the so-called " anorthosite problem ". The discovery that the mega-opx - an ubiquitous mineral in all massif-type anorthosites - were Ca-tschermakitic has thrown new

light on the question. Though experimental data on the plagioclase - Al-opx system are still scarce compared to the garnet - or spinel - bearing systems, there is little doubt that the mega-opx from the central anorthosite have started to crystallize at high P,T conditions (around 10-12 kb and 1250°C) and, being interstitial to plagioclase crystals, plagioclase was also stable on the liquidus under those conditions. Accordingly, the P,T conditions for the crystallization or the opx from the margin were not so high: the opx contains less Al and the plagioclase is more Ca-rich, in agreement with experimental data (Green 1970; Fram & Longhi 1992). The composition of the minerals from the noritic matrix also points to a final consolidation at an even shallower depth.

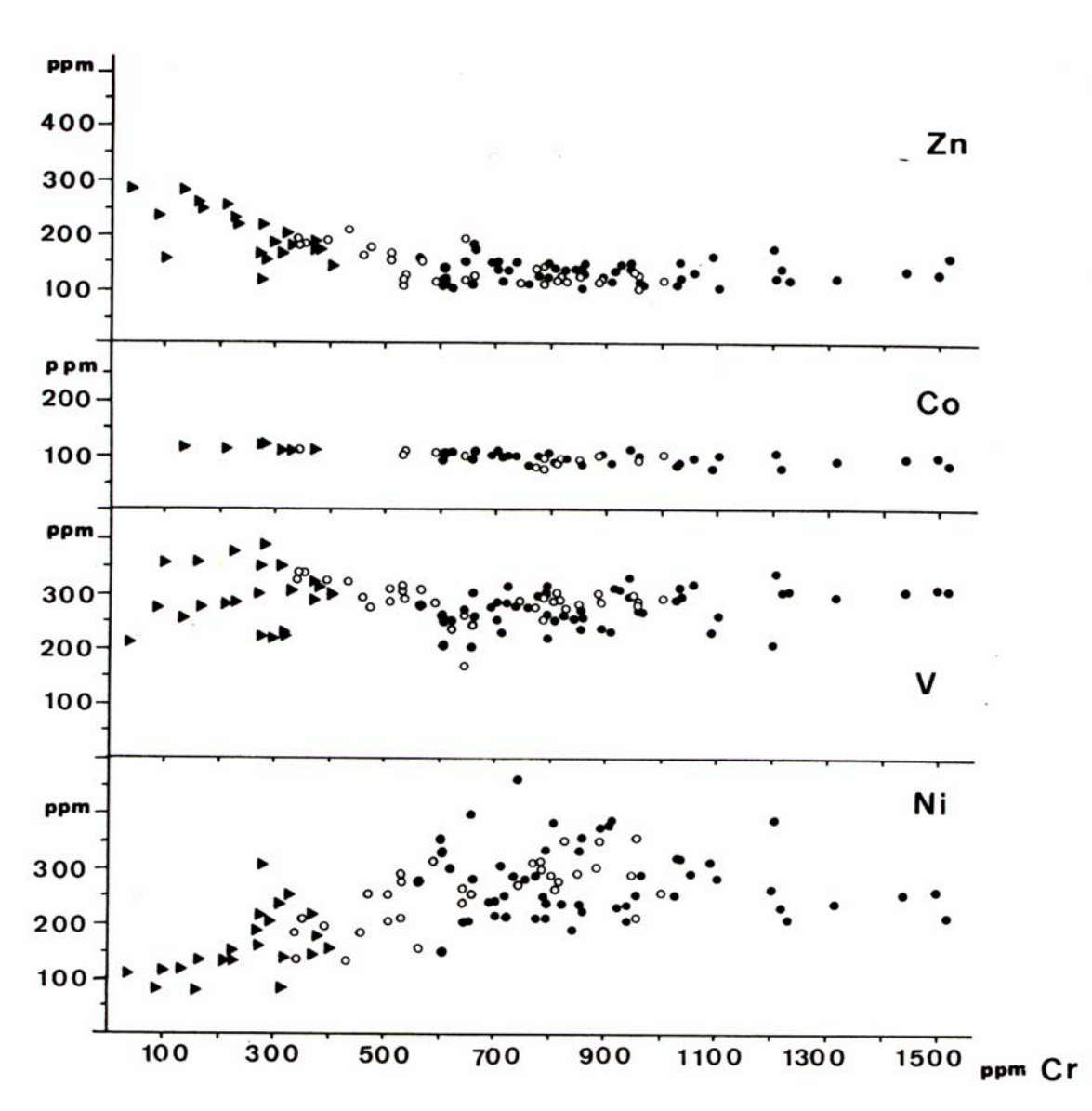

Fig. 2.4. Transition element content vs Cr content in opx from the EGOG massif (ppm). Legend: Open circle: mega-opx from the central anorthosite: filled circle: mega-opx from the margin; triangle: opx from norite pegmatite.

The nature of the parental magma of EGOG is not known. No " chilled " margin has been unambiguously recognized, though fine-grained noritic rocks occurring locally at the contact with the migmatitic gneiss envelope and septa are potential candidates. The contrast in composition between the plagioclase and the mega-opx from the central part and the foliated margin is still partly enigmatic. The variation in Sr content of the plagioclase (low in the margin and high in the center) does not result from a variation in the partition coefficient

value between plagioclase and melt with pressure, though pressure significantly increases the partitioning of Cr between opx and melt (Vander Auwera et al. 2000). This opens the possibility that a jotunitic magma could be parental to the central anorthosite and a high-alumina basalt to the foliated margin. This confirms the possible existence of two different parental magmas to account for the Rogaland massifs, as already suggested by Duchesne et al. (1985) but now with an important difference: a basaltic magma produces the labradorite anorthosite massifs, and a jotunitic magma gives rise to andesine anorthosite, such as the central part of EGOG, the BKSK succession of rocks, the Hidra Massif, etc.

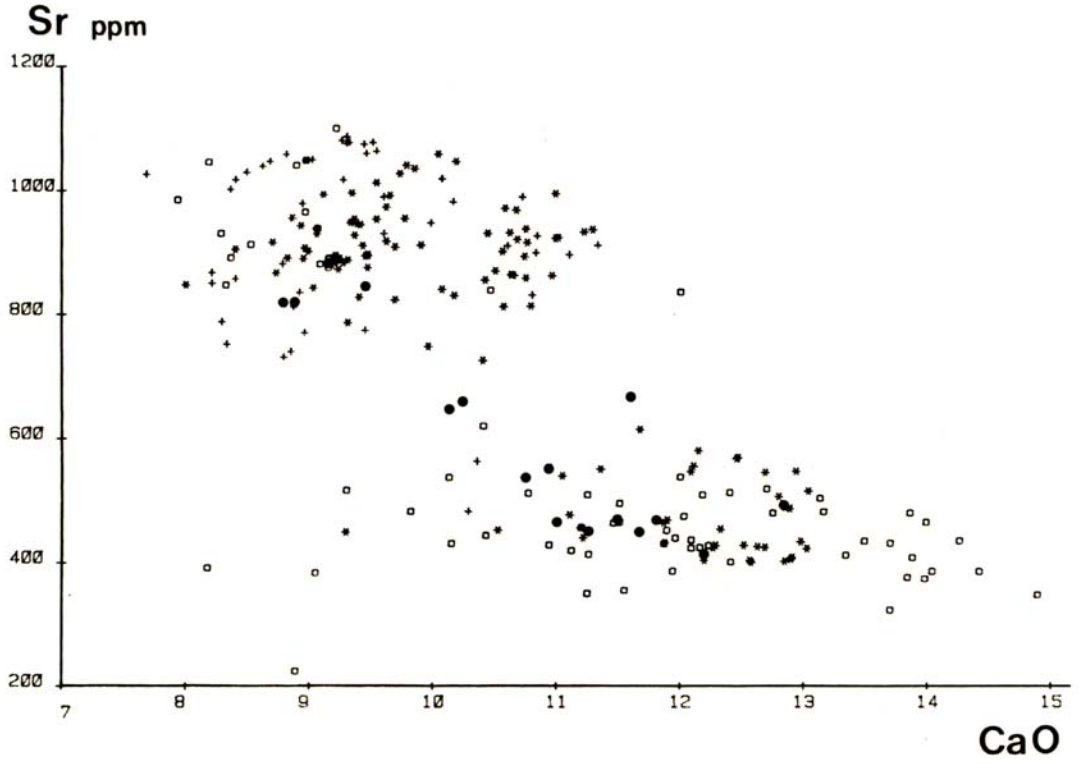

Fig. 2.5. Sr (ppm) vs CaO (%) in plagioclases form EGOG massif. Legend: (asterisk): phenocryst from the central part and from the margin; (cross): matrix plagioclase from the central part; (square) matrix plagioclase from the margin; (dot): plagioclase from inclusion.

Though many points remain unsolved, a general model for the crystallization and emplacement of the EGOG massif can be tentatively proposed (Duchesne & Maquil 1981; Maquil & Duchesne 1984). It basically accounts for the following features:

1. occurrence in the field of all transition terms between magmatic and metamorphic textures, particularly coincidence of the foliation plane with the compositional layering, and also between protoclastic and granoblastic structures points to various degrees of deformation.
2. indication of successive deformations in the margin.
3. evidence that the deformation leading to granoblastic structure was already completed when large parts of the massif were still capable of intrusion (gneissic inclusions, unfoliated noritic dyke in the margin, etc.).
4. occurrences of different compositions between phenocrysts and matrix minerals (particularly mega-opx with different Al and Cr contents).

5. indications from available geothermometers (cpx-opx) and barometers (Al in pyroxenes) of crystallization (and recrystallization) processes along a P-T gradient.

These points of evidence are in favour of an emplacement process in which the anorthosite, in a mushy stage, lubricated by a minor amount of interstitial liquids and containing megacrysts or aggregates of megacrysts, forms at depth, rises diapirically in the crust and produces its own deformation along the walls and within the mass. A ballooning process locally leads to the foliation of marginal parts and also sufficiently deforms the external metamorphic envelope (syn-emplacement deformation) to achieve parallel structure on both sides of the contact. A final telescopic flattening of the whole system extends the area of the massif by bringing the root of the diapir near its roof in a central position.

This interpretation of the EGOG body, proposed by Duchesne & Maquil (1981) and Maquil & Duchesne (1984), was confirming a model of diapiric emplacement suggested by Martignole & Schrijver (1970) for the Morin anorthosite (but later on disproved by Martignole 1996). Maquil & Duchesne (1984) showed that the emplacement mechanism was not necessarily linked to a regional deformation, but this one could not be precluded until accurate age measurements (U-Pb on zircon extracted from mega-cryst aggregates) gave an age of 931±3 Ma (Schärer et al. 1996), some 70 m.yr. younger than the last recognized regional deformation.

The various structural and petrographic characteristics of the EGOG pluton together with thermo-mechanical properties of anorthosite and mid- and lower crustal rocks were used by Barnichon et al. (1999) to build up a finite element mechanical model of diapiric rise and emplacement. This model confirms that diapirism of an anorthosite mush through the lower crust can indeed take place in the relatively small time interval measured, and gives rise to a strain regime in agreement with field observations.

The other large anorthositic massifs (Åna-Sira and Helleren) also contain the EGOG " trilogy " i.e. (1) mega-crysts of Al-rich opx, (2) anorthosite-norite complex, (3) large parts made up of foliated rocks as well as gneissic inclusions. As far as the emplacement mechanism is concerned, the similarities with EGOG are striking and basically the same diapiric process can be accounted for. The interaction between the uprising anorthosite diapirs and the surrounding rocks, namely the BKSK layered intrusion and the migmatitic gneiss envelope, has led to a gravity controlled tectonic in which the BKSK intrusion was folded in a (rim) syncline to accommodate the uprise of the EGOG and Helleren massifs to the East and of the Helleren and Åna-Sira massifs on both sides of the Sokndal lobe (Bolle et al. 2000).

***

Chapter 3

THE BJERKREIM-SOKNDAL LAYERED INTRUSION

(by Brian Robins and J. Richard Wilson)

Introduction

The Bjerkreim-Sokndal Intrusion (BKSK) (Michot 1960; 1965; Duchesne 1987a; Wilson et al. 1996) is a large (40 km long and up to 15 km wide), Late Proterozoic layered intrusion that occupies an area of about 230 km^2 (Fig. 3.1). Lithologically the intrusion consists of virtually all of the rock types belonging to the anorthosite kindred, i.e. andesine anorthosite, troctolite, leuconorite, norite, gabbronorite, jotunite (hypersthene monzodiorite), mangerite (hypersthene monzonite), quartz mangerite and igneous charnockite (hypersthene granite). Anorthosite, leuconorite and norite are accompanied by ilmenite-rich rocks.

The BKSK is emplaced in granulite-facies quartzo-feldspathic and mafic gneisses as well as anorthosite and leuconorite belonging to the Egersund-Ogna (Michot & Michot 1970; Duchesne & Maquil 1987), Håland-Helleren (Michot 1961) and Åna-Sira (Krause et al. 1985; Duchesne & Michot 1987) massifs, and xenoliths of all these host rocks are common within the intrusion itself (Duchesne 1970).

The BKSK and the various anorthosite massifs are cut by members of a suite of small plutons and wide, laterally-persistent dykes of jotunite, some of which are differentiated (Duchesne et al. 1989; Wilmart et al. 1989). The most voluminous of the jotunites that cut the northern part of the BKSK is the Lomland dyke/sill complex (Duchesne et al. 1989). The BKSK is also cut by members of the Egersund swarm of basaltic dykes.

Shape and internal structure of the Bjerkreim-Sokndal intrusion

The Bjerkreim-Sokndal Intrusion has generally been described as a lopolith, but recent detailed mapping shows it to be a trough-like, discordant intrusion. Modelling of the associated +10-30 mgal gravity anomaly (Smithson & Ramberg 1979) and a seismic reflection profile (Deemer & Hurich 1997) shows that the base of the intrusion lies at a depth of 4-5 km.

Layering within the intrusion is deformed into a deep, doubly-plunging syncline that branches in the south around a dome cored by the Åna-Sira anorthosite massif (Fig. 3.1). The core of the syncline is occupied by quartz mangerite and charnockite, which do not exhibit modal or textural layering, and these are separated in places from the underlying mangerite by a zone with abundant wall-rock xenoliths. The magnitude of the gravity lows over the granitoids suggests a maximum thickness of about 2 km (Smithson & Ramberg 1979). There is no evidence that the roof of the intrusion is preserved anywhere within the confines of the present outcrop.

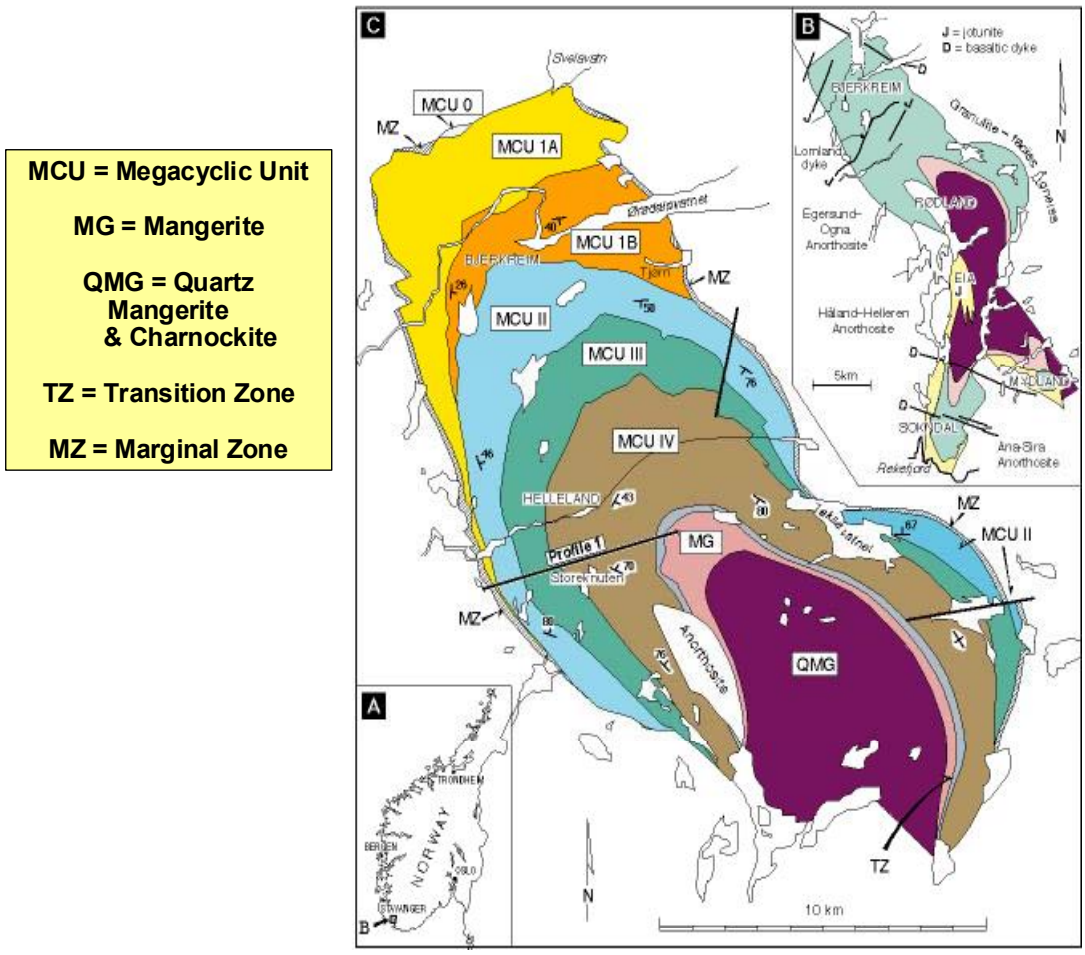

Fig. 3.1. Location (A), sketch map (B), and stratigraphic subdivision of the Bjerkreim lobe (C) of the Bjerkreim-Sokndal Intrusion.

The BKSK consists of three lobes; the Bjerkreim lobe in the north-west, and the smaller Sokndal and Mydland lobes to the south and south-east respectively (Fig. 3.1B). Modal layering and phase contacts in the Bjerkreim lobe are disposed in a syncline that plunges south-east at 20-40°. In the steep limbs of the syncline the cumulates are foliated, generally in the plane of modal layering. In places, cumulus minerals form augen in a foliated matrix, small shear zones are developed, and there is a strong mineral lineation. Linear mineral and magnetic fabrics dominate in the core of the syncline (Paludan et al. 1994 ; Bolle et al. 2000). Cumulus plagioclases are strained or recrystallised to shape-oriented polygonal aggregates, whereas prismatic Ca-poor pyroxenes are commonly kinked or bent. Uniform paleomagnetic vectors in different parts of the intrusion (Poorter 1972) suggest that the deformation and development of the synformal disposition of the layering took place at temperatures in excess of the Curie point (550-650°C). The synformal disposition of the layering is inferred to be due to gravitational foundering (Paludan et al. 1994 ; Bolle et al. 2000).

The layered series

The Layered Series in the Bjerkreim lobe has a thickness of >7000m in the axial region of the syncline and can be divided into 6 megacyclic units (MCU 0 to IV) which exhibit characteristic sequences of cumulates (Figs. 3.1 and 3.2). The megacyclic units can be further subdivided into zones a-f, based on assemblages of cumulus minerals (Figs. 3.2 and 3.3).

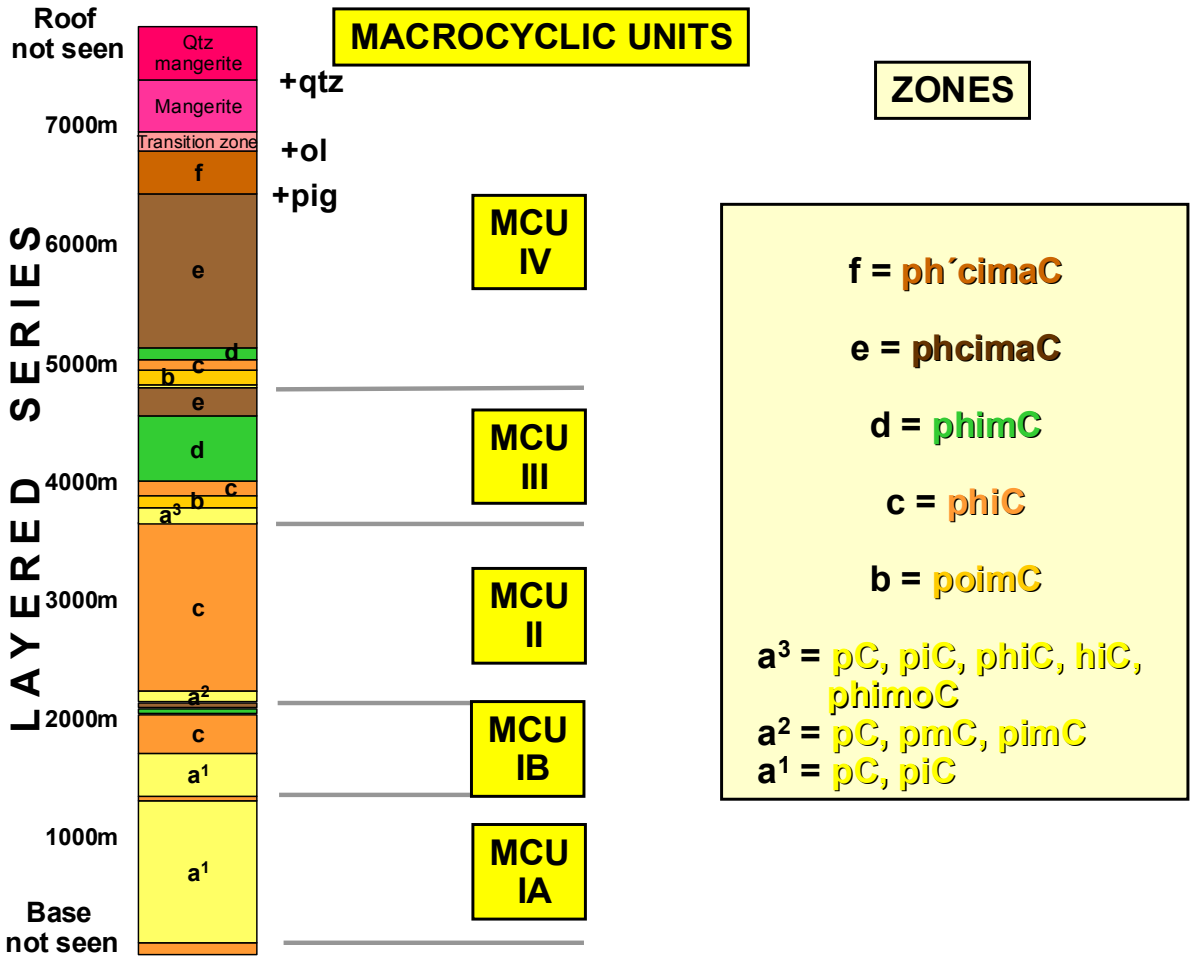

Fig. 3.2. Stratigraphy of the Layered Series of the Bjerkreim-Sokndal Intrusion as developed in the axial region of the Bjerkreim lobe and its subdivision into macrocyclic units and cumulate zones.

The megacyclic units vary in stratigraphic thickness, lateral persistence and in the nature of the layer sequences they exhibit. The lower three megacyclic units, exposed only in the northernmost part of the intrusion, are individually as much as 1300m thick but show a pronounced southward thinning in the western limb of the syncline and are not developed in the southern parts of the Bjerkreim lobe.

The lowermost cumulates are exposed in the north-western part of the Bjerkreim lobe and consist of plagioclase-hypersthene-ilmenite cumulates (phiC). They are regarded as the top of MCU 0, the rest of which, together with an unknown thickness of cumulates, is hidden. These cumulates are overlain successively by pC, piC and phC belonging to MCU IA (~1300m thick in a profile along the axial trace of the syncline).

This sequence is repeated in MCU IB (~875m thick) which locally also displays more evolved lithologies with the entry of cumulus Ca-rich pyroxene, followed by apatite and magnetite. MCUs 0-IB are characterised by the presence of plagioclase megacrysts (up to 10 cm long) in all rocks with the exception of the most evolved cumulates at the top of MCU IB MCU II (reaching a thickness of 1600m) consists of a thin layer of magnetite-bearing piC overlain exclusively by phiC. The appearance of cumulus magnetite in the leuconorites at the base of MCU II and its absence in the overlying cumulates suggests affinities with the olivine-bearing zones near the bases of succeeding MCUs. The base of MCU II is characterised by a marked regression in the composition of cumulus plagioclase (Fig. 3.3).

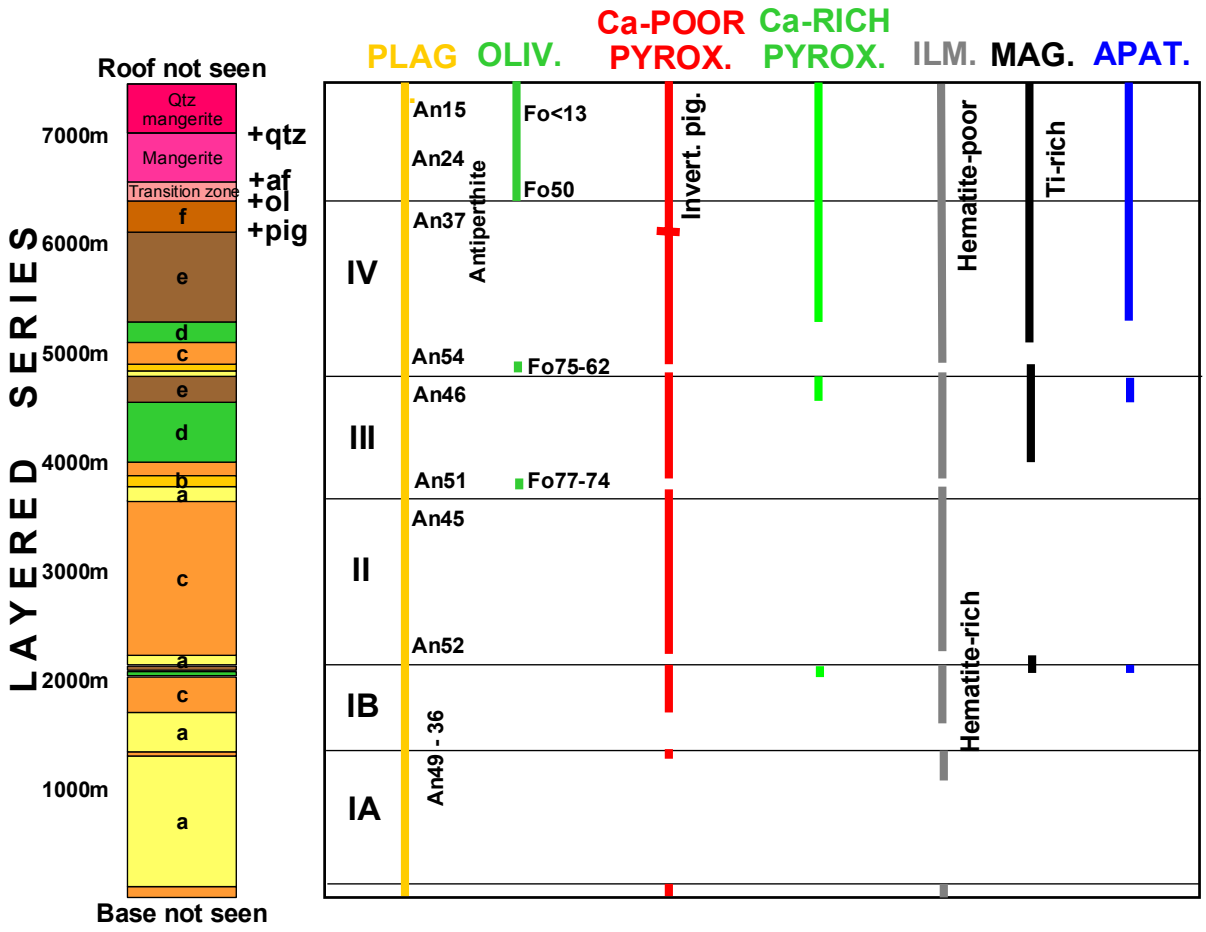

Fig. 3.3. Generalised stratigraphy and cryptic layering of the Bjerkreim-Sokndal Layered Intrusion. After Wilson et al. (1996).

MCU III (maximum ~1100m thick) generally has a lower zone (Zone IIIa in Fig. 3.3) up to 140m thick that consists mainly of pC, but with interlayered iC, phiC and hiC. The base of the zone is marked by a thin (<10m) sulphide-bearing subzone, unique in the Layered Series, that consists of ilmenite norite, mafic ilmenite norite or massive orthopyroxenite. Zone a is characterised by a stratigraphic regression to higher-temperature mineral compositions. In the axial region of the intrusion and on the southern flank, zone a is overlain by leucotroctolite (zone b) that contains cumulus magnetite in addition to plagioclase, olivine and ilmenite. Together with the similar rocks near the base of MCU IV, the zone IIIb cumulates are the most primitive cumulates in the intrusion. The leucotroctolite is in turn overlain by phiC of zone c, followed by magnetite norite (Zone d) and gabbronorite (Zone e) with the successive (re-)entry of cumulus magnetite and then apatite together with Ca-rich pyroxene. In the eastern flank of the intrusion MCU III is relatively condensed and zone b is absent. Zone e is only developed in the flanks of the lobe. In the axial region the base of MCU IV rests on zone d cumulates.

MCU IV (maximum thickness ~1800m) displays a sequence similar to MCU III. MCU IV contains, however, additional, more-evolved cumulates. Michot (1960) recognised the prominent olivine-bearing zone b near the base of MCU IV and referred to it as the "Svalestad horizon". It has a thickness of about 100m and is laterally persistent along strike for about 24km. Olivines in the olivine-bearing zones near the bases of MCU III and IV are partially or completely replaced by orthopyroxene-Fe-Ti oxide symplectites, but the zones are texturally distinctive even where no olivine remains. Small amounts of biotite and hornblende also occur in the olivine-bearing zones. Ca-poor pyroxene is inverted pigeonite in the upper part of

MCU IV (Zone f) which grades into overlying mangerite through a jotunitic Transition Zone (TZ) whose base is defined by the re-entry of olivine (~Fo_{50}), which more or less coincides with the appearance of interstitial alkali feldspar (Duchesne et al. 1987). With the appearance of cumulus mesoperthite the rocks grade upwards from jotunite to mangerite, which in turn passes into massive quartz mangerite and, locally, charnockite. Even in these highly-evolved rocks, hydrous phases are not abundant: Calcic amphibole is generally a minor mineral (except in the uppermost part of the granitoids where it may occur as large oikocrysts) and biotite is generally an accessory mineral. The combined thickness of the mangerite, quartz mangerite and charnockite is >350m (Rietmeijer 1979) and may be as much as 2km (Smithson & Ramberg 1979).

Viewed on a broad scale (Figs. 3.2 and 3.3), the lower part of the Layered Series is dominated by plagioclase cumulates, the middle part by plagioclase-hypersthene-ilmenite cumulates and the upper part by plagioclase-hypersthene/pigeonite-augite-ilmenite-magnetite-apatite cumulates. Combined with the reversals to relatively primitive mineral assemblages at the bases of the MCUs, this is strong, first-order evidence that the Layered Series crystallised in a continuously fractionating, periodically replenished magma chamber. Replenishment events were few in number and widely spaced in time. The bulk composition of the magma occupying the chamber after each replenishment event can be judged by the relative volumes of the respective types of cumulate that constitute the successive macrocyclic units. In the lowermost units the cumulates represented are predominantly high-temperature varieties and the proportion of more-evolved cumulates generally increases in the upper units. This pattern suggests that the bulk composition of the magma occupying the chamber became progressively more evolved with time.The base of MCU IV seems to reflect the last major influx of magma into the BKSK chamber. This replenishment event appears to have involved a large volume of magma and was associated with very significant expansion of the chamber. The regressive layered sequences beneath the most-primitive leucotroctolitic cumulates in MCUs III and IV are up to 120m thick, showing that replenishment of the magma chamber must have taken place over a prolonged period of time. After the influx of magma reflected by the MCU III/IV transition, fractional crystallisation was apparently uninterrupted and we interpret the stratigraphic transition to mangerite, quartz mangerite and charnockite as reflecting progressive differentiation of the residual magma, probably containing a significant crustal component due to assimilation of country rocks and hybridisation with roof melts.

Fe-Ti oxides in the Bjerkreim-Sokndal intrusion

Ilmenite is an early-crystallising, almost ubiquitous mineral in the Bjerkreim-Sokndal intrusion. Substantial concentrations of ilmenite are restricted, however, to the regressive sequences that occur at the bases of the upper MCUs, especially units III and IV. Ilmenite and plagioclase-ilmenite cumulates are prominent in zone IVa in the axial region of the intrusion, and ilmenite-rich melanorites are found at the base of MCU III to the east of Teksevatnet. This relationship indicates that the generation of ilmenite-rich cumulates was related to replenishment of the Bjerkreim-Sokndal magma-chamber and was probably a consequence of turbulent mixing of the resident magma with inflowing more-primitive jotunitic magma.

Ilmenite exhibits a general decrease in hematite content through the Layered Series, from 16-20% in the lower part of the series where it is the only cumulus Fe-Ti oxide, to about 2% in the mangerite and quartz mangerite (Duchesne 1972a). This pattern is repeated on a smaller scale in the individual MCUs. Ilmenite contains about 0.3% V_2O_3 in the lower part of the Layered Series and shows an identical variation to hematite content. Manganese in ilmenite, however, increases almost continuously through the Layered Series, from about 0.3% MnO in leuconorites near the base to 1.0% MnO in mangerite; breaks in the trend at contacts between MCUs are slight. Nickel and chromium are enriched in ilmenite at the bases of MCUs where concentrations can be as high as 1000 ppm Ni and 1.4% Cr_2O_3.

Magnetite is a cumulus phase in the upper parts of MCUs IB, III and IV, in the TZ where it occurs in oxide-rich layers, and in the leuconorites and/or leucotroctolites near the bases of MCUs II, III and IV. Its TiO_2 content increases systematically from <2% in zone d of MCU III to as much as 19% (corresponding to $Usp_{58}Mt_{42}$) in the TZ. As with ilmenite, the Mn-concentrations increase (to ~0.25% MnO at the top of MCU IV) and vanadium decreases upwards through the Layered Series (from ~1.3% to 0.02% V_2O_3 at the top of MCU IV) (Duchesne 1972a). Magnetite in leucotroctolite at the base of MCU IV contains lower V concentrations (1.0-0.75% V_2O_3) than the magnetite in the uppermost part of MCU III and on its reappearance in the upper part of MCU IV, possibly due to the presence in the leucotroctolite of small amounts of amphibole that has a high partition coefficient for V (Jensen et al. 1993). Ni concentrations are generally low (< 40 ppm), except in the leucotroctolites at the bases of MCUs III and IV where concentrations are 900-600 ppm. Nickel decreases with stratigraphic height in the leucotroctolite at the base of MCU IV. Chromium exhibits the same behaviour as Ni, concentrations in the leucotroctolite at the base of MCU IV varying from 1.4-0.4% Cr_2O_3. Chromium contents in magnetite elsewhere in the BKSK are very low.

Parental magma

Fine to medium-grained, granular jotunites are present at several places along the steep, discordant northern margin of the BKSK. They occur along the outer margin of an up to 100m thick Marginal Series that separates cumulates belonging to MCU IA and IB and the high-grade gneisses of the metamorphic envelope (Fig. 3.1). The marginal jotunites are generally sparsely to markedly porphyritic and are considered to be chilled representatives of the magma that was parental to the oldest part of the Layered Series.
The jotunites are evolved basic rocks characterised by high FeO^t (11.1-12.9 wt%) and TiO_2, MgO in a narrow range between 3.8 and 5.0 and low CaO (5.4-6.7 wt%) (Fig. 3.4). They exhibit light REE-enriched chondrite-normalised rare-earth patterns with either a small positive Eu-anomaly or none at all, suggesting that previous fractionation or accumulation of plagioclase phenocrysts was very limited. Their compositions are similar to the jotunite trapped between anorthosite blocks enclosed within the plagioclase cumulates of MCU IB at Tjørn that likewise has been claimed to be representative of a parental magma (Duchesne & Hertogen 1988), and also to marginal jotunites of the Hidra Leuconorite (Duchesne et al. 1974).

The marginal jotunites have features that are consistent with a status as the parental magma for the cumulates of MCU IA and IB of the Layered Series of the BKSK. Textures show clearly that plagioclase was the first phase to crystallise from the jotunite magma and was followed by Ca-poor pyroxene and Fe-Ti oxides. The jotunites are rich in TiO_2 and poor in diopside components, compatible with the early crystallisation of cumulus ilmenite and the delayed appearance of cumulus Ca-rich pyroxene. The chemistry of the minerals in the jotunites is also comparable with the BKSK Layered Series: Plagioclases in the jotunites are slightly more sodic and the pyroxenes decidedly more iron-rich than the equivalent highest-temperature minerals in the BKSK cumulates. The presence of interstitial K-feldspar and quartz in the marginal rocks also demonstrates that the jotunite magma had the potential to produce a significant amount of an acid residual magma, as required by the presence of the granitoids at the top of the BKSK Layered Series.

Dry melting experiments on a jotunite collected from Tjørn show that such melts have plagioclase as the sole liquidus phase to ~7kb at temperatures of 1150-1165°C and oxygen fugacities of between FMQ-2 and FMQ-4 (Vander Auwera & Longhi 1994). Olivine, ilmenite and Ca-poor pyroxene (which crystallises together with olivine) appear successively at lower temperature within ~55°C of the liquidus at pressures up to ~5 kb. Allowing for the low oxygen fugacity in the melting experiments, which stabilises olivine relative to Ca-poor

pyroxene and suppresses magnetite saturation, and the lower TiO_2 of the experimental starting material (3.5wt. %) compared with the marginal jotunites, that reduces ilmenite saturation, the experimental crystallisation sequence of the jotunite at moderate pressure (5-7 kb) (plagioclase-hypersthene/olivine-ilmenite) is reasonably similar to that in the lower part of the BKSK Layered Series, that crystallised at 4-6 kb based on the contact-metamorphic mineral assemblages (Jansen et al. 1985).

TYPICAL MARGINAL JOTUNITE (B90)

SiO_2	49.8	Q	6.7
TiO_2	4.2	or	5.3
Al_2O_3	15.0	ab	20.3
FeO*	14.2	an	27.5
MgO	5.0	di	4.8
CaO	6.7	hy	26.1
Na_2O	2.4	mt	1.6
K_2O	0.9	il	8.0
P_2O_5	0.8	ap	1.8

Fig. 3.4. Major-element composition and CIPW norm of a typical chilled jotunite from the northern margin of the Bjerkreim-Sokndal Intrusion. From Robins et al. (1997).

Phase equilibria show that jotunitic magmas have compositions that reside on a thermal divide at pressures where they coexist with plagioclase and two pyroxenes and cannot be decendants of mantle-derived basalts (Longhi et al. 1999). They appear to have originated by melting of lower crustal gabbronorites. Recent investigations of the Re-Os systematics of the Rogaland Igneous Province (Schiellerup et al. 2000) also support a crustal origin.

Processes in the Bjerkreim-Sokndal magma chamber

Initial emplacement, subsequent replenishment and expansion

The distribution and contact relationships of the oldest cumulates in the Bjerkreim lobe of the BKSK indicate that the magma chamber during the earliest phases of its evolution was approximately wedge shaped and relatively limited in horizontal and vertical extent. It is probable that the initial development of the magma chamber was controlled by displacements along a normal fault, space being created by more pronounced subsidence of the hanging wall beneath the floor of the embryonic intrusion than the roof rocks. Thus the cumulates forming MCU 0-IB crystallised at the base of a chamber with the form of a half graben, the deepest part of the chamber being along its steep, fault-controlled, north-eastern margin.

The high frequency of anorthositic xenoliths in the early cumulates suggests that the margins of the early magma chamber were mainly composed of rocks belonging to the Egersund-Ogna anorthosite massif while part consisted of granulite-facies quartzofeldspathic and mafic gneisses. The incorporation of large numbers of blocks of anorthosite and

leuconorite suggests either that extensive stoping took place along the roof and walls of the chamber or that large numbers of xenoliths were transported into the chamber as it was filled.

During the early stages of evolution of the BKSK chamber there were at least two major episodes of magma recharge, represented by the bases of MCUs IA and IB. Each of these were followed by the crystallisation of exceptionally thick sequences of plagioclase-rich, zone a cumulates on the floor of the magma chamber. The cumulus plagioclase in MCUs IA and IB is distinctly more sodic (An_{46-39}) and the orthopyroxene has a lower mg# than in the succeeding units. Plagioclase is commonly antiperthitic and interstitial quartz and apatite occur in some of the plagioclase-rich cumulates, features that are uncommon in the higher-temperature cumulates elsewhere in the Bjerkreim lobe of the BKSK. These observations suggest that the early, plagioclase-rich cumulates may have crystallised from lower-temperature, more-differentiated magmas than both those emplaced later in the evolution of the magma chamber and those represented by the jotunite marginal chills. Systematic stratigraphic variations in the composition of plagioclase in these rocks are not conspiquous, despite their considerable thicknesses. These relatively evolved magmas emplaced early in the development of the BKSK must have had densities sufficiently low to permit the settling of leuconorite and anorthosite xenoliths and, by inference, also plagioclase primocrysts. The thicknesses of pC and piC, the inconspiquous cryptic variation and the presence of plagioclase and rarer orthopyroxene megacrysts in MCUs IA and IB suggest that the magmas may have been emplaced with significant amounts of crystals, particularly plagioclase, in suspension.

Crystallisation of the multiphase cumulates at the top of MCU IB was interrupted by emplacement of a voluminous batch of jotunite magma from which the cumulates of MCU II were formed. This influx of magma led to elevation of the roof and substantial lateral enlargement of the chamber. Stratigraphic relations show that the edge of the chamber was displaced by >6 km to the southeast and in the southern part of the Bjerkreim lobe cumulates belonging to MCU II are separated from the floor of the intrusion by only a thin marginal zone of plagioclase-rich rocks. The new stretch of floor produced during lateral enlargement of the chamber was not planar. An elevated ridge existed in the Teksvatnet area, and the MCU II sequence and later cumulates thin markedly over this topographic feature. The ~2m thick sequence of phiC that intervenes between the low-temperature cumulates (phci±m±aC**)** forming the uppermost part of MCU IB and the higher-temperature zone a cumulates in the lower part of MCU II indicates that the replenishment event was not instantaneous but persisted for a period of time. The regressive stratigraphic sequence that crystallised during the prolonged influx of magma was the result of mixing of some of the resident with the inflowing magma. Subsequent to replenishment, the magma chamber was occupied by a lens of liquid residing on a floor of earlier cumulates that dipped inwards at low angles to an axial depression. Continuous cooling and fractional crystallisation of the magma led to formation of a thick sequence of pimC and phiC (MCU II). The magma did not differentiate sufficiently to re-attain saturation in magnetite, Ca-rich pyroxene or apatite before the emplacement of a further batch of magma.

The replenishment event that terminated the crystallisation of MCU II resulted in a further expansion of the magma chamber similar to that accompanying the preceeding magma influx. Judging by the degree of cryptic layering in MCU III, the increase in the depth of the magma occupying the chamber was, however, much less than during the earlier influx and the extent of expansion of the chamber appears to have been more limited. Expansion of the chamber took place by lateral wedging of 1600-3000m towards the south. The edge of the magma chamber in the southernmost part of the Bjerkreim lobe advanced further into the Helleren anorthosite massif, and during this processes numerous blocks of anorthosite and leuconorite were incorporated into the magma chamber.

The final major replenishment event took place after the resident magma had undergone a degree of fractional crystallisation sufficient to stabilise first magnetite, then Ca-rich

pyroxene and apatite as liquidus minerals along the more distal (and higher) parts of the floor of the magma chamber while in the axial region of the magma chamber, magnetite-bearing noritic cumulates were still crystallising. This phase of magma influx appears to have been very voluminous and it resulted in a major lateral enlargement of the magma chamber to the south and the development of the Sokndal and Mydland lobes of the BKSK, where only the equivalents of cumulates belonging to MCU IV in the Bjerkreim lobe are represented. During the lateral migration of the edge of the magma chamber from its previous location near the present southern margin of the Bjerkreim lobe, myriads of large blocks and slabs of anorthositic rocks and quartzofeldspathic gneisses were stoped from the enlarging roof of the chamber. Whilst new, high-temperature magma flowed into the lowest part of the magma chamber, the less-dense residual magma was probably decanted southwards into the new Sokndal and Mydland lobes. This major replenishment was followed by almost continuous differentation that eventually led to the formation of mangeritic cumulates.

Duchesne and Wilmart (1997) have proposed that the crystallisation of mangerite was terminated by the emplacement of magmas that varied in composition from jotunite to charnockite. The thick uppermost unit of quartz mangerite and charnockite in the BKSK then crystallised from a viscous, inhomogeneous mixture of residual acid magmas and externally-derived, differentiated magma, possibly with additional admixture of anatectic melts derived from the gneisses that formed part of the roof of the magma chamber. In the Bjerkreim lobe of the intrusion there is, however, an uninterrupted cryptic variation from the TZ into the overlying granitoids, suggesting continued cooling and fractional crystallisation of residual magma.

Crustal contamination

The BKSK magma chamber was emplaced into quartzo-feldspathic and mafic gneisses as well as massif-type anorthosites. Xenoliths of these country rocks are enclosed in the BKSK cumulates and are exceptionally abundant in places. It is unlikely that the plagioclase-saturated BKSK magmas could have assimilated anorthositic rocks or dry mafic gneisses, but extensive interaction between the magmas occupying the chamber and xenoliths of quartzo-feldspathic gneiss seems very probable. In addition, the granitoids that form the uppermost part of the BKSK may have resulted in part from partial melting of gneisses that formed part of the roof of the magma chamber, and anatectic acid magmas may have mixed with the underlying more basic magmas occupying the bulk of the chamber.

The initial $^{87}Sr/^{86}Sr$ ratios (Sr_0) of cumulates in the Bjerkreim lobe vary substantially and provide robust evidence of extensive assimilation within the magma chamber. Sr_0 shows a general evolution with stratigraphic height in the Bjerkreim Layered Series from 0.705 in MCU II to 0.7086 in the upper part of MCU IV (zone e) (Fig. 3.5). The trend of increasing Sr_0 is interrupted by regressions to values as low as 0.7048 associated with the lower boundaries of MCU III and IV. With the exception of the uppermost part of the Layered Series there is a remarkable antipathetic relation between the cryptic variation as defined by the composition of cumulus minerals (An%, mg# in pyroxenes) and Sr_0.

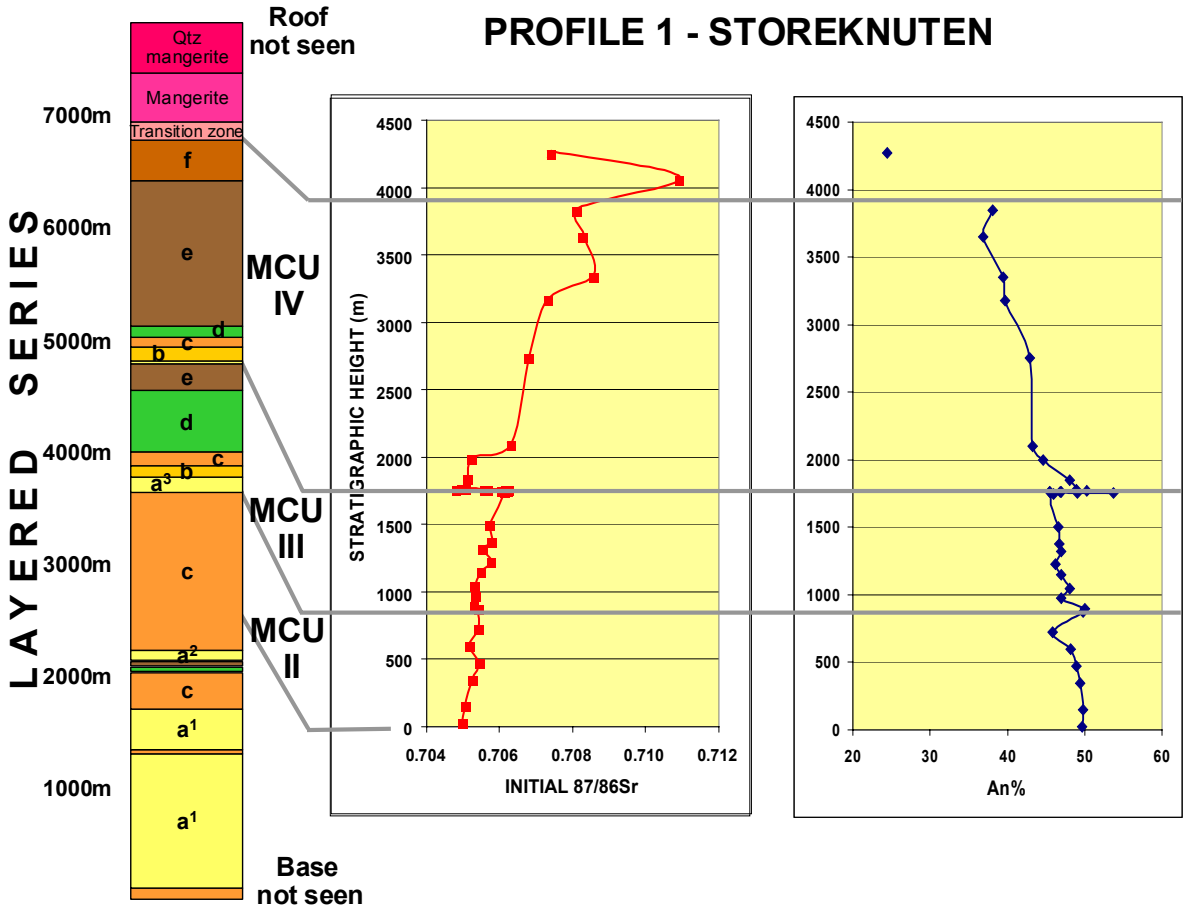

Fig. 3.5. Cryptic variation in plagioclase compositions and initial Sr^{87}/Sr^{86} for bulk-rock samples collected through the Layered Series in the southern flank of the Bjerkreim lobe (after Nielsen et al. 1996). The location of sample profile 1 is given in Fig. 1. The stratigraphic column to the left is for the Layered Series as developed in the axial region of the lobe. Note the pronounced cryptic regression associated with the MCU III/IV contact.

There is relatively little isotopic data for the granitoids that form the uppermost part of the BKSK, and certain aspects of it indicates disturbance of the Rb-Sr system. Wielens et al. (1980) calculated an isochron that gave an initial Sr isotope ratio of 0.7075±0.0028 on the basis of some of the data for these rocks reported by Versteeve (1975). Demaiffe et al. (1986) estimated Sr_0 for the quartz mangerite to be ~0.7085. Both of these values coincide with that in the upper part of MCU IV, eliminating earlier isotopic arguments for a separate origin of the granitoids, and in accord with an origin as residual, highly-differentiated magmas. Currently, there is no isotopic evidence that supports an origin for all or part of the quartz mangerites and charnockites exclusively through anatexis of country-rock gneiss. The $^{87}Sr/^{86}Sr$ ratios (at 930-920Ma) for the gneisses in the vicinty of the BKSK are extremely variable, but generally higher than that of the quartz mangerite (e.g. 0.7196 for gneisses in Gydalen, a short distance to the east of the margin of the BKSK (Versteeve 1975)). The variation in Sr_0 in the Bjerkreim Layered Series is open to interpretation in several different ways. Assimilation of country rocks (either in situ or as xenoliths) or incorporation of anatectic melts may have taken place continually during the cooling and fractional crystallisation of magma that was well-mixed on a chamber scale. Alternatively, the degree of contamination may have increased towards the chamber roof in a stratified magma, due to assimilation of increasing numbers of buoyant xenoliths in the upper parts of the magma chamber or variable amounts of physical mixing with a separate, low-density, anatectic roof melt. Additionally, a contaminated isotopic signature may have diffused from the roof downward through a stratified magma column (see below). In view of the evidence in the

BKSK for magma stratification during at least part of the evolution of the chamber, it would seem likely that some or all of these processes were operating during the crystallisation of the cumulates at the base of the magma chamber. Assuming simultaneous assimilation and fractional crystallisation (AFC), the available Sr isotope data are consistent with a ratio between the rates of assimilation and fractional crystallisation of ~0.2 (Tegner et al. 2000).

Compositional stratification of the magma chamber

Several features of the stratigraphic organisation of the cumulates in the Bjerkreim lobe of the BKSK indicate that the magma from which they crystallised was compositionally stratified and that the density stratification was stable over substantial periods of time.

Detailed mapping of phase contacts has demonstrated that the zone a cumulates at the base of MCUs IB and II thin dramatically as they are traced from the north-eastern margin of the intrusion to the south-west, and both zones eventually pinch out within ilmenite norites. These plagioclase-rich cumulates must be contemporaneous with the lower-temperature cumulates into which they pass along the strike of the modal layering towards the margins of the intrusion. The zone a cumulates at the base of MCUs III and IV exhibit a similar geometrical relationship: They are thickest in the axial region of the intrusion but thin towards both margins, and wedge out completely to the east towards the Teksvatnet ridge. The converse relationship is apparent in the uppermost part of MCU III, where the lowest-temperature cumulates (phcimaC) occur in the more marginal parts of the unit but are absent in the axial region of the Bjerkreim lobe where the basal cumulates of MCU IV rest on higher-temperature phimC. These stratigraphic relationships suggest gradients in magma composition and temperature across the floor of the chamber during fractional crystallisation. We suggest that the magma occupying the chamber was stably stratified with density and temperature decreasing and the degree of magma differentiation increasing upwards through the column of magma, while the cumulate-melt interface was sloping, either uniformly towards the north-east margin of the chamber (during the crystallisation of MCU IB) or generally inwards towards the axis of the chamber (during the crystallisation of MCU III). An exception to this generalisation is the ridge in the chamber floor represented near Teksevatnet that existed during the crystallisation of MCU II and later units. The cumulates of MCU II-IV thin over this feature and certain zones wedge out eastwards towards it (e.g. zone IIIb). Evidently, at the stage in the accumulation of the Layered Series represented by MCUs II and III, higher-temperature cumulates were forming in the adjacent basins than on the ridge itself. During the crystallisation of MCU IV, the Teksevatnet topographic high appears to have been largely eliminated.

The angles of 2-15° that exist between certain of the phase contacts and the boundaries between the megacyclic units in the Bjerkreim lobe provide a reasonable minimum estimate of the original slopes of the temporary floor of the magma chamber beneath a stratified magma. The fact that discordances between cryptic and modal layering exist both near the base and the top of MCU III suggest that magma stratification was extremely stable. It persisted for at least as long a period of time as the up to 1050m-thick megacyclic unit took to crystallise.

Whether the column of stratified magma in the BKSK chamber was divided into horizontal liquid layers separated by diffusive interfaces is not clear from field relations. A continuously-stratified magma excludes convective mixing. There is, however, clear evidence within the cumulates of the BKSK for convection during their crystallisation, including cross-lamination, erosional unconformities and troughs. We therefore suggest that the magma was discontinuously stratified, and consisted of horizontal, independantly-convecting and internally homogeneous liquid layers separated by relatively-sharp, diffusive interfaces. Several processes that appear to have operated in the BKSK magma chamber could have led to the development of stratification: Entrainment of resident magma and hybridisation in

turbulent fountains during the emplacement of new, less-differentiated and denser magma (Campbell 1996); Repeated emplacement of hot, dense magma along the floor of the chamber, with little mixing with the overlying resident magma (Huppert & Sparks 1980); Varying degrees of mixing between the resident magma and anatectic melts generated along the inclined walls and roof of the magma chamber or assimilation of varying amounts of buoyant wall-rock xenoliths (Campbell & Turner 1987); Compositional convection driven by density differences arising from crystallisation along inclined surfaces (McBirney et al. 1985).

Hydridisation

The cryptic variation in mineral chemistry and particularly in initial Sr, Nd and Pb isotope ratios exhibited by a section through the sequence of zone a cumulates above the base of MCU IV (see Figs. I.2.7 & 8 in the description of excursion localities) suggests that the final influx of magma into the Bjerkreim-Sokndal chamber was prolonged and associated with the elevation of the differentiated, contaminated and compositionally-zoned column of resident magma (see Fig. I.2.9 in the description of excursion localities) as well as hybridisation of the inflowing and resident magmas (Jensen et al. 1993; Barling et al. 2000). This resulted in a modal regression from phcmiaC to phiC/piC and culminated in the crystallisation of high-temperature, plagioclase (An_{53})-olivine (Fo_{74}) cumulates. The modal regression is accompanied by a reverse cryptic variation in mineral compositions and a systematic variation in initial isotopic ratios (e.g. a steady upward decrease in $^{87}Sr/^{86}Sr$ from 0.7061 to 0.7048), demonstrating that the cumulates crystallised from hybrid magmas with an increasing proportion of the inflowing, more primitive jotunite. Recharge of the magma chamber took place after prolonged fractional crystallisation of magnetite and consequent decrease in the density of the resident magma. Hybridisation is envisaged as taking place in a turbulent fountain with the efficiency of hybridisation of the inflowing magma with the less-dense resident magma decreasing with time.

In contrast, differentiation of the resident magma was arrested at a relatively early stage by the influx of magma marked by the MCU II/III contact. MCU II consists exclusively of a thin basal sequence of plagioclase cumulates and a thick series of phiC. Cumulus magnetite does not make an appearance in MCU II, and it is likely that the resident magma was differentiating with increasing density during its crystallisation. The MCU II/III boundary is characterised by a sulphide-enriched subzone associated with a discontinuous layer of orthopyroxenite or mafic ilmenite norite. This is succeeded by a general regression in mineral compositions that culminates in the zone IIIb troctolitic cumulates in the central and western part of the Bjerkreim lobe. Zone b cumulates are, however, absent in the eastern flank.

The stratigraphic relations appear to be consistent with prolonged magma-chamber recharge associated with progressive mixing of the inflowing jotunitic magma and the resident, stratified magma whose basal portion was more dense than the replenishing magma. The sulphide-enriched orthopyroxenite and related melanocratic ilmenite norite that represent the initial response to the replenishment event are explained by crystallisation of hybrid magmas residing in the pyroxene phase volume. Their chamber-wide distribution is inferred to result from mixing taking place some distance above the floor at a level where the plume formed by the inflowing magma reached a level of neutral buoyancy in the compositionally-stratified magma column and then spread laterally throughout the chamber (Fig. 3.6). As the influx proceeded the resident magma was stripped from the base of the chamber and mixed into the ascending plume as the hybrid layer increased in thickness and became compositionally stratified. Eventually the lower boundary of the hybrid layer reached the floor of the magma chamber. The highest-temperature cumulates (poC, zone IIIb) crystallised from the lowest part of this hybrid layer and were restricted to the central trough on the chamber floor (corresponding to the axial region of the intrusion), while lower-temperature cumulates crystallised simultaneously on the eastern “shelf” from magma higher up in the hybrid layer.

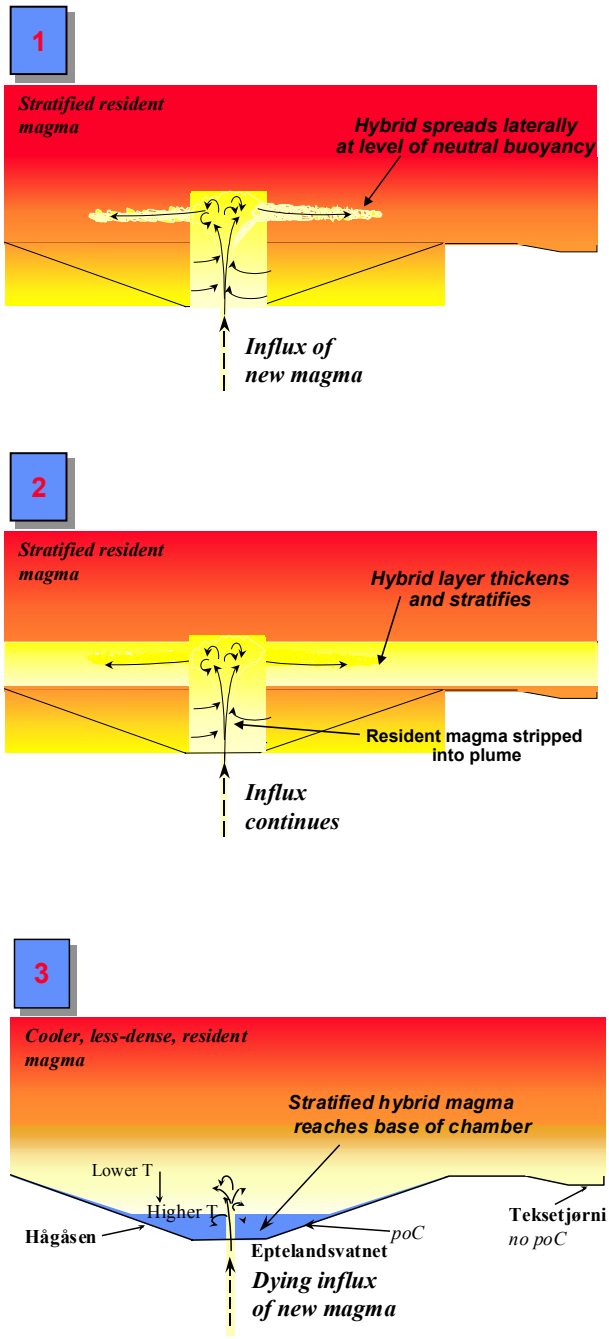

Fig. 3.6. The sequence of events during the influx of magma reflected by zones IIIa and IIIb depicted in schematic W-E sections: A) Magma flowed in as a turbulent plume and the hybrid spread laterally some distance above the floor of the chamber; B) The hybrid layer thickened and stratified and its lower boundary sank as resident, denser magma beneath was mixed into the plume. Crystallisation in the hybrid layer resulted in the sulphide-bearing orthopyroxenite and equivalents. C) The stratified hybrid layer reached the floor of the chamber. Troctolite (zone b) crystallised in the axial trough while more evolved cumulates formed on the eastern shelf.

***

Chapter 4

THE JOTUNITIC AND THE ACIDIC IGNEOUS ROCKS

(by J. Vander Auwera, O. Bolle and J.C. Duchesne)

The Jotunite suite

Proterozoic massif anorthosites are usually associated with variable amounts of a characteristic suite of intermediate rocks. The least evolved rocks of this suite are enriched in mafic minerals (low- and high-Ca pyroxenes, Fe-Ti oxides, apatite), and in some cases very high concentrations of these phases give rise to hypermelanic rocks. Different names including ferrodiorite, monzonorite, jotunite, Fe-Ti-P-rich rocks (FTP) or oxide-apatite gabbronorite have been used; however, Vander Auwera et al. (1998) referred to them by the collective term of jotunite (Fe-Ti-P-rich hypersthene monzodiorite). Evolved rocks of the suite include mangerite (hypersthene monzonite), quartz mangerite (hypersthene quartz monzonite) and charnockite (hypersthene granite). Vander Auwera et al. (1998) accordingly referred to the suite as a whole as the jotunite suite.

The origin of jotunites has been the subject of considerable debate, despite their similar textural and geochemical characteristics from one anorthosite complex to another. Several hypotheses, not mutually exclusive, have been proposed: (1) jotunites are residual liquids after anorthosite crystallization (Emslie 1978, Morse 1982, Wiebe 1992, Ashwal 1993, Emslie et al. 1994) (evolved jotunites: Vander Auwera et al. 1998); (2) jotunites are the parental magmas of the andesine anorthosite suite (Duchesne et al. 1974; Duchesne & Demaiffe 1978; Demaiffe & Hertogen 1981) (primitive jotunites: Vander Auwera et al. 1998); (3) jotunites are products of partial melting of the lower crust with necessary heat produced by anorthosite emplacement (Duchesne et al. 1985b; 1989; Duchesne 1990); (4) jotunites are transitional rocks in a comagmatic sequence from anorthosite to mangerite (Wilmart et al. 1989; Owens et al. 1993; Mitchell et al. 1996; Duchesne & Wilmart 1997); (5) jotunites are derived by fractionation of mafic magmas unrelated to the anorthositic suite (Emslie 1978; 1985); (6) jotunites are immiscible liquids conjugate to mangerites (Philpotts 1981); (7) primitive jotunites are produced by partial melting of a lower crustal gabbronoritic source (Longhi et al. 1999) and are parent magmas of the andesine anorthosites (Vander Auwera et al. 1998).

In the Rogaland intrusive complex (Fig. 1.3) (Michot 1960; Michot & Michot 1969), jotunitic rocks and the products of their differentiation are particularly abundant compared to the other anorthositic provinces. Jotunitic rocks mainly occur in a system of dykes and small intrusions (Duchesne et al. 1985a; 1989). Some dykes are petrographically homogeneous along strike, such as the Varberg dyke (jotunitic), the Vaersland and Ørsland dykes (quartz mangerite) and the Vettaland dyke (antiperthite norite). Others show a variation of composition along strike, such as the Lomland dyke (from norite to mangerite), the Tellnes dyke (from jotunite to charnockite), and the Håland dyke (from norite to quartz mangerite).

The Rogaland jotunites, first briefly described by Michot (1960), were extensively studied by Duchesne, Demaiffe and coworkers in several papers reviewed by Duchesne (1990). Jotunites are typically medium-grained and contain plagioclase (usually antiperthitic), some perthitic to mesoperthitic (in the evolved facies) K-feldspar, poikilitic inverted pigeonite, augite, Fe-Ti oxides, apatite, and quartz in the evolved facies (Duchesne 1990). They occur mostly as dykes crosscutting massif-type anorthosites (Fig. 1.3) but those that have been dated have similar absolute ages in the range close to 930 Ma (Schärer et al. 1996). Among them, the Tellnes dyke in the Åna-Sira massif as well as the Varberg and Lomland dykes in the EGOG massif (Fig. 1 3) have been studied in most detail (Duchesne et al. 1985a; Wilmart et al. 1989). The Tellnes dyke varies continuously from jotunitic to charnockitic lithologies. It has a well-defined Rb-Sr whole rock isochron giving the same age as the U-Pb

zircon age and its compositional variation can be explained not by mixing but by a process of fractional crystallization without progressive contamination (Wilmart et al. 1989). Modelling of the fractional crystallization process was achieved in two steps by least square calculation, the mineral compositions of the subtracted assemblages being constrained by Ford et al. (1983) of the olivine composition and for the coexisting minerals by considering the relevant cumulus mineral associations in the BKSK Layered Series.

Whole-rock Rb-Sr isotopic data from other dykes such as Lomland do not fit tightly to isochrons and there is considerable variation in I_{Sr} from dyke to dyke (0.704 - 0.710) that does not correlate with other geochemical parameters (Demaiffe et al. 1986, Duchesne et al. 1989). There is also distinct trace element signatures from dyke to dyke: for the same major element contents, significant variations in REE, Zr, Ba and Rb are observed (Duchesne et al. 1989; Bolle 1996). Taken together these data suggest sources with variable mineralogy and degrees of contamination and of melting.

Jotunites also form small intrusions (Fig. 1.3) (e.g. Eia-Rekefjord), mingling facies (e.g. in the southern part of the Apophysis of BKSK: Demaiffe 1972; Wiebe 1984; Bolle 1998), as well as chilled margins to the Hidra and Garsaknatt leuconoritic bodies (Demaiffe & Hertogen 1981) and, locally, to the BKSK layered intrusion (Duchesne & Hertogen 1988; Wilson et al. 1996, Robins et al. 1997). One of these chilled margins, the Tjörn facies (sample 80123a of Duchesne & Hertogen 1988), has been studied experimentally (Vander Auwera & Longhi 1994) and it has been shown that, in this composition, the near liquidus assemblages are plagioclase (An_{49}) + olivine (Fo_{64}) at 5 kb and plagioclase (An_{47}) + low-Ca pyroxene (En_{66}) at 7 kb. Clearly the succession of cumulate rocks in the BKSK intrusion can be reasonably accounted for by fractional crystallization ca. 5 kb of a melt similar to the Tjörn chilled liquid, but slightly more An-rich and with a somewhat larger MgO/FeO ratio.

A liquid line of descent (LLD)

Among the Rogaland jotunites, the least differentiated compositions (high MgO, low K_2O) correspond to the chilled margins and, in most variation diagrams (Fig. 4.1), they form a group distinct from the jotunites of the dyke system (Duchesne 1990). Vander Auwera et al. (1998) referred to the chilled margin samples as *primitive* jotunites and to the least differentiated samples of the dyke trend as *evolved* jotunites. Using experimental data, these authors showed that the gap between primitive and evolved jotunites only results from a lack of exposure of an early fractionation stage which probably took place below the intrusion level of dykes. Indeed, in variation diagrams, the gap between the primitive and evolved jotunites is filled by experimental liquids residual to the Tjörn primitive jotunite (Vander Auwera & Longhi 1994). Combined experimental and geochemical data have thus enabled these authors to define a complete liquid line of descent (LLD) ranging from primitive jotunites to evolved jotunites and then to charnockites. Modelling of this LLD supports the hypothesis that extensive fractionation of primitive jotunites produces quartz mangerites with REE concentrations in the range of jotunites, strong depletions in U, Th, Sr, Ti, P and smaller to no relative depletions in Hf and Zr. Moreover, experimental and petrographic data indicate that the FTP rocks represent accumulations of a dense oxide-apatite-pigeonite assemblage into coexisting multisaturated jotunitic to mangeritic liquids.

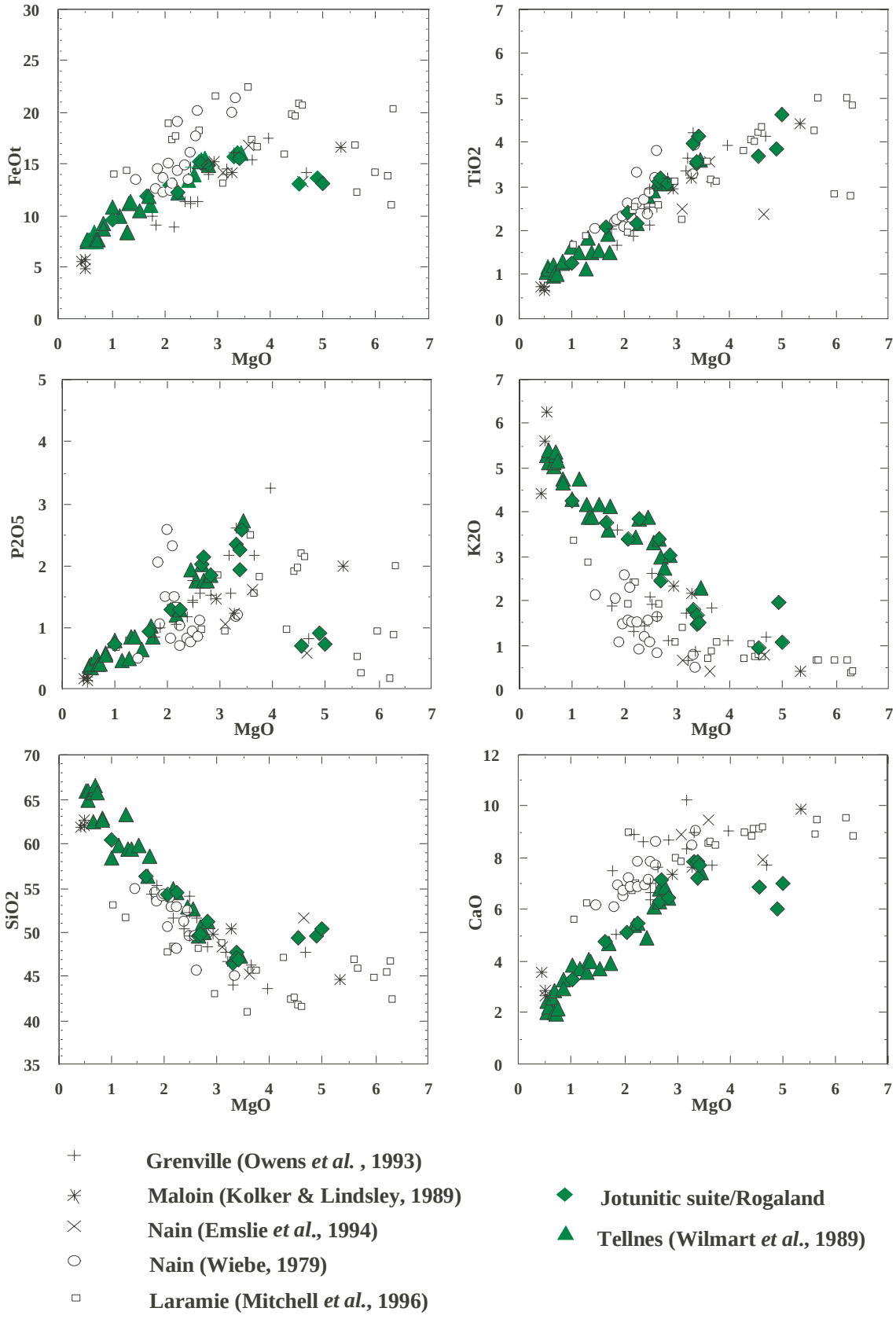

Fig. 4.1 Major element variation diagrams of the jotunitic suite (after Vander Auwera et al. 1998). Data from fine-grained samples (chills), from the Tellnes dike (Wilmart 1988; Wilmart *et al.* 1989) and from other localities {Grenville Province, Quebec: Owens et al. (1993); Laramie: Kolker & Lindsley (1989); Mitchell et al. (1996); Nain: Wiebe (1979); Emslie et al. (1994)} are shown for comparison.

In conclusion, the Rogaland jotunitic-charnockitic trend is the latter part of a multi-stage process of polybaric fractional crystallization, crystal accumulation, and probably flow differentiation within dykes. The early stage of fractionation passing from primitive jotunite to evolved jotunitic melts is not displayed in the dyke system. It probably took place in a chamber several kilometers below the intrusion level of dykes to produce andesine anorthosites and layered rocks. The jotunitic dykes ranging in composition from evolved jotunites to quartz mangerites or charnockites were also probably spawned by fractionation either within a deeply seated anorthositic intrusion or in a layered mafic body, such as the BKSK intrusion.

Crustal origin of the primitive jotunite

Experimental data on the liquidus equilibria in the range of 1 bar to 13 kbar relevant to the anorthosite petrogenesis have brought new constraints on the nature of the source rocks of the jotunite parental magmas (Longhi et al. 1999). Between 10 and 13 kbar, i.e. the pressure conditions of a deep-seated magma chamber where Al-rich megaopx coexist with plagioclase, the phase diagram shows a thermal barrier and the Tjörn jotunite sits close to that barrier. Consequently, the primitive jotunite cannot be derived by fractionation of melt of an olivine-dominated mantle and can only be produced by melting of a source rock whose composition lies on the barrier, i.e. a gabbronoritic rock, which cannot be a mantle rock.

These experiments have constrained the composition of the source rocks. Mafic granulites - a major component of the lower crust - have adequate average compositions, although they greatly vary between different tectonic provinces (Rudnick & Fountain 1995). The best candidates are layered intrusions of basaltic kindred such as the Stillwater Complex which have higher mg-numbers than average lower crust.

Because of the thermal barrier at high pressure, mixing with silica-rich (crustal) material has no effect on the major element chemistry of basaltic liquids. Whatever the amount of mixing, these liquids are inexorably brought back to the ol+opx cotectic by decreasing temperature and forced to follow it. Crustal contamination of a basaltic magma in a deep-seated magma chamber is thus possible, especially at the radiogenic isotope level, but fractionation does not lead to silica-rich liquids.

The acidic igneous rocks

Another main component of the AMCG suite are acidic rocks. They also occur in the Rogaland anorthosite province. They are found in the upper part of the BKSK layered intrusion, in the Apophysis and in the Farsundite body as well as in the small Breimyrknuten charnockite. The Lyngdal granodiorite, formerly considered as belonging to the anorthosite province (Falkum 1966; Pasteels et al. 1970), is nowadays preferably connected to the post-collisional plutonism related to the Mandal Line. The granodiorite contains no opx but hornblende + biotite + titanite and resembles the Svofjell granite, one of the Mandal Line largest pluton (Vander Auwera et al. 1999; Bogaerts et al. 2001; Vander Auwera et al. 2001).

The BKSK upper part: C-type magmas

The upper part of the BKSK intrusion comprises mangerite, quartz mangerite and charnockite (Duchesne & Wilmart 1997)(Table 4.1). They form a suite of K_2O-rich alkali-calcic granitoids. Their high fe-# and HFSE contents give them A-type affinities. The agpaicity index varies between 0.87 and 0.94, thus the suite is not peralkaline but can be considered as alkaline (Liégeois & Black 1987; Maniar & Piccoli 1989). The high abundance in K_2O, TiO_2, P_2O_5 and low CaO are typical of C-type magmas (Kilpatrick & Ellis 1992).

Mangerites lie stratigraphically above the Layered Series defined by Wilson et al. (1996) (see Figs. 3.1 and 3.2), more precisely above the transition zone marked by the appearance of a ferrous olivine in the cumulus minerals (Michot 1960; 1965; Duchesne et al. 1987b). Geochemically they display evidence of mesoperthite accumulation (large Eu positive anomaly, high Ba contents, low Zr contents) and must be assimilated to cumulates, capping the MCU IV and the transition zone (see Fig. I 3.3). Quartz mangerites and charnockites form the top of the intrusion and its most central part. They are coarse-grained and massive, with a faint foliation, hardly visible in the field, but clearly unravelled by anisotropy measurement of magnetic susceptibility (Bolle et al. 2000).

The petrogenesis of this rock suite has long been debated. Michot (1960; 1965) considered they were produced by fractional crystallization together with the underlying anorthosites, leuconorites and norites, thus giving strong evidence of a continuous evolution from anorthosite to quartz mangerites. This concept was however questioned when isotopic evidence of contamination by crustal material became available (see the review by Demaiffe et al. 1986). Moreover the Layered Series was shown to result from repeated influxes of magma (Duchesne 1972; Nielsen & Wilson 1991) and assimilation was recognized as a constantly operating mechanism during fractional crystallization, the contaminant being anatectic melts from country rock gneisses at the roof of the intrusion (Nielsen et al. 1996). The granitoid rocks from the upper part were therefore considered either as the contaminated residual liquid of the cumulate pile (Nielsen et al. 1996) or, following a suggestion of Wiebe (1984), as the melted roof itself.

Detailed work in the Ørsland area (see Itinerary 3) has suggested another scenario (Duchesne & Wilmart 1997): the transition from mangerite cumulates to quartz mangerites takes place in a zone of enclaves crowded with jotunite microgranular enclaves, pods and rafts of leucogranitic material and countless gneiss xenoliths. This zone was identified by Michot (1960; 1965) as a discontinuous " xenolithic septum " at the same level of the stratigraphic column. This enclave zone also marks a discontinuity in the evolution (Duchesne & Wilmart 1997): the quartz mangerites above that zone were less evolved than the liquid in equilibrium with the underlying mangerite cumulates (Figs. I 3.2 and I 3.3). The later (the resident liquids) were swept by several magmas and particularly by a new influx of less evolved magma.

Two series of liquids

Petrography and geochemistry permit to divide the granitoids into two distinct series: the main LLD (fe# close to 0.85), which passes from jotunites through 2-pyroxene quartz mangerites to amphibole charnockites, and the olivine trend (fe#= 0.94), which encompasses olivine-bearing quartz mangerites and charnockites and is rooted into mangeritic liquids. Both series are intimately mixed in the field. They evolve through fractional crystallization with assimilation of a crustal leucogranitic component, which has been identified in fine-grained leucogranitic enclaves, particularly abundant in the uppermost part of the massif, close to the now eroded roof. These enclaves display very irregular shape with long dyke-like fingers (Photo I 3.1). Curiously they have a very peculiar geochemical signature: they are strongly depleted in incompatible elements, namely REE except Eu, which shows a huge positive anomaly. Similar characteristics have been described in leucosomes from migmatites (Barbey et al. 1989; Sawyer 1991; Fourcade et al. 1992; Vander Auwera 1993), which corroborates the origin of these enclaves as migmatitic melts from the envelope.

The main LLD is similar in major elements to the Tellnes evolution up to the charnockites. Then due to a higher water activity of 0.3, it moves to amphibole charnockites representing a granitic eutectic with higher SiO_2 content (Wendlandt 1981; Ebadi & Johannes 1991). Some trace elements are however quite different than in the Tellnes trend. Rb, Cs and Th increase much quicker here, and zircon saturates at 60-62% SiO_2, earlier than in the Tellnes trend. These differences are possibly related to the higher water fugacity and/or to the

assimilation process. The olivine trend displays an evolution similar to that of the main LLD, with also contamination by the same leucogranitic material. Nothing can preclude the hypothesis that they were produced by the evolution of the resident magma in equilibrium with the mangerite cumulates. They also contain olivine and their fe# matches the expected values at equilibrium.

Zircons from both rock series reveal complex structures (Duchesne et al. 1987a). U-mapping unravels U-rich cores or U-poor cores rimmed by a U-rich envelope, both within U-poor outer shells. This points to hybridization processes and/or heritage from the source rock.

In the major replenishment event taking place before complete crystallization of the mangerite cumulates, the resident magma was brought in close contact with the incoming magma and partly mixed with it while preserving olivine-bearing rocks at places. The incoming magma was more evolved than the jotunitic influx at the basis of each macrocyclic unit. The main LLD points to a same jotunitic kindred, but its provenance is not known. The Apophysis has been suggested as a possible feeder conduit, where a similar range of rocks is represented and in which mingling of magmas is conspicuous (Duchesne et al. 1987a; Bolle 1998).

The Apophysis

In the Apophysis southern part, as e.g. near Fidsel (see Itinerary 4), mingling and mixing relationships between a primitive jotunitic magma (similar to the Hidra chilled margin) and a mangeritic melt are conspicuous (Duchesne 1989; Bolle, 1998). In the northern part of the Apophysis, detailed mapping (Bolle 1996; 1998) has shown that the (quartz) mangeritic magma is dominating and contains a network of elongated lenses made up of mafic-rich jotunite that represents FTP facies. The contact zone between the Åna-Sira massif and the envelope was therefore swept by various magmas. Moreover, these magmas have cut across the noritic to mangeritic cumulates of the Mydland lobe, confirming an intrusive event posterior to the cumulate formation.

Interestingly the Apophysis (quartz) mangeritic magma defines a short trend, from 58 to 66.5% SiO_2, plotting in many variation diagrams close or in between the main LLD and the olivine-trend defined in the upper part of BKSK. Is this an indication that rather than a feeder conduit, the Apophysis could have acted as an escape conduit for the two acidic magmas mingled at the top of the BKSK, the Apophysis (quartz) mangeritic magma resulting from the complete mixing of part of the other two? Actually, the intermediate geochemical character of the Apophysis (quartz) mangeritic magma compared to both trends defined in the BKSK acidic rocks is not so systematic, and, moreover, preliminary Sr-Nd isotope data obtained on quartz mangerites from the BKSK and the Apophysis (Bolle et al. in prep.) preclude that the latter may have formed by mixing of the former without simultaneous, unsupported, crustal contamination. The Apophysis (quartz) mangerite is therefore best seen as resulting from the crystallization of a third acidic magma, preferentially intruded along the eastern contact of the Åna-Sira massif.

Table 4.1 Average composition of various petrographic facies in BKSK and its Apophysis (after Duchesne & Wilmart, 1997; Bolle, 1998). AC: amphibole charnockite; OC: olivine charnockite; PQM: 2-pyroxene quartz mangerite; OQM: olivine quartz mangerite; PM: 2-pyroxene mangerite; j: jotunite.

	BKSK AC		**BKSK OC**		**BKSK PQM**		**BKSK OQM**		**Apophysis PM**		**Apophysis PQM**		**North Apophysis J (FTP facies)**		**South Apophyse J (enclaves)**	
	M (n = 14)	**σ**	**M (n = 17)**	**σ**	**M (n = 15)**	**σ**	**M (n = 8)**	**σ**	**M (n = 8)**	**σ**	**M (n = 36)**	**σ**	**M (n = 7)**	**σ**	**M (n = 7)**	**σ**
SiO2	71.24	*2.52*	68.03	*1.18*	63.82	*2.04*	63.57	*1.64*	58.37	*0.49*	62.67	*1.80*	47.97	*2.86*	52.34	*1.02*
TiO2	0.47	*0.20*	0.61	*0.08*	1.19	*0.26*	0.85	*0.11*	1.29	*0.11*	0.97	*0.17*	3.30	*0.50*	3.19	*0.23*
Al2O3	12.94	*0.42*	13.39	*0.39*	13.79	*0.50*	14.24	*0.75*	15.92	*0.66*	15.27	*0.57*	11.93	*0.96*	13.80	*0.61*
Fe2O3	1.80	*0.43*	2.26	*0.37*	1.95	*0.55*	2.23	*0.46*	2.92	*0.50*	2.12	*0.53*	4.25	*0.77*	2.63	*0.77*
FeO	2.67	*1.02*	3.97	*0.42*	5.84	*1.31*	5.82	*0.65*	6.79	*0.66*	5.58	*0.80*	14.15	*1.97*	10.81	*0.51*
MnO	0.08	*0.05*	0.11	*0.05*	0.14	*0.04*	0.14	*0.04*	0.17	*0.01*	0.13	*0.03*	0.30	*0.03*	0.18	*0.02*
MgO	0.43	*0.14*	0.32	*0.14*	1.13	*0.31*	0.44	*0.10*	0.87	*0.20*	0.69	*0.22*	3.04	*0.50*	3.86	*0.46*
CaO	1.20	*0.33*	1.63	*0.24*	2.76	*0.48*	2.49	*0.31*	3.72	*0.18*	2.78	*0.39*	7.37	*0.60*	6.01	*0.27*
Na2O	3.87	*0.28*	4.05	*0.17*	4.14	*0.24*	4.51	*0.27*	5.05	*0.28*	4.80	*0.41*	3.42	*0.30*	4.14	*0.19*
K2O	5.26	*0.19*	5.50	*0.16*	4.81	*0.22*	5.47	*0.12*	4.51	*0.15*	4.81	*0.23*	1.82	*0.38*	2.20	*0.20*
P2O5	0.11	*0.05*	0.13	*0.04*	0.45	*0.12*	0.20	*0.05*	0.35	*0.05*	0.30	*0.06*	2.10	*0.45*	1.13	*0.09*
Total	100.07	*0.52*	100.00	*0.64*	100.02	*0.56*	99.95	*0.34*	99.97	*0.43*	100.13	*0.53*	99.66	*0.52*	100.44	*0.25*
FeO/FeO+MgO	0.86	*0.03*	0.93	*0.03*	0.84	*0.02*	0.93	*0.01*	0.89	*0.02*	0.89	*0.03*	0.82	*0.02*	0.74	*0.03*
U	1.67	*0.81*	1.07	*0.35*	1.08	*0.38*	0.84	*0.31*	0.68	*0.08*	0.86	*0.28*	0.63	*0.13*	0.90	*0.16*
Th	4.49	*2.62*	2.94	*1.74*	3.01	*0.93*	2.86	*2.75*	1.14	*0.31*	1.76	*1.33*	2.15	*0.73*	2.65	*0.90*
Pb	24.7	*8.2*	20.3	*4.0*	22.5	*2.7*	19.4	*7.5*	17.2	*5.5*	19.9	*3.7*	9.72	*3.13*		
Zr	566	*190*	785	*79*	857	*149*	760	*187*	1141	*178*	1030	*151*	520	*173*	379	*52*
Hf	15.2	*4.7*	19.6	*2.0*	23.2	*4.8*	18.9	*4.8*	26.1	*3.8*	26.2	*3.4*	11.6	*3.8*	10.7	*1.4*
Nb	21.3	*9.3*	28.3	*5.3*	32.3	*6.2*	30.3	*4.7*	20.3	*6.2*	24.3	*6.7*	37.5	*7.2*		
Ta	1.19	*0.45*	1.64	*0.26*	2.01	*0.38*	1.88	*0.36*	1.11	*0.25*	1.34	*0.32*	2.13	*0.41*	1.48	*0.20*
Th/U	2.5	*0.5*	2.6	*0.8*	2.9	*0.6*	3.0	*1.7*	1.7	*0.4*	2.0	*0.6*	3.4	*0.7*	2.9	*0.6*
Zr/Hf	35.9	*5.3*	41.0	*5.0*	37.3	*4.4*	40.3	*3.4*	44.5	*3.0*	39.5	*4.4*	44.8	*3.8*	35.2	*4.1*
Nb/Ta	17.8	*4.0*	17.6	*1.9*	16.1	*1.4*	16.2	*1.1*	18.6	*3.4*	17.8	*1.9*	17.7	*1.9*		
Rb	152	*29*	135	*10*	103	*19*	117	*9*	59.8	*8.9*	84.2	*13.8*	24.3	*6.0*	28.0	*9.3*
Cs	0.42	*0.22*	0.26	*0.06*	0.26	*0.13*	0.23	*0.08*	0.27	*0.10*	0.25	*0.09*	0.17	*0.08*		
Sr	90.7	*21.3*	80.4	*9.7*	177	*33*	110	*15*	257	*24*	190	*26*	359	*37*	359	*17*
Ba	639	*169*	741	*77*	831	*109*	1057	*142*	1642	*190*	1324	*128*	891	*167*	738	*56*
K/Rb	295	*47*	340	*24*	396	*61*	389	*35*	641	*84*	484	*70*	623	*53*	709	*212*
K/Ba	73.3	*22.6*	62.3	*6.7*	49.0	*8.0*	43.5	*5.6*	23.3	*3.3*	30.5	*4.0*	16.7	*1.4*	24.8	*1.6*
Sc	6.95	*2.27*	10.2	*1.0*	13.0	*2.5*	15.3	*1.8*							20.8	*1.4*
V					39.2	*10.8*			25.9	*4.9*	20.7	*4.1*	81.0	*24.2*	156	*16*
Cr					10.9	*6.4*										
Co	3.12	*1.09*	2.83	*0.32*	9.93	*2.24*	3.82	*0.35*	9.52	*1.80*	8.10	*1.27*	31.0	*4.6*	40.4	*3.8*
Ni					4.09	*1.66*										
Zn	92.5	*30.2*	121	*17*	144	*25*	147	*54*	173	*21*	146	*21*	295	*24*	152	*14*
Ga	27.0	*2.5*			28.0	*1.7*			26.5	*0.8*	27.1	*1.5*	26.6	*1.0*		
La	50.5	*20.6*	48.2	*11.8*	66.8	*11.5*	50.6	*30.1*	46.2	*5.6*	55.0	*10.8*	83.3	*5.3*	45.4	*4.0*
Ce	110	*41*	108	*25*	153	*25*	118	*69*	105	*13*	119	*20*	202	*21*	109	*8*
Pr									15.1	*2.1*	17.3	*3.2*	30.2	*2.7*		
Nd							60.7	*9.3*	71.1	*7.7*	75.5	*12.5*	133	*11*	68.0	*5.0*
Sm	15.1	*9.6*	14.2	*2.4*	18.5	*3.2*	15.2	*4.7*	16.7	*1.7*	16.9	*2.6*	28.1	*2.9*	14.9	*1.3*
Eu	2.71	*0.76*	3.33	*0.35*	3.92	*0.58*	4.74	*0.64*	6.21	*1.01*	5.01	*0.59*	6.18	*0.28*	4.38	*0.33*
Gd									16.9	*2.4*	17.0	*3.3*	28.2	*4.2*		
Tb	1.83	*0.61*	1.90	*0.32*	2.50	*0.41*	2.10	*0.74*	2.45	*0.37*	2.55	*0.43*	3.75	*0.34*	2.19	*0.20*
Dy									13.5	*1.6*	14.7	*1.9*	19.8	*1.9*		
Ho									2.83	*0.38*	3.13	*0.40*	3.89	*0.41*		
Er									7.05	*0.87*	8.12	*1.06*	9.33	*1.12*		
Tm									1.03	*0.21*	1.14	*0.18*	1.13	*0.17*		
Yb	5.36	*1.05*	4.94	*0.46*	6.56	*1.43*	6.00	*1.74*	6.52	*0.87*	7.48	*1.12*	6.97	*0.99*	4.89	*0.41*
Lu			0.76	*0.11*					1.02	*0.16*	1.16	*0.16*	1.02	*0.16*	0.75	*0.05*
Y	58.7	*20.8*	59.6	*13.2*	85.8	*17.1*	68.6	*31.2*	77.2	*8.8*	84.1	*11.4*	99.7	*13.2*	64.0	*2.5*
(La/Yb)n	6.7	*2.2*	7.0	*1.5*	7.5	*1.4*	5.7	*1.8*	5.1	*0.3*	5.3	*1.0*	8.7	*0.7*	6.7	*0.4*
Eu/Eu*	0.70	*0.41*	0.75	*0.16*	0.66	*0.09*	1.02	*0.22*	1.16	*0.29*	0.91	*0.14*	0.69	*0.07*	0.90	*0.05*

The Breimyknuten charnockite

This relatively small body (Itinerary 4, Table I 4.1) is entirely located in the country rock gneisses in between the Apophysis and the Hidra body. This location inside the Vardefjell strongly migmatized zone makes it a good candidate, and the best available up to now, to represent a product of charnockitic anatexis, triggered by the heat coming from the nearby

intrusions. The charnockitic mineralogy and composition together with the presence of CO_2-rich fluid inclusions (Wilmart & Duchesne 1987; Wilmart et al. 1991) matches the experimental eutectic obtained by Wendlandt (1981) under granulite facies conditions. No other data can, as yet, corroborate that model. The relatively small volume of the body suggests that the dry anatexis was not a very efficient process, at least at the level of final intrusion of the anorthosites.

The Farsund charnockite

The Farsund charnockite is still unperfectly known. Rather homogeneous, it shows a restricted range of composition (Table I 4.1). More data are needed to decide whether it is a differentiate of a jotunitic melt or a product of charnockitic anatexis. Isotopic signature are up to now ambiguous (Demaiffe et al. 1986)

Conclusions

Rogaland jotunites proved decisive in filling the Daly gap between basic and acidic rocks. A continuous LLD - the Tellnes trend - has been identified with chilled melts. It is a rare case of FC in a close system of a dry magma. Modelling by various methods was confirmed by experimental petrology. The Tellnes trend thus appears an excellent reference to better define the C-type granite LLD (a typology that we now prefer to A-type used by (Duchesne & Wilmart 1997)

Starting from this relatively simple case (dry system, no contamination), we can now better decipher the influence of assimilation and of a low activity of water on the position of the LLD and on the behaviour of trace elements. The identification of a leucogranitic (leucosomic) material, unexpectedly depleted in incompatible element, as a possible contaminant can also question classical views on the effect of contamination.

The origin of the jotunite as parental to andesine anorthosite at mid-crust pressures, as proposed long ago by Duchesne & Demaiffe (1978), is now confirmed by experiments and modelling. This view can now be extended to massif-type andesine anorthosites at the pressure of the deep-seated magma chamber (10-13 kb). Moreover, experimental data now show that jotunites lie on thermal highs in the relevant phase diagrams at 10-13 kbar, indicating that these magmas cannot be derived by fractionation of peridotitic mantle melts but by melting of gabbronoritic sources in the lower crust at 40-50 km depths. One can now question the capability of the underplating process to yield intermediate magma through crustal contamination of mantle-derived magmas.

Chapter 5

THE IRON-TITANIUM DEPOSITS

(by J.C. Duchesne and H. Schiellerup)

Introduction

Numerous Fe-Ti deposits of economic or sub-economic grade occur in the Rogaland Anorthosite Province. They include the famous world-class deposit of Tellnes, discovered in 1954 and operative since 1960, which is the second most important ilmenite deposit in crystalline rocks after the Lake Tio deposit, Allard Lake district, Quebec. The Storgangen deposit, which closed in 1964, is another famous mining site. Total production at the two deposits exceeds 20 million tons of ilmenite (Force 1991). The old Blåfjell mine, active from 1863 to 1876, produced some 90,000 tons of ore. Apart from these economic deposits, numerous smaller occurrences are found disseminated in the anorthosite massifs. Krause et al. (1985) tabulated 23 small mines or prospects in the Åna-Sira anorthosite massif, 7 in the Sokndal lobe of the Bjerkreim-Sokndal intrusion, and 39 in the Håland-Helleren anorthosite. There are also disseminated ilmenite + magnetite ± apatite occurrences in banded norite horizons of the Bjerkreim-Sokndal layered intrusion and in numerous jotunite (Fe-, Ti-, P-rich hypersthene monzodiorite) dykes and intrusions (a.o. Eia-Rekefjord massif, Lomland dyke).

Mining activity in the Rogaland province began at Kolldal, southeast of Egersund, in 1785 and reached a maximum between 1861 and 1881 in that region. After a 20 year break in Fe-Ti oxide ore exploitation, activity moved definitively to Sokndal which became the mining center for the Blåfjell, Storgangen and Tellnes orebodies.

Exceptional exposure, lack of a metamorphic overprint (that typically affects the North American deposits), and a great variety of concordant and discordant occurrences, large compositional variations and beautiful varieties of microstructures are features giving considerable interest to the Rogaland mineralizations. It is thus not surprising that the orebodies are cited in numerous papers and textbooks (a.o. Vogt 1893; Foslie 1928; Ramdohr 1960).

Hubaux (1956; 1960) described a large number of occurrences in the Egersund district. He was able to distinguish variation in microtextures in the various deposits. However, his conclusions on the genesis of Rogaland Fe-Ti deposits were strongly influenced by Michot's (1955; 1956) interpretation of the Norito-Granitic Zone (NGZ) located between the Egersund-Ogna and the Håland-Helleren massifs (Fig. 5.1B). Michot (1956) suggested a metasomatic origin for the Fe-Ti ore-bodies, which were considered to represent a mafic front in a complex transformation of a norite. Duchesne (1970, 1973) showed that the microtextures and the compositions of ilmenite and magnetite from the "metasomatic" bodies were quite similar to those found in the Bjerkreim-Sokndal layered rocks as well as in other, smaller deposits far away from the NGZ. Duchesne (1972) used trace elements to classify the deposits in a simple magmatic sequence. He further suggested that the metasomatic hypothesis was not necessary to account for the data. Later, new trace element data, including REE on apatite, led Roelandts & Duchesne (1979) to propose an origin for the deposits by segregation of Fe-Ti oxide minerals from comparable magmas at various stages of differentiation.

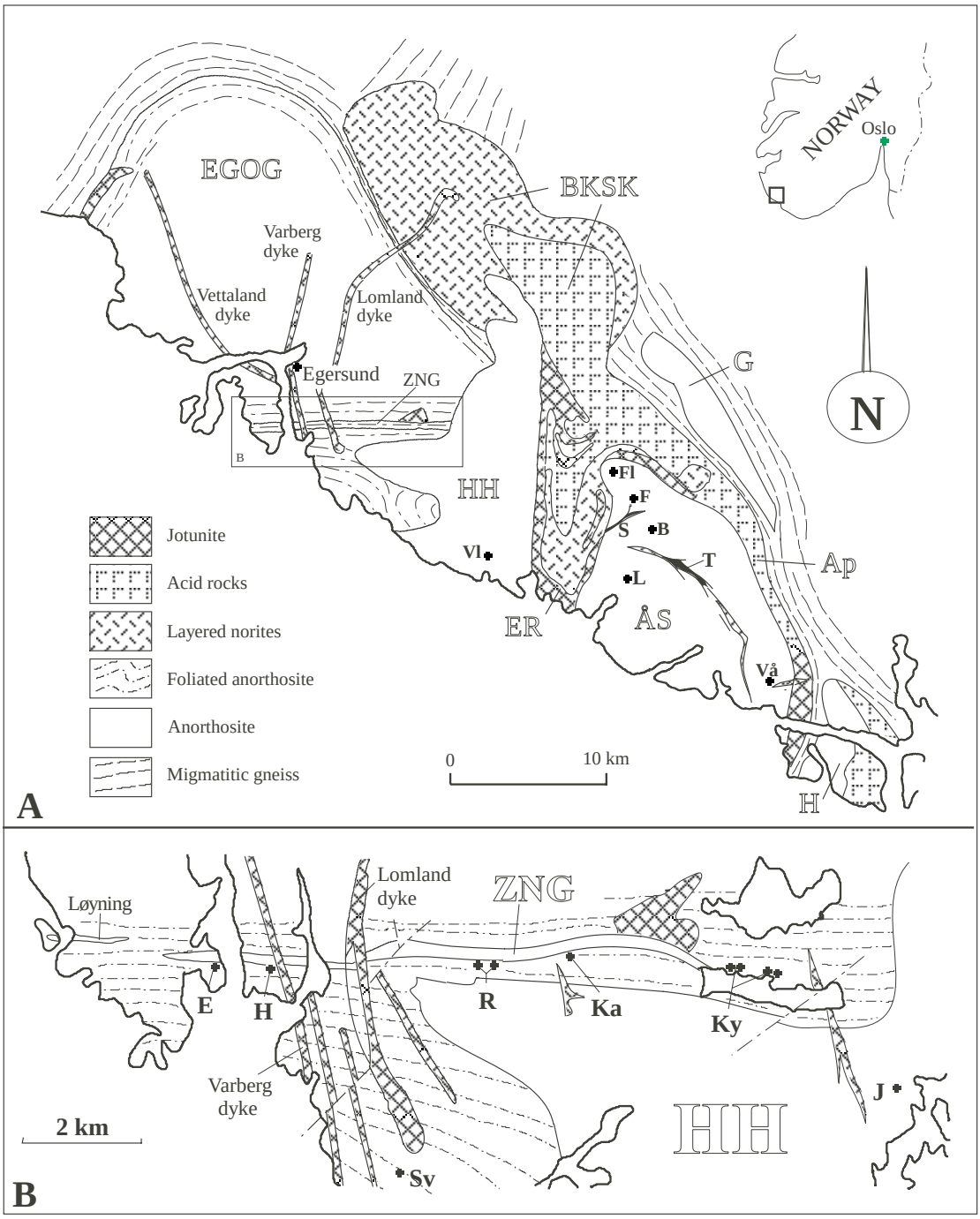

Fig. 5.1. A. Schematic geological map of the Rogaland anorthosite province. Main geological units: EGOG, Egersund-Ogna massif; HH: Håland-Helleren massif; ÅS: Åna-Sira massif; H: Hidra massif; BKSK: Bjerkreim-Sokndal intrusion; Ap: Apophysis; G: Garsaknat massif; ER: Eia-Rekefjord intrusion. Fe-Ti deposits: B: Blåfjell; F: Flordalen; Fl: Frøtlog; L: Laksedal; S: Storgangen; T: Tellnes; Vl: Vatland. B. Schematic geological map of the contact zone between the Egersund-Ogna and Håland-Helleren massifs (adapted from Hubaux 1960). Same shading as A. ZNG: Norito-granitic Zone; Fe-Ti deposits: E: Eigerøy; H: Hestnes; J: Jerneld; Ka: Kagnuden; Ky: Kydlansvatn; R: Rødemyr; Sv: Svånes.

Table 5.1. List of deposits mentioned in this review and their location (coordinates EUREF 89 (WGS84) in zone 32VLK)

Tellnes (T)	490 690
Storgangen (S)	445 722
Blåfjell (B)	469 714
Laksedal (L)	461 688
Kydlansvatn (Ky)	325 797
Kagnuden (Ka)	297 800
Rødemyr (R)	284 798
Hestnes (H)	249 797
Eigerøy (E)	239 799
Svånes (Sv)	270 764
Jerneld (J)	349 778
Vardåsen (Vå)	544 623
Flordalen (F)	447 761
Vatland (Vl)	346 710
Frøytlog (Fl)	457 736

Krause and co-workers have documented the Blåfjell (Krause & Zeino-Mahmalat 1970), Storgangen (Krause & Pape 1975) and Tellnes (Gierth & Krause 1973) deposits in great detail (Fig. 5 1). Although they were rather reluctant to propose detailed models for the formation of the orebodies, they did suggest a connection among all the orebodies and the Bjerkreim-Sokndal intrusion. They also invoked a complex fractional crystallization process to give rise to the anorthosite series of rocks and orebodies (Krause & Pedall 1980; Krause et al. 1985). Wilmart et al. (1989) showed that the relationship between the Tellnes deposit and the associated jotunite dyke system (see below) was more complex than formerly suspected, and ruled out a strict comagmatic origin (without contamination).

More recently, new studies have been devoted to the deposits: Schärer et al. (1996) determined the U-Pb age of the Tellnes ore-body; Duchesne (1999) revisited some of the typical ore-bodies; Schiellerup et al. (2000) investigated the Re-Os isotopes in several deposits and the related anorthosites; Kullerud et al. (in prep.) produced a first interpretation of the Titania A/S data base on the Tellnes deposit (2000 analyses for major elements and S, Cr, V, Zr, Sr, Ni, Cu, Co, Nb, and Pb); Diot et al. (1999) studied the anisotropy of magnetic susceptibility of the Tellnes deposit in order to better constrain its structure; many aspects on the origin of the deposits have also been resolved by experimental petrology (Vander Auwera & Longhi 1994; Vander Auwera et al. 1998) and theoretical considerations (Duchesne 1996).

Table 5.2. Representative compositions of Ti and P-rich rocks from various occurrences

	PUNT	75192	GNOR	8059	6482	80146D	TELN	STORG	TJØRN
SiO_2	43.88	38.41	44.70	33.89	18.71	25.67	30.37	27.9	49.7
TiO_2	4.44	7.38	3.59	6.82	12.27	7.88	18.40	19.6	3.63
Al_2O_3	12.89	8.00	14.55	7.53	1.65	1.33	11.70	8.3	15.78
Fe_2O_3	5.13	6.00	5.34	9.25	21.79	17.63	7.25	11.7	5.00
FeO	13.20	18.19	9.52	15.68	27.80	33.20	18.10	19.2	8.37
MgO	3.94	6.11	5.33	9.15	10.06	8.01	6.13	7.0	4.44
CaO	8.76	9.94	8.87	10.00	5.23	5.20	4.39	3.3	6.81
Na_2O	3.26	1.82	3.86	1.60	.11	n.d.	2.40	n.a.	3.88
K_2O	1.02	0.27	0.81	0.32	n.d.	n.d.	0.60	n.a.	1.05
P_2O_5	2.99	4.05	2.54	4.71	1.99	1.83	0.09	0.04	0.64
S							0.21	0.3	

PUNT: average of 4 analyses of the Puntavoll facies -Lomland dyke (Duchesne et al, 1985)
75192: Fe-Ti-P rich melanorite - Varberg dyke (Duchesne, unpublished)
GNOR: average of 38 apatite-bearing gabbronoritic cumulates of the BKSK massif (Duchesne, unpublished and Michot, pers. comm.)
8059: melanocratic apatite gabbronoritic layer in the BKSK massif (Michot, pers.comm.)
6482: ultramafic layer - noritic transition zone Ørsland (Duchesne et al., 1987)
80146D: ultramafic layer - mangeritic transition zone Ørsland (idem)
TELN: Tellnes ilmenite norite (ore); average from Krause et al., (1985) and Force (1991)
STORG Storgangen average ilmenite norite; integrated composition from 1963 average mill feed (Force, 1991)
TJØRN: typical chilled jotunite from the BKSK massif (Duchesne and Hertogen, 1988)
n.a. : not analysed; n.d.: not detected

The various Fe-Ti deposits

A first classification of the deposits into low-grade and high-grade types based on the oxide mineral content is convenient to circumscribe the petrological problem of formation. The low-grade type (or disseminated type) is represented by the common rocks (cumulates or liquids) found in BKSK and the jotunite dyke system (see Chapters 3 and 4). Accumulation in a magma chamber or direct crystallization from a jotunite melt can obviously account for their formation. TiO_2 and P_2O_5 concentrations of 13% and 5% respectively (Table 5.2) are employed here to separate high-grade from low-grade deposits. All high-grade deposits are of magmatic origin and are discordant, that is, they form dykes, pods, veins or stockwork into enclosing rocks. The most significant high-grade deposits will be examined here. Their locations can be found in Fig. 5.1 and Table 5.1. The largest deposits (Tellnes, Storgangen, Blåfjell - Laksedal) are crosscutting the Åna-Sira massif, as are the Flordalen, Frøytlog and Vardåsen occurrences.

Kydlandsvatn, Kagnuden, Rødemyr, Hestnes and Eigerøy are located in the Håland-Helleren massif, close to the Norito-Granitic Zone (Fig. 5.1B). The Jerneld, Vatland and Svånes deposits lie inside the Håland- Helleren massif. Some deposits are still rich in silicate minerals (e.g. Storgangen, Tellnes) and there is a continuous transition towards pure oxide minerals (e.g. Jerneld, Kydlandsvatn), or oxide minerals and apatite (e.g. Hestnes). Except for Tellnes, which is an undeformed late dyke, and Blåfjell and Laksedal, which are contained in a pegmatitic norite crosscutting the ÅS massif, all deposits occur in anorthosite massifs.

A short description of each occurrence is given in the Appendix. Table 5.3 synthesizes their main characteristics together with their possible origin, which is discussed below. The minor and trace element contents of separated ilmenite, magnetite, and apatite are reported in Tables 5.4-7 and illustrated in Figs. 5.2-5.

Table 5.3 - Principal characters of the Fe-Ti high-grade deposits in Rogaland.

Name	Setting	Rock type	Oxide paragenesis	Suggested origin
Tellnes (T)	dyke-like intrusion in ÅS anorthosite	Homogeneous ilmenite norite. Locally laminated	hemo-ilmenite ± magnetite	cumulate enriched by crystal sorting in a noritic liquid
Blåfjell (B)	bodies in noritic pegmatite intruded in ÅS	massive ilmenite	hemo-ilmenite (Cr-, V-, Mg-rich) ± magnetite (only in L)	cumulate in a noritic liquid
Laksedal (L)				
Storgangen (S)	concordantly layered dyke intruded in ÅS	melanoritic layers in slightly deformed layered norite	hemo-ilmenite + Cr-, V-rich magnetite	cumulate in differentiated sill
Kydlandsvatn (Ky)	strongly dipping ilmenite lenses and layers in the contact zone between EGOG and HH	ilmenite layer in layered anorthosite and leuconorite	hemo-ilmenite (medium in Cr, V, Mg) ± magnetite	cumulate in a differentiated sill plastically deformed by the anorthosite emplacement process
Vardåsen (Vå)	elongated body associated with a norite dyke	transitional contacts with the norite	hemo-ilmenite ± magnetite	same
Frøytlog (Fl)	associated with a norite dyke	same	hemo-ilmenite ± traces of magnetite	same
Svånes (Sv)	deformed layered body intruded in HH	same	hemo-ilmenite (medium in Cr, V, Mg)	same
Flordalen (F)	dyke-like body in massive anorthosite	ilmenite containing plagioclase crystals	hemo-ilmenite	same
Vatland (Vl)				
Rødemyr I (RI)	dyke intruded in HH close to the contact with the NGZ	oxide minerals vein	hemo-ilmenite (low Cr) + magnetite (V-rich)	probably cumulate
Rødemyr II (RII)	raft in the NGZ (RII) or at the contact with HH	oxide-rich lenses	ilmenite (low Cr) + Ti-magne-tite + apatite (medium REE)	cumulate or immiscibility
Kagnuden (Ka)				
Hestnes (H)	Veins intruded in HH	vein of nelsonite with planar orientation of apatite and oxide mineral	ilmenite (Cr-poor) + Ti-magne-tite + apatite (REE-rich)	immiscibility of a P-, Ti-, Fe- rich liquid
Eigerøy (E)				
Jerneld (J)	Veins in HH	massive hemo-ilmenite	hemo-ilmenite (very Cr- and Mg-rich)	high temperature solid state segregation and recrystal-lisation (dynamic recrystal-lisation)

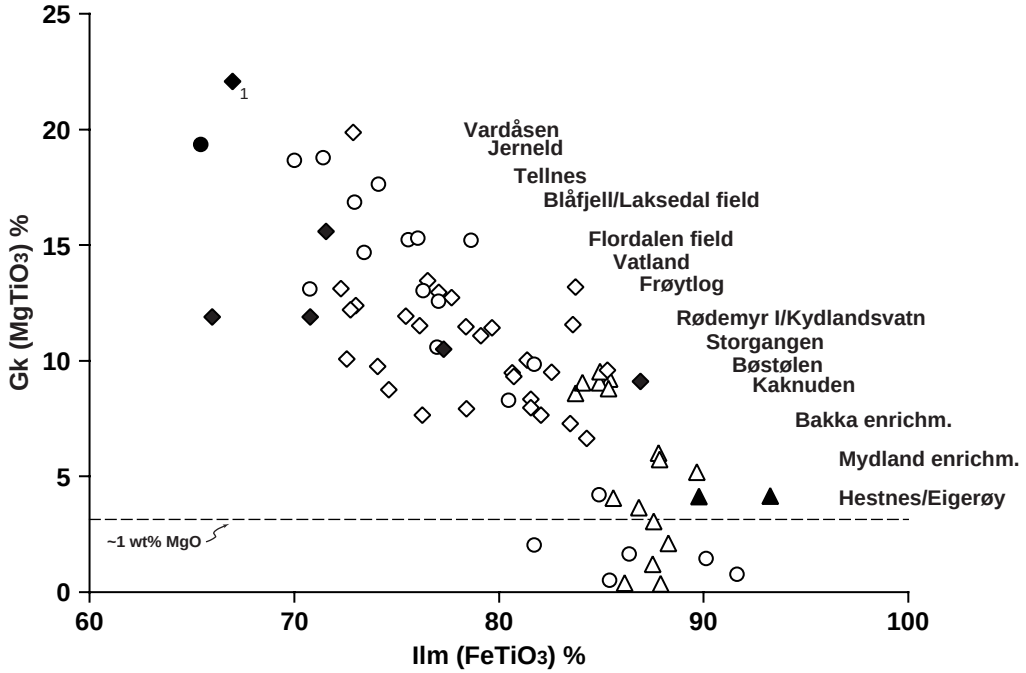

Fig. 5.2. Composition of ilmenites from various ilmenite-rich intrusions and deposits in Rogaland in terms of molar geikielite ($MgTiO_3$) vs. molar endmember ilmenite ($FeTiO_3$). Type 1 = circles. Type 2 = squares. Type 3 = triangles. Open symbols represent electron microprobe data (Schiellerup et al., in prep.), solid symbols are compositions determined by XRF on ilmenite separates (Duchesne, 1999). [1] Tellnes ilmenite composition from Krause et al. (1985). Type 3 compositions are generally characterized by low geikielite contents, whereas type 1 deposits have ilmenites rich in geikielite. Low-geikilite type 1 ilmenites have only been found in the Bjerkreim-lobe of the Bjerkreim-Sokndal intrusion.

Irrespective of their relationship with enclosing rocks, the high-grade deposits can be conveniently classified on the basis of their mineralogy and particularly their oxide association. Three types have been defined (Duchesne 1973, 1999):

Type 1 oxide assemblage (hemo-ilmenite as the only oxide), rich in Cr, Ni, Co, Mg, is found in Jerneld, Blåfjell, Flordalen, Vatland, and Svånes;

Type 2 oxide assemblage (hemo-ilmenite + magnetite) characterizes Storgangen, Tellnes, Bøstølen, Vardåsen, Kydlandsvatn and Rødemyr I;

Type 3 oxide assemblage (ilmenite + Ti-magnetite + apatite) is found in Hestnes, Eigerøy, Kagnuden and Rødemyr II, with lower Cr, Ni, Co and higher Zn contents in the oxides as well as high REE contents in the apatite.

As pointed out by Duchesne (1973; 1999), the variations in the nature of the oxide assemblage and in the trace element composition are indeed quite similar to the evolution in the BKSK intrusion. The 3 types of oxide assemblages correspond to 3 successive stages of evolution in the cumulate series (see Chapter 3). Moreover, evidence of layering are commonly found in several deposits (Svånes, Flordalen, Vardåsen, Storgangen, Bøstølen and Kydlandsvatn). In BKSK, hemo-ilmenite is the second mineral to appear on the liquidus, subsequent only to plagioclase. Similarly, layers of pure hemo-ilmenite in anorthosite occur in the Kydlandsvatn deposits (see locality I.16), and a cumulate origin involving magmas, in which ilmenite was the first mafic mineral to crystallize, is plausible. The trace element evolution, particularly the Mg and Cr content of ilmenite, also mimics the BKSK-trend. The

variation in MgO-content of ilmenite may be expressed by the amount of geikielite ($MgTiO_3$) dissolved in ilmenite. The geikielite content decreases systematically with differentiation and, as may be observed in Fig. 5.2, the composition of ilmenites from discordant deposits throughout the province are correlative with ilmenite compositions in the BKSK. The trend observed reflects similarities in origin and evolution among discordant deposits and the BKSK. In the Bjerkreim-lobe, however, a reduced MgO content is evident, possibly due to subsolidus reactions. The similarities point to a fractional crystallization process, with accumulation of Fe-Ti oxides as the main controlling mechanism, to explain the variety of deposits.

However, there do exist compositional, morphological and textural differences between BKSK and the high-grade deposits do exist: (1) some deposits contain several mineral assemblages side by side: Tellnes, Laksedal and Kydlandsvatn have types 1 and 2 and, in the latter, apatite can be also present in type 2; (2) the trace element content in the deposits is usually much higher than in BKSK: type 3 has a magnetite with much higher Cr contents (200 to 1300 ppm) than in BKSK (< 50 ppm). Type 1 such as Jerneld ilmenite is also much richer in Cr and in MgO than in BKSK. Similarly, the REE in Hestnes and Eigerøy apatites are higher by a factor of 3 than in BKSK;

In some cases, as in Tellnes as shown by Gierth (1983), the Cr content of ilmenite is distinctly lower when magnetite is present in the oxide assemblage. Indication of a similar behavior is also given here in Laksedal (compare ilmenites 78.29.1 and 78.29.2 in Table 5) and in Kydlansvatn (ilmenite 66-182 is richer than the others). It is clear that these distributions do not reflect mineral/melt equilibrium in which the element content is controlled by partition coefficients with the melt, but could result from exchange of Cr between the two oxide minerals during subsolidus evolution at high temperature. Compared to ilmenite, magnetite, with a spinel structure, is particularly eager to concentrate Cr.

The discrepancies between the deposits and BKSK might result from the more complex evolution of the massive anorthosites compared to BKSK. The latter is a magma chamber evolving at a roughly constant pressure of c. 5 kb. In contrast, the massive anorthosites have crystallized over a large interval of pressure with deformation starting in the magmatic stage and continuing in the solid stage. Igneous textures and mineral compositions may therefore have been modified in the solid stage (annealing texture, Ostwald ripening) at relatively high temperature (500-1000°C). Because crystallization and deformation were synchronous, filter press mechanisms could have expelled magmatic liquids, crystal-laden liquids, or even crystal mushes from more rigid crystal matrixes. Hence, typical intrusive contacts, as observed in dykes or pods, do not necessarily imply that the intruded material was liquid. It could equally well represent an injected crystal mush or a crystal-laden liquid.

Table 5.4. Composition of Fe-Ti oxides in selected Rogaland deposits. Analyses by XRF on minerals separated by standard methods (dense liquids and Frantz separator). FeO calculated by charge balance. T°C , fO_2 (expressed as logfO_2) and DFMQ (difference to FMQ buffer) by use of QUIlF equilibria (Lindsley and Frost, 1992) and program QUILF (Andersen et al. 1993). Detection limits (<): Ni: 10 ppm; SiO_2: 0.01%; MnO: 10 ppm. Co in magnetite not analysed.

	Jerneld	Kydlandsvatn		Storgangen		Tellnes		Rødemyr I		Kagnuden		Hestnes		Eigerøy	
	6623	64 96		64 146		64 145		66 16		66 11		66 33		66 150	
	Ilm	Ilm	Mgt	Ilm	Mgt	Ilm	Mgt	Ilm	Mgt	Ilm	Mgt	Ilm	Mgt	Ilm	Mgt
FeO	31.6	31.5	30.4	36.5	29.3	34.1	29.6	33.8	29.9	40.9	32.7	42.7	36.2	44.1	43.0
MnO	0.23	0.25	0.002	0.3	<	0.29	0.005	0.49	0.006	0.48	0.066	0.62	0.13	0.65	0.2
MgO	5.3	3.2	0.6	2.8	1.2	4.2	0.8	2.9	0.7	2.4	1.3	1.1	0.4	1.1	0.5
CaO		0.04	0.01	0.1	0.02	0.13	0.07		0.06	0.02	0.06	0.12	0.14		
ZnO	0.014	0.002	0.019	0.008	0.023	0.007	0.16	0.05	0.022	0.006	0.1	0.012	0.26	0.014	0.23
Fe_2O_3	15.8	23.0	64.5	12.1	65.5	13.0	62.3	18.1	65.4	3.2	57.5	5.0	49.8	1.2	39.4
Al_20_3	0.6	0.1	0.8	0.3	0.8	0.4	1.4		1.2	0.08	2.9	0.1	3.2	0.02	2.4
V_2O_3	0.33	0.41	1.08	0.27	0.96	0.2	0.75	0.14	1.12	0.07	1.04	0.02	0.34	0.02	0.3
Cr_20_3	0.43	0.05	0.36	0.069	1.06	0.055	1.16	0.02	0.1	0.003	0.06	<	0.019	<	0.043
TiO_2	45.8	41.7	1.0	46.4	0.5	46.5	0.9	43.7	0.5	50.8	4.03	50.3	7.0	51.9	13.8
SiO_2		<	0.07	0.13	0.46		0.39		0.28	<	0.26	0.02	0.38		0.52
Total	100.1	100.3	98.8	99.0	99.8	98.9	97.6	99.1	99.3	97.9	100.0	100.1	97.8	99.0	99.8
Ni (ppm)	640	200	940	170	820	140	3600	170	380	40	280	<	80	30	30
Co (ppm)	200			70		90		130		80		50		50	
Hem/Usp %	18.2	24.6	1.8	12.9	1.5	14.5	2.8	18.8	1.5	3.3	12.3	5.0	21.8	1.2	41.4
T°C			595		500		557		523		548		653		493
fO_2			-15.3		-18.2		-17.3		-16.9		-22.5		-18.4		-27.8
DFMQ			4.8		5.6		4.3		5.9		-0.6		-0.1		-3.6

Table 5.5 Compositions of some trace elements in ilmenites All elements were measured by XRF on ilmenite separated by standard methods. MgO and MnO are expressed in wt.%, the other elements in ppm

			MgO	Cr_2O_3	V_2O_3	Ni	Co	Ni/Co	MnO	Zn	Rem
Storeknuten		JL-5	4.40	690	1500	230	140	1.6	0.34	50	+MGT
(BKSK)		JL-12	3.65	280	1500	170	130	1.3	0.36	100	id
Jerneld	J	66-23	5.25	4300	3200	520	130	4.0	0.23	140	
		79-15-2	5.40	4500	3200	410	110	3.7	0.22	70	
Blåfjell	B	66-62	5.70	2790	3000	690	170	4.1	0.24	50	
		66-133	3.20	1690	2900	180	100	1.8	0.28	160	
Laksedal	L	78-29-1	5.00	2700	2700	490	110	4.5	0.25	40	
		78-29-2	5.50	520	1900	340	100	3.4	0.32	30	+MGT
Svånes	Sv	78-26-1	3.20	870	3500	170	130	1.3	0.25	140	
		79-21-1	4.00	870	3600	140	130	1.1	0.27	140	
Kydlandsvatn	Ky	64-96	3.20	500	4100	200			0.20	20	+MGT
		66-182	3.70	850	4100	220	140	1.6	0.22	110	
		66-181	3.06	310	4000	120	170	0.7	0.30	80	+MGT +AP
		79-19-1	3.60	300	3700	85	130	0.7	0.28	100	id
		90-I	2.56	430	5000	270	160	1.7	0.23	120	id
		90-J	2.68	480	5000	210	110	1.9	0.23	30	id
Tellnes	T	64-145	4.17	550	2000	130	90	1.4	0.49	150	+MGT
Storgangen	S	64-146	2.76	690	2700	170	70	2.4	0.30	80	+MGT
		64-149	3.50	230	2100	190	80	2.4	0.33		id
Rødemyr I	RI	66-16	2.86	220	1400	170	130	1.3	0.34	510	+MGT
Rødemyr II	RII	66-15	1.86	100	1700	50	150	0.3	0.44	100	+MGT +AP
Kagnuden	Ka	66-11	2.40	30	700	40	80	0.5	0.48	60	+MGT +AP
Hestnes	H	66-33	1.07	<10	200	0	50	0.0	0.62	120	+MGT +AP
		92-23D	1.50	60	700	80	60	1.3	0.55	480	id
Eigerøy	E	66-04	1.40	<10	700	15	60	0.3	0.73	20	+MGT +AP
		66-150	1.10	4	200	30	50	0.6	0.65	140	id

.

Though many ambiguities sill remain, *fractional crystallization* with accumulation of Fe-Ti oxides may approximately account for the Storgangen, Kydlandsvatn, Flordalen, Frøytlog, Vatland, Svånes and Tellnes deposits (obvious layering in the first three, cryptic layering of the two oxide minerals in Storgangen, REE distribution in Tellnes indicating accumulation of plagioclase). The Blåfjell and Laksedal ilmenite deposits are integral parts of a large mass of norite pegmatite and most likely represent concentration of cumulus minerals in that noritic liquid. The Jerneld deposit may have originated as a hemo-ilmenite cumulate in a transient magma chamber, which was subsequently deformed along with its enclosing anorthosite at high temperature during emplacement. Due to its wetting properties and ability to recrystallize, ilmenite could have migrated in the solid state during deformation to form veins. Considering the usually high contents in Cr and MgO in ilmenite, the parent magmas of all these deposits were probably less evolved than that of BKSK, but they belonged to the same kindred, with early ilmenite crystallization. The possible influence of pressure on the oxide composition may explain the variable MgO and Cr contents, but this remains to be tested by experimental petrology.

Immiscibility cannot be rejected as an alternative enrichment mechanism. Though the supporting experimental evidence are currently lacking (see the discussion in Duchesne 1999), it is a convenient mechanism to generate vein deposits of almost pure material. The Hestnes and Eigerøy nelsonites probably represent the best field evidence in favor of the

existence of such immiscible liquids. They display evolved characteristics (high REE content in the apatite, high TiO_2 and Zn contents in magnetite, lower Ni/Co ratios) together with primitive characteristics (from 190 to 1300 ppm Cr_2O_3 in magnetite – Table 5.6), features difficult to reconcile with fractional crystallization.

The Kagnuden and Rødemyr deposits show characteristics intermediate between the Kydlandsvatn deposits and Hestnes-Eigerøy nelsonites: hemo-ilmenite is present with (Ti-) magnetite (type 2 association) and locally with apatite (type 3 association); the Cr content in magnetite is comparable to Hestnes; the V content in both oxides resemble Kydlandsvatn; the REE content in apatite is also intermediate between Kydlandsvatn and Hestnes; magnetite is more abundant and richer in Ti in Kagnuden. It is thus hard to decide whether these deposits were derived from an immiscibility process, such as might be the case in the Hestnes-Eigerøy nelsonites, or were formed by a cumulus process.

Table 5.6 Compositions of some trace elements in magnetites. All elements were measured by XRF on magnetites separated by standard methods. TiO_2 and Al_2O_3 are expressed in wt%; the other elements in ppm. Detection limit (<): 10 ppm MnO.

			TiO_2	Cr_2O_3	V_2O_3	MnO	Ni	ZnO	Al_2O_3
Storeknuten		JL-5	2.4	14600	9800	660	1080	620	2.5
(BKSK)		JL-12	1.5	4100	7800	280	940	1000	1.7
Laksedal	L	78-29-2	1.8	8230	9600	170	850	560	1.5
Kydlandsvatn	Ky	64-96	1.0	3600	10800	20	940	190	0.8
		79-19-1	3.2	2030	9700	170	460	320	1.5
		90I	0.5	3100	11900	<	940	430	1.2
		90J	0.5	3100	12400	<	950	200	1.0
		66-181	4.2	2060	8800	210	490	180	1.1
Tellnes	T	64-145	0.9	11600	7500	50	3600	1600	1.4
Storgangen	S	64-146	0.5	10600	9600	<	820	230	0.8
		64-149	2.6	2400	9600	220	850	1180	1.4
Rødemyr I	R I	66-16	0.5	1000	11200	60	380	220	1.2
Rødemyr II	R II	66-15	3.6	730	7600	480	310	680	
Kagnuden	Ka	66-11	4.0	600	10400	660	280	1000	2.9
Hestnes	H	66-33	7.0	190	3400	1300	80	2600	3.2
		92-23D	7.2	950	3900	1300	50	2340	3.1
Eigerøy	E	66-04	14.1	1300	2700	2500	100	2000	2.4
		66-150	13.8	430	3000	2000	30	2300	2.0

Table 5.7 REE contents (ppm) of apatites from various Rogaland Fe-Ti deposits. Data from the BKSK intrusion are from Roelandts and Duchesne, 1979. Analyses by ICP-MS, except 66-15 and BKSK samples by NAA (Roelandts and Duchesne, 1979).

	MCU III	MCU IVg	79.19.1	90-I	90-J	66-15	66-11	66-163	66-150	66-33	92-23D
	BKSK	BKSK	Ky	Ky	Ky	R II	Ka	Ka	E	H	H
La	152	354	194	181	127	269	269	217	801	951	929
Ce	431	946	551	537	424	729	751	623	2236	2649	2588
Nd	504	709	487	497	400	609	608	538	1737	2108	1994
Sm	96.9	182	123	149	116	158	138	139	395	466	439
Eu	20.2	32.9	26.8	32.5	28.0	30.5	27.6	29.3	42.5	44.5	43.7
Gd	85	167	131	162	134	168	142	145	385	423	425
Tb	13	25	17	20	20	23	18	19	55	68	61
Dy	52	99	85	101	112	93	85	95	301	300	321
Ho	10.2	18.7	12.6	15.2	17.6	18.1	14.7	14.6	51.0	55.1	55.0
Er	21.2	42.9	33.2	39.4	47.2	33.8	36.3	38.7	128	142	138
Yb	11.1	24.1	17.2	21.3	28.9	24.7	18.8	19.5	80	83.9	83.4
Lu	1.1	2.3	2.2	2.6	3.5	2.1	2.3	2.5	8.7	10.4	9.2
Eu/Eu*	0.68	0.59	0.65	0.64	0.69	0.57	0.60	0.63	0.33	0.30	0.31

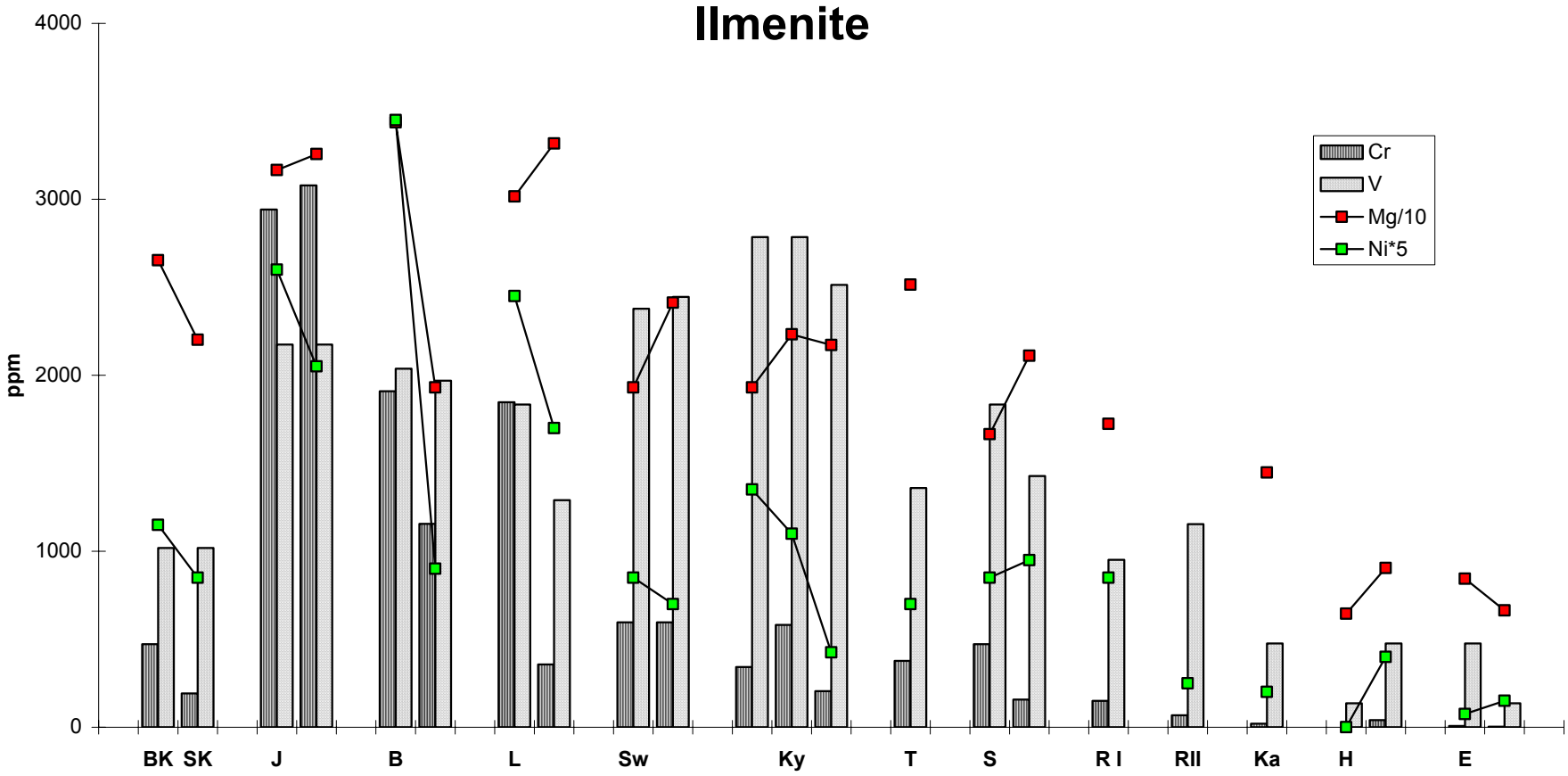

Fig. 5.3 Cr, V, Mg, and Ni in ilmenites separated from the Fe-Ti deposits (see Table 5.5).

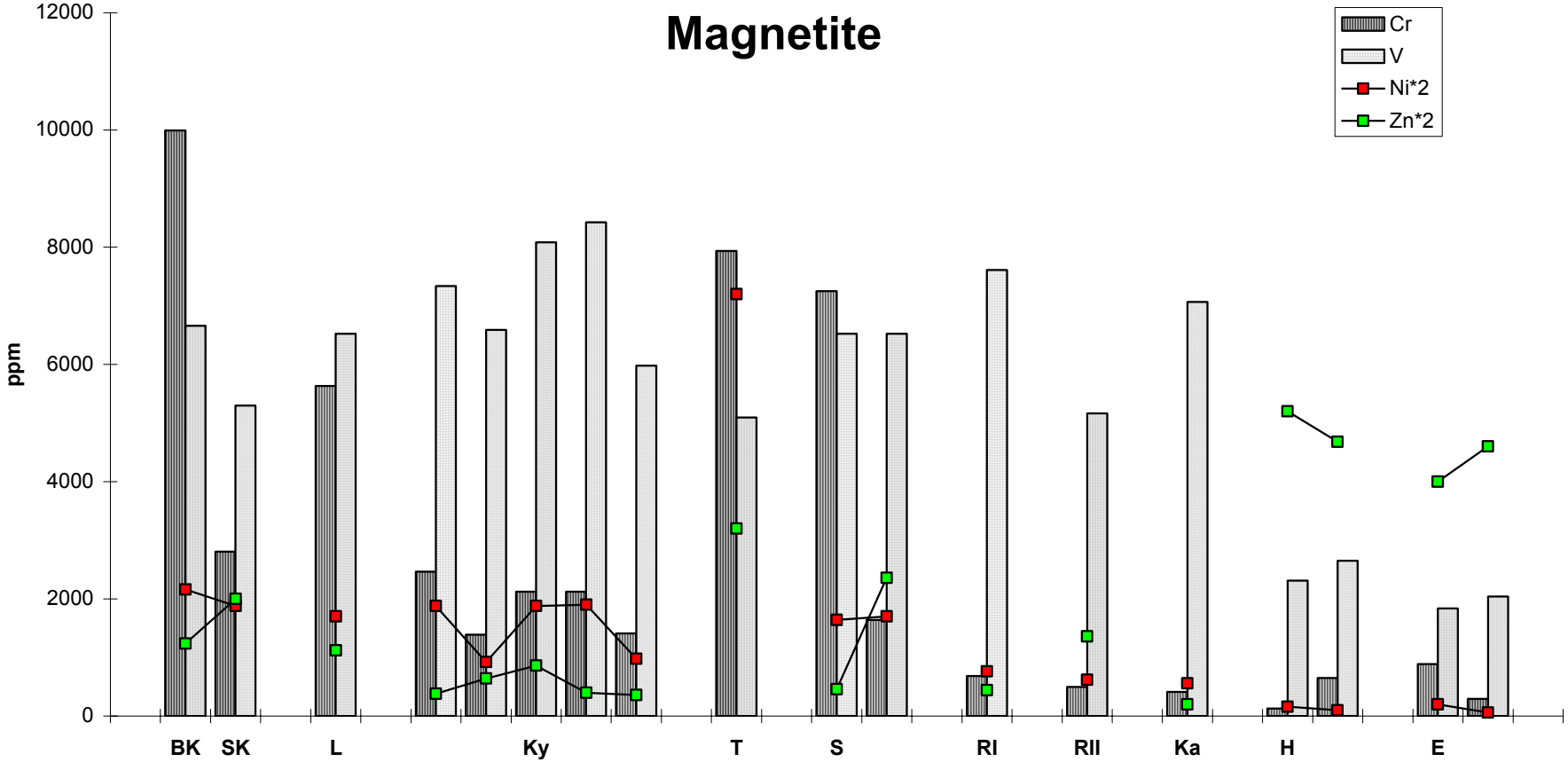

Fig. 5.4 Cr, V, Zn, and Ni in magnetites separated from the Fe-Ti deposits (see Table 5.6).

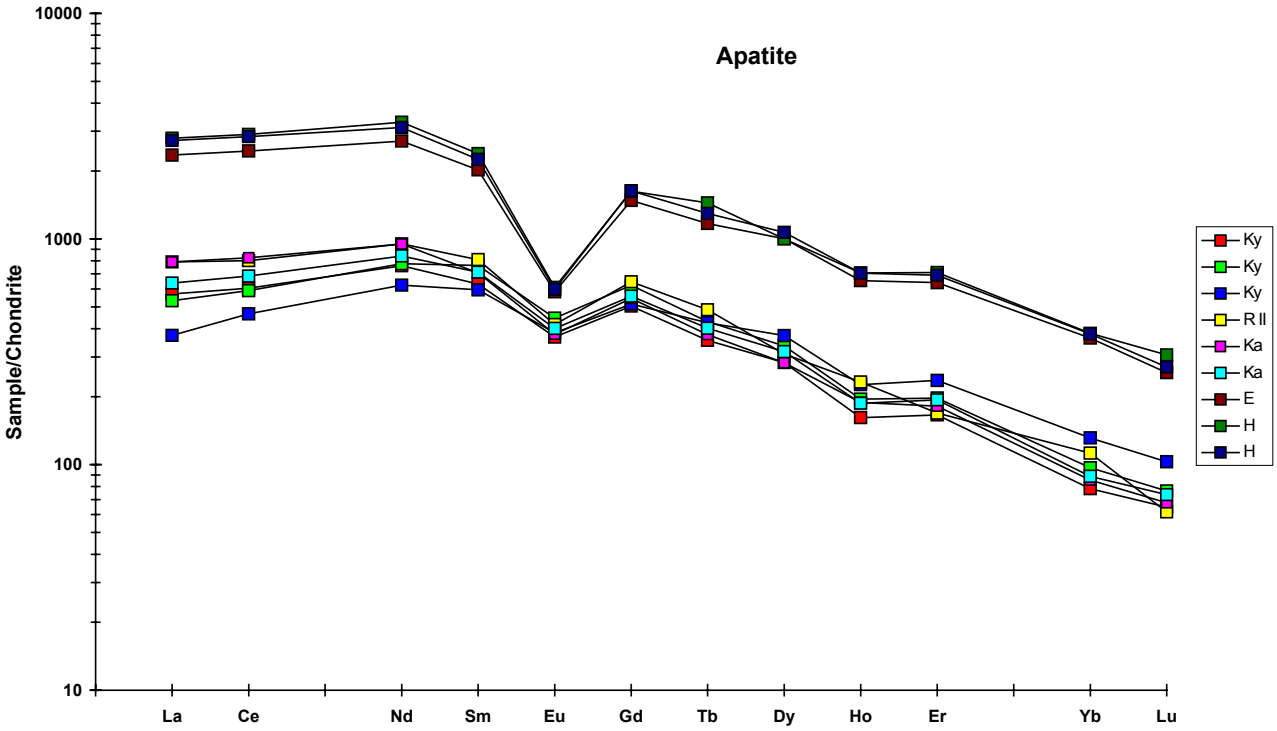

Fig. 5.5. Chondrite-normalized REE distribution in apatites from Fe-Ti deposits (see Table 5.7)

APPENDIX: SHORT DESCRIPTION OF THE SIGNIFICANT DEPOSITS

Tellnes (T)

The Tellnes deposit is a sickle-shaped ilmenite-rich noritic body more than 2700 m long and, in the central part, more than 400 m wide. It is intrusive into the ÅS anorthosite, as evidenced by sharp contacts, numerous apophyses cutting the surrounding anorthosite, intrusive breccias, and xenoliths of anorthosite. The deposit has been extensively studied by Krause and his group (Gierth & Krause 1973; Krause et al. 1985). The ilmenite norite orebody extends on both ends into a jotunite dyke - called the main dyke -, which is 5 to 10 m thick and ranges in composition from jotunite to quartz mangerite. In the south-eastern end, a zone of interfingering of leuconoritic and mangeritic dykes makes the transition with the main dyke. The latter cuts across the anorthosite for more than 4 km in the north west and for more than 10 km in the south west. U-Pb ages on zircon and baddeleyite from the ilmenite orebody are 920 ± 3 Ma, thus slightly younger than the jotunite dyke (931 ± 5 Ma) (Schärer et al. 1996). The two intrusions are not strictly comagmatic as evidenced by differing Sr isotope initial ratios, as well as the conspicuous difference in emplacement ages. Wilmart et al. (1989) have discussed in detail the mechanisms by which the two intrusions can be related. Isotopically, the ilmenite norite can be derived from the crystallization of a noritic liquid related to the crystallization of the ÅS anorthosite. Liquids of appropriate compositions are, however, not known elsewhere in the massif, and the exact nature of the parent magma to the Tellnes deposit remains ill-defined.

The ilmenite norite is homogeneous on a large scale: euhedral plagioclase (An_{45-42}), only locally slightly bent and granulated, and euhedral bronzite (En_{77-75}) with subordinate olivine (Fo_{80}) are enclosed by an interstitial hemo-ilmenite (Hem_{13}). Fe-Ni-Co-Cu sulfides and Ti-biotite are present in minor amounts. Apatite and magnetite occur in some facies; the latter, showing lamellae of zinciferous spinel (sample 64-145, Tables 5.4-6, Figs. 5.2-3). It is rich in Cr, V and Zn with the highest Cr/V ratio (1.6) and ZnO content (0.16%) in the area. Gierth (1983) has shown that hemo-ilmenite associated with magnetite contains less Cr (250-600 ppm) and Zn (c. 70 ppm) than ilmenite in magnetite-free samples (700-1400 ppm Cr and c. 130 ppm Zn), an important consideration for mining methods and for petrogenetic models. An average composition of the ore is reported in Table 2. REE and other trace elements are given by Wilmart et al. (1989). A distinct positive Eu anomaly indicates accumulation of excess plagioclase. Subtle variations in chemical composition have been put forward by extensive sampling of the deposit (Kullerud et al. in prep.). Rocks along the contact and in some apophyses are richer in modal plagioclase without significant change in the composition of the minerals (the plagioclase goes down to An_{39} and the pyroxene Mg# varies from 0.77 to 0.60). Magnetite is more abundant in the upper part of the body. Apatite is slightly more enriched along the inclined NE floor of the intrusion (Fig. 5.6).

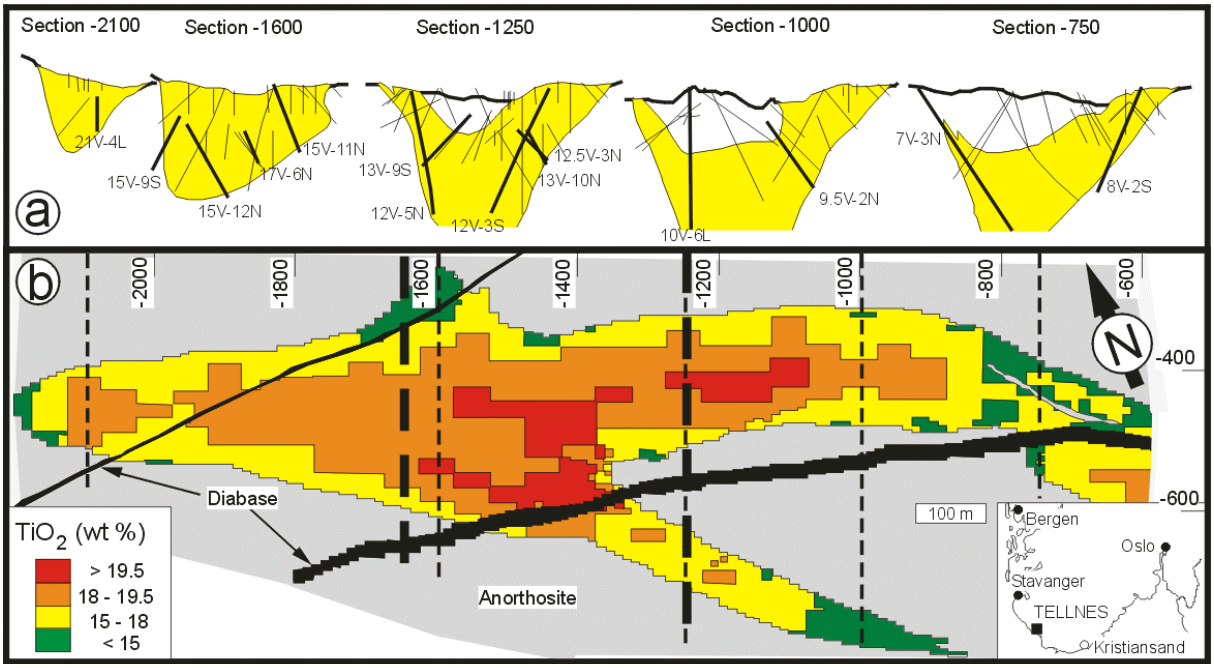

Fig. 5.6. A three-dimensional block model of the Tellnes ore compiled on the basis of approximately 4900 analyses of the ore, using DATAMINE®. a) Vertical sections showing the sampling density of drill cores. b) Horizontal section showing the variations in the TiO_2-content of the ore. Light dotted lines show the positions of vertical sections in a), heavy dotted lines show the position of the vertical sections given in c). c) Vertical sections showing the variations in the contents of TiO_2, Cr, P_2O_5, S and magnetite (from Kullerud et al. in prep.).

The ilmenite norite locally shows mineral lamination and lineation, well evidenced by the study of anisotropy of magnetic susceptibility (Diot et al. 1999). These mineral orientations are likely to be formed by the flow of the intruding material. Wilmart et al. (1989) have suggested that the deposit and the related plagioclase-rich rocks, can be explained as sorted cumulates, injected as a crystal mush lubricated by 3 to 10% interstitial Fe-Ti-rich silicate liquid.

Blåfjell (B) and Laksedal (L)

In the Blåfjell deposit, massive bodies of hemo-ilmenite (20% Hem) (0.25% Cr2O3; 3.22% MgO) (analyses of Krause & Zeino-Mahmalat 1970) occur in a pegmatitic norite close to its contact with the enclosing ÅS anorthosite. Our analysis of hemo-ilmenite 66-62, separated from a plagioclase-rich massive ore, agrees with previous determinations (Table 5.5, Fig. 5.2). Sample 66-133 is a hemo-ilmenite (15-18% Hem) separated from a magnetite-free noritic pegmatite (Table 5.5, Fig. 5.2). The norite pegmatite distinctly shows two oxide assemblages (Krause & Zeino-Mahmalat 1970). In the first one, hemo-ilmenite is the only oxide mineral (>

2100 ppm Cr); in the second one, magnetite is present together with ilmenite and apatite (Cr contents are very low in ilmenite and magnetite). Duchesne (1973) proposed that these assemblages represented two stages in the fractional crystallization of noritic liquids. The Laksedal deposit occurs in the same pegmatite body and also shows types 1 and 2 oxide parageneses. When hemo-ilmenite is the only Fe-Ti oxide, it is rich in Cr and V (sample 78.29.1 in Table 5.5), but when accompanied by magnetite (78.29.2), hemo-ilmenite is distinctly lower in Cr and V, and magnetite is richer in both elements (Table 5.6).

Storgangen (S)

The Storgangen orebody forms a dyke in the ÅS massif (4 km long, up to 50 m thick) with numerous offshoots. The anorthosite which constitutes the hanging wall of the dyke is always foliated concordantly with the contact. Strong foliation in the westernmost part of the intrusion, close to the ÅS margin, is also evident, and accompanied by deformation and granulation of plagioclase grains. The observations imply that the Storgangen dyke had intruded and solidified prior to the final deformation of ÅS, which was possibly related to the gravitationally induced subsidence of the neighboring Bjerkreim-Sokndal intrusion (Paludan et al. 1994; Bolle et al. 2000). The orebody is concordantly layered on a cm to m scale, locally with some irregularities. The layering is generally dipping in a northerly direction at an angle of 40-60°, and is conspicuously isomodal throughout the sequence. In the westernmost outcrops, modal layering strikes parallel to the layering in the adjacent parts of the BKSK. The BKSK cumulates crystallized from a much larger magma chamber, where modal layering developed sub-horizontally. The concordant and parallel behavior of the BKSK and Storgangen layerings seem to indicate that the latter originated as a sill-like body. The mineralogy comprises plagioclase, Ca-poor and Ca-rich pyroxene, apatite, Fe-Ti oxides, green chromian spinel and a variety of minor sulfides, as well as baddeleyite. Cumulus Ca-rich pyroxene is rare and only seems to be present in the uppermost part of the layered sequence. Late entry of Ca-rich pyroxene is in accordance with up-section being equivalent to stratigraphic up, and the hanging wall thus represents the roof of the Storgangen magma chamber. Apatite is highly accessory but does not seem to be stratigraphically confined. The complete section is generally rich in oxides, but the most extensive oxide-rich zones occur in the lower half of the stratigraphy. At the footwall, the norite contains a hemo-ilmenite (Hem_{13}) associated with magnetite and pleonastc spinel. The mafic mineral content decreases somewhat upwards, and there is a systematic decrease in An content of plagioclase (An_{55} to An_{43}) and En content of Ca-poor pyroxene (En_{75} to En_{66}), though distinct lateral variation exists (Krause et al. 1985, and current contribution). The MgO content of ilmenite is strongly correlated with the En content of coexisting Ca-poor pyroxene, and ilmenite in Storgangen evolves from 3-3.5% MgO to around 2% MgO. Strong upwards decreases in contained Cr, Ni and Cu in the Storgangen cumulates reflect fractionation of oxides and, apparently, fractional segregation of sulfides. In addition, Gierth (1983) observed a distinct decline in V and Zn concentrations, the Ni/Co ratio, as well as an increase in Mn in both oxides from the base to the top of the dyke. Cryptic layering is thus conspicuous in the dyke.

Two analyses are presented in Tables 5.5-6 and Figs 5.2-3 (64-146, 64-149). Both samples have been obtained from the lowermost part of the intrusion. These data agree with Gierth's: the Cr content in the magnetite is high as well as the Cr/V ratio compared to the other occurrences.

Kydlandsvatn (Ky)

The Kydlandsvatn deposits belong to the Kolldal-Liåsen type defined by Michot (1956). Lenticular orebodies (1 to 2 m-thick) in anorthosite are elongated parallel to the contact between the HH and EGOG anorthosite massifs, and to the norito-granitic septum (NGZ),

which is itself intercalated between the two massifs (Fig. 5.1B). In Liåsen, the orebodies are made up of bundles of parallel layers (up to 20 cm-thick) of massive ore, interbedded with anorthosite, leuconorite or norite layers. All gradations between a very pure oxide ore and noritic varieties exist. Similarly, the accompanying "gangue" rocks pass progressively from norite to anorthosite by decreasing the amount of mafic minerals.

Although these features were interpreted by Michot (1956) as bunches of veins emplaced in anorthosite, the layered character calls for a different explanation: the orebodies and associated rocks accumulated from a fractionally crystallizing melt that intruded as a concordant sill in the contact zone between the two anorthosite massifs. The strongly dipping lamination plane (70°S), together with the frequent lenticular structures and overall granulation and recrystallization of the plagioclase indicate that the layered sill was also involved in the same syn-emplacement deformation as the surrounding anorthosite massif. In the westernmost contact zone between the EGOG and HH massifs, the occurrence of a layered sill - the Løyning sill (Fig. 5.1B) should also be noted. The Løyning sill was injected and deformed concordantly with the foliation of the EGOG margin (Ernst & Duchesne 1991) (see locality I.14). These occurrences may suggest that the marginal zones of the diapiric anorthosite massifs contained a number of small mafic magma chambers, in which layering could develop.

The Kydlandsvatn deposits are made up of hemo-ilmenite (Hem_{20}) with or without Ti-poor magnetite. When hemo-ilmenite is the only oxide mineral (sample 66-182) it shows Cr, V and Mg contents comparable to the Svånes deposit (Fig. 5.2). A variety of ore (sample 66-181) contains abundant apatite (up to 26 vol%) with relatively low REE content (Table 5.7; Fig. 5.4).

Svånes (Sv)

Svånes is an irregularly deformed mass of banded and layered norite (modally graded) with distinct lamination. It occurs in the HH anorthosite far from the contact with the EGOG massif: hemo-ilmenite (15-18% Hem) and some droplets of sulfides are concentrated in melanoritic layers (plag + opx ± biotite). The layered character of the body points to an origin as a cumulate rock in a small magma chamber inside the anorthosite mass. The structure indicates that the intrusion was plastically deformed during the emplacement of the anorthosite. Compared to the Kydlansvatn ore, the hemo-ilmenite is moderately enriched in Cr but the V content is somewhat lower (small Cr/V ratio) (Table 5.5; fig. 5.2).

Rødemyr (RI and RII)

The Rødemyr deposits are located in a more or less brecciated vein at the contact between the HH massif and the NGZ. The ore is made up of hemo-ilmenite (c. 18% Hem) and Ti-poor magnetite, rich in pleonastic spinel exsolutions, together with sulfides and independent grains of (green) spinel. Some varieties are noritic and coarsely layered. The Cr content of hemo-ilmenite and magnetite is low but the V content remains relatively high (Tables 5.5-6; Figs. 5.2-3).

Not far from the main vein is an apatite-bearing lens of ilmenite and Ti-magnetite (called Rødemyr II; sample 66-15), within the NGZ but close to the contact with the Håland massif. The composition of the two oxides and the apatite is very similar to the Kagnuden minerals.

Kagnuden (Ka)

Kaknuden is a small deposit located at the contact between the NGZ and the HH massif, which is made up of homogeneous ilmenite (Hem 3) , Ti-magnetite (with Al-spinel exsolutions), sulfides and some apatite. As in Rødemyr I and II, the magnetites are Cr- poor (Table

5.6, Fig. 5.3). The ilmenite is however less rich in V than Rødemyr II (lower Hem content) (Table 5.5, Fig. 5.2). The REE in the apatite from Kagnuden and Rødemyr II are richer than in Kolldal-Liåsen (Table 5.7; Fig. 5.4).

Hestnes (H) and Eigerøy (E)

Both deposits intruded the HH massif, close to the contact with the NGZ. The ore bodies are made up of almost equal quantities of oxide minerals and apatite with insignificant amounts of silicates. The deposits may thus be classified as nelsonites. A recent factory building now covers the Eigerøy deposit. The Hestnes vein comprises several varieties of ore defined by the grain size of apatite and magnetite (apatite may vary from 0.5 mm to 5 mm in length, magnetite locally coalesces into 1-2 cm long and 2-4 mm wide "platy" grains), on the apatite content (from 0 - c. 50%), and on the structure of the ore (homogeneous with oriented euhedral apatite or grain size- or modally-layered on a cm to dm scale). The main oxide mineral is an Al-spinel- and Ti-rich magnetite (c. 7% TiO_2 in Hestnes, c. 14% TiO_2 in Eigerøy) with subordinate amounts of homogeneous ilmenite (Tables 5.4-6, Figs 5.2-3). The ilmenites are Cr- and V-poor in the two deposits. The Eigerøy and Hestnes magnetites are quite rich in Cr (c. 1300-190 ppm) compared to the Kagnuden and Rødemyr II magnetites (< c. 600-730 ppm). Apatites in both deposits are REE-rich with large negative Eu anomalies (Table 5. 7; Fig. 5.4). Sulfides are remarkably abundant in the coarse-grained magnetite variety.

Jerneld (J)

The Jerneld deposit consists of several dykes and veins, cutting across the HH anorthosite, far away from the contacts of the massif. The orebodies are made up of coarse-grained hemo-ilmenite (18% Hem) with traces of green spinel and sulfides (predominantly pyrite). Except for rare blebs of plagioclase, the ore is massive and very pure. It displays sharp contacts with the enclosing anorthosite, which is completely devoid of oxide minerals. No magnetite was ever found in this deposit. The hemo-ilmenite shows relatively high contents in V (c. 3200 ppm), the highest amount of Cr (c. 4500 ppm) in the province, high MgO (~5.3%) and Ni (400-500 ppm) contents, as well as a high Ni/Co ratio (Tables 5.4-5; Fig. 5.2).

Vardåsen (Vå)

The Vardåsen deposit is located close to the eastern margin of the ÅS anorthosite. Vardåsen is an elongated body of almost pure ilmenite associated with a north-south striking norite dyke. The contact between the norite and the ilmenite body is transitional, and the relationship is most adequately explained by fractionation processes in a common magma. The norite is poorly layered and consists of plagioclase, ilmenite and Ca-poor pyroxene. Magnetite can be locally present, whereas chromium-rich green spinel is abundant in the ilmenite-rich rock. The Vardåsen ilmenites are very magnesian containing 5.4% MgO.

Flordalen (F)

The Flordalen deposits consist of two essentially bi-mineralic occurrences (Florklev and Store Ålgård gruber) carrying plagioclase in addition to ilmenite. The two deposits are found in a dyke striking northwest-southeast through the Åna-Sira anorthosite. The width of the dyke is up to 15 m but contact relations are ambiguous and the dyke is poorly exposed apart from the sites of former activity. The mineralogy is composed of hemo-ilmenite (4.2-4.8% MgO), with coarse grained hematite exsolutions, and plagioclase, as well as minor amounts of green spinel and occasionally biotite and Ca-poor pyroxene. Texturally, ilmenite is thoroughly equilibrated, forming polygonal aggregates surrounding dispersed euhedral and undeformed

plagioclase grains. The dyke is characterized by an irregular modal layering into plagioclase and oxide-rich layers and lenses. The Flordalen dyke extends for several hundred m and do not qualify as a stable magma chamber within the massive anorthosite. However, the composition and irregular modal layering imply that the dyke most likely did form as a cumulate, possibly fractionating from magma moving along a structural weakness.

Vatland (Vl)

The Vatland deposit is located in the southeastern part of the Håland-Helleren anorthosite. The deposit may be described as a set of veins and dykes, compositionally ranging from pure ilmenite to ilmenite-rich anorthosite. The veins and dykes are from few cm to 1.5 m thick, and have been mined at least three sites over a distance of 200 m in a north-south direction. The dykes are either made up by massive ilmenite or by euhedral plagioclase phenocrysts suspended in an ilmenite matrix. The ilmenite is Mg-rich containing in excess of 4% MgO, and appears to be similar to the Flordalen deposits in the Åna-Sira anorthosite.

Frøytlog (Fl)

Frøytlog is another small ilmenite occurrence associated with a noritic dyke. Generally the mineralogy is made up of hemo-ilmenite, plagioclase and Ca-poor pyroxene, though dispersed grains of magnetite also seem to be present. The ilmenite contains around 4% MgO. The dyke is layered with ilmenite concentrated in cm to dm thick layers.

***

Part II

Itineraries

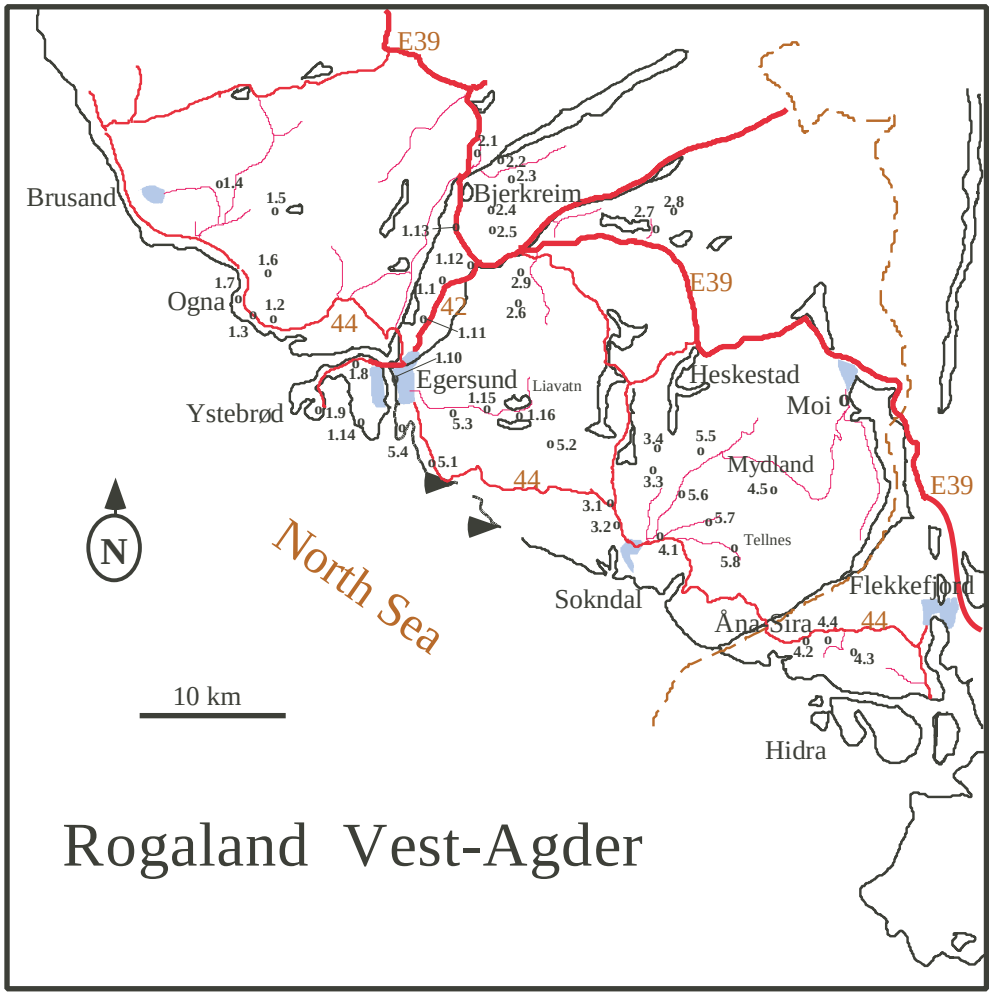

Fig. I 1.0. Itineraries in the Rogaland anorthosite Province

Itinerary 1

THE EGERSUND OGNA MASSIF

(by J.C. Duchesne, J. Vander Auwera, H. Diot, H. Schiellerup and R. Maquil)

The Egersund-Ogna massif is the main topic of this itinerary (Fig. I 1.1). The localities will show various field relationships illustrating its characteristics and demonstrating its emplacement mechanism. En route outcrops of dyke rocks (jotunite, norite or dolerite) will also be visited, as well as remarkable features of the neighbouring units, particularly an ilmenite deposit.

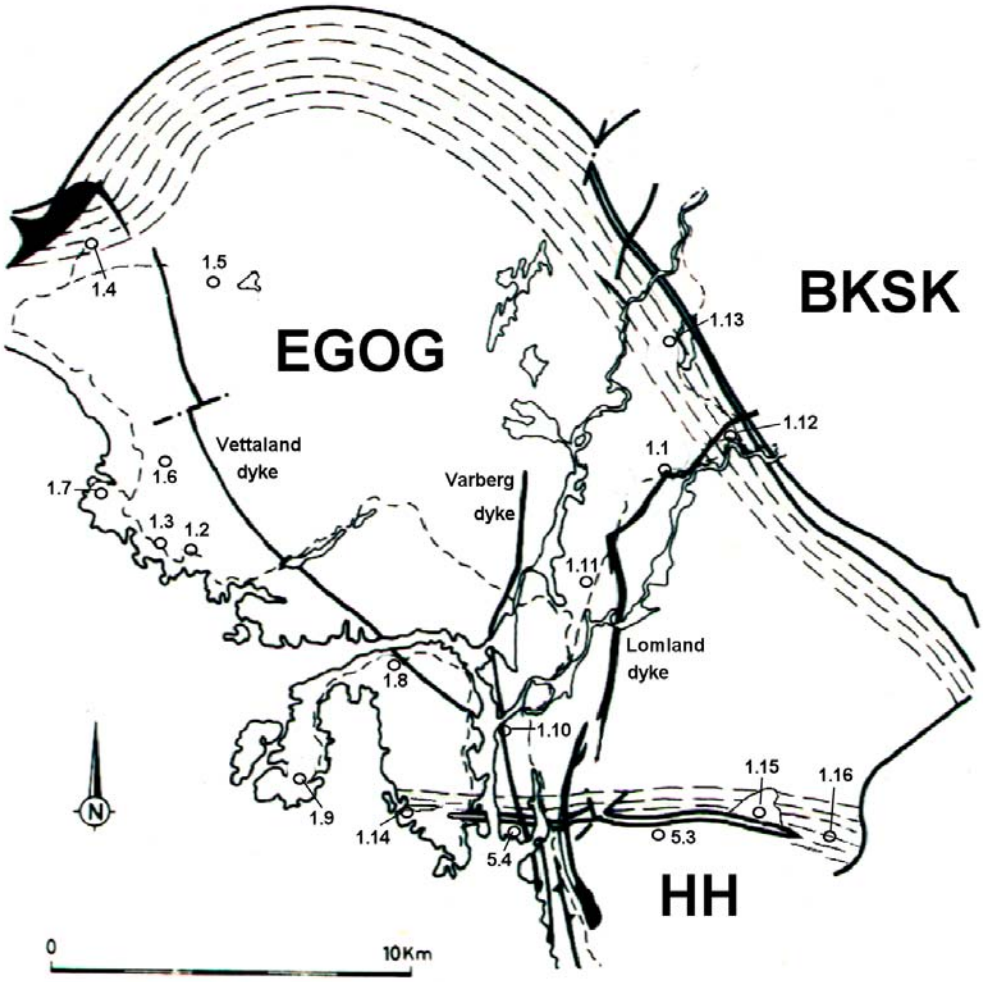

Fig. I 1.1. Itinerary 1 on a schematic geological map of the EGOG massif and its neighbouring massifs Bjerkreim-Sokndal (BKSK) and Håland-Helleren (HH) anorthosite massifs. Figures refer to the stop numbers.

From Moi, take road E39 (E18) to the north. After driving through the Drangsdalen, the road enters the Bjerkreim-Sokndal layered intrusion at Eide. Follow the road through Helleland, then at Krossmoen, take to the left road 9 to Egersund.

Locality 1.1 (1212.2; LK298-900) NESE: THE EGERSUND ANORTHOSITE AND THE LOMLAND DYKE

Road-cut along road 9, at the Klungland bridge over the railway.

- Pinkish to violet, medium-grained anorthosite with some coarser, ill-defined phenocrysts of plagioclase of the same composition as the matrix plagioclase.
- Cutting across the anorthosite, the Lomland dyke of jotunitic to monzonitic composition, which extends over more than 25 km across the Egersund-Ogna massif and its neighbours, the Håland and the Bjerkreim-Sokndal massifs. Fine-grained inclusions and chilled margins. The rock represents the Klungland type (see Duchesne et al. 1985a; 1989), which characterizes the north part of the dyke and contrasts with the Puntavoll type, more noritic (FTP), which occurs in the southern part of the dyke.

Take the road to the Egersund railway station then along road 40 to next point.

Locality 1.2 (1211.1; LK163-867) PIGGSTEIN: THE ANORTHOSITIC-NORITIC COMPLEX.

Stop the car at the boundary of the Egersund District (15 km from Egersund city). Walk over the hills, due north, and follow the district boundary.

- Typical coarse-grained anorthosite, usually weathered, from the central part of the massif, with lenses of leuconorite, megacrysts of orthopyroxene and locally veinlets of hemo-ilmenite.
- On the W side of the valley between the two ponds (Piggsteintjörni and Auratjörni), the outcrops beautifully display the anorthositic-noritic complex. Aggregates of megacrysts of plagioclase (up to 30 cm in length, labradorescent, granulated) forming anorthositic lenses, and of megacrysts of Al-rich opx and plagioclases in sub-ophitic texture (leuconoritic lenses) are embedded in a matrix of finer-grained leuconorite (without opaque minerals), in which the opx display an interstitial “ cuspate ” structure. The aggregates from 2 to 10 m in size are elongated parallel to a plane which also corresponds to a rough orientation of the plagioclase network in the matrix. Rapid variation in grain size of the matrix leuconorite can be observed locally. Some of the leuconoritic aggregates display a recrystallized medium-grained sugar-like texture with granulated and stretched opx. Such texture is transitional to that of leuconoritic gneisses of the marginal zone of the massif.

This outcrop beautifully illustrates the polybaric evolution of the anorthosite. The megacryst aggregates were formed at high pressure (the high Al content of the opx megacrysts indicate 11 to 13 kb) and rose diapicrically in a leuconorite to anorthosite crystal mush lubricated by some leuconorite melt (with Al-poor opx, also Cr poor). The occurrence of deformed and recrystallized inclusions suggests that the deformation took place before the end of the intrusive process and was thus synintrusive.

A short walk SW leads to a small body of brownish leuconorite with a typical fine-grained granular texture and some layering (pyroxene layers), outcropping on the W flank of a small hill. At the roof of the intrusion, several mushrooms of leuconorite penetrate the anorthosite (gravity instabilities) with an ill-defined gneissic texture; clusters of plagioclases constitute small inclusions in the norite. Sulfides (pyrrhotite and pyrite) are concentrated in a pyroxene layer at the wall of the intrusion.

Table I 1.1. Chemical compositions of various rocks from the Egersund-Ogna massif.

Analyse	1	2	3	4	5	6	7	8	9	10	11	12	13
SiO2	53.61	47.63	53.70	53.23	52.67	48.26	51.11	53.28	49.01	50.00	48.21	51.00	54.47
TiO2	0.11	5.45	0.31	1.01	2.11	4.74	1.30	0.17	0.30	0.38	0.30	0.12	0.09
Al2O3	24.84	15.75	17.75	18.41	18.08	15.48	16.48	22.97	24.95	25.23	21.07	24.36	27.85
Fe2O3	1.17	4.04	5.18	2.30	2.71	4.33	2.52	1.14	1.99	1.04	1.94	2.25	0.37
FeO	1.48	10.31	4.53	5.82	7.47	10.52	8.82	3.51	2.87	2.86	5.49	2.51	ND
MnO	0.07	0.15	0.14	0.13	0.13	0.15	0.18	0.18	0.04	0.06	0.09	0.07	0.01
MgO	3.46	6.67	6.87	6.82	4.39	4.71	7.37	5.61	5.49	5.39	9.27	5.17	0.22
CaO	10.04	5.33	6.94	7.84	8.03	7.34	9.02	9.34	10.76	10.97	9.64	10.79	11.39
Na2O	4.80	4.12	3.87	4.17	4.48	3.78	3.42	4.10	3.51	2.98	2.73	3.42	4.99
K2O	0.35	0.61	0.68	0.74	0.79	0.65	0.37	0.25	0.27	0.32	0.43	0.26	0.41
P2O5	0.02	0.06	0.02	0.07	0.11	0.12	0.19	0.03	0.08	0.09	0.06	0.03	0.05
Total	99.95	100.12	99.99	100.54	100.97	100.08	100.78	100.58	99.27	99.32	99.23	99.98	99.85

Sample location and description

1. RMPIG - Piggstein (see loc. 1.2) – Coarse-grained leuconorite of the anorthosito-noritic complex (average of analyses RM79.205, RM79.204.1 and 2)
2. RM78.63 - id. – Fine-grained norite in stockwork
3. RM79.115 - S.Revtja - Noritic pegmatite (without Fe-Ti oxides) (dykes)
4. RM79.108 – Ystebröd - Noritic pegmatite (without Fe-Ti oxides) (dykes)
5. JCD79.10 – Holmevatn - Fine-grained antiperthitic norite (dyke)
6. JCD79.33 – Revtja - Antiperthitic norite (dyke)
7. JCD79.14 – Saglandsvatn (E18) (see loc. 1.13) - Granular norite (dyke)
8. RM77.66.16 - id - Foliated leuconorite
9. JCD64.100 – Krossheim (see loc. 1.12) - Foliated leucotroctolite
10. JCD66.67 - id. Foliated leuconorite
11. JCD66.46 – Kydlandsvatn - Foliated leucotroctolite (se loc. 1.16)
12. RM78.124 – Sirevåg - sugar-like leuconorite (inclusion)
13. JCD00-35 –Sørskog - Labradorescent anorthosite (An_{54}) (see loc. 1.6)

Walk down to the road (parking place) and back to the starting point. Road-cuts display typical coarse-grained, granulated, locally labradorescent anorthosite in which some interstitial opx megacrysts can be observed. Good samples can be found in the embankment of the road. Proceed along road 40 to the North.

Locality 1.3 (1211.1; LK157-875) KALVSHAGEN CENTRAL ANORTHOSITE

(see P. Michot, 1960, point I.B, p.27)

Small abandoned quarry on the right side of the road on top of a small gradient; numerous drill holes in rock and minerals.

- Typical aggregates of granulated, labradorescent, phenocrysts of plagioclase with interstitial megacrysts of Al-rich opx with plagioclase exsolutions (visible with the naked eye), some hemo-ilmenite grains.

The labradorescent plagioclase (Böggild intergrowth) have the following chemical characters: CaO = 11.1% (i.e. An = 55% wt%; K_2O = 0.33%; Sr = 950 ppm; Ba = 62 ppm; Ti = 580 ppm and Rb = 1.3 ppm). Its Sr isotopic ratio is 0.7029 (Demaiffe, pers. comm.). An analysis of the opx megacryst 66.119 is given Table 2.1, anal. 1 and is plotted on Fig. 2.2. NO SAMPLING, PLEASE (sampling is possible at Locality 1.2).

Proceed along road 40 to Brusand, via Ogna. At Brusand, take to the right a gravel road to Brusali and proceed to Haugsenga.

Locality 1.4 (1211.1; LK122-965) W. HAUGSENGA: THE GNEISSIC MARGIN (I)

(see P. Michot 1960, point I.e, p.27).

Stop at the outbuildings of the Haugsenga farm (a few hundred m. south of the main farm). Walk N60E following the tops of the hill towards summit 182 m.

- Leuconoritic and anorthositic gneisses of the inner border of the massif in various stages of deformation and recrystallization. Conformity of the foliation and the place of chemical layering. Megacrysts of Al-opx forming hyge (several metre long) aggregates with plagioclases. Some mega-opx display well-preserved undeformed cores. A variety of deformational textures including granulations, kinkings, granoblastic zones. In less deformed parts the structure can be compared to what is observed at Piggstein (Locality 1.2).
- Dykes of pegmatitic norite, discordant on the general foliation and locally foliated.
- Dykes of undeformed jotunite (N.Rudla) and quartz-norite, with inclusions of quartzo-feldspathic gneisses from the envelope (N.Högeli).

From Haugsenga, go back to the first crossing and take to the left. At the next crossing, take to the right, to Heresvela.

Locality 1.5 (1212.2 ; LK174-949) THE HOMSEVATNET SULFIDE DEPOSIT

At the Heresvela farms, take a gravel road to the East. South of Revtja pound, take to the left up to a private parking place. Walk the path to the summer houses along the eastern Hellevatn, then walk uphill.

The Homsevatnet sulfide deposit is located in the north-central part of the Egersund-Ogna anorthosite about 12 km north-northwest of Egersund (Fig. I 1.1) and is the most significant sulfide deposit in the province. Exploitation took place during the early 1870's (Larsen 1931). A number of small and possibly related occurrences have been found in an elongated area covering 2 to 3 km^2 around Bjørndalsnipa and Ualand, south of the Homsevatnet deposit (Stadheim 1968, Hovland 1975). Mining operations have left a 10-15 m long and 4 m wide incision in the anorthosite host and an 8 m deep shaft sunk into the main sulfide ore (Richter 1943). The shaft is now filled with water.

The deposit is situated within massive anorthosite well away from the foliated and deformed margin of the body. The main occurrence at Homsevatnet and the local geology are shown on Fig. I 1.2. The sulfides occur within a norite pegmatite intrusive into the Egersund-Ogna anorthosite (Henriette 1984).The pegmatite is characterized by numerous metre-sized subangular anorthosite enclaves forming a complex zone with interconnected xenoliths. The grain size varies, and the norite is not universally pegmatitic, and contacts with the surrounding anorthosite may be either sharp or diffuse. The pegmatite consists of equigranular crystals of plagioclase, 3-5 cm in diameter, and a composition of An_{40-43} (965 ppm Sr; 400 ppm Ba) kinked and bent orthopyroxene (En_{52-58}; 2.7-3.6 %Al_2O_3; 70-120 ppm Cr) as well as abundant and large poikilitic grains of hemo-ilmenite (Hem_{20}) and magnetite (Henriette 1984).

A fine grained gabbronoritic dyke striking NW-SE is also present in the Homsevatnet area. The dyke cuts across both the anorthosite and norite pegmatite, but no contacts with the sulfides have been observed. The gabbronorite consists of granulated equigranular ~1 mm

plagioclase (An_{40}) and oriented subhedral orthopyroxene ($En_{54}Fs_{44}Wo_2$) of similar size. The amount of clinopyroxene ($Wo_{44}En_{36}Fs_{20}$) is somewhat smaller than that of orthopyroxene, and the dyke also contains small amounts of hemo-ilmenite (Hem_{12}) (Henriette 1984). The dyke represents the youngest magmatic event in the area.

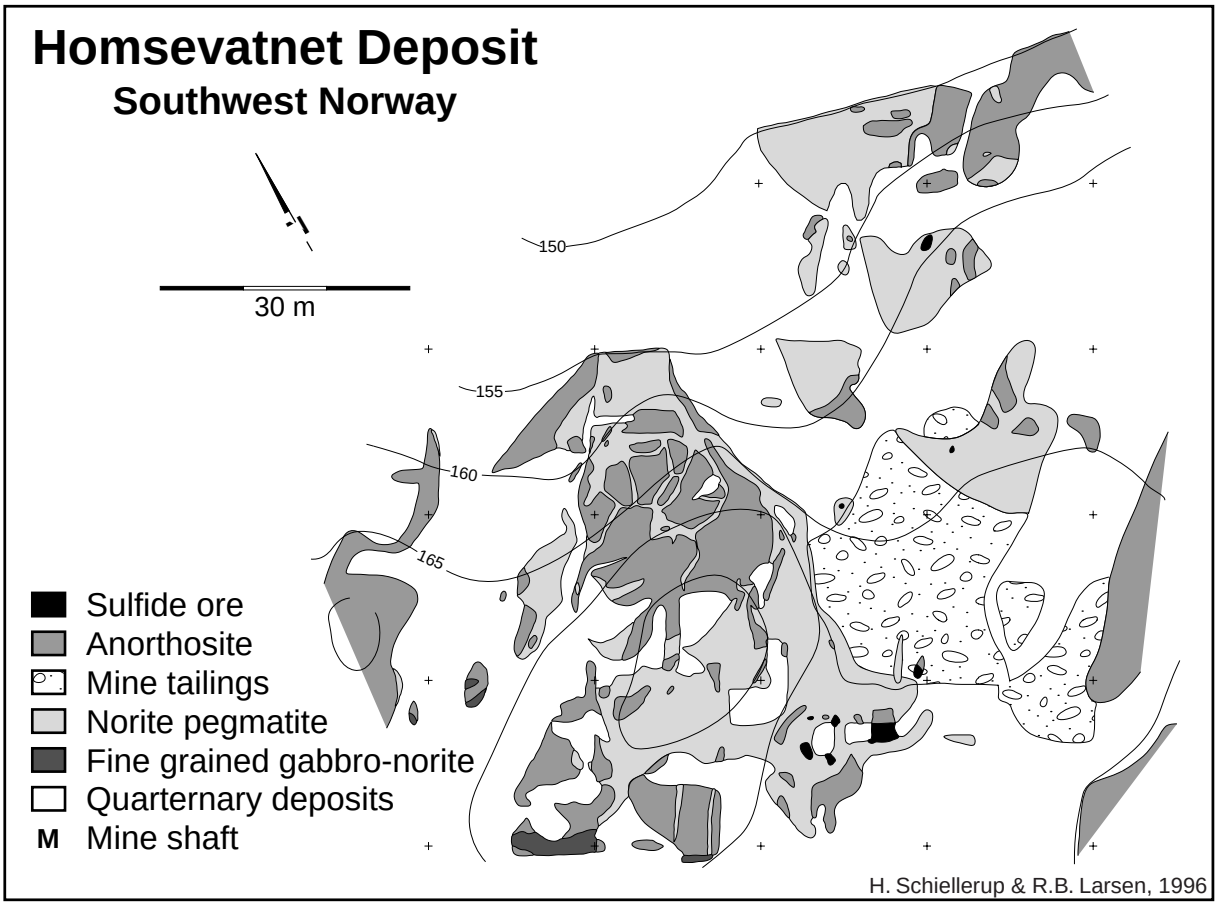

Fig. I 1.2. Geological map of the Homsevatnet sulfide deposit in the EGOG anorthosite.

The main sulfides are found in massive form as a m-sized dyke-like or lenticular body, whose primary outline and characteristics have been obscured by exploitation. The sulfides are dominated by 2-5 cm large subhedral grains of pyrrhotite. Large pyrrhotites are often twinned or kinked in response to stress, implying that sulfide deposition (and formation of mono-sulfide solid solution (mss)) took place prior to the final emplacement of the anorthosite. A Ti-magnetite (with rare ilmenite lamellae and rims) is also present and was most likely the first phase to precipitate from the sulfide melt. Pyrite is a subordinate phase and appears as sub- to euhedral 0.5 mm grains, generally in elongated aggregates along grain boundaries of larger pyrrhotite grains. These pyrites are often enveloped by chalcopyrite. Early pentlandite forms larger (~1 mm) grains or aggregates included in pyrrhotite along cracks or grain boundaries. A later generation of pyrrhotite is found in veins transecting both the early pyrrhotite phenocrysts and the chalcopyrite. The Homsevatnet deposit is zoned with a central massive pyrrhotite-dominated ore surrounded by a marginal disseminated or stringer-type ore dominated by chalcopyrite. Sulfide-filled stringers and fractures in silicate grains surrounding the ore bodies are almost universally monomineralic, consisting entirely of chalcopyrite. This mode of occurrence does not seem to be consistent with an origin of chalcopyrite exclusively by exsolution from a homogeneous monosulfide solid solution (mss) but requires that the marginal chalcopyrite-dominated ore crystallized from a copper-enriched sulfide melt. In this

respect the Homsevatnet deposit is a small scale representative of world class magmatic sulfide systems such as Noril'sk and Sudbury where marginal "breccia matrix ore" or "footwall" orebodies are similarly enriched in Cu (Schiellerup et al. in prep.).

Subsequently, the pentlandite grains were almost completely replaced by violarite, in rare cases leaving small equant grains of pentlandite embedded in violarite (Photo I 1.1). Incipient alteration of pyrrhotite along cleavage and grain boundaries is conspicuous, the alteration products most likely being the magnetic monoclinic pyrrhotite also detected by XRD. Later dissolution along cracks led to the formation of goethite veins transecting all ore minerals and, to a lesser extent, veins filled with fine-grained marcasite and pyrite aggregates.

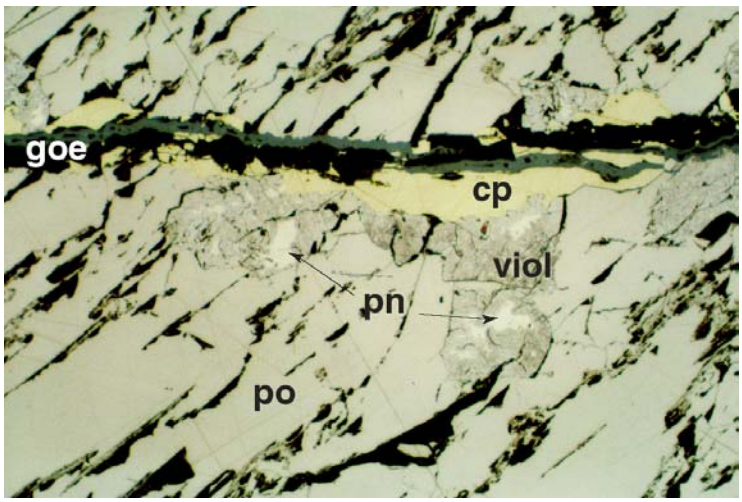

Photo I 1.1. Sulfide sample from the Homsevatnet deposit showing pyrrhotite (po) partly embedding violarite (viol). The violarite grains contain small angular relicts of pentlandite (pn). Exsolved chalcopyrite forms along pyrrhotite grain boundaries and is, in this section, transected by a late goethite-filled crack. Displayed section is 0.5 mm wide.

The primary sulfide paragenesis consisting of pyrrhotite, pentlandite, chalcopyrite and subsidiary amounts of pyrite is conspicuously magmatic in character and a hydrothermal origin is very unlikely. Average Cu, Ni and Co contents of the sulfides are 0.7, 0.7 and 0.15%, respectively (Henriette 1984; Schiellerup et al. in prep.). Pt is <4.3 ppb and Pd ranges from 3 to 9 ppb (Schiellerup et al. in prep.).

The massive sulfide contains several types of inclusions (Henriette 1984): (1) equal sized granoblastic anorthosite inclusions (also found in the noritic pegmatite). The plagioclase has a composition (An_{58}, 834 ppm Sr, 111 ppm Ba) similar to high pressure plagioclase megacrysts (see Fig. 2.6); (2) 1-3 cm sized plagioclase phenocrysts: An_{39-40} with c. 800 ppm Sr and c. 350 ppm Ba, similar to plagioclase from the noritic pegmatite; (3) opx mega-phenocrysts (undeformed) chemically similar to the pegmatite pyroxene; (4) “ocellar” aggregates of interfingered opx ($En_{48}Fs_{49}Wo_3$) and cpx (from $Wo_{33}En_{36}Fs_{31}$ to $Wo_{45}En_{34}Fs_{21}$), with interstitial plagioclase and homogeneous ilmenite (<Hem_9) and some sulfides. Similarities in composition between the plagioclase and opx phenocrysts included in the sulfide and the same minerals in the norite pegmatite point to an origin of the sulfide as an immiscible liquid in the norite pegmatite. On the other hand, the ocellar pyroxenite cannot have crystallized from an immiscible silicate melt in the sulfide liquid, as the rounded shape would suggest, because it contains ilmenite and not Ti-magnetite as is the case in the sulfide. Equilibrium between two immiscible melts indeed requires crystallization of identical phases in the two melts. The most likely mechanism of formation of these ocellar pyroxenite is thus fractional crystallization from the sulfide melt itself (Henriette 1984).

Re-Os isotopes and R-factor modeling of trace elements suggest that an external source of sulfur is not required. The sulfide occurrences most likely result from the differentiation of primary, relatively sulfur-rich silicate magmas (Schiellerup et al. in prep.). The isochronous relationships recorded between anorthosites, mafic rocks, Fe-Ti ore deposits and sulfides, as

discussed by (Schiellerup et al. 2000), imply that the sulfides and their host intrusions were derived from sources of similar composition. Os and Nd isotopic modeling give strong indications that the sulfides, as well as the unmineralised anorthosites and norites, are primarily crustal derivatives (Schiellerup et al. 2000).

Back to Brusand, then take road 40 towards Egersund. Circa 400 m. before the bridge over the railway at Sirevåg, take a gravel road to the left.

Locality 1.6 (1212.3 ; LK161-895) SØRSKOG : DIMENSION STONE QUARRY

Take a gravel road from Sørskog farms to the East (private road) and climb up to a quarry in operation.

- Beautiful exposures of anorthosite and leuconorite showing 3-5 cm iridescent zoned plagioclase with blue and green colors (An_{55}). Small opx megacrysts.
- Fine-grained dolerite dykes related to the Egersund dyke swarm.

Back to road 40 towards Egersund. Circa 500 m. past the bridge over the railway at Sirevåg, take a gravel road to the right and follow the indication to a “Krigsminne” (war monument).

Locality 1.7 (1211.1; LK133-891) VETEN: GNEISSIC INCLUSIONS IN THE ANORTHOSITE (I)

Stop at the parking place of the“ Krigsminne ” of Veten and walk on top of the hills, around second world war fortifications.

- Typical medium-sized equigranular pinkish anorthosite, with rare phenoclasts of plagioclase, containing various metre-sized inclusions of anorthositic to leuconoritic, granoblastic (sugar-like) gneisses, tilted in all orientations.

Back to Egersund by road 40. En route, at the end of Hellvik pool, overview from the road on a “ White Stone ” quarry - altered anorthosite (kaolinitization). At about the Egersund railway station, after crossing the bridge, take to the right the road to Ystebrød.

Locality 1.8 (1211.1; LK216-846) STIGEL: VETTALAND DYKE

- The dyke is crossed by the road. It has a granular texture and a quartz noritic composition. Though its major element composition is very similar to the rest of the dyke, the trace element composition is frankly different: here the dyke displays the Eigeröy type (depletion in large ion lithophile elements, bell-shaped REE distribution with a positive Eu anomaly) (Duchesne et al. 1985b; 1989)).

Follow the road to the end, then a small path southward.

Locality 1.9 (1211.1: LK195-815-191 810) YSTEBRØD: NORITIC PEGMATITE AND GNEISSIC INCLUSIONS (II).

(See P. Michot 1960, Point I.B, P.27)

- The path cuts across a stockwork of noritic pegmatites (with Fe-Ti oxides), forming dykes with sharp contacts with the anorthosite and extending over the entire northern side of the bay. Two types of opx and plagioclases can be distinguished in the field: (1) small opx megacryst (up to 10 cm) with plagioclase exsolutions, locally kinked and granulated, coexisting with large plagioclases, usually irregularly granulated; (2) oikocrysts of Al-poor opx (up to 10 cm in diameter) containing small euhedral, locally undeformed plagioclases.

Ilmenite can also form smaller oikocrysts. Our interpretation is that the intruded material consists in aggregates of plagioclase and opx megacrysts formed at a higher pressure and lubricated by a noritic melt which crystallises in the interstices to form oikocrysts (Duchesne 1984).

Some of the blocky inclusions are obviously xenolithic (see below) and have been carried in the noritic pegmatite. This raises the possibility that all blocky anorthosites might be inclusions in the norite pegmatite (Robins, pers. comm.).

- Further south, on the other side of the bay, several large xenoliths of anorthositic and leuconoritic banded gneisses, tilted in various positions, are embedded in the noritic pegmatite. The inclusions are similar in texture and plagioclase geochemistry (Fig. 2.6) to the leuconoritic gneisses of the margin of the massif (Duchesne & Maquil 1981). A small vein of anorthositic material is injected across an inclusion and merges into noritic pegmatite.

Photo I 1.2. Blocky inclusion of leuconoritic banded gneiss embedded in noritic pegmatite. Ystebrød, locality 1.9.

Note that the tilted inclusions were good evidence for Michot (1960) of an igneous origin of the anorthosite in contrast with the metasomatic views of that period) and also of the existence of an old anorthosite basement, rejuvenated by leuconoritic anatexis. These inclusions are now interpreted as fragments of the deformed margin of the massif (due to syn-emplacement deformation) (Maquil & Duchesne 1984).

Back to Egersund.

Locality 1.10 (1211.1; LK245-828) VARBERGKAIEN: THE VARBERG DYKE

In the town centre take the Strandgata (street) to the mouth of the harbour. Behind the Customs building along the Varbergkaien, the road cut exposes the Varberg dyke. This is ca. 150m thick, dipping 60 W and is typical jotunite (with large poikilocrysts of opx of about 1 cm in diameter) (Duchesne et al. 1985b; 1989). Fine-grained chilled margin (also with poikilocrysts of opx!) of 5-10 cm thick can be found at the wall of the dyke. At the roof of the dyke, a satellite dykelet (50 cm thick) also of fine-grained jotunite is present.

Back to centre of town. Take road 9 northward.

Locality 1.11 (1212.2; LK281 895) SLEVELAND: DOLERITIC DYKE

Just opposite the entrance of the gravel road to Sleveland's farm is a doleritic dyke ca.1m thick, with aphanitic (vitrous margins). It belongs to the Egersund WNW-ESE dolerite dyke system (Bingen et al. 1998).

Proceed along road 9 towards the junction with road E39 (E18).

Locality 1.12 (1212.2; LK293-935) KROSSMOEN: THE GNESSIC MARGIN (II)

Last road-cut on the left before the junction with road E39 (E18).

Typical leuconoritic gneisses, with some leucotroctolitic layers (Fo_{70} + An_{67}) (difficult to identify without a microscope) from the marginal deformed zone of the Egersund-Ogna massif. Some discontinuous layers of recrystallized opx, locally with preserved cores.

The plagioclases of the gneisses of this outcrop are amongst the highest in anorthite content found in the massif (up to An_{74}); they are low in Sr (350-450 ppm), K_2O (<0.1-0.3%), Ba (<100 ppm) and Rb (< 0.5 ppm) (see Fig. 2.5 (Duchesne 1967; Duchesne & Demaiffe 1978)). The $^{87}Sr/^{86}Sr$ initial ratio is 0.7040 (Duchesne & Demaiffe 1978).

Proceed along road E39 (E18) to the North.

Locality 1.13 (1212.2; LK293-935) SAGLANDSVATN: THE GNEISSIC MARGIN (III).

Spectacular road-cut along Saglandsvatn (about 3 km north of the preceding locality) showing on both sides of the road coarse-grained leuconoritic gneisses. Giant opx stretched along the foliation plane (80°E) over distances up to tens of metres. Various degrees of deformation of the opx can be observed: (nearly) undeformed cores, kinkings, granulated zones, recrystallized granoblastic lenses and layers.

The anorthosite content of the plagioclases varies between An_{60} and An_{70} (Fig. 2.5). As in the preceding outcrop, the Sr content is remarkably low (ca 380 ppm) as well as K_2O (0.16-0.40%) and Ba (<20 ppm-75 ppm).

The opx varies between En_{70} and En_{60}. (Fig. 2.2) and the Al content between 1.5 and 3.0% Al_2O_3, the more recrystallized varieties tending to have the lowest Al contents (Maquil and Duchesne 1984). Undeformed cores still show plagioclase exsolutions and have a bulk Al-content of about 5.5% Al_2O_3 (see Table 1.1 and Fig. 2.3). The transition trace element contents are similar to those from opx megacrysts from the central part of the massif, except for Cr which is definitely higher in the opx from the margin (Figs. 2.3-4).

Photo I 1.3 Leuconoritic foliated margin of the EGOG massif. Road E39, locality 1.13.

Back to Egersund.

Locality 1.14 (1212.2; LK218-802) THE LØYNING LAYERED SILL

At the Egersund railway station, take the road to the Eigerøya island, cross the bridge and immediately after take to the left. After 2.8 km take the small road to the right up to Løyning. After the farms, walk along a path down to the seashore.

The small Löyning body (1.5 km x 200 m) is a layered sill, intruded in the contact zone between the southern foliated margin of the Egersund-Ogna anorthosite and the Håland anorthosite (Ernst 1990; Ernst & Duchesne 1991) (Fig. I 1.3). The contacts between the Löyning body and the enclosing anorthosite are sharp and concordant. The layering dips 70°S and, as indicated by small-scale modally graded layers, the body is slightly overturned. The body is made up of two units: a lower layered mafic to ultramafic unit and an upper more massive leuconoritic unit. The Lower Unit is composed of norites, melanorites as well as of a minor amount of pyroxenites occurring as dm to pluri dm-thick layers. An olivine-bearing melanorite has also been recognized close to the southern contact. The Upper Unit is made of a relatively homogeneous leuconorite. Several anorthositic to leuconoritic dykes originating from the Upper Unit crosscut the anorthosite (Duchesne et al. 1991). Rocks of the two units are fine-grained and the contact between both Units is progressive. Field and petrographic evidence suggest that the Löyning body has been deeply deformed: a lineation is locally present.. Mineral compositions display a modest variation from base to top: An_{59} to An_{38} for plagioclase, Fo_{68} to Fo_{63} for olivine, Mg#68 to 58 for orthopyroxene, Hem>18 to < 9 for ilmenite (Ernst 1990). In thin section, orthopyroxene and plagioclase are usually

hypidiomorphic whereas ilmenite and clinopyroxene are interstitial. The texture is granoblastic. Mineral compositions and modal abundances suggest that the parent magma of the Löyning body is close to a primitive jotunite (Vander Auwera et al. 1998).

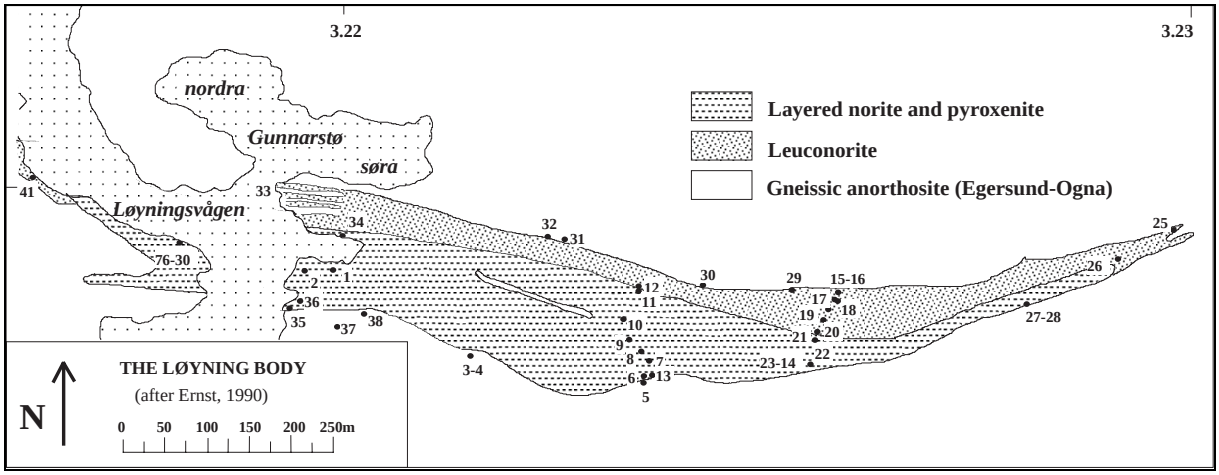

Fig. I 1.3. Geological map of the Løyning layered sill (after Ernst 1990)

Back to Egersund.

Locality 1.15 (1212.2; LK306-804) THE KOLLDAL LAYERED INTRUSION

From Egersund take the road to Kolldal.

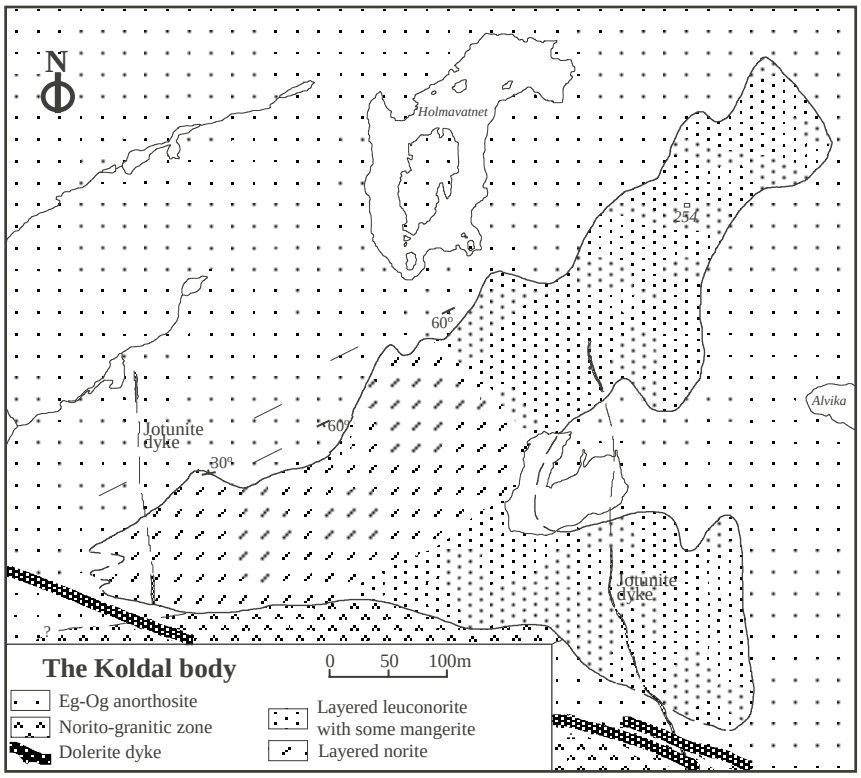

Fig. I 1.4. Geological map of the Kolldal layered intrusion.

The Kolldal body is also intruded in the southern marginal border of the Egersund-Ogna anorthosite at the contact between this anorthosite and the norito-granitic zone of Puntevold-Lien (Piron 1981) (Fig. I 1.4). The contacts between the body and the surrounding rocks are discordant and numerous inclusions have been observed. Detailed field data suggest that this small massif is lens-shaped and dips slightly towards the north. It clearly crosscuts the sub-vertical foliation of the Egersund-Ogna margin. In the south it displays a sub-vertical contact with the norito-granitic zone of Puntervold-Lien. It can be divided in two broad zones grossly oriented NE-SW: a noritic to leuconoritic zone containing some mangerites to the North and a coarse grained leuconorite to the South. The northern contact of the body with Egersund-Ogna is sub-horizontal and underlined by a fine-grained leuconorite. A m-sized jotunitic dyke is intruded in the anorthosite roof parallel to the contact. Mineral compositions display the following ranges: An_{38}-An_{44} (plagioclase), En_{53-66} (orthopyroxene), Hem_{7-20} (ilmenite). Apatite is absent in the coarse grained leuconorite and present in the upper part of the intrusion. Moreover, magnetite is more abundant in the upper part.

Locality 1.16 (1212.2; LK326-801 to 330-796) THE LIÅSEN SECTOR

From Kolldal, carry on by the same road to Heggdal and at the crossing take to the left up to the Liavatn mouth. Walk southward on the eastern bank of the stream.

This cross-section permits to observe a continuous transition from typical foliated leuconorite from the margin of the EGOG massif to the Håland anorthositic massif and an ilmenite deposit.

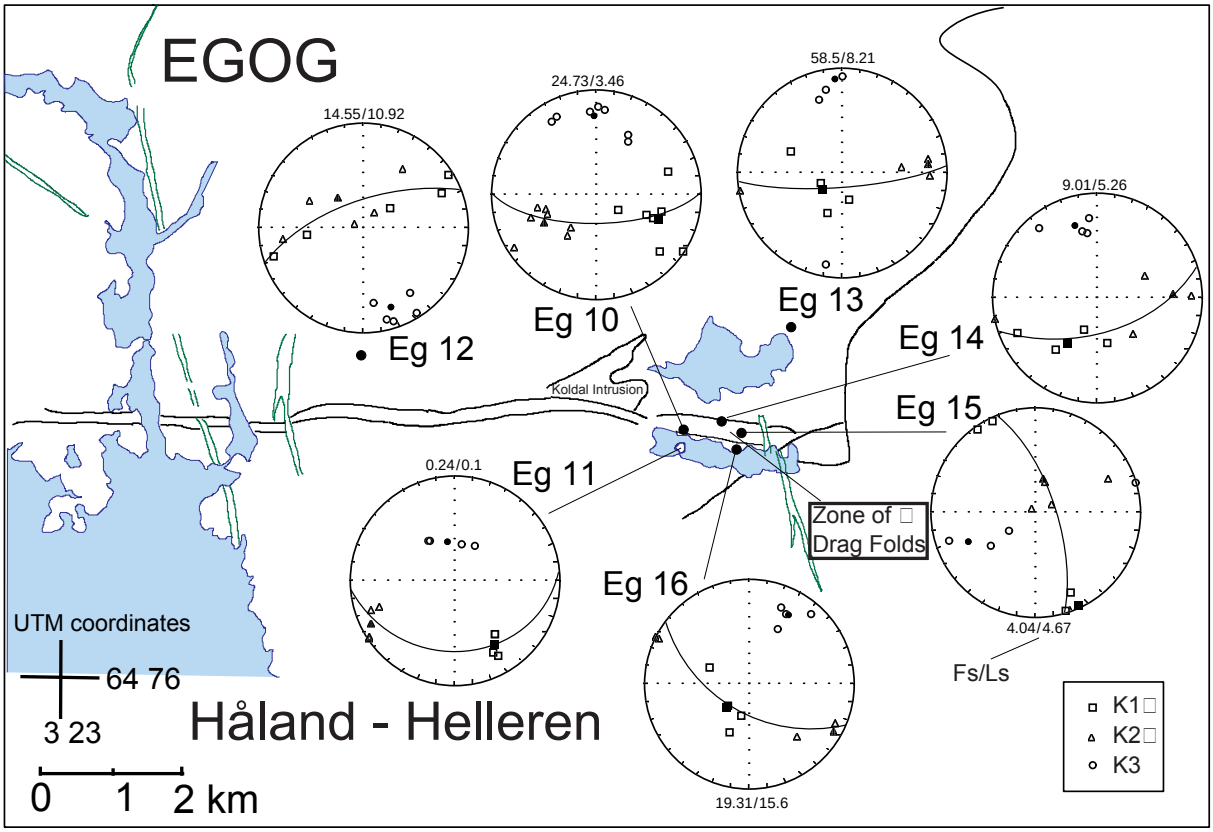

Fig. I 1.5 Magnetic foliations and lineations in the anorthosite and leuconoritic gneisses. Schmidt projections of K_1(□), K_2(Δ) and K_3(○) axes of the magnetic susceptibility ellipsoid (full symbols represent average values) at various localities (from Lambert 1998).

Typical E-W trending deformed margin of the EGOG massif made up of foliated leuconorite dipping to the South (Fig. I 1.5). The rocks display all variants in deformation intensity of an anorthosito-leuconoritic complex with variable grain size yielding a variety of lithologies from coarse- to fine-grained anorthositic, noritic and pyroxenitic gneiss. The texture is strongly granoblastic with granulated opx stretched along the foliation plane sometimes over distances of several metres. The rock becomes gradually enriched southwards in quartz lenses and bands. Lenticular bodies alternating layers of granitoidic and noritic composition become more common (most probably inclusions of migmatitic gneiss from the envelope). Metric to decametric folds are beautifully exposed. One of them shows an asymmetrical shape resulting from a cinematic amplification of a mechanical discontinuity, which points to the uprise of the central part of the massif relative to its border (Fig. I 1.6). This relative shear movement of EGOG and Håland (diapirism of EGOG - sinking of Håland) has first produced the strong foliation of the EGOG margin and then the folding of this foliation. The B-axes of these folds evolve from a "b" to an "a" position but never reach a sheath fold shape, and their attitude never overtake a 45° dipping. No lineation is preserved on the foliation surfaces because of the strong recrystallisation of the rock during deformation. The sense of shear is mainly recorded by the asymmetric shape of stretched mega-opx and of drag folds.

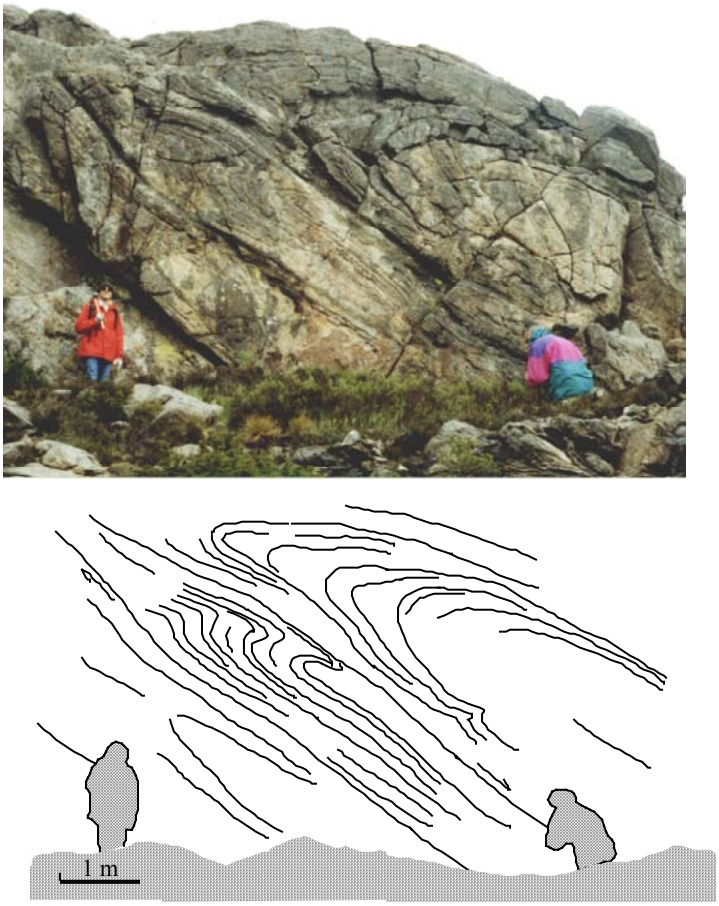

Fig. I 1.6. Drag fols in the EGOG foliated margin. The central part of the EGOG massif is on the left of the photo and the foliation is dipping to the south.

- This formation is followed by a 100-150 m-thick leuconoritic unit, less deformed, more massive but with thin lenses and discontinuous mafic layers. The rocks are coarser-grained, the occurrence of Fe-Ti oxides is conspicuous and the opx displays an interstitial poikolitic

structure. This overall igneous-looking aspect was noted by Michot who considered it as resulting from an in situ leuconoritic anatexis (in Hubaux 1960). This hypothesis is no more considered nowadays.

- A 50m-thick unit follows. It is made up of a fine-grained sugar-like norite containing lenses of anorthosite and of pyroxenite. Petrographically the grain size does not appear to result from a deformation process: the plagioclase is antiperthitic, much larger than the mafics and with irregular contours, a granular texture which suggests a rapidly cooled magma. Geochemically is a high-alumina gabbro with relatively high Al_2O_3 (18.6 %) and TiO_2 (2.4 %), low K_2O (0.37%) and P_2O_5 (0.01%) and Mg#=0.45 (Lambert 1998), similar in composition to the high-alumina gabbros in the Laramie anorthosite complex (Mitchell et al. 1995). A distinct positive Eu anomaly and the presence of anorthosite and pyroxenite inclusions suggest a crystal laden liquid.

Photo I 1.4 Layers of ilmenite ore in anorthosite (Kydlandsvatn deposit, Liaasen sector).

- After a more foliated zone resembling EGOG highly deformed margin (but with oxide minerals!), one enters an anorthosite with layers of Fe-Ti oxide minerals. This zone extends on the whole northern shore of the Kydlansvatn where evidence of old mining activities in the thickest layers (1-2 m) are numerous (see Appendix of Chapter 5 for more extended description of the Kydlansvatn deposit). Here in this section, the mafic layers (1-5 cm thick), interleaved with anorthosite layers, are made up of hemo-ilmenite (ca Hem_{20}) with traces of aluminous spinel, characteristic of type I deposits (though the major Kydlansvatn occurrences belong to type II, see Chapter 5). Ilmenite layers form bundles that wrapped anorthosite lenses and boudins, and display folds and other evidence of high-

temperature deformation. Cr_2O_3 contents in ilmenite vary between 343 and 1547 ppm (12 samples) and a southward increase is suggested. V_2O_3 varies between 0.3 and 0.4 %, and Ni between 187 and 317 ppm, with a very coarse positive correlation between Ni and Cr (0.5). An interpretation of the Kydlansvatn deposit is given in the Appendix of Chapter 5.

- The section ends in the Håland massif which shows beautiful relationships between anorthosite enclaves and coarse grained ilmenite bearing leuconorite.

Back to Egersund and Moi.

***

Itinerary 2

THE BJERKREIM - SOKNDAL INTRUSION

(by Brian Robins and J. Richard Wilson)

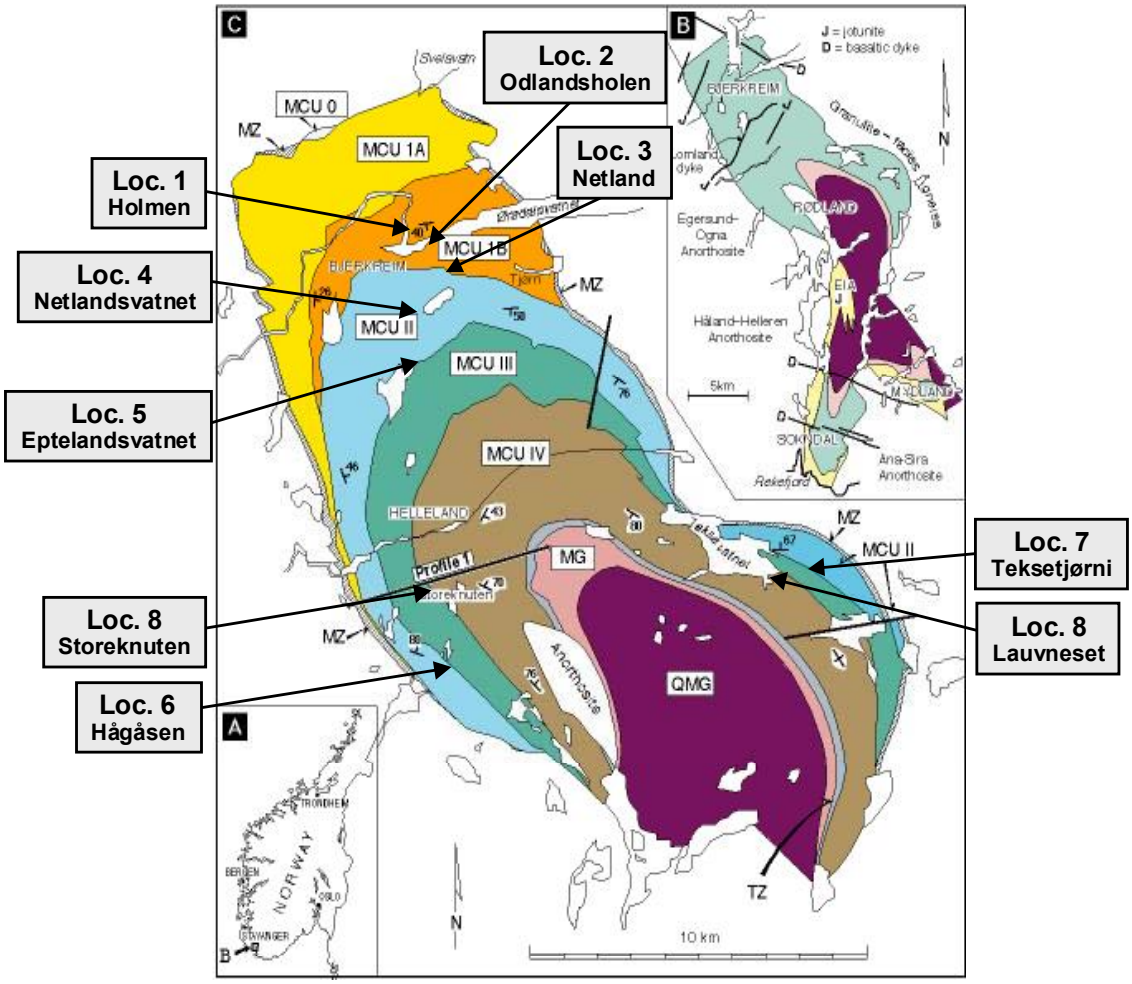

Fig. I 2.1. Localities in the Bjerkreim-Sokndal Intrusion described in the guide

Locality 2.1 (1212 II; LK319-001 to LK320-985): TRAVERSE THROUGH THE LOWER PART OF MEGACYCLIC UNIT IB. HOLMEN TO ODLANDSHÖLEN.

(by Brian Robins)

Description: The traverse commences in plagioclase cumulates (pC) (mainly leuconorite) southeast of the farm at Holmen, near the base of MCU IB. They contain plagioclase with a bimodal size distribution and intercumulus orthopyroxene and ilmenite. Both the megacrystic and smaller plagioclase crystals are laminated. Xenoliths of anorthosite similar to that found in the nearby Egersund - Ogna Massif are common. Note the substantial thickness of pC. To the southwest this zone gradually thins and eventually disappears near the Berse lake. Further southwards along the traverse, pC is succeeded stratigraphically by plagioclase-ilmenite cumulates (piC) with faint modal layering and numerous rafts of mafic granulite and then strongly-layered plagioclase-orthopyroxene-ilmenite cumulates (phiC). The succession reflects the sequence of crystallisation (plagioclase → ilmenite → orthopyroxene) of the parental magma. In the upper part of the zone of piC there is a horizon particularly notable for

its content of anorthosite blocks. In the phiC at the south end of the traverse there are abundant, thin but laterally-persistent modally-graded layers, in which plagioclase megacrysts are concentrated in the plagioclase-rich layer tops. The modally-graded layers are separated by thicker isomodal phiC layers, and the basal contacts of some modally-graded layers are disconformities. The more mafic cumulates which form a knoll on the opposite (west) side of the river are more-evolved plagioclase-orthopyroxene-Ca-rich pyroxene-ilmenite cumulates (phciC) that occur higher up in MCU IB. They are preserved in a downthrown fault block.

Mineral compositions. Plagioclase in pC towards the base of MCU IB along this traverse is around An_{45}, significantly more calcic than at the top of the underlying phiC (An_{41}). Variation within the pC zone is slight, but in the phiC and overlying phciC the An content decreases from 45 to 42. No clear systematic variation in the Mg# of Ca-poor pyroxenes has been detected in this traverse; it varies in the range of 68.5-67. The lowest of these values are, however, found in the phciC towards the top of the unit.

Locality 2.2 (1212 II ; LK324-985): XENOLITHIC pC (MCU IB). SOUTH SIDE OF ODLANDSHOLEN.

(by Brian Robins)

Description: A major NE-SW fault (with a downthrow to the north) repeats the succession seen in the previous traverse on this southern side of the Ørsdalen valley. In this recently excavated surface numerous large blocks and slabs of anorthosite and leuconorite are clearly visible enclosed in leuconorite (pC) belonging to the lowermost unit of MCU IB. These xenoliths appear to have been derived from the adjacent Egersund-Ogna Anorthosite Massif, and are particularly abundant in the lowermost parts of MCUs IA & IB.

Locality 2.3 (1212 II ; LK334-983): BOUNDARY BETWEEN MCU IB AND II. ROADSIDE EXPOSURES BETWEEN NETLAND AND HYTLAND.

(by Brian Robins)

Description: Proceeding down the hill, road cuts expose the transition from phiC, forming the central zone of MCU IB, to plagioclase-orthopyroxene-Ca-rich pyroxene-ilmenite cumulates (phciC) (hand lenses are essential!), the most evolved cumulates in MCU IB in this area. Further to the west, the phciC is overlain by a thin layer of gabbronorite in which magnetite and apatite are cumulus minerals. In the lowest exposures, a 2m thick ilmenite-rich transition zone between the top of MCU IB and pC forming the lower part of the thick MCU II can be examined. This regressive zone of phiC reflects the entry of more-primitive magma into the chamber in which the cumulates were crystallising. The overlying pC characteristically contains magnetite, as do the troctolites that occur near the bases of MCUs III and IV, but evidence of cumulus olivine has only been discovered at a single locality near the base of MCU II.

Mineral compositions. The upper part of MCU IB at this locality contains An_{43} and pyroxenes with Mg#s of 64-68 (Ca-poor) and 72-78 (Ca-rich). The pC at the base of MCU II contains An_{49-51}.

Locality 2.4 (1212 II, LK321-970): Cm-SCALE LAYERING AND CROSS BEDDING. ROADSIDE EXPOSURE ABOVE A SMALL STREAM, W. OF NETLANDSVATNET.

(by Brian Robins)

Description: At this locality phiC in the central part of MCU II exhibits several sets of cross-lamination. Such structures are fairly rare in the intrusion, but are important in indicating the ability of currents moving along the floor of the magma chamber to erode unconsolidated cumulates and to transport and redeposit cumulus crystals elsewhere.

Locality 2.5 (1212 II, LK327-956): BOUNDARY BETWEEN MCUs II AND III. EPTELANDSVATNET - SHORT TRAVERSE FROM NORTH TO SOUTH ALONG THE BLUFFS ABOVE THE NE-END OF EPTELANDSVATNET.

(by Brian Robins)

Description: The traverse starts in rather massive phiC at the top of MCU II. This is followed stratigraphically by a thin sulphide-bearing subunit that occurs at the base of MCU III. This subunit consists of rusty, massive ilmenite norite, strongly- to intensely-layered mafic ilmenite norite or massive orthopyroxenite. This subunit can be traced discontinuously around the whole of the Bjerkreim lobe of the BKSK, a distance of more than 30 km. The main sulphides are pyrrhotite, chalcopyrite and pentlandite (Cu/Cu+Ni ≈ 0.5). Sparse secondary pyrite occurs locally.

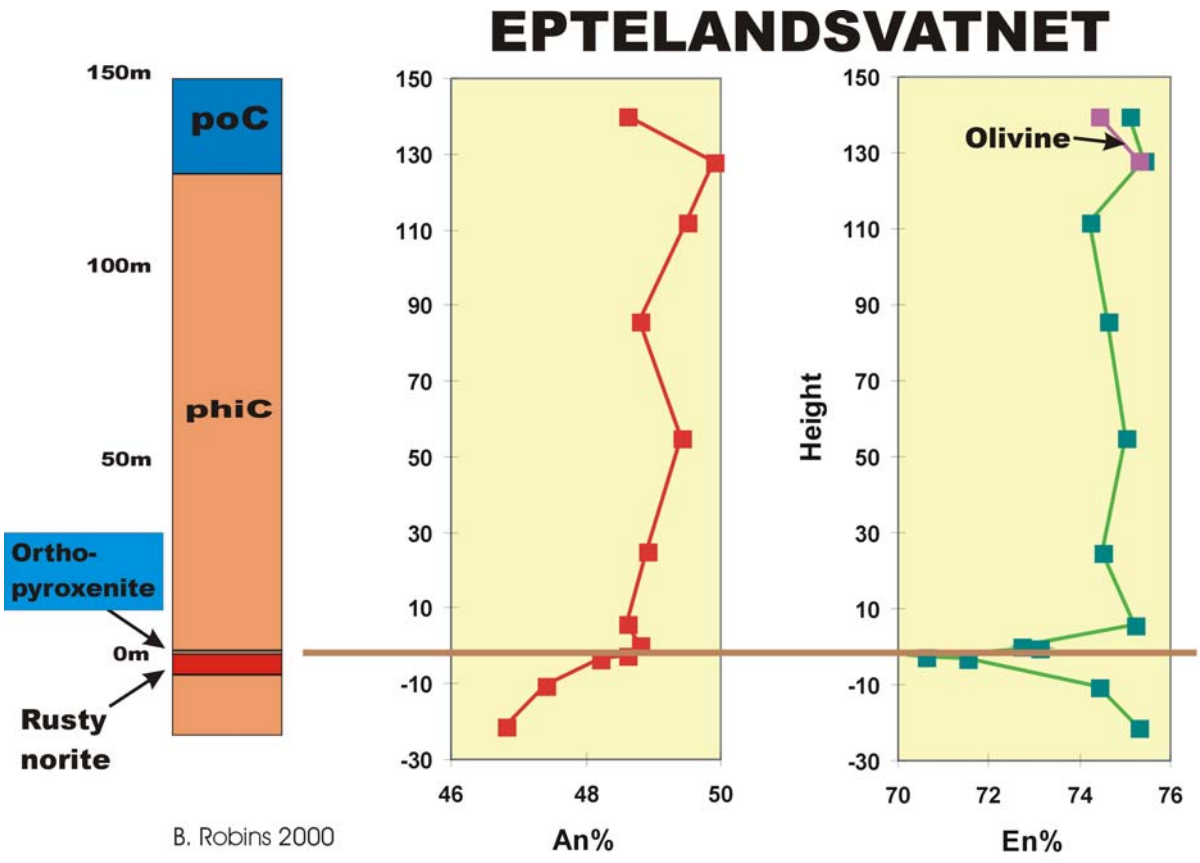

Fig. I 2.2. Cryptic variation in plagioclase and orthopyroxene across the MCU II/III contact at Eptelandsvatnet (loc. 2.5). Based on work by Kristine Krogh Jensen.

Assays have shown that the sulphides contain insignificant concentrations (< 40ppb) of PGE + Au. The sulphide-bearing subunit is overlain by leuconorites that in places are characterised by pronounced modal layering in which layers rich in cumulus plagioclase alternate with ilmenite and orthopyroxene-rich layers (intruded in this traverse by a basalt sheet probably belonging to the Egersund dyke swarm). These are followed by rather massive pC or phiC which grades(?) into coarse-grained, plagioclase-olivine, zone IIIb cumulates. Cumulus olivine is not always visible in the poC; it is commonly replaced by orthopyroxene (due to reaction with intercumulus melt) or fine-grained, symplectitic intergrowths of orthopyroxene and magnetite (due to subsolidus oxidation). Olivine can, however, be identified with a hand lens on glaciated pavements along the sides of the stream at the southern end of the traverse. Further to the south, the troctolites are succeeded by modally-layered phiC with rare slump structures. The traverse demonstrates a stratigraphic sequence different from that of MCU IB & II suggesting that the magmas which periodically flowed into the chamber varied in composition.

We can return by walking to the northeast and then following the sulphide-rich subunit southwestwards back to Eptelandsvatnet. This subunit is generally underlain by up to 10 metres of rusty leuconorite with disseminated sulphides, and overlain by a thinner zone of sulphide-bearing norite. The subunit itself is up to 1m thick and consists of either pyrrhotite pyroxenite or modally-graded layers of pyrrhotite norite, in places containing norite xenoliths. It varies considerably in thickness and in places is totally absent, although the norite with disseminated sulphides persists. The subunit appears to be the result of the collection of droplets of an immiscible sulphide melt in depressions on the floor of the magma chamber. The subunit probably reflects the initial response to the inflow of new magma into the chamber, mixing of new and more-evolved, resident magma and the formation of a hybrid magma that was saturated only in othopyroxene and sulphides. Continued magma inflow (and a reduction in the efficiency of mixing) eventually led to the crystallisation of poC, that are among the highest-temperature cumulates present in the intrusion. The thickness of the zone a cumulates here is ~120m, showing that magma replenishment persisted for a considerable period of time.

Mineral compositions. The An-content of plagioclase in a 30m thick interval beneath the sulphide-rich subunit increases from An_{47} to An_{49}. Immediately above the subunit it varies from An_{50-49} and in poC of zone IIIb from An_{52-48}. The Mg# of Ca-poor pyroxene decreases rapidly from 76 to ~71 through 20m of phiC forming the upper part of MCU II and increases to 75 just above the sulphide-rich subunit. The unusually Fe-rich pyroxenes at the top of MCU II may be a result of subsolidus re-equilibration with the sulphides present, particularly in connection with the oxidation of pyrrhotite to pyrite. Above this subunit the Mg# of Ca-poor pyroxene remains fairly constant but increases slightly (to 77-76) in the poC. Olivine varies between Fo_{77-74} in poC. Although the minerals show irregular and uncorrelated changes in composition (possibly due to magma mixing and disequilibrium), there appears to be a slight reverse cryptic variation in An% through the zone a cumulates.

Locality 2.6 (1212 II, LK353-886): CONTACT OF MCUs II AND III. HÅGÅSEN.

(by Brian Robins, based on work by Kristine Krogh Jensen)

Description: Hågåsen is a hill located on the southern flank of the Bjerkreim lobe of the Bjerkreim Sokndal intrusion, on which the layered sequence across the boundary between MCUs II and III is well exposed. The sequence of cumulates is similar to that at Eptelandsvatnet (see loc. 2.5) but condensed in thickness. We shall walk from the road northeastwards up the layered sequence to the top of Hågåsen.

The stratigraphically-lowest cumulates exposed along the traverse are massive to weakly modally-layered ilmenite leuconorites (phiC) forming the uppermost part of MCU II. These are succeeded by 20cm of intensely modally-layered melanorite and a massive layer of sulphide-bearing pyroxenite up to 2m thick that mark the base of MCU III. The orthopyroxenite is exceptionally thick here and as it dies out in both directions along strike it appears to occupy a shallow and >200m broad trough. The orthopyroxenite is overlain by phiC with laterally-persistent and remarkably rythmic modal layering that gradually dies away upwards into massive phiC about 15-20m above the orthopyroxenite. The base of the succeeding poC is encountered a few metres further up the sequence (25-30m above the orthopyroxenite).

Mineral compositions. Mg#s of orthopyroxenes in the upper part of MCU II are ~74, decreasing rather abruptly to 70 immediately beneath the orthopyroxenite, as at Eptelandsvatnet. The orthopyroxenite itself contains pyroxene with a Mg# of 72.5 and in the overlying phiC the Mg# shows a slight regressive trend from 72 to 74. The poC contains olivine of Fo_{74-76}. Plagioclase exhibits no systematic variations in composition. PhiC in the upper part of MCU II contains plagioclase of fairly constant composition (An_{47}) while in the sequence above the orthopyroxenite plagioclase compositions vary irregularly between An_{46} and 49.

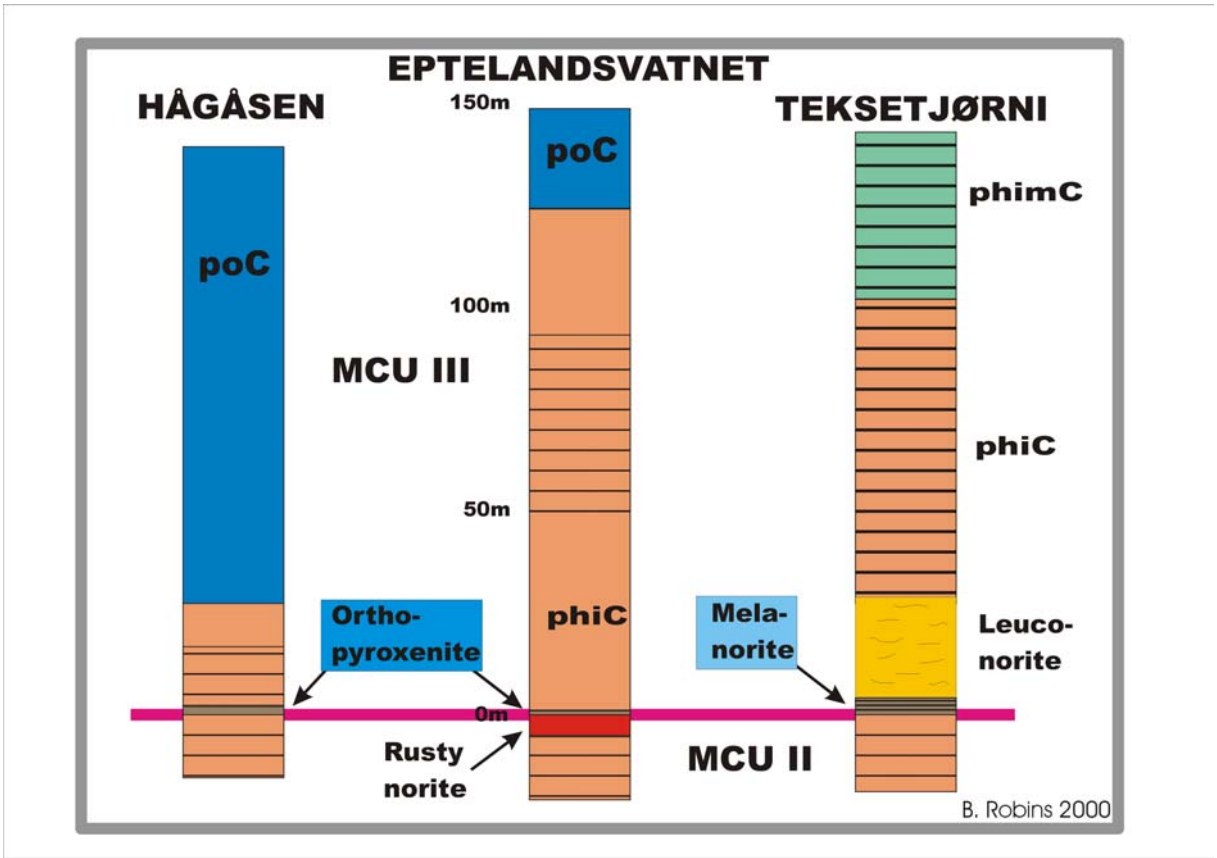

Fig. I 2.3. Comparison of the stratigraphic sequences across the MCU II/III contact at Eptelandsvatnet (loc. 2.5), Hågåsen (loc. 2.6) and Teksetjørni (loc. I 2.7). Note the thicker sequence of zone a cumulates in the axial region of the intrusion at Eptelandsvatnet compared the equivalent in the southern flank (at Hågåsen), and the lack of zone b (poC) at Teksetjørni in the eastern flank of the intrusion.

Locality 2.7 (1312 III, LK433-935): CONTACT OF MCUs II AND III. BETWEEN TEKSEVATNET AND TEKSETJØRNI.

(by Brian Robins)

Description: This locality lies on the eastern flank of the Bjerkreim lobe of the Bjerkreim Sokndal intrusion, to the east of the Teksevatnet re-entrant. Cumulates in this part of the intrusion are believed to have crystallised on an elevated portion of the floor of the magma chamber and as a result the Layered Series is condensed relative to the axial regions of the intrusion and certain stratigraphic zones are absent. The cumulates along a short N-S traverse at this locality can be compared with those present at Eptelandsvatnet and Hågåsen, illustrating some of the lateral stratigraphic variations that occur in the Layered Series. The locality also demonstrates the relationship that exists between ilmenite-rich cumulates and replenishment of the magma chamber.

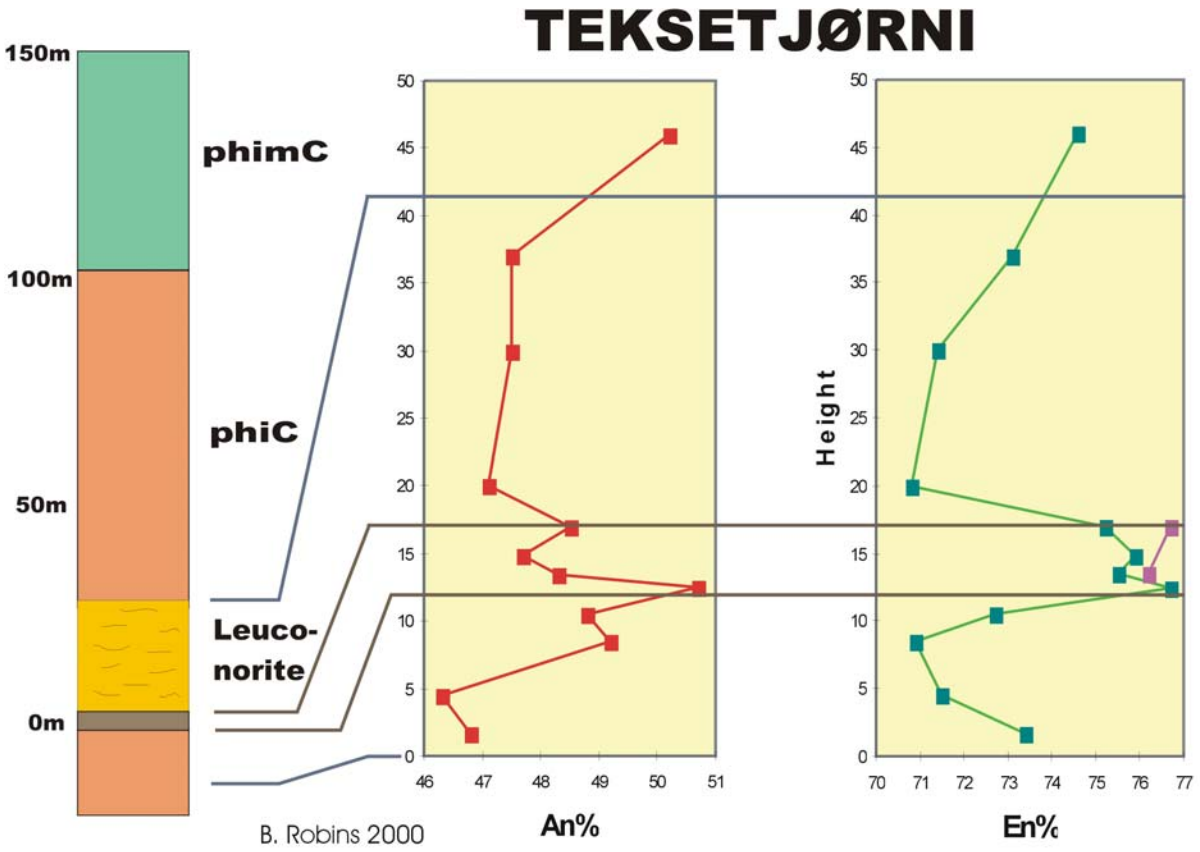

Fig. I 2.4. Cryptic variation in plagioclase, orthopyroxene (green) and olivine (violet) across the MCU II/III boundary at Teksetjørni.

The traverse starts from the track leading to Teksetjørni in ilmenite norites (phiC) belonging to the upper part of MCU II. These cumulates exhibit steeply-dipping to overturned small-scale modal layering, minor unconformities and abundant, generally tabular xenoliths. They are succeeded by ~5m of ilmenite-rich melanorite with sulphides and sparse olivine at the base of MCU III, then rather massive leuconorite containing discontinuous ilmenite-rich layers and a thin sequence of modally-layered ilmenite norite. The latter are overlain by magnetite-bearing norite enclosing numerous blocks and slabs up to 100m across of massive norite or leuconorite. Note that the prominent poC seen at Eptelandsvatnet and Hågåsen is

absent here. The unit of olivine-bearing melanorite is the lateral equivalent of the layer of sulphide-bearing orthopyroxenite developed locally elsewhere.

Mineral compositions. The compositional variations in plagioclase, orthopyroxene and olivine in the sequence developed at this locality are illustrated in Fig. I 2.4. Note the cryptic regression through the uppermost 5m of MCU II as well as the presence of more calcic plagioclase, more magnesian orthopyroxene and magnesian olivine in the melanorite, all suggesting that the formation of the melanorite was a response to magma-chamber replenishment. Orthopyroxene (and to a lesser degree plagioclase) near the base of the overlying leuconorite returns to compositions similar to those in the upper part of MCU II, and it exhibits a slight but consistent cryptic regression through the leuconorite into the phiC. This trend does not persist further upwards in the sequence, the majority of MCU III in this region being characterised by a normal cryptic variation (Fig. I 2.5).

Interpretation. Recently we have studied the lithostratigraphic relationships and cryptic layering in a series of sections across the boundary between MCUs II and III spaced over a distance of 25km along strike. This boundary is particularly instructive with respect to processes during replenishment since lateral variations in the thicknesses of MCU II and III are pronounced and reflect the topography that existed on the chamber floor at the time of magma replenishment. In the central region of the BKSK, around the hinge of the deep syncline defined by the layering, MCU III has a thickness of 900-1050m while in the SW limb of the syncline its thickness is reduced but fairly constant at ~800m. To the east of the axial region MCU III decreases to <350m in thickness over a step of gneiss in the substrate, then increases slightly to ~450m before thinning and wedging out further to the SE against the base of the intrusion. The thickness of MCU II varies in a similar but even more dramatic way. These variations are considered to be due to crystallisation of the megacyclic units in a central trough on the magma-chamber floor and on an elevated "shelf" or shallow trough to the east. In addition, differentiation of the resident magma was arrested at a relatively early stage by the influx of magma marked by the MCU II/III transition. MCU II consists exclusively of a thin basal sequence of plagioclase cumulates and a thick series of phiC. Cumulus magnetite does not make an appearance in MCU II, and it is likely that the resident jotunitic magma was differentiating with increasing density during its crystallisation.

The stratigraphically lowest cumulates in MCU III are a thin sequence of strongly-layered melanocratic, orthopyroxene- and ilmenite-rich norite (phiC), or a discontinuous layer of orthopyroxenite up to 3m thick, all characterised by elevated amounts of disseminated sulphides (pyrrhotite, pentlandite, chalcopyrite and pyrite). The layer of orthopyroxenite is unique in the Bjerkreim Layered Series. Although it shows considerable lateral variations both in thickness and modal composition, this sequence can be recognised everywhere at the base of MCU III. A distinctive feature of the sequence as developed on the "shelf" is the local occurrence of sparse cumulus olivine in melanocratic ilmenite norite and the correlative layer of orthopyroxenite. The basal sulphide-bearing cumulates are succeeded in the majority of the Bjerkreim lobe by 25-130m of massive to strongly-layered phiC (zone a cumulates), then a massive unit of troctolite (pomC, zone b) up to 100m thick, that constitute the highest-temperature cumulates in MCU III. The troctolites reside beneath lower-temperature phiC, phimC and eventually phcmiaC that form the remainder of MCU III. In the eastern part of the lobe the sequence immediately above the basal cumulates of MCU III is much thinner (25-45m) and consists of either rather massive leuconorite with discontinuous thin layers of ihC (resembling zone a cumulates elsewhere in the intrusion), or modally-layered, melanocratic ilmenite norite. With the exception of a locally-developed 1m-thick layer, troctolite (zone b) is conspicuously absent in this shelf region and the leuconorite or melanocratic norite is succeeded by "normal" phiC.

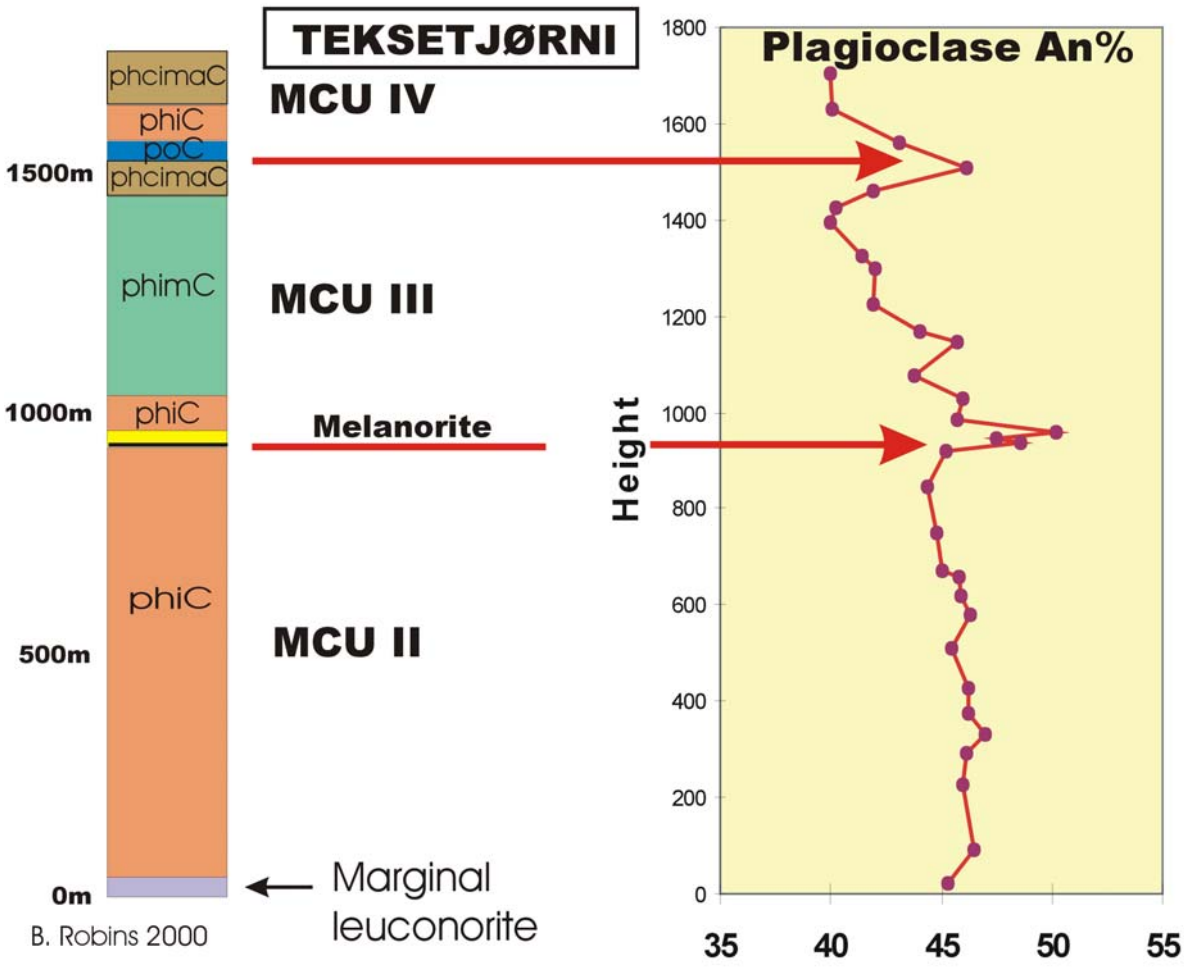

Fig. I 2.5. Cryptic variation in plagioclase through MCU II, III and the lower part of IV in the eastern flank of the Bjerkreim lobe as displayed in a series of samples collected along a traverse from the margin of the intrusion, through the Teksetjørni locality (loc. I 2.7) to Lauvneset (loc. I 2.8).

The cryptic variation across the MCU II/III boundary is characterised by a regression in mineral compositions (and $^{87}Sr/^{86}Sr$) from the phiC forming the upper part of MCU II to the most primitive compositions that are found either in the troctolites forming the zone b cumulates of MCU III in the central and western part of the lobe or in the cumulates above the sequence of leuconorite/melanocratic norite in the eastern, "shelf" area. This is consistent with prolonged magma-chamber replenishment associated with progressive mixing of the inflowing and resident jotunitic magmas. The sulphide-enriched orthopyroxenite and related melanocratic ilmenite norite are explained by crystallisation of hybrid magmas residing in the pyroxene phase volume during the initial stages of replenishment. Their "global" distribution is inferred to result from mixing taking place some distance above the chamber floor at a level where the plume formed by the inflowing magma reached a level of neutral buoyancy in the compositionally-stratified magma column and spread laterally throughout the chamber. As the influx proceeded the resident magma was stripped from the base of the chamber and mixed into the ascending plume as the hybrid layer increased in thickness and became

compositionally stratified. Eventually the lower boundary of the hybrid layer reached the floor of the magma chamber. The highest-temperature cumulates (poC, zone b) crystallised from the lowest part of this hybrid layer and were restricted to the central trough on the chamber floor, while lower-temperature cumulates crystallised simultaneously on the eastern "shelf" from magma higher up in the hybrid layer.

Locality 2.8 (1312 III, LK428-931): MAGNETITE, ILMENITE AND APATITE-BEARING CUMULATES (MCU IV) . LAUVNESET, nr. TEKSE.

(by Brian Robins)

Description: Cumulates containing apatite together with magnetite, ilmenite and Ca-rich pyroxene occur in the upper parts of MCUs IB, III and IV. Apatite in the Bjerkreim-Sokndal Intrusion generally makes its entry as a cumulus mineral at about the same stratigraphic level as Ca-rich pyroxene but may preceed or postdate it stratigraphically by some tens of metres. The late appearance of Ca-rich pyroxene is a reflection of the unusually Ca-poor composition of the parental jotunite magmas. Apatite is most abundant immediately after its appearance as a cumulus mineral when it may constitute as much as 10% of the rocks. This locality on the shore of Teksevatn exhibits apatite- and oxide-rich gabbronoritic cumulates with pronounced modal layering immediately above the apatite-in phase contact within MCU IV. The sequence of MCU IV cumulates in this area is different from the axial region of the intrusion: The thickness of zone c (phiC) is reduced and zone d (phimC) seems to be absent (Fig. I 2.5).

Mineral compositions. In keeping with the evolved cumulus assemblage, the minerals in this part of the Layered Series have relatively low-temperature compositions: Plagioclase is ~An_{40}; Ca-poor and Ca-rich pyroxene have Mg#s of ~63 and ~70 respectively.

Locality 2.9 (1212 II, LK342-905): BASAL CONTACT OF MCU IV. STOREKNUTEN.

(by J. Richard Wilson)

Description: Storeknuten is a rounded hill, located on the southern flank of the Bjerkreim lobe of the Bjerkreim Sokndal intrusion (Fig. I 2.1), where the boundary between Megacyclic Units III and IV has been studied in detail (Jensen et al. 1993, Nielsen et al. 1996, Barling et al. 2000). There is a good view of the Bjerkreim lobe from the summit of Storeknuten. The strike of the layering here is NW-SE and the dip is about 50-60° to the NE into the core of the Bjerkreim synform. Olivine-bearing rocks in the Layered Series are restricted to two zones just above the bases of MCUs III and IV and form pronounced topographic ridges. Storeknuten belongs to the uppermost olivine-bearing zone which Paul Michot called the Svalestad unit (referred to as zone IVb here).

We shall approach Storeknuten from the southeast, along a farm track. There are sporadic exposures of gabbronorite (phcimaC) belonging to the uppermost part of MCU III (zone e) in the fields. On the left of the track (at LK344902) is a particularly instructive exposure of modally-layered gabbronorite in which several gneissic xenoliths are embedded. Structures due to blocks of gneiss impacting and slicing into partly-crystallised cumulates are preserved and allow discussion of layering-forming processes (Photo I 2.1).

Photo I 2.1. Modally-graded layering in MCUIII, Storeknuten section.

At the base of Storeknuten, the MCU IIIe cumulates are overlain by a zone (about 30m thick) of plagioclase-rich cumulates belonging to MCU IVa (Fig. I 2.6). MCU IVa consists dominantly of pC and piC, with magnetite and Ca-poor pyroxene occurring as sporadic early phases. A characteristic feature is the presence of thin ilmenite-rich layers, many of which are discontinuous and deformed by slump folds. These ilmenite-rich layers, particularly abundant in the axial region of the intrusion at this stratigraphic level, suggest that magma-chamber replenishment and magma mixing were a prerequisite for ilmenite concentration.

The entry of olivine as a cumulus phase defines the base of MCU IVb. This boundary is exposed on the southern slopes of Storeknuten. MCU IVb consists dominantly of massive leucotroctolite containing oikocrysts of Ca-poor pyroxene. MCU IVb is about 100m thick and contains sporadic cumulus magnetite (and possibly ilmenite and Ca-poor pyroxene), as well as small quantities of biotite and brown hornblende. Most olivines are partly or completely replaced by orthopyroxene-oxide symplectites. The summit of Storeknuten is composed entirely of rocks belonging to MCU IVb. The disappearance of olivine and magnetite, and the entrance of cumulus Ca-poor pyroxene in the slopes to the north define the base of MCU IVc (phiC). This phase contact is accompanied by the development of an igneous lamination and modal layering. Modal layering becomes increasingly well developed up through MCU IVc.

Mineral compositions and Sr-isotope ratios. There is a cryptic regression in mineral compositions through the uppermost part of zone IIIe that continues through zone IVa (Fig. I 2.7). The upper part of MCU IIIe has Ca-poor pyroxene with En_{68-70}, plagioclase with An_{44-46} and an initial Sr-isotope ratio of 0.7061; the base of MCU IVb has En_{76}, An_{53} and Sr_o 0.7049, together with olivine Fo_{74}. There is an extremely systematic upward decrease in Sr-isotope ratios through the upper part of MCU IVa (Fig. I 2.8). The variation in initial Sr isotope ratios appears to be delayed relative to the regression in mineral compositions.

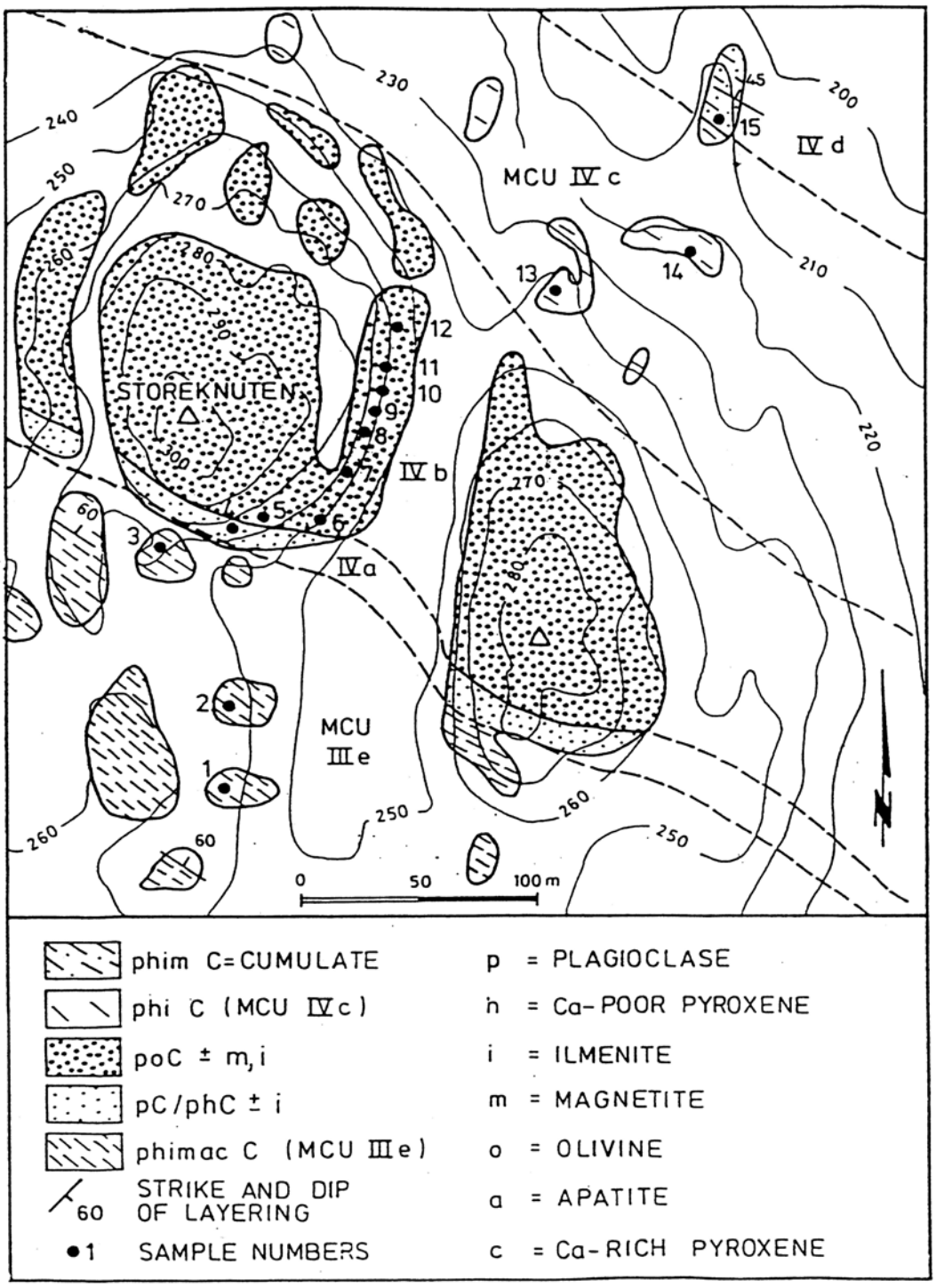

Fig. I 2.6. Geological map of the Storeknuten area showing the distribution of major outcrops, lithologies, strike and dip of layering, and sample locations. The legend explains the abbreviations used for the cumulate nomenclature. From Jensen et al. (1993)

Plagioclases show a rather erratic trend to more evolved compositions upwards through MCU IVb, while olivines first become more Fe-rich and then more Mg-rich (Fig. I 2.7). The olivine trends may have been influenced by trapped-liquid shift. Sr-isotope ratios increase systematically from 0.7049 at the base of zone IVb to 0.7053 at its top, reach 0.7058 in zone IVd and returns to 0.7061 in zone IVe (Figs. I 2.7 & I 2.8).

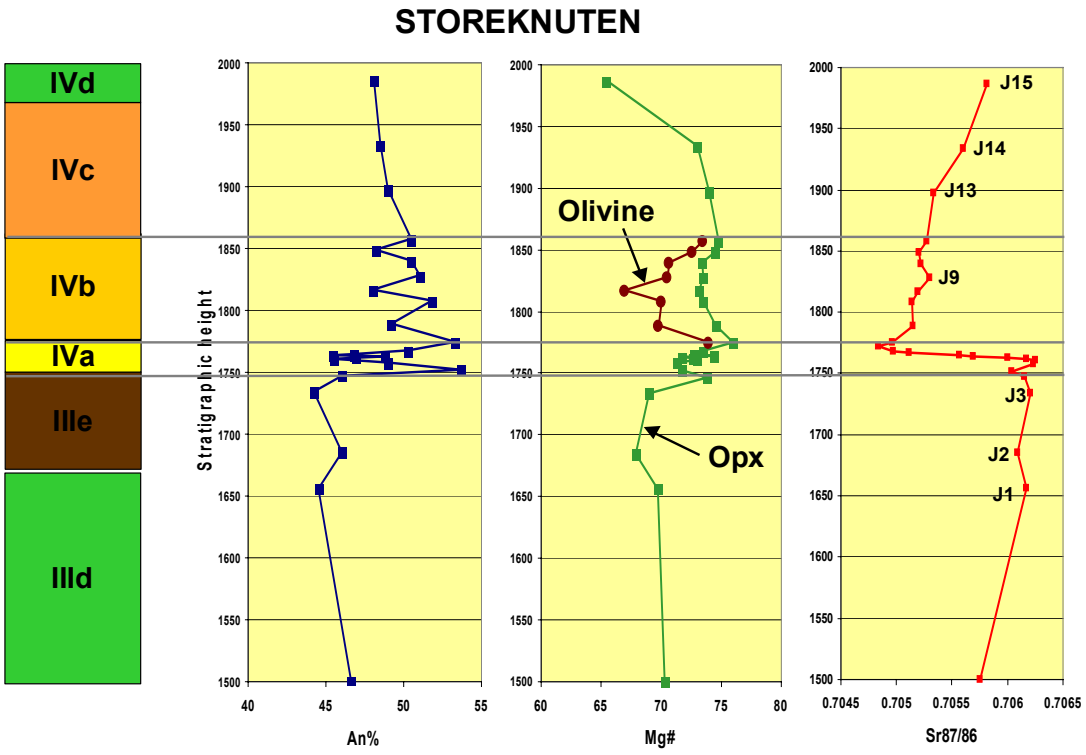

Fig. I 2.7. Cryptic variation through the upper part of MCU III and the lower part of MCU IV at Storeknuten. The sample numbers (J1-15) correspond to those marked in Fig. I 2.6. Based on data from Jensen et al (1993) and Nielsen et al. (1966).

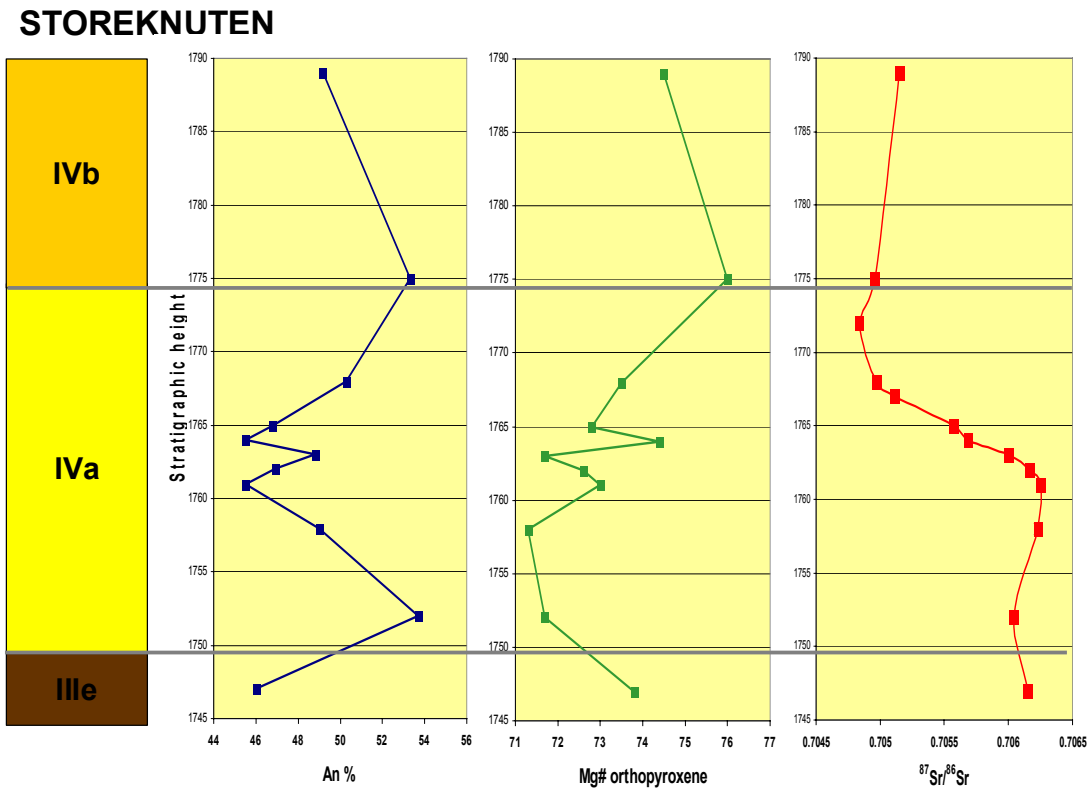

Fig. I 2.8. Cryptic variation through the basal, regressive zone of MCU IV at Storeknuten. From Nielsen et al. (1996).

The significance of the MCU III/IV boundary for magma mixing. The cryptic variations across the boundary between MCUs III and IV clearly indicate the operation and importance of magma mixing during magma-chamber replenishment. The magma residing in the chamber when the influx marked by the base of MCU IV took place was compositionally zoned (Fig. I 2.9), and assimilation of gneissic country rock at the roof had resulted in an elevated Sr-isotope ratio that may have increased upwards through the magma column. The inflowing magma had an Sr-isotope ratio of about 0.7049 while the resident magma had a ratio of 0.7061 at the floor in the Storeknuten area. The inflowing magma mixed with the basal layer(s) of the resident magma as a result of the new magma fountaining into the chamber. A decreasing degree of mixing between the inflowing and resident magma with time led to hybrid magmas with decreasing Sr-isotope ratios. Crystallisation of these hybrid magmas during replenishment= produced the isotopic regression in the upper part of MCU IVa. Initially, influx led to elevation of the zoned magma column, exposing the base of the chamber in the Storeknuten area, located some distance up the inwardly-sloping floor, to progressively more primitive magma. It took some time before the hybrid magma flooded this point on the floor, causing the delay in the regression in isotope ratios relative to that defined by the mineral compositions. When the magma inflow ceased, olivine-bearing rocks of MCU IVb began to crystallise at the base of the chamber. The leucotroctolites at the base of MCU IVb are amongst the most primitive rocks in the entire intrusion.

Calculations based on geochemical modelling, the thickness of cumulate stratigraphy repeated (from the top of zone IIIe to the appropriate part of zone IVe) and Sr-isotope ratios indicate that the layer of hybrid magma generated during replenishment had a thickness of 350-500m in the Storeknuten area and that the leucotroctolites of MCU IVb represent about 20-30% crystallisation of this layer.

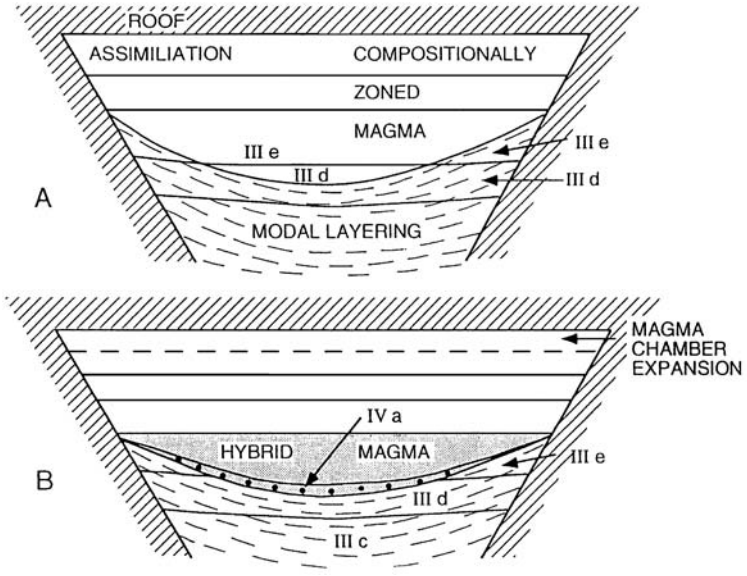

Fig. I 2.9. Sketches of the Bjerkreim-Sokndal magma chamber during formation of the MCU III/IV boundary. From Jensen et al. (1993). A. Crystallisation of the upper part of MCU III. The magma layer parental to zone IIId is only present in the central, lowest part of the saucer-shaped chamber. Zone IIIe is crystallising from the overlying magma layer(s) towards the margins. The Storeknuten profile is located near the margin, where zone IIIe cumulates are present. B. Magma replenishment elevated the residual magma and produced a hybrid magma layer at the floor. Zone IIIa crystallised during influx to produce a modal and cryptic regression. ***Note that the vertical scale has been greatly exaggerated in these sketches.***

***

Itinerary 3

THE SOKNDAL LOBE AND THE UPPER PART OF THE BJERKREIM-SOKNDAL INTRUSION

(by J.C. Duchesne and E. Wilmart)

The itinerary starts at Rekeland on road 44.

Locality 3.1 (1311.4; LK401-728) REKELAND: EIA-REKEFJORD INTRUSION

The road cuts across the Eia-Rekefjord jotunitic body which intrudes the contact between the Helleren anorthositic body on the West and norites of the Bjerkreim-Sokndal lopolith on the East.

Several types of jotunites are displayed. Near the bridge, along the contact with the anorthosite, typical homogeneous jotunite which grades upwards into a faintly layered unit with coarse-grained porphyritic layers. A fine-grained rock, lying conformably (several metre-thick inclusions?) and an anorthositic inclusion can be seen near the foot-bridge over the road.

The homogeneous jotunite averages the composition of the samples taken around Rekefjord (among them, 66-125 - Duchesne et al. 1974) and of the Varberg dyke (see locality 1.8). The fine-grained rock is petrologically and chemically similar to the chilled-margin of the Varberg dyke: equigranular texture, with poikilocrysts of opx, fine-grained, needle-like apatite crystals and subhedral oxides, the latter minerals being dispersed in all other minrals (Duchesne et al. 1985a; 1989; Vander Auwera et al. 1998) . This rock provide good evidence in favour of the existence of (chilled) jotunitic liquids.

Proceed a few hundred metres to the South along road 44

Locality 3.2 (1311.4; LK404-740 to 402-725) N.HAUGE: LAYERED NORITES OF BJERKREIM-SOKNDAL (SOKNDAL LOBE)

The road follows the W flank of the lopolith and displays discontinuous outcrops of layered norites with various characters of cumulate rocks (planar and linear lamination, banding, small-scale rhythmic layering, modally graded layers, etc.). The rocks belong to the upper macro-rhythmic units of P. Michot's stratigraphy (Michot 1960; 1965)). They are commonly apatite and cpx-bearing.

Proceed to Hauge and carry on towards Åna-Sira; at Åmot, take the bridge to the left and the road to the North. At the first crossing (500 m after the bridge) take to the left. The road runs through the norites of the lopolith. About 2 km further North, after the bridge, at Bakka schoolhouse, take to the left towards Slatten and Herveland.

Locality 3.3 (1311.4; LK423-741) HERVELAND: MANGERITES FROM THE BJERKREIM-SOKNDAL LOPOLITH

(See P. Michot, 1960, III h, p.37).

When reaching the plateau, after Slatten, the outcrops are on the left side of the road.

Typical Mangerite: irregular mosaic of spectacular mesoperthite with interstitial fayalitic olivine ($Fa_{92}Fo_8$), ferroaugite ($Mg_{16}Fe_{41}Ca_{43}$), minor ferrohypersthene ($Mg_{18}Fe_{80}Ca_2$),

ilmenite (Hem_3Ilm_{97}), Ti-magnetite ($Usp_{50}Mt_{50}$) and apatite) (for details on the mineralogy and chemical composition - major and trace element - see Duchesne 1970; 1972b; Duchesne & Demaiffe 1978; Duchesne et al. 1987a; Duchesne & Wilmart 1997). Some fine grained inclusions (with " chilled facies ") of jotunitic to olivine-bearing mangeritic composition.

Back to Bakka schoolhouse, take on the left the road to Bakka (farms). It passes into the banded norites of the lopolith (dipping 40°-60°W).

Locality 3.4 (1311.4; LK433-742 to 431-754 and 425754) ØRSLAND: TRANSITION FROM NORITES TO MANGERITES AND QUARTZ MANGERITES

This itinerary (illustrated in Fig. I 3.1) permits to observe a nearly continuous section starting in the layered norites, passing through the transition zone into the mangerites and from the latter to the quartz mangerites through the so-called xenolithic septum of Michot (1960). For more details see (Duchesne et al. 1987a; Duchesne & Wilmart 1997).

a. From the last hairpin turn at the Bakka pond, walk uphill the path to Ørsland farm:

- norite (cpx and apatite bearing) with a strong planar lamination (40-50°W) and some mafic layers, belonging to the eastern flank of the lopolith;
- fine-grained dyke of quartz-monzonite with inclusions of norite;
- after the farms, the mafic layers increase in number and become more irregular.

b. In a small gully, rusty ultramafic layers (c. 1m thick), intercalated with norites: the association in the ultamafic layer is 35% olivine (Fo_{50}), 12% cpx ($Mg_{38}Fe_{17}Ca_{45}$), 17% ilmenite ($Hem_{2.6}Ilm_{97.4}$), 30% magnetite (TiO_2 = 11%, $Usp_{33.2}$ $Mt_{66.8}$), 5% apatite (sample 6482 - (Duchesne 1970; 1972a; Duchesne et al. 1987)

c. At the end of the meadows, quartz mangeritic Ørsland dyke (Duchesne & Wilmart 1997) containing inclusions of anorthosite and of mangero-monzonite.

d. 750 m further North, the path reaches a pass on the left flank of which a 50-80 m pile of rocks can be observed. It is made up of a series of ultramafic layers (0.5 to 4 m thick) dipping 60-70°W intercalated in the lower part with noritic layers and in the upper part with mangeritic layers. On top of the series, massive mangerites. This relatively thin pile of rocks is to the author's knowledge the best exposed section in the intrusion displaying the transition between layered norites and the mangerites. Cryptic layering is conspicuous in the pile of rocks. All minerals progressively and rapidly change in chemical composition (e.g. olivine Fo_{45} to Fo_{19}; TiO_2 in magnetite from 10% to 19%, etc.) and modal proportion. The detailed evolution is described in Duchesne et al. (1987a). Petrographic and geochemical evidence indicate that crystal fractionation (not immiscibility), is the leading mechanism of differentiation. A typical association is 34% olivine (Fo_{29}), 32% cpx ($Mg_{29}Fe_{28}Ca_{42}$), 2% ilmenite ($Hem_{1.5}$), 31% Ti-magnetite (19%TiO_2 i.e. Usp_{58}), 1% apatite (sample 66.216 - Duchesne 1970; 1972a; Duchesne et al. 1987a).

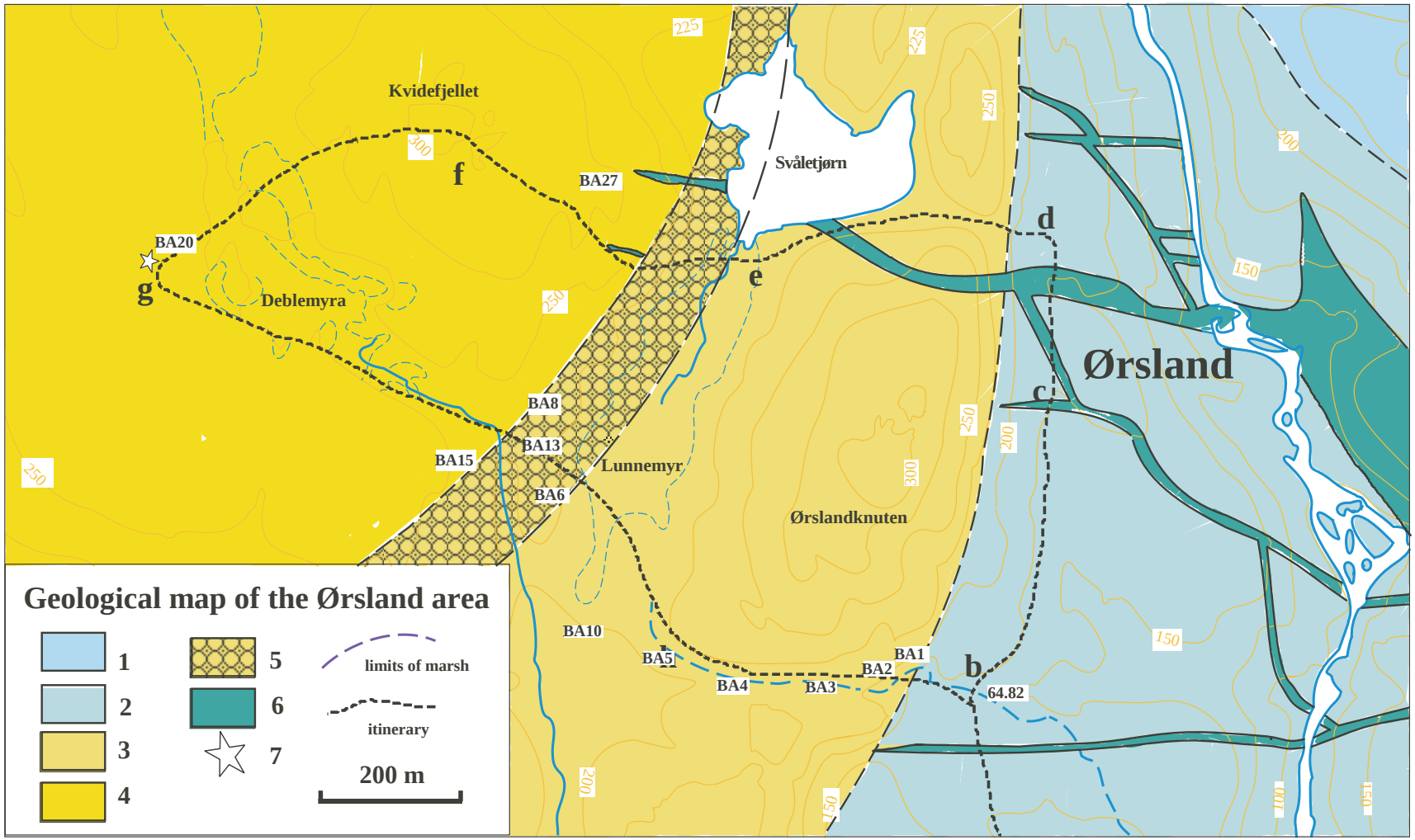

Fig. I 3.1. Geological map of the Ørsland area (after Duchesne & Wilmart, 1997). Sample numbers refer to samples detailed in Fig. I 3.2.

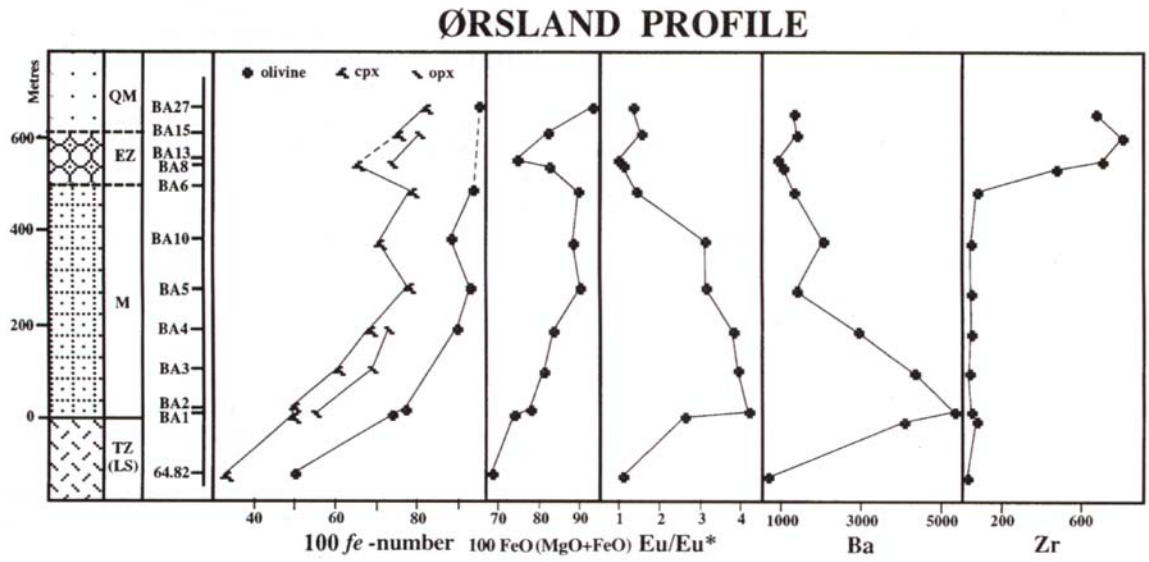

Fig. I 3.2. Compositional variations in the rock sequence from the Transition zone (TZ) through the mangeritic unit (M) and the enclave-rich zone (EZ) to the quartz mangerite unit (QM). From left to right, stratigraphic heights relative to the top of the TZ; lithologies; stratigraphic zone distribution; sample numbers; variation of fe# in olivine, Ca-poor pyroxene and Ca-rich pyroxene; variation of fe# in whole rock; Eu anomaly; Ba content (ppm). Sample location in fig. I.3.2. Note that samples BA8 and BA15 are devoid of olivine and sample BA13 was not studied under the microprobe (from Duchesne & Wilmart, 1997).

e. Walk uphill into massive (weakly foliated) mangerites and go round the Svaletjorn pool to its southern outlet: mangerite become heterogeneous and overcrowded with xenoliths of various dimensions, lithologies and grain size (jotunite, porphyritic mangerite, patches of graphic pegmatite, pillows of fine-grained chilled jotunite, angular-shaped amphibolite). This zone of 100-200 m thick, which extends on the flank of Kvidefjellet up to the beginning of the plateau at altitude 250 m, belongs to what P. Michot has called the xenolithic septum. It straddles the contact between mangerites and quartz mangerites, and according to Duchesne and Wilmart (1997), indicates a new influx of acidic magma mixing and mingling with the resident magma on top of the cumulate pile.

f. En route to the Kvidefjellet which is on typical quartz mangerites with or without olivine (Duchesne & Wilmart 1997). Metre-sized rafts, dykes or inclusions with finger-shaped contours of fine-grained sugar-like leucogranites (73-78% SiO_2) interpreted on the basis of their trace element composition as back-veining material: leucosome material from surrounding migmatites remobilized and injected into the magma chamber. These inclusions also points to the proximity of the roof of the intrusion. The lack of inclusions made up of the basic (restitic) component of the migmatites precludes an origin of the quartz mangerite by in situ anactectic melting of the roof.

g. On the plateau at LK417-753 a large leucogranitic inclusion with anastomosed contours (sample BA20 in Duchesne & Wilmart 1997) (Photo I 3.1);

Photo I 3.1. Part of a leucogranitic enclave (sample BA20) showing dyke-like fingers in quartz mangerite. The very peculiar REE signature permits to identify the origin as migmatitic melts from the envelope.

h. On the way back, the path is taking a gully, south east of Lunnemyr, which cuts across the pile of mangerite cumulates (see Duchesne & Wilmart 1997).

Back to Bakka and then to Hauge and Moi.

***

Itinerary 4

THE ROGALAND INTRUSIVE MASSIFS: EASTERN PART

(by J.C. Duchesne, D. Demaiffe, O. Bolle, J. Vander Auwera and E. Wilmart)

This itinerary will be briefly devoted to the Åna-Sira massif type anorthosite (Fig I 4.1), and will focus mainly on its relationship with the envelope, the Apophysis and the Hidra

leuconoritic body. The Tellnes deposit will be visited on itinerary 5.

From Moi, take the E39 (E18) to the north. At Heskestad, follow the road to Hauge. It crosses the upper part of the Bjerkreim-Sokndal intrusion till Eia. Then it follows the contact between the Eia-Rekefjord jotunitic intrusion and the Håland-Helleren massif till Rekeland. The road then enters the southern lobe of the Bjerkreim-Sokndal massif and, at Hauge, in the lows formed by the norites, crosses the axial plane of the syncline. Proceed along road 44 to Flekkefjord, which enters the Åna-Sira massif (Fig. I 4.1) at the hill foot.

Locality 4.1 (1311.4; LK446-704): AGGLOMERATE OF ORTHOPYROXENE MEGACRYSTS

A huge agglomerate of megacrysts of opx and plagioclase can be seen from the road in the anorthosite, on the other side of the small gully which runs down the road.

The orthopyroxene is En_{74} and its Al content is close to 9.0% Al_20_3 (specimens EC74-73 of Emslie (1975).

Locality 4.2 (1311.4; LK523-627): BOTNEVATN

Along Botnevatn, spectacular outcrop seen from the road on the northern flank of the small hill, facing the Botnevatn, immediately on the eastern side of the lake outlet to Åsnes.

The so-called Barth's inclusion of folded leuconoritic gneiss embedded in common anorthosite and crosscut by a 1m-thick anorthosite dyke (Photo I 4.1). The anorthosite contains small opx megacrysts.

This outcrop has a long scientific history. It has been interpreted in three different ways, thus reflecting the evolution of ideas on the genesis of anorthosite. It was shown to Paul Michot (pers. comm.) by T.F. Barth in the fifties as evidence of a metasomatic origin of the Åna-Sira anorthosite: the folded leuconoritic gneiss body was considered as a relic of an uncompletely transformed gneiss. For Paul Michot it was an inclusion within an igneous anorthosite. Later, Michot forged the concept of leuconoritic anatexis (Michot 1955)which was further extended into the theory of basic palingenesis (Michot 1961b): the gneissis inclusion became a remnant of an unmelted old leuconoritic gneiss which was the substrate of the migmatitization. Nowadays, following Maquil and Duchesne (1984) and Duchesne et al. (1985b), the inclusion is interpreted as a fragment of the margin of the intrusion, deformed by emplacement of the central part of the massif and engulfed in it (cf. Itinerary 1, localities 1.2, 1.5 and 1.7).

200 m further, the road cuts across the Tellnes main dyke, made up of typical quartz mangerite.

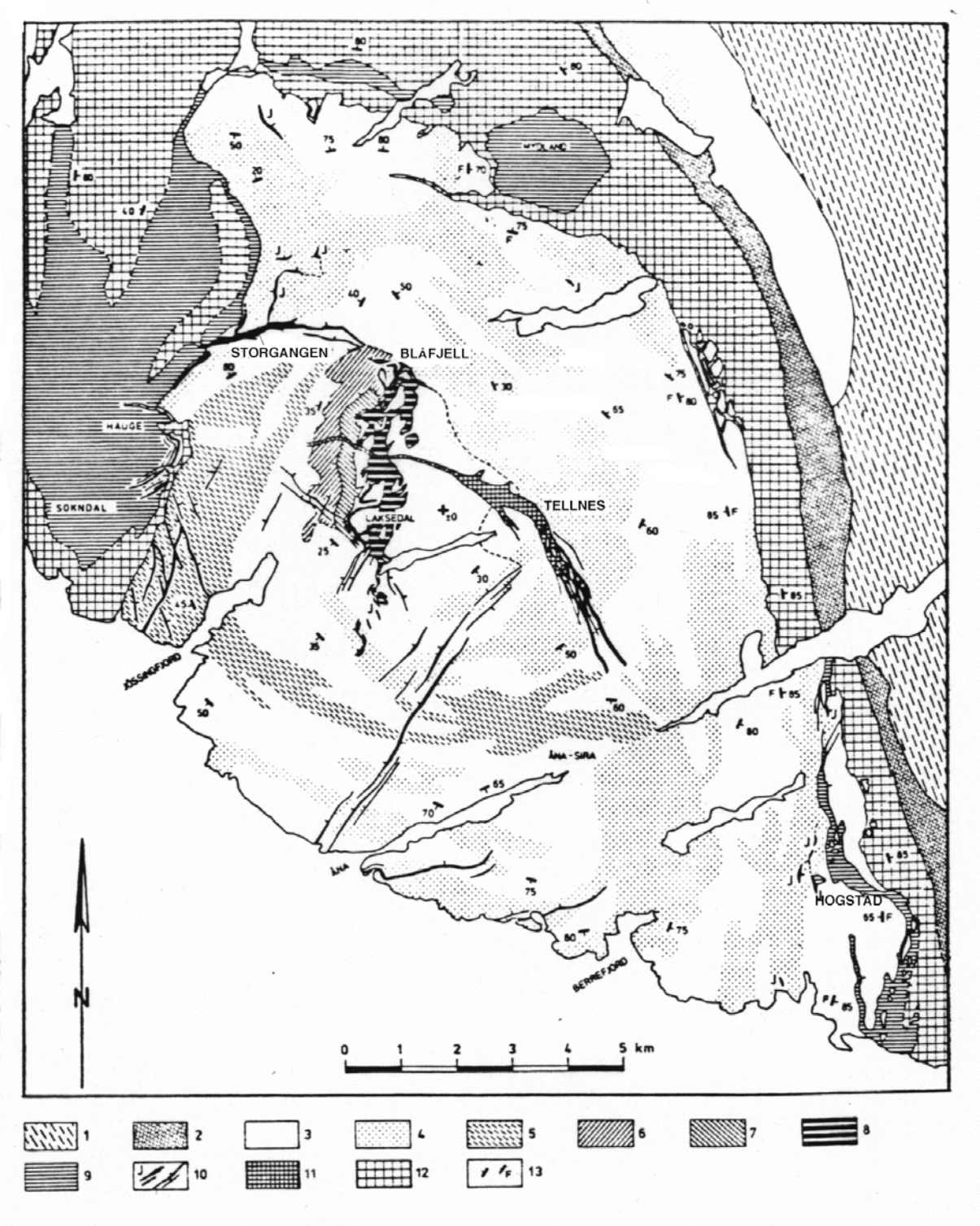

Fig. I 4.1 Geological sketch map of the Åna-Sira anorthosite and related rocks (after Krause and Pedall, 1980). Legend: 1. Charnockitic migmatites and gneisses; 2: Banded noritic-charnockitic gneisses; 3. Anorthosite (0-10 vol% mafics); 4: Leuconorite (10-25% mafics); 5: Anorthositic-noritic complex; 6-8: Internal norites; 6: Layered intrusion of Bøstølen, poorly stratified upper part; 7: Layered intrusion of Bøstølen, stratified lower part; 8: Norite-pegmatite body of Blåfjell; 9: external norite (J) and ilmenite dykes; 11; Ilmenite-norite body of Tellnes; 12: Mangeritic units (Lopolith of Bjerkreim-Sokndal); 13: Igneous layering and secondary foliation (F).

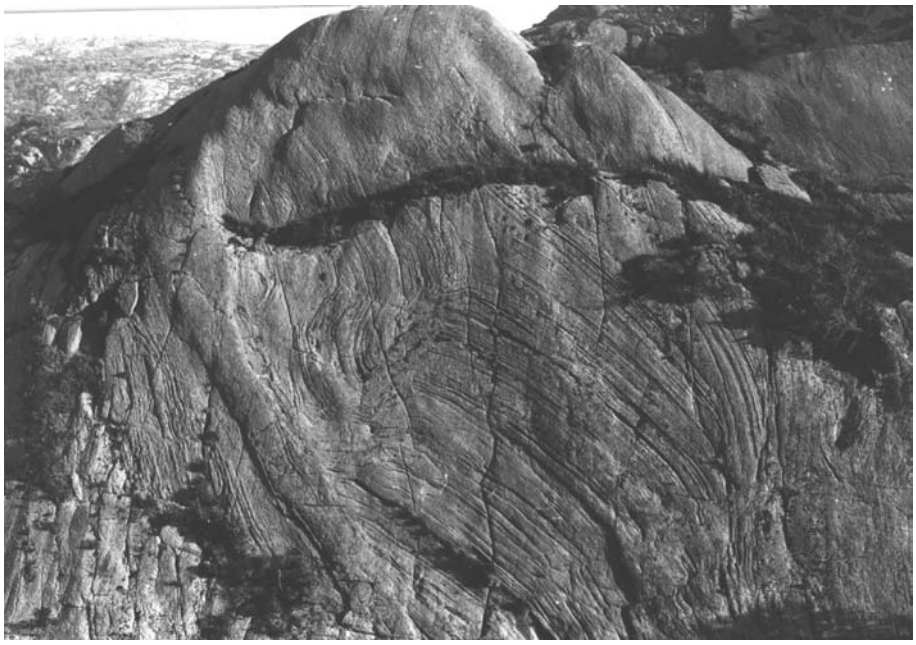

Photo I 4.1. Spectacular outcrop along the Botnevatnet: the so-called Barth's enclave.

Proceed to Kvanvik, on road 44 (Åna-Sira - Flekkefjord).

Locality 4.3 (1311.4; LK563-621to 591-605) FIDSEL-VARDEFJELL: APOPHYSIS, HIDRA MASSIF AND COUNTRY GNEISS

At Kvanvik, the road enters the green hollows of the norites of the Apophysis, an intrusion between the massive anorthosite and the enveloppe of country gneisses. Take a gravel road to Fidsel. Leave the car at the houses and walk along the path (which starts at the first farm to the left) towards the Vardefjell. The path has been marked with red stripes by a local touristic organisation.

Fig. I 4.2 gives a schematic geological map and Fig. I 4.3, two cross sections on which the various points of interest are reported. The itinerary enables the following units to be observed:

1. Various facies of jotunites (= hypersthene diorites) and their mingling relationships with mangeritic hybrid rocks from the Apophysis.
2. A series of supracrustal gneisses in granulite facies from the envelope.
3. The small charnockitic intrusion of Breimyrknutan.
4. The leuconoritic massif of Hidra and its fine-grained " chilled " margin (porphyritic jotunite).
5. The foliated Farsund charnockite (Farsundite).

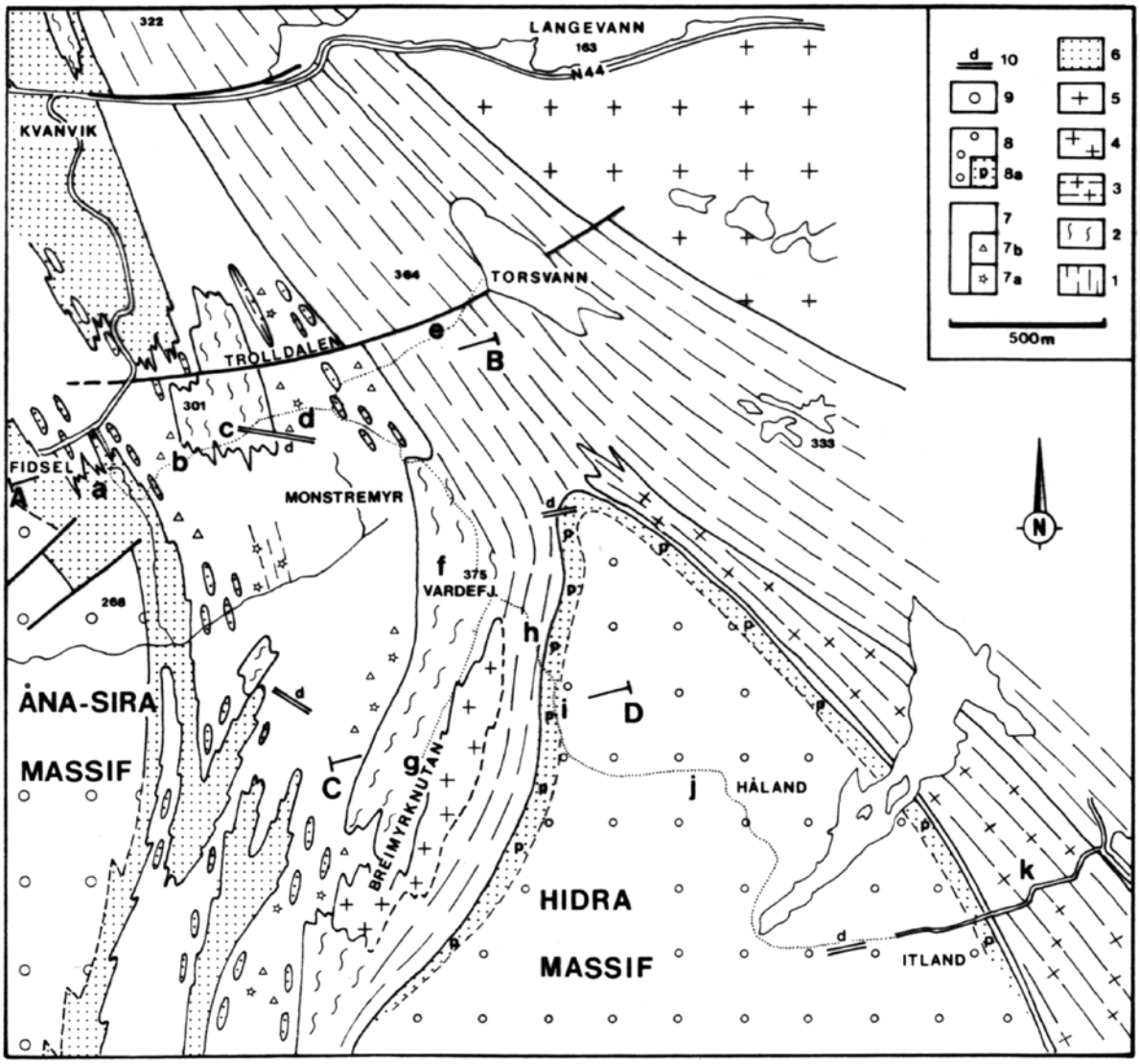

Fig. I 4.2. Geological map of the Kvanvik-Fidsel-Vardefjell area**.** Legend: 1. Banded gneiss series (supracrustal gneisses); 2. Vardefjell migmatitic complex; 3. Charnockitic gneisses (Farsund (meta)-charnockite); 4. Charnockite (Breimyrknutan); 5. Granite-gneiss unit; 6. Jotunite (usually fine-grained, some varieties are medium-gained); 7. Porphyroïdic monzonite/mangerite including porphyritic jotunite with abundant mesoperthite phenocryst varieties, 7a. with poikilocrysts of amphibole, 7b. with angular, zoned metabasite inclusions; 8. Coarse-grained leuconorite, 8a. fine-grained porphyritic jotunite; 9. Anorthosite; 10. Doleritic dyke. a to k: points described in the itinerary. AB and CD: cross-sections (see fig. I 4.3).

The points are the following:

a. Near the Fidsel farms, the meadows are situated on a medium-grained jotunite, showing igneous lamination (and lineation) (Table I 4.1; anal. 3 and Fig. I 4.3). Some layering can be observed along the path, as well as more complex structures (mingling?) with local concentration of mafics and small fine-grained inclusions. Late acidic dykes.

b. Coarse-grained (porphyroïdic = large amount of phenocrysts) mangerite (anal. 8 and 11) with rounded inclusions of fine-grained jotunite (anal. 7) of various size and shapes and elongated in the oriented texture. Angular inclusions of amphibolite with dehydrated noritic rims (Vander Auwera 1993) are common near the contact with rocks from the envelope, as well as interfingered raft of leucogranitic material.

Table 4.1. Chemical analyses and normative composition of various samples.

No	1	2	3	4	5	6	7	8	9	10	11	12	13	14	15	16	17
SiO_2	48.00	49.53	47.99	52.03	52.10	54.03	55.71	55.65	59.27	58.87	58.47	61.53	67.62	65.38	69.67	72.44	73.09
TiO_2	4.61	3.82	3.75	3.26	2.39	2.24	2.00	1.71	1.19	1.15	1.28	1.44	0.76	0.97	0.85	0.45	0.35
Al_2O_3	14.20	14.50	14.15	13.71	15.48	15.58	15.10	16.25	15.52	15.94	15.83	13.40	13.85	13.60	13.26	13.30	13.37
Fe_2O_3	5.00	2.13	3.42	2.67	5.97	3.16	2.11	4.06	1.75	2.37	3.80	1.70	2.34	1.47	0.64	0.58	1.35
FeO	10.40	11.70	12.84	11.20	8.08	8.19	9.32	7.40	7.24	7.46	6.09	7.08	3.40	5.09	3.37	2.37	1.84
MnO	0.18	0.17	0.25	0.19	0.21	0.17	0.19	0.16	0.15	0.17	0.15	0.14	0.10	0.11	0.09	0.06	0.04
MgO	4.60	4.80	4.40	3.62	1.41	2.04	2.05	1.44	0.75	0.55	0.69	1.38	0.70	0.34	0.49	0.34	0.31
CaO	6.41	6.46	7.14	6.25	5.85	5.93	5.07	4.33	3.77	3.61	3.71	3.01	2.31	2.78	2.39	1.56	0.91
Na_2O	3.65	3.51	4.11	4.35	4.69	4.97	4.98	5.42	4.79	5.04	4.49	4.10	3.75	3.42	2.85	2.89	3.86
K2O	1.08	2.04	1.23	2.23	3.07	2.79	3.28	3.56	4.09	4.57	4.64	4.70	4.54	5.49	5.05	5.14	5.31
P_2O_5	0.80	1.01	1.24	1.19	0.91	1.07	0.87	0.76	0.38	0.30	0.32	0.58	0.23	0.34	0.30	0.14	0.14
Fe_2O_3t	16.54	15.12	17.67	15.10	14.94	12.25	12.46	12.27	9.79	10.65	10.56	9.56	6.11	7.12	5.41	3.21	3.39
Total	99.80	99.68	100.52	100.70	100.16	100.17	100.68	100.74	98.90	100.03	99.47	99.06	99.60	98.98	99.99	99.27	100.57
Normative compositions (wt%)																	
Or	6.5	12.1	7.2	13.1	18.1	16.5	19.3	20.9	24.5	27.0	27.6	28.1	27.0	32.8	29.9	30.6	31.2
Ab	30.7	29.8	34.6	36.5	39.6	41.9	41.8	45.5	40.9	42.6	38.1	35.0	31.8	29.2	24.1	24.6	32.4
An	19.6	17.8	16.4	11.2	12.1	11.9	9.1	9.4	8.8	7.3	9.3	4.3	7.5	5.6	8.4	7.0	3.4
Q	2.7				0.4				4.7	1.6	5.2	10.0	22.2	17.4	27.4	31.2	27.4
Cpx	5.9	7.0	9.7	10.6	9.8	9.4	9.2	6.4	6.8	7.7	6.3	6.3	2.2	5.6	1.4		0.2
Opx	16.5	16.3	7.0	13.5	4.9	8.4	9.6	4.7	8.6	7.5	4.7	9.8	3.9	4.7	4.0	4.1	2.4
Ol		4.4	10.4	2.5		0.7	2.3	2.5									
Mt	7.3	3.1	4.9	3.8	8.6	4.6	3.0	5.8	2.6	3.4	5.5	2.5	3.4	2.2	2.4	0.8	1.9
Ilm	8.9	7.3	7.1	6.2	4.5	4.2	3.8	3.2	2.3	2.2	2.4	2.8	1.4	1.9	1.6	0.9	0.7
Ap	2.0	2.2	2.7	2.6	2.0	2.3	1.9	1.6	0.8	0.7	0.7	1.3	0.5	0.7	0.7	0.3	0.3

Sample location and description: 1. Matrix of porphyric jotunite JCD70.20 - Fine-grained border facies of Hidra massif, E. Vardebakkan (Duchesne et al., 1974); 2. Fine-grained jotunite JCD72.34 - E. contact of Hidra massif (Duchesne et al., 1974); 3. Medium-grained jotunite JCD78.33 – Fidsel; 4. Fine-grained jotunite occurring as rounded inclusions in 5 (average of 4 samples) – Trolldalen; 5. Porphyric jotunite (associated with 4) JCD81.12.82 – Trolldalen; 6, id. JCD81.12.6 – Trolldalen; 7. Fine-grained jotunite (rounded inclusion) embedded in (8) JCD75.69.2 – Erratic; 8. Porphyroidic jotunite mangerite, associated with 7, JCD75.69.1 Erratic; 9. Porphyroidic jotunite mangerite, JCD81.12.9 – Trolldalen; 10. Id. JCD80.28.2 - NW Montremyr; 11. id. JCD80.28.1 – Sturlaknuten; 12. (Hypersthene-bearing) quartz-mangerite jotunite (average of 10 samples from the upper part of the Bjerkreim-Sokndal intrusion); 13. Charnockite (average of 2 samples) – Breimyrknutan; 14. Farsund charnockite (average of 37 analyses) (Wilson and Annis, 1973); 15. Foliated farsundite (average of 2 analyses) – Itland; 16. Leucogranitic gneiss JCD80.30 - contact zone of Hidra massif, Vardebakkan; 17. id. JCD78.34.1 - Septum, E. - E. Sturlaknuten.

c. Large inclusion (septum) from the envelope made up of banded gneisses which comprises quartzitic and amphibolitic to noritic layers associated with lenses of leucogranitic gneiss and followed by a thick fine-grained leucogranitic unit (ca 200 m) faintly oriented (anal. 17). Small doleritic dyke with aphanitic borders.

d. Porphyroïdic to porphyritic (quartz-) mangerite (anal. 5, 6, 9 and 10) extending on both sides of Monstremyr, locally with quartzo-feldspathic patches showing large poikocrysts of brown amphibole (diam. up to 10 cm) (ferro-edenitic hornblende (Dekker 1978)). Metre-sized rounded, sharply bound, jotunitic inclusions (anal. 4) and interfingeredleucogranitic lenses. Swarm of inclusions.

At the northern tip of Monstremyr take the gravel road which follows Trolldalen towards Torsvatn.

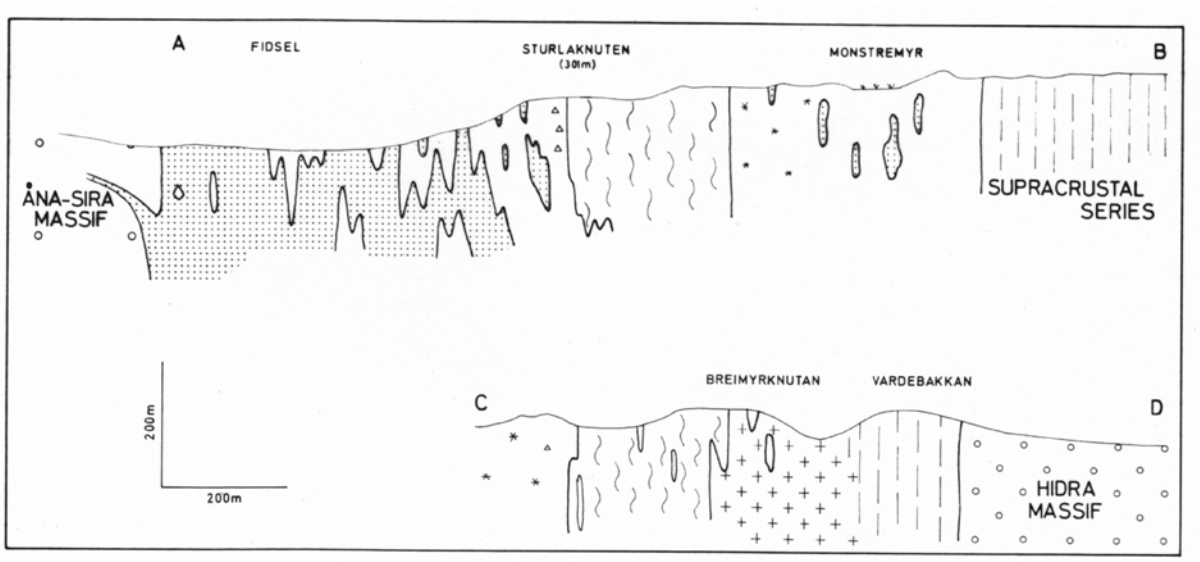

Fig. I 4.3. Cross sections in the geological map. Same legend as in fig. I.4.2.

e. Series of supracrustals comprising metaquartzites, fine-grained granitic gneisses locally migmatitic, banded norito-granitic gneisses, metanorites, kinzigitic gneisses (garnet - cordierite - sillimanite - spinel gneisses), amphibolites, noritic gneisses, and augen gneisses. The rock show evidence of intense stretching (boudinage, blastomylonite texture, small-scale banding, etc.) and several episodes of migmatization.

Return to Monstremyr and follow the path to Vardefjell.

f. Vardefjell: complex rock formed at the contact between the envelope and the (quartz-) mangeritic unit: small angular mafic-rich inclusions in a mixture of quartzo-feldspathic leucocratic material with porphyritic jotunite. Leuco-granitic patches. Continue to the South and follow the banded gneisses up to the Breimyrknutan body.

g. Breimyrknutan: small body of charnockite (= hypersthene granite) showing intrusive contact against the banded gneiss unit. It is a massive, unfoliated, coarse-grained rock (anal. 13) emplaced in a late tectonic stage possibly in close chronological relationship with the Hidra body.

h. Banded gneisses from the envelope and immediately at the contact with the Hidra body, continuous unit of leucogranitic gneiss (vertical lineation) (anal. 16).

i. Porphyritic jotunite (anal. 1 and 2) at the margin of the Hidra body containing large (up to 30 cm) phenocrysts of blue plagioclase. Variation in the phenocrysts/matrix ratio. Increasing proportion of phenocrysts towards the centre of the body. Coarse-grained leuconorite of the Hidra body (orthoculumate structure) (Demaiffe and Hertogen 1981). Stockwork of acidic dykes.

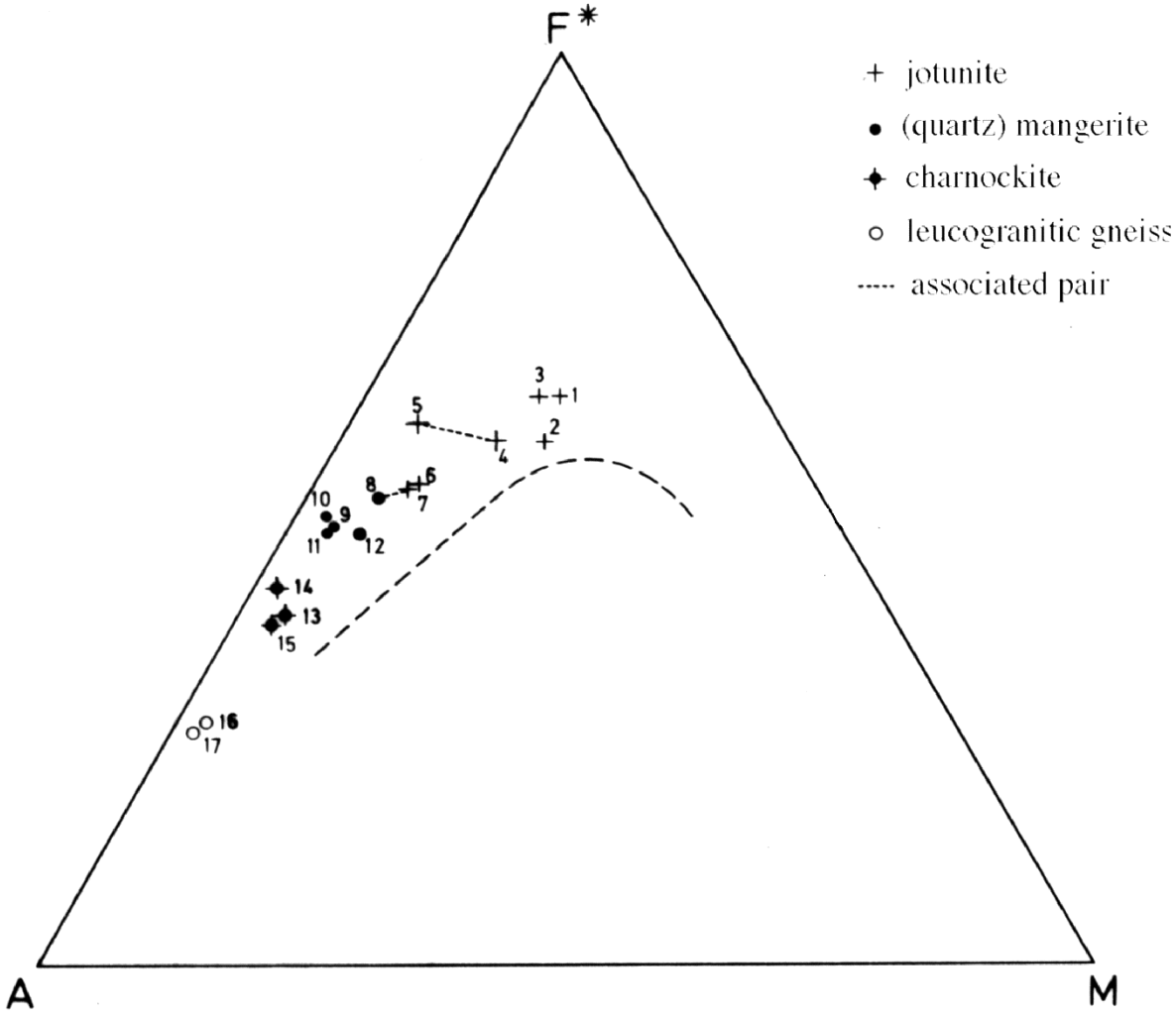

Fig. I 4.4. AFM diagram ($Na_2O + K_2O$ - FeO + 0.9 Fe_20_3 - MgO) of rocks given in Table I.4.1.

View on the Hidra body and its eastern contact with the envelope. Follow the path eastward through Håland (abandoned) to Itland.

j. Cross-section through the monotonous coarse-grained Hidra leuconorite. Locally blue plagioclase phenocrysts (c. 20 cm) and acidic (graphic) pegmatitic dykes.

After Itland, follow the gravel road on 300 m and stop on top of the slope.

k. Foliated Farsund charnockite (anal. 15) with conspicuous blastomylonitic texture.

Return to road 44, follow it to Flekkefjord and then to Moi.

Comments

A. The intrusion situated between Åna-Sira and the envelope has been considered as the southern prolongation of the Bjerkreim-Sokndal lopolith (Demaiffe 1972) and, consequently, called the Apophysis of Bjerkreim-Sokndal. Field studies and geochemical data (Bolle 1998) have revealed that this intrusion in its northern part is a conduit by which (quartz) mangeritic material (anal. 12) from the uppert part of the Bjerkreim-Sokndal has escaped. South of Lundevatn, this material is mingled with a jotunite magma (anal. 3, 4) giving rise to fine-grained rounded inclusions (anal. 4, 7), hybrid porphyroidic jotunite (anal. 5, 6) and mangerite (anal. 8-11).

B. The Breimyrknutan charnockitic body (Wilmart 1982) matches the experimental eutectic obtained by Wendlant (1981). It could have been produced by virtually in situ anatexis under granulite facies conditions (dry conditions or high P_{CO2} of the supracrustal series, in which it is emplaced. CO_2-rich fluid inclusions are present (Wilmart & Duchesne 1987). The necessary heat for the charnockitic anatexis can have been provided by the nearby Hidra intrusion. Both bodies are undeformed and thus late in the tectonic evolution.

C. The supracrustal character of the envelope is evidenced by the occurrence of aluminous gneisses (pelitic rocks), as well as by metaquartzites. Metabasites are likely to represent former volcano-sedimentary material. Preliminary data on the major and trace element geochemistry of these rocks indicate that no simple answer can be given to the question of the origin of the basic rocks (Jacques de Dixmude 1978; Wilmart 1982). Metasomatic enrichment of alkalis is obvious in F-rich biotite-bearing amphibolites (K_2O up to 2.3%; K/Rb = 50; F up to 2000 ppm) (Roelandts et al. 1987). The augen gneisses and the granitic gneisses interbedded in the series were possibly former grauwackes and rhyolitic tuffs, respectively.

   Application of various orthopyroxene-clinopyroxene geothermometers to the metabasites yields the following equilibrium temperatures (Wilmart & Duchesne 1987): 840° (Wells 1977), 800°C (Wood & Banno 1973) and 650° (Lindsley & Andersen 1983). Garnet-cordierite-plagioclase-sillimanite-quartz assemblages in neigbouring metapelites give values around 600°C and 3 ± 0.5 kb by means of several geothermobarometers (Thompson 1976; Martignole & Sisi 1981; Newton & Haselton 1980; Aranovitch & Podlesskii 1983).

   Armoured relics of symplectic quartz + spinel in garnets suggest peak temperature around 1000°C and a final equilibrium attained by decreasing temperature (Wilmart & Duchesne 1987). In the Breimyrknutan charnockite, opx-cpx geothermometry gives a minimum temperature of 800°C (host-pyroxene and exsolution lamellae), in agreement with the high T conditions one would expect for dry anatexis.

   Application of Bohlen and Boettcher's (1981) experimental results on the opx-olivine-quartz equilibrium yields a minimum pressure of 5 kb for the emplacement of the Hidra charnockitic dykes (see below). It appears that the pressures recorded are 1-3.5 kb lower that those recorded in the quartz mangerites of the Bjerkreim-Sokndal lopolith (Wilmart & Duchesne 1987; Wilmart et al. 1991). Though the aluminous gneisses on which the thermobarometry is calculated are closed to the contact with Åna-Sira and the Apophysis, it can be suspected that the P,T conditions measured do not relate to the emplacement of the igneous masses, but to a later stage of retrograde evolution.

D. The Hidra massif provides a rare opportunity for observing the relationship between the central coarse-grained leuconorite and the border facies, which is a fine-grained (300 to 500 μm) porphyritic (phenocrysts An_{45} from 2 to 20 cm) (Duchesne 1971; Demaiffe et al. 1973) (anal. 1 and 2). Trace element geochemistry (Duchesne et al. 1974) of the jotunite shows no Eu anomaly (fig. I 4.5) and a relatively high Sr content. These data are strong evidence in favour of the jotunite being the parental magma of the body and the border facies being the equivalent of the chilled margin of shallower intrusions. On these grounds, Duchesne & Demaiffe (1978) have suggested that jotunitic/jotunitic magmas can be parental to andesine anorthosites. Demaiffe & Hertogen (1981) and Weis & Demaiffe (1983) provided a description of the petrology, geochemistry and Sr and Pb isotopic compositions of various rock-types from the Hidra massif and have calculated a fractional crystallization model with assimilation (AFC) starting from a jotunitic magma and producing anorthosite and leuconorite complementary to the acidic dyke network. They have to assume the early separation of an Fe-Ti-P-rich cumulate in order to account for the evolution towards acidic rocks.

Geochronological studies (Pasteels et al. 1979) give an age close to 930 Ma, which is late in the magmatic evolution of the province. The lack of any deformation structure of the plagioclase precludes any tectonic movement during or after the crystallization process (a rather unusual feature for an anorthosite body!). The magma chamber was created by the opening of the supracrustal series, a movement possibly initiated by the emplacement of the nearby, older Farsund charnockite intrusion.

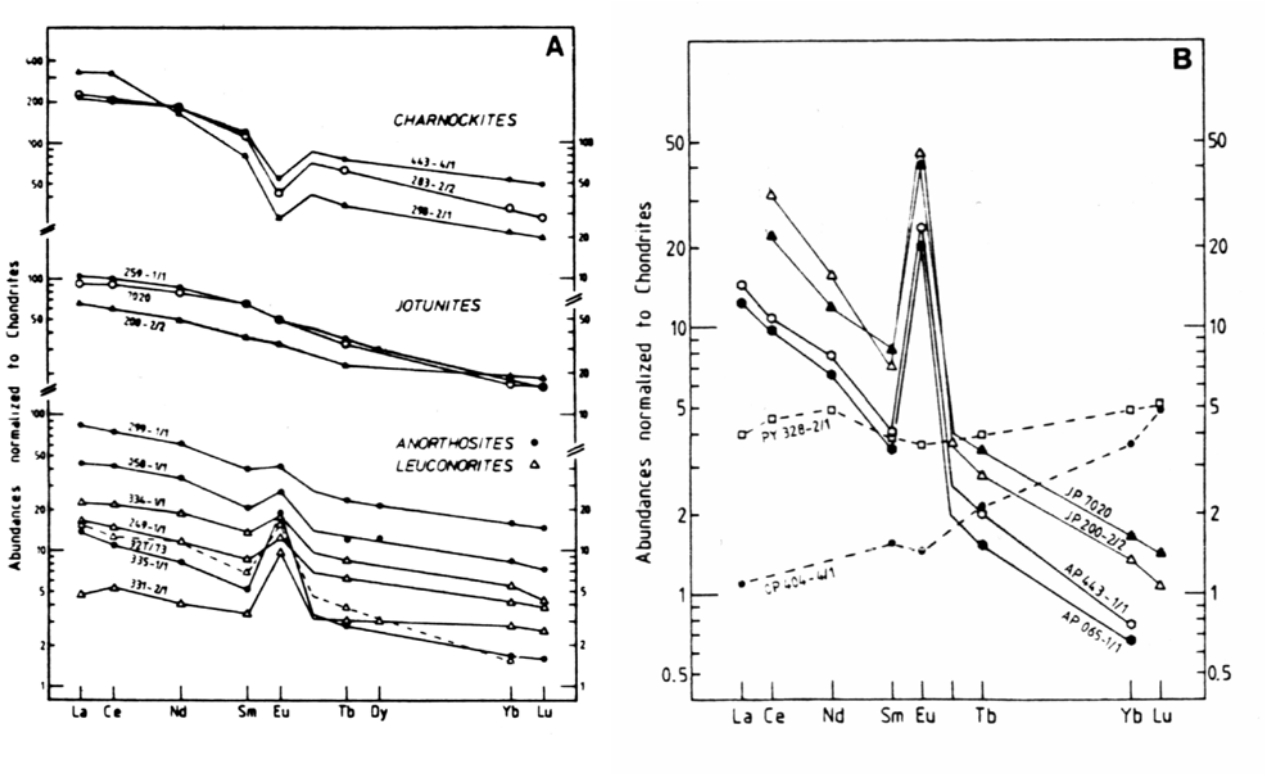

Fig. I 4.5. Rare earth element distribution in the Hidra massif (chondrite-normalized REE patterns). A: whole-rock samples. B: unzoned cores of two large plagioclase crystals from anorthositic orthocumulates (AP) and of two composite plagioclase phenocryst samples from the border jotunites (JP). Also plotted are the data for a pyroxenite (PY) and an orthopyroxene (OP) megacryst (from Demaiffe & Hertogen, 1981).

Locality 4.4 (1311.4; LK550-625) THE HOGSTAD LAYERED INTRUSION

From Kvanvig along road 44, take a small road to the south.

This small intrusion (2 km x 200 m) has been subdivided into three units which are from the base to the top : banded norites, spotted leuconorites (with opx oikocrysts) and homogeneous norites (Boutefeu 1973; Castellani 1993; Vander Auwera & Duchesne 1996) (Fig. I 4.6). The rocks display a subvertical planar lamination and locally, a subvertical lineation. The norites and leuconorites are essentially made up of plagioclase and orthopyroxene with minor augite and accessory apatite, ilmenite and magnetite. Late biotite and amphibole locally occur around Fe-Ti oxides. Plagioclase, orthopyroxene and ilmenite are cumulus phases in the whole sequence. Magnetite, apatite and clinopyroxene are postcumulus phases in the banded norites and become cumulus phases in the middle (magnetite) and upper parts (apatite, clinopyroxene) of the intrusion (Fig. I 4.6). Plagioclase and orthopyroxene show evidence of granulation and deformation (bent twinning, kinks, ondulous extinction).

Microprobe data display a restricted range of cryptic layering in plagioclase (An_{49}-An_{37}), orthopyroxene (En_{64}-En_{50}) and augite (Mg# = 0.75 to 0.65), which indicates a small extent of

fractionation (Fig. I 4.7). The Cr, Ni and Co content of ilmenite and magnetite as well as the REE content of plagioclase suggest that the spotted leuconorites correspond to a new magma influx and thus that the intrusion results from fractional crystallization of two distinct magma batches.

Major and trace elements content of minerals indicate that the parent magma of the intrusion is similar in composition to a primitive jotunite slightly less magnesian than the Tjörn chilled margin of the nearby Bjerkreim-Sokndal intrusion (sample 80123a of Duchesne & Hertogen 1988, and of Vander Auwera & Longhi 1994). Moreover, although this small magma chamber is enclosed in the Åna-Sira anorthosite, these intrusions have different parent magmas. Finally, the Hogstad body was emplaced at a pressure of 5 kb or less and the deformed textures observed in the intrusion were likely induced by the synemplacement deformation linked to the diapiric uprise of the Åna-Sira anorthosite. This process has probably also induced the subvertical position of the layering.

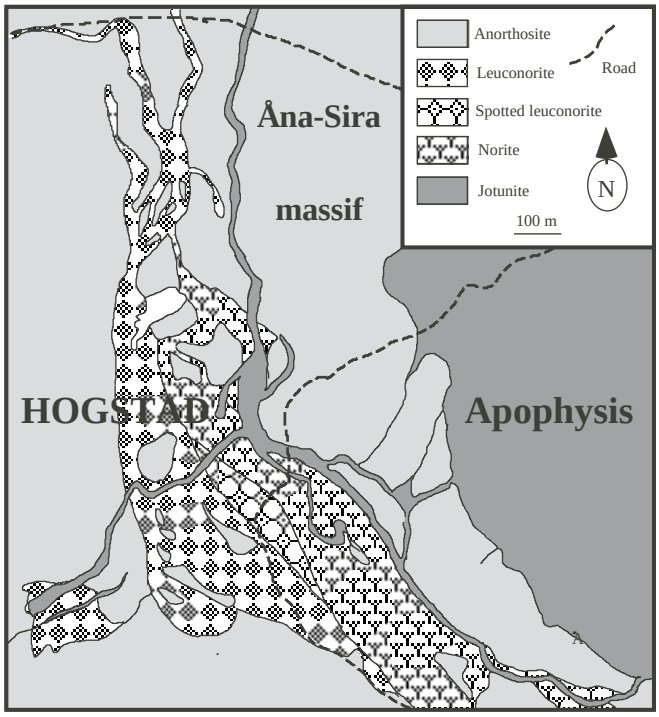

Fig. I 4.6. Geological map of the Hogstad layered intrusion. Legend: 1: (banded) norite; 2: spotted leuconorite; 3: homogeneous norite; 4: anorthosite (Åna-Sira massif); 5: undifferentiated rocks from the Apophysis (after Vander Auwera & Duchesne, 1996). probably also induced the subvertical position of the layering.

UNITS	Samples	Plag An %	Opx Ens %	Ilm Cr (ppm)	Mgt Cr (ppm)	Cpx Mg#	Apa Modal Prop.(%)	Ilm Modal Prop.(%)	Mgt Modal Prop.(%)
	TOP								
HOMOGENEOUS NORITES	73-82 (N)								
	92HG14(N)	37	51			0.65			
	92HG16(N)	44	50						
	70-34 (N)	41	56	59	452	0.66	4.9	6.8	5.3
	70-33 (L)	44	62			0.72	1.8	5.1	0
SPOTTED LEUCONORITES	73-85 (L)								
	72-69 (L)	47	60	486	4419		2	7.2	1.5
BANDED NORITES	73-02 (N)	43	61	<25					
	72-66 (N)	46	64				0	11.2	5.5
	72-61(L)						0.5	4.9	1.5
	92HG19(L)	44	61			0.75			
	72-63 (L)	44	63				0.6	7.4	2.1
	72-62 (L)	49	62	178	1115		0.5	5.4	0.7
	BOTTOM								

Fig. I 4.7. Generalized cumulus sequence and cryptic layering in the Hogstad body. Sample numbers refer to the most representative samples of the different units. Petrographic type in brackets: leuconorite (L) or norite (N). Dashed line: intercumulus status; continuous line: cumulus status. Plagioclase and pyroxene composition correspond to the most An-rich and most magnesian compositions respectively observed in each sample. Modal proportions of minerals from Boutefeu (1973).

Return to Moi.

Locality 4.5 (1311.4; LK539-711) VOREKNUDEN: ACIDIC QUARTZ MANGERITE FROM THE APOPHYSIS

Coming from Moi or Mydland, take the road to Navrestad-Åvedal. Drive ca 500 m to attain the Voreknuten track which starts on the western side of the road. Turn into the track and, a bit further on, pass through a barrier closed with a padlock (the key may be obtained at the *Kraftverk* of Moi). For ca 750 m, from the barrier to the eastern shore of a small lake (Kvedlandsvatnet), the track cut across the southern tip of the Garsaknatt leuconorite outlier (some outcrops are visible along the track); and after the lake, in the (steep!) slope to the Vorknuten, it scores a ca 500-m-large unit of granulite-facies banded gneisses which separates the Garsaknatt massif from the Apophysis (Fig. I 4.8). Park at the end of the track, near a small building, at the foot of the antenna which caps the Voreknuten (542 m).

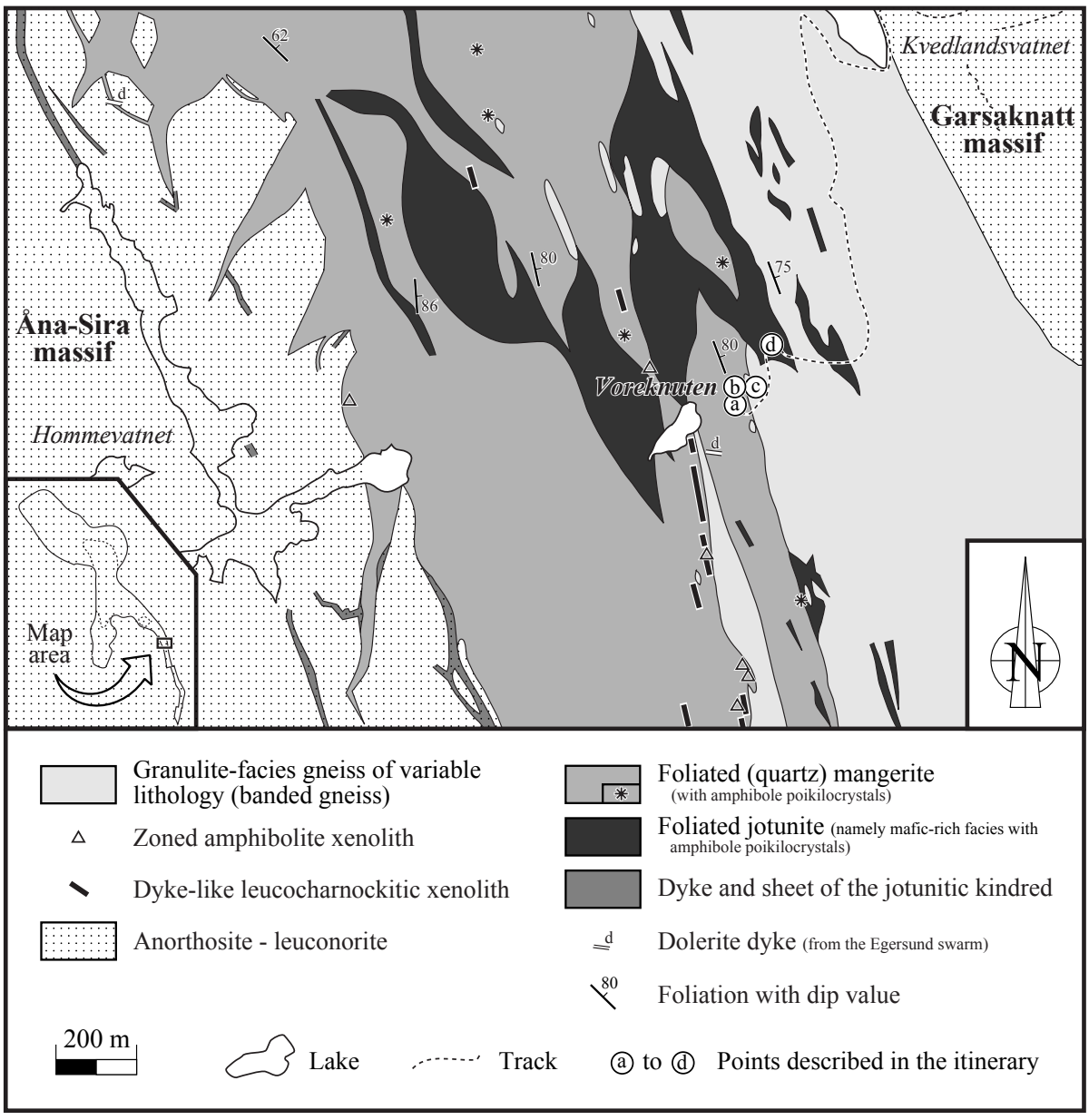

Fig. I 4.8. Geological sketch map of the Apophysis in the Voreknuten surroundings.

a. Fresh outcrops of coarse-grained quartz mangerite. The rock is strongly deformed, and displays sub-vertical mineral foliation and lineation. Note the winged aspect (usually symmetrical) of K-feldspar porphyroclasts. Presence of some elongated, cm- to dm-sized, zoned amphibolite xenoliths from the high-grade country rocks, which are transposed parallel to the lineation.

   This mangeritic rock is the dominant component of the Apophysis in the area and is usually more evolved than in the southern part (see Chapter 4 and Table 4.1 for information about the geochemistry). The foliated aspect, with steep dips, is a typical feature of the whole Apophysis and of a marginal zone developed in the BKSK acidic rocks, along their eastern contact. This strongly deformed area has been interpreted as a sub-vertical, syn- to post-magmatic shear-zone, possibly accomodating differential gravity-induced movements between the eastern part of the Rogaland anorthosite province and the gneissic country rocks (Bolle et al. 1997; 2000). More structural data on the granulitic gneisses and the Åna-Sira anorthosite adjacent to this zone are however needed to better constrain this thesis.

Climb up to the Voreknuten top.

b. Viewpoint. Strong contrast in the landscape between the Apophysis naked hills, mainly made up of quartz mangerite, and the hollows immediately to the east and the SE, occupied by rocks from the metamorphic envelope; straight contact beautifully displayed to the south and which runs a few metres below the Voreknuten top. Towards the NE, the wooded hills are made up of leuconorite from the Garsaknatt outlier; and to the west, towards the sea, dark coloured mounds belong to the Åna-Sira anorthosite massif.

Go down to the east, towards the track along which it will be proceeded northward for some tens of metres.

c. Contact between the Apophysis foliated quartz mangerite and the banded gneisses, followed by a small cross-section through these latter. Centimetre- to decimetre-scale, irregular alternances of felsic (charnockitic) and mafic (amphibolitic, metanoritic) layers and lenses, with some metaquartzite intercalations. Local migmatitization.

d. Outcrops of coarse-grained jotunite, with poikilocrystals of brown amphibole, some of them being included in dm-sized quartzofeldspathic patches with pegmatitic texture.

   These outcrops are part of an off-shoot, escaped from a network of jotunite lenses associated with the (quartz) mangerite in the Apophysis northern part. The jotunite lenses correspond to pockets of liquid laden with pyroxenes, oxides and apatite, as demonstrated by the relatively high mafic-mineral content (40-55%) and important Fe-Ti-P enrichment (Table 4.1) of many samples (FTP rocks) (Chapter 4). The aspect of the jotunite lens network, a kind of huge *shlieren* structure, suggests that the pockets where elongated and dislocated in the flowing (quartz) mangerite magma (Bolle et al. 1997). Major and trace element geochemistry, and Sr-Nd isotopes (Bolle 1998; Bolle et al. in prep.) preclude however any comagmatic relationship with the acidic host, in the form e.g. of a flow differentiaton.

***

Itinerary 5

THE ROGALAND IRON-TITANIUM DEPOSITS

(by J.C. Duchesne and H. Schiellerup)

This itinerary will allow us to visit a few spectacular outcrops of typical orebodies with easy access, including the world-class ilmenite deposit of Tellnes in operation by Titania A/S.

From Moi, take the E39 (E18) to the North, after driving through the Drangsdalen, at Eide, take road 501 to Rekeland and Hauge. At Rekeland turn right on road 44 and drive to Svånes.

Locality 5.1 (12111.1 ; LK270-764) THE SVÅNES DEPOSIT

Outcrops of the Svånes deposit can be observed along the road. The deposit is described in the Appendix of Chapter 5.

Drive to Egersund and in the locality take on the right the road to Koldal. Drive to Koldal, Heggdal and on the south side of the Kydlandsvatn and stop at Kydland.

Locality 5.2 (1211.1 ; LK349-778) THE JERNELD DEPOSIT

The path to the Jerneld deposit follows a 30 m-thick dolerite dyke. After some 1300 m, when the Spjodevatnet lake comes into view, turn right. The Jerneld deposit is described in the Appendix of Chapter 5.

Drive back along the same road and stop at the houses 500 m east of Stokkatjørna. Take the path to the SE.

Photo I 5.1. Norito-charnockitic septum (Norio-granitic zone of P. Michot) in the surroundings of the Rødemyr deposit. A late leucocharnockitic dyke cuts across the septum.

Locality 5.3 (1211.1 ; LK284-798) THE RØDEMYR DEPOSIT

On the path to the old mining site, one cuts across the Puntavoll-Lien norito-granitic zone (NGZ), as defined by Michot (1955) (see Chapter 1), which is some 50 m thick here. It is made up of alternating layers of equigranular norite and blastomylonitic leucocharnockite (Photo I 5.1). An inclusion of anorthosite (10 cm in diameter) can be observed. A thin

undeformed magnetite-bearing charnockitic dyke cuts the septum at a high angle. The Rødemyr deposit is described in the Appendix of Chapter 5.

Drive back to Egersund, take road 44 to the south and at the first crossing, turn right toward Hestnes. Stop in the village at a small playground. Walk uphill towards Lårabakken. The deposit is not easy to find in a small gully at the contact with ZNG rocks. The accurate location is 3 24843-64 797793.

Locality 5.4 (1211.1 ; LK249-797) THE HESTNES NELSONITE DEPOSIT

The Hestnes deposit is described in the Appendix of chapter 5.

Drive back to Hauge, then take the road to Flekkefjord and shortly after leaving the centre, take the bridge to the left and the small road to Mydland. Some 4 km further on, take a small road on the left to Løtupt. Drive ca. 2.5 km and stop some 500 m before Løtupt.

Locality 5.5 (1311.4 ; LK447-761) THE FLORDALEN DEPOSIT

The Flordalen deposit is described in the Appendix of Chapter 5. The outcrops are along the road and at the entry of an old shaft.

Drive back the same road and at Sandbekk, take the bridge entering the old buildings of Titania and immediately after the bridge, take to the right to the end of the road.

Locality 5.6 (1311.4 ; LK445-722) THE STORGANGEN DEPOSIT

The Storgangen deposit is described in the Appendix of chapter 5.

Drive back in direction of Hauge and before the bidge, turn left along a small road to Åmot and Blåfjell

Locality 5.7 (1311.4 ; LK469-714) THE BLÅFJELL DEPOSIT

The Blåfjell deposit is described in the Appendix of chapter 5. A description of the mining history can be found at the site.

Drive back to the bridge and after it take road 44 to Flekkefjord. Some 2km further on, take the private road to Tellnes (Titania A/S).

Locality 5.8 (1311.4 ; LK490-690) THE TELLNES DEPOSIT

The Tellnes deposit is described in the Appendix of chapter 5.

Drive back to Moi through Rekeland and Eide (road 504) or through Mydland, Liland, and Skåland along Lundevatnet.

References

Åhäll, K.-I., Cornell, D. H., & Armstrong, R. 1998: Ion probe zircon dating of metasedimentary units across the Skagerrak: new constraints for early Mesoproterozoic growth of the Baltic Shield. Precambrian Res. 87, 117–134.

Åhäll, K.-I. & Gower, C. F. 1997: The Gothian and Labradorian orogens: variations in accretionary tectonism along a late Paleoproterozoic Laurentia–Baltica margin. *Geol. Fören. Stockholm Förhan. 119*, 181–191.

Andersen, D.J., Lindsley, D.H. & Davidson, P.M. 1993: QUILF: a Pascal program to assess equilibria among Fe-Mg-Ti oxides, pyroxenes, olivine, and quartz. *Comput. Geosci. 19*, 1333-1350**.**

Andersson, J., Möller, C., & Johansson, L. submitted: Zircon chronology of migmatite gneisses along the southern Mylonite Zone: a major Sveconorwegian terrane boundary in the Baltic Shield. *Precambrian Res.*

Andersson, J., Söderlund, U., Cornell, D., Johansson, L., & Möller, C. 1999: Sveconorwegian (-Grenvillian) deformation, metamorphism and leucosome formation in SW Sweden, SW Baltic Shield: constraints from a Mesoproterozoic granite intrusion. *Precambrian Res. 98*, 151–171.

Andersson, M., Lie, J.E. & Husebye, E.S. 1996: Tectonic setting of post-orogenic granites within SW Fennoscandia based on deep seismic and gravity data. *Terra Nova 8*, 558-566**.**

Aranovitch, L.Y. & Podlesskii, K.K. 1983: The cordierite-garnet-sillimanite-quartz equilibrium: experiments and applications. *In*: Saxena, S.K. (ed) *Adv. in Physical Geochemistry.* Springer, Heidelberg, 3, 173-198.

Ashwal, L.D. 1993: Anorthosites. Springer, Heidelberg, 422 p.

Barbey, P., Bertrand, J.M., Angoua, S. & Dautel, D. 1989: Petrology and U/Pb geochronology of the Telohat migmatites, Aleksod, Central Hoggar, Algeria. *Contrib. Miner. Petrol. 101*, 207-219**.**

Barling, J., Weis, D. & Demaiffe, D. 2000: A Sr-, Nd-, and Pb-isotopic investigation of the transition between two megacyclic units of the Bjerkreim-Sokndal layered intrusion, south Norway. *Chemical Geology 165*, 47-65**.**

Barnichon, J.-D., Havenith, H., Hoffer, B., Charlier, R., Jongmans, D. & Duchesne, J.C. 1999: The deformation of the Egersund Ogna massif, South Norway: Finite Element modelling of diapirism:. *Tectonophysics 303*, 109-130**.**

Berthelsen, A. 1980: Towards a palinspastic tectonic analysis of the Baltic Shield. *Int. Geol. Cong.*, 5–21.

Bingen, B., Boven, A., Punzalan, L., Wijbrans, J.R. & Demaiffe, D. 1998a: Hornblende $^{40}Ar/^{39}Ar$ geochronology across terrane boundaries in the Sveconorwegian Province in S. Norway. *Precambrian Res. 90*, 159-185**.**

Bingen, B., Birkeland, A., Nordgulen, Ø., & Sigmond, E. M. O. in press: Correlation of supracrustal sequences and origin of terranes in the Sveconorwegian orogen of SW Scandinavia: SIMS data on zircon in clastic metasediments. *Precambrian Res.*

Bingen, B., Birkeland, A., Nordgulen, Ø., Sigmond, E. M. O., & Whitehouse, M. 1999: Abstract. Detrital zircon ages from sediments in Hardangervidda, Telemark and Kongsberg, S Norway, and implications for Proterozoic crustal building in the Sveconorwegian province. *J. Conf. Abs. 4-1*, 126.

Bingen, B., Demaiffe, D. & Hertogen, J. 1990: Evolution of feldspars at the ampphibolite-granulite-facies transition in augen gneisses (SW Norway): geochemistry and Sr isotopes. *Contrib. Mineral. Petrol. 105*, 275-288**.**

Bingen, B., Demaiffe, D. & Hertogen, J. 1996: Redistribution of rare earth elements, thorium, and uranium over accessory minerals in the course of amphibolite to granulite facies metamorphism:

The role of apatite and monazite in orthogneisses from southwestern Norway. *Geochim. Cosmochim. Acta 60*, 1341-1354**.**

Bingen, B., Demaiffe, D., Hertogen, J., Weis, D. & Michot, J. 1993: K-rich calc-alkaline augen gneisses of Grenvillian age in SW Norway: mingling of mantle-derived and crustal components. *J. Geology 101*, 763-768**.**

Bingen, B., Demaiffe, D. & van Breemen, O. 1998b: The 616 Ma old Egersund Basaltic dike swarm, SW Norway, and Late Neoproterozoic opening of the Iapetus Ocean. *J. Geology 106*, 565-574**.**

Bingen, B. & van Breemen, O. 1998a: Tectonic regimes and terrane boundaries in the high-grade Sveconorwegian belt of SW Norway, inferred from U-Pb zircon geochronology and geochemical signature of augen gneiss suites. *J. Geol. Soc. London 155*, 143-154**.**

Bingen, B. & van Breemen, O. 1998b: U-Pb monazite ages in amphibolite- to granulite-facies orthogneiss reflect hydrous mineral breakdown reactions: Sveconorwegian Province of SW Norway. *Contribution to Mineralogy and Petrology 132*, 336-353**.**

Bogaerts, M., Scaillet, B. & Vander Auwera, J. 2001: Experimental determination of phase equilibria of the Lyngdal granodiorite (Southern Norway) (abstract) EUG XI, Strasbourg, p770

Bohlen, S.R. & Boettcher, A.L. 1981: Experimental investigations and geological applications of orthopyroxene geobarometry. *Amer. Mineral. 66*, 951-964**.**

Bolle, O. 1996: L'Apophyse du massif stratiforme de Bjerkreim-Sokndal (Rogaland, Norvège): une intrusion composite de la suite charnockitique. *In*: Demaiffe, D. (ed) *Petrology and geochemistry of magmatic suites of rocks in the continental and oceanic crusts (J. Michot volume).* MRAC-ULB, Brussels, 129-144.

Bolle, O. 1998: *Mélanges magmatiques et tectonique gravitaire dans l'Apophyse de l'intrusion de Bjerkreim-Sokndal (Rogaland, Norvège). Pétrologie, géochimie et fabrique magnétique.* Thèse de doctorat, Université de Liège, 204 p.

Bolle, O., Demaiffe, D. & Duchesne, J.C. in prep: Petrognesis of jotunitic and acidic members of an AMCG suite (Rogaland anorthosite province, southwestern Norway): a Nd-Sr isotope assesment.

Bolle, O., Diot, H. & Duchesne, J.C. 1997: Anisotropie de la susceptibilité magnétique dans une intrusion composite de la suite charnockitique: l'apophyse du massif stratiforme de Bjerkreim-Sokndal (Rogaland, Norvège). *C. R. Acad. Sci. Paris (série IIa) 325*, 799-805**.**

Bolle, O., Diot, H. & Duchesne, J.C. 2000: Magnetic fabric and deformation in charnockitic igneous rocks of the Bjerkreim-Sokndal layered intrusion (Rogaland, Southwest Norway). *J. Struct. Geol. 22*, 647-667**.**

Boutefeu, A. 1973: *La lentille noritique de Hogstad (Norvège méridionale).* Unpubl. Licence Thesis, University of Liège.

Campbell, I.H. 1996: Fluid dynamic pocesses in basaltic magma chambers. *In*: Cawthorn, R.G. (ed) *Layered igneous rocks.* Elsevier, Amsterdam, 45-76.

Campbell, I.H. & Turner, J.S. 1987: A laboratory investigation at the top of a basaltic magma chamber. *J. Geology 95*, 155-172**.**

Castellani, M. 1993: *La lentille de Hogstad (Rogaland, Norvège): étude pétrologique et géochimique.* Unpub. Licence Thesis, Université of Liège.

Christoffel, C. A., Connelly, J. N., & Åhäll, K.-I. 1999: Timing and characterization of recurrent pre-Sveconorwegian metamorphism and deformation in the Varberg–Halmstad region of SW Sweden. *Precambrian Res. 98*, 173–195.

Connelly, J. N., Berglund, J., & Larson, S. A. 1996: Thermotectonic evolution of the Eastern Segment of southwestern Sweden: tectonic constraints from U–Pb geochronology. *In*: Brewer, T. S. (ed.) *Precambrian crustal evolution in the North Atlantic Region*, Vol. 112 , pp. 297–313. Geological Society, London, Special Publications.

Cosca, M. A., Mezger, K., & Essene, E. J. 1998: The Baltica–Laurentia connection: Sveconorwegian (Grenvillian) metamorphism, cooling, and unroofing in the Bamble Sector, Norway. *J. Geol. 106*, 539–552.

Dahlgren, S., Heaman, L., & Krogh, T. 1990: Geological evolution and U-Pb geochronology of the Proterozoic Central Telemark area, Norway. *Geonytt 17*, 38–39.

Davidson, A. 1995: A review of the Grenville orogen in its North American type area. *J. Australian Geol. Geophys. 16*, 3–24.

de Haas, G.J.L.M., Andersen, T. & Vestin, J. 1999: Detrital zircon geochronology: new evidence for an old model for accretion of the Southwest Baltic Shield. *J. Geology 107*, 569-586**.**

Deemer, S. & Hurich, C. 1997: Seismic image of the basal portion of the Bjerkreim-Sokndal layered intrusion. *Geology 25*, 1107-1110**.**

Dekker, A.G.C. 1978: Amphiboles and their host rocks in the high-grade metamorphic Precambrian of Rogaland/Vest Agder, SW. Norway. *Geol. Ultrajectina 17*, 275 p.

Demaiffe, D. 1972: Etude pétrologique de l'Apophyse sud-est du massif de Bjerkrem-Sogndal. *Ann. Soc. Géol. Belg. 95*, 255-269**.**

Demaiffe, D., Duchesne, J.C., Michot, J. & Pasteels, P. 1973: Le massif anorthosito-leuconoritique d'Hidra et son faciès de bordure. *C.R. Acad. Sc. Paris 277*, 14-20**.**

Demaiffe, D. & Hertogen, J. 1981: Rare earth element geochemistry and strontium isotopic composition of a massif-type anorthositic -charnockitic body: the Hidra massif (Rogaland, SW. Norway). *Geochim. Cosmochim. Acta 45*, 1545-1561**.**

Demaiffe, D., Weis, D., Michot, J. & Duchesne, J.C. 1986: Isotopic constraints on the genesis of the anorthosite suite of rocks. *Chem. Geol. 57*, 167-179**.**

Diot, H., Lambert, J.M., Bolle, O. & Duchesne, J.C. 1999: Magmatic intrusion and mineralization along a strike-slip fault into the Åna-Sira anorthosite: the Tellnes case (Rogaland, Norway). *4th Hutton Conference* , Clermont-Ferrand.

Dons, J. A. 1960: Telemark supracrustals and associated rocks. *In*: Holtedahl, O. (ed.) *Geology of Norway*, Vol. 208, pp. 49–58. Norges geologiske undersøkelse.

Duchesne, J.C. 1966: Séparation rapide des minéraux des roches. *Ann. Soc. Géol. Belg. 69*, 347-356**.**

Duchesne, J.C. 1967: Les relations Sr-Ca dans les plagioclases des anorthosites du Rogaland méridional. *Ann. Soc. Géol. Belg. 90*, 643-667**.**

Duchesne, J.C. 1970: Microstructures of Fe-Ti oxide minerals in the South Rogaland anorthositic complex (Norway). *Ann. Soc. Géol. Belg. 93*, 527-544**.**

Duchesne, J.C. 1971: Le rapport Sr/Ca dans les plagioclases du massif de Bjerkreim-Sogndal et son évolution dans la cristallisation fractionnée du magma plagioclasique. *Chem. Geol. 8*, 123-130**.**

Duchesne, J.C. 1972a: Iron-titanium oxide minerals in the Bjerkrem-Sogndal massif, South-Western Norway). *J. Petrol. 13*, 57-81**.**

Duchesne, J.C. 1972b: Pyroxènes et olivine dans le massif de Bjerkrem-Sogndal (Norvège méridionale). Contribution à l'étude de la série anorthosite-mangérite. *24ème Congrès Géologique International* , Montréal

Duchesne, J.C. 1973: Les gisements d'oxides de Fe et Ti dans les roches anorthositiques du Rogaland (Norvège méridionale). *In*: *Les roches plutoniques dans leur rapport avec les gîtes minéraux.* Masson, Paris, 241-248.

Duchesne, J.C. 1984: Massif anorthosites: another partisan review. *In*: Brown, W.S. (ed) *Feldspars and feldspathoids.* NATO Adv. Stud. Inst., Reidel, Dordrecht, C137, 411-433.

Duchesne, J.C. 1987a: The Bjerkreim-Sokndal massif. *In*: Maijer, C. & Padget, P. (ed) *The geology of southernmost Norway: an excursion guide.* Norges Geol. Unders., Special publication, 1, 56-59.

Duchesne, J.C. 1987b: The Rogaland intrusive massifs: eastern part. *In*: Maijer, C. & Padget, P. (ed) *The geology of southermost Norway: an excursion guide.* Norges Geol. Unders., Special publication, 1, 63-66.

Duchesne, J.C. 1990: Origin and evolution of monzonorites related to anorthosites. *Schweiz. Mineral. Petrogr. Mitt. 70*, 189-198**.**

Duchesne, J.C. 1996: Liquid ilmenite or liquidus ilmenite: a comment on the nature of ilmenite vein deposit. *In*: Demaiffe, D. (ed) *Petrology and geochemistry of magmatic suites of rocks in the continental and oceanic crusts*: ULB-MRAC, Brussels, 73-82.

Duchesne, J.C. 1999: Fe-Ti deposits in Rogaland anorthosites (South Norway): geochemical characteristics and problems of interpretation. *Miner. Deposita 34*, 182-198**.**

Duchesne, J.C., Caruba, R. & Iacconi, P. 1987a: Zircon in charnockitic rocks from Rogaland (South-West Norway): petrogenetic implications. *Lithos 20*, 357-368**.**

Duchesne, J.C. & Demaiffe, D. 1978: Trace elements and anorthosite genesis. *Earth Planet. Sci. Lett. 38*, 249-272**.**

Duchesne, J.C., Demaiffe, D., Roelandts, I. & Weis, D. 1985a: Petrogenesis of monzonoritic dykes in the Egersund-Ogna anorthosite (Rogaland, S.W. Norway): trace elements and isotopic constraints. *Contr. Mineral. Petrol. 90*, 214-225**.**

Duchesne, J.C., Denoiseux, B. & Hertogen, J. 1987b: The norite-mangerite relationships in the Bjerkreim-Sokndal layered lopolith (SW Norway). *Lithos 20*, 1-17**.**

Duchesne, J.C., Ernst, G.J. & Hertogen, J. 1991: Leuconoritic dykes: new evidence for injected crystal mushes from the Løyning lens (Egersund-Ogna massif, Rogaland, Norway) (abstract). *IGCP 290* , Adirondack meeting.

Duchesne, J.C. & Hertogen, J. 1988: Le magma parental du lopolithe de Bjerkreim-Sokndal (Norvège méridionale). *C.R. Acad. Sci. Paris 306*, 45-48**.**

Duchesne, J.C., Liégeois, J.P., Vander Auwera, J. & Longhi, J. 1999: The crustal tongue melting model and the origin of massive anorthosites. *Terra Nova 11*, 100-105**.**

Duchesne, J.C. & Maquil, R. 1981: Evidence of syn-intrusive deformation in South-norwegian anorthosites (abstract). *Terra Cognita Special issue 1*, 94**.**

Duchesne, J.C., Maquil, R. & Demaiffe, D. 1985b: The Rogaland anorthosites: facts and speculations. *In*: Tobi, A.C. & Touret, J.L.R. (ed) *The deep Proterozoic crust in the North Atlantic Province.* NATO Adv. Stud. Inst., Reidel, Dordrecht, C158, 449-476.

Duchesne, J.C., Roelandts, I., Demaiffe, D., Hertogen, J., Gijbels, R. & De Winter, J. 1974: Rare-earth data on monzonoritic rocks related to anorthosites and their bearing on the nature of the parental magma of the anorthositic series. *Earth Planet. Sci. Lett. 24*, 325-335**.**

Duchesne, J.C. & Wilmart, E. 1997: Igneous charnockites and related rocks from the Bjerkreim-Sokndal layered intrusion (Southwest Norway): a jotunite (hypersthene monzodiorite)-derived A-type granitoid suite. *J. Petrol. 38*, 337-369**.**

Duchesne, J.C., Wilmart, E., Demaiffe, D. & Hertogen, J. 1989: Monzonorites from Rogaland (Southwest Norway): a series of rocks coeval but not comagmatic with massif-type anorthosites. *Precambrian Research 45*, 111-128**.**

Ebadi, A. & Johannes, W. 1991: Beginning of melting and composition of first melts in the system Qz - Ab - Or - H_2O - CO_2. *Contrib Mineral Petrol 106*, 286-295**.**

Eliasson, T. & Schöberg, H. 1991: U–Pb dating of the post-kinematic Sveconorwegian (Grenvillian) Bohus granite, SW Sweden: evidence of restitic zircon. *Precambrian Res. 51*, 337–350.

Emslie, R.F. 1975: High pressure pyroxene megacrysts from anorthositic rocks and their bearing on the genesis of the parent magma (abstract). *Geol. Soc. Am., Abstr. with Progr. 7*, 752-753**.**

Emslie, R.F. 1978: Anorthosite massifs, Rapakivi granites, and the late Proterozoic rifting of North America. *Precambrian Res. 7*, 61-98.

Emslie, R.F. 1985: Proterozoic anorthosite massifs. *In*: Tobi, A.C. & Touret, J.L.R. (ed) *The deep Proterozoic crust in the North Atlantic Province.* NATO Adv. Stud. Inst., Reidel, Dordrecht, C158, 39-60.

Emslie, R.F., Hamilton, M.A. & Thiérault, R.J. 1994: Petrogenesis of a Mid-Proterozoic Anorthosite - Mangerite - Charnockite - Granite (AMCG) complex: isotopic and chemical evidence from the Nain plutonic suite. *J. Geology 102*, 539-558.

Ernst, G. 1990: *La lentille de Løyning, Egersund, Rogaland, Norvège méridionale.* Unpubl. Licence Thesis, University of Liège.

Ernst, G.J. & Duchesne, J.C. 1991: Evidence of ultra-small layered intrusion : the Löyning lens, Egersund, Norway (abstract). *Terra Abstracts 3*, 426-427.

Falkum, T. 1966: Structural and petrological investigations of the Precambrian metamorphic and igneous charnockite and migmatite complex of the Flekkefjord area, Southern Norway. *Norges Geol. Unders. 242*, 19-25.

Falkum, T. 1982: Geologisk kart over Norge, berggrunnskart Mandal, 1:250000.

Falkum, T. 1985: Geotectonic evolution of southern Scandinavia in light of a Late-Proterozoic plate collision. *In*: Tobi, A.C. & Touret, J.L.R. (ed) *The deep Proterozoic crust in the North Atlantic Province.* NATO Adv. Stud. Inst., Reidel, Dordrecht, C158, 309-322.

Falkum, T. 1998: The Sveconorwegian magmatic and tectono-metamorphic evolution of the high-grade Proterozoic Flekkefjord complex, South Norway. *Norges geol. Unders. Bulletin 434*, 5-33.

Falkum, T. & Pedersen, S. 1979: Rb-Sr age determination on the intrusive Precambrian Homme granite and consequence for dating the last regional folding and metamorphism in the Flekkefjord region, SW Norway. *Norsk Geol. Tidsskr. 59*, 59-65.

Force, E.R. 1991: Geology of titanium mineral deposits. *Geol. Soc. Amer. Spec. Paper 259*, 1-112.

Ford, C.E., Russell, D.G., Craven, J.A. & Fisk, M.R. 1983: Olivine-liquid equilibria: temperature, pressure and composition dependence on the crystal/liquid cation partition coefficients for Mg, Fe2+, Ca and Mn. *J. Petrol. 24*, 256-265.

Foslie, S. 1928: Gleichgewichtsverhältnisse bei einigen Titaneisenerzen. *Fennia 50*, 1-15.

Fourcade, S., Martin, H. & de Brémond d'Ars, J. 1992: Chemical exchange in migmatites during cooling. *Lithos 28*, 43-53.

Fram, M.S. & Longhi, J. 1992: Phase equilibria of dikes associated with Proterozoic anorthosite complexes. *Amer. Mineral. 77*, 605-616.

Gierth, E. 1983: Types and trace elements of titanium ores in the Tellnes area, South Rogaland. *In*: (ed) Monograph series on mineral deposits,: Gebrüder Borntraeger, Berlin, Stuttgart, 22, 47-57.

Gierth, E. & Krause, H. 1973: Die Ilmenitlagerstätte Tellnes (Süd-Norwegen). *Norsk Geol. Tidsskr. 53*, 359-402.

Gorbatschev, R. & Bogdanova, S. 1993: Frontiers in the Baltic Shield. *Precambrian Res. 64*, 3–21.

Green, T.H. 1970: Experimental fractional crystallization of quartz diorite and its application to the problem of anorthosite origin. *In*: Isachsen, Y.W. (ed) *Origin of anorthosite and related rocks.* N.Y. State Mus. Sci. Serv. Mem., 18, 23-30.

Hageskov, B. 1985: Constrictional deformation of the Koster dyke swarm in a ductile sinistral shear zone, Koster islands, SW Sweden. *Bull. Geol. Soc. Denmark 34*, 151–197.

Heaman, L. M. & Smalley, P. C. 1994: A U–Pb study of the Morkheia Complex and associated gneisses, South Norway: implications for disturbed Rb–Sr systems and for the temporal evolution of Mesoproterozoic magmatism in Laurentia. *Geochim. Cosmochim. Acta 58*, 1899–1911.

Henriette, A. 1984: *Les indices de sulfures dans le massif anorthositique d'Egersund-Ogna (Rogaland - Norvège méridionale)*. Unpub. Licence Thesis, University of Liège.

Hermans, G.A.E.M., Tobi, A.C., Poorter, R.P.E. & Maijer, C. 1975: The high-grade metamorphic Precambrian of the Sirdal-Ørsdal area, Rogaland/vest-Agder, SW Norway. *Norges geol. Unders. 318*, 51-74.

Holland T. J., Babu E. V., & Waters D. J. (1996) Phase relations of osumilite and dehydration melting in pelitic rocks: a simple thermodynamic model for the KFMASH system. *Contrib. Mineral. Petrology 124*, 383-394.

Hovland, R. 1975: Nikkelprospektering I Egersund - anorthositfelt. *Malmgeologisk symposium BVLI Bergforskningen, referat fra møte i Trondheim, "Nikkelprospektering i Norge »*

Hubaux, A. 1956: Différents types de minerais noirs de la région d'Egersund (Norvège). *Ann. Soc. Géol. Belg. 79*, 203-215.

Hubaux, A. 1960: Les gisements de fer titané de la région d'Egersund (Norvège). *N. Jb. Miner. Festband Ramdohr 94*, 926-992.

Huppert, H.E. & Sparks, R.S.J. 1980: The fluid dynamics of a basaltic magma chamber replenished by inlux of hot, dense, ultrabasic magma. *Contrib. Mineral. Petrol. 75*, 279-289.

Jacques de Dixmude, S. 1978: Géothermométrie comparée de roches du faciès granulite du Rogaland Norvège méridionale). *Bull. Mineral. 101*, 57-65.

Jansen, J.B.H., Blok, R.J., Bos, A. & Scheelings, M. 1985: Geothermometry and geobarometry in Rogaland and preliminary results from the Bamble, S. Norway *In*: Tobi, A.C. & Touret, J.L.R. (ed) *The deep Proterozoic crust in the North Atlantic Province.* NATO Adv. Stud. Inst., Reidel, Dordrecht, C158, 499-516.

Jarl, L.-G. 1992: New isotope data from the Protogine Zone and southwestern Sweden. *Geol. Fören. Stockholm Förhan. 114*, 349–350.

Jensen, J.C., Nielsen, F.M., Duchesne, J.C., Demaiffe, D. & Wilson, J.R. 1993: Magma influx and mixing in the Bjerkreim-Sokndal layered intrusion, South Norway: evidence from the boundary between two megacyclic units at Storeknuten. *Lithos 29*, 311-325.

Johansson, L., Lindh, A., & Möller, C. 1991: Late Sveconorwegian (Grenville) high-pressure granulite facies metamorphism in southwest Sweden. *J. Metamorphic Geol. 9*, 283–292.

Johansson, L., Möller, C., & Söderlund, U. in press: Geochronology of eclogite facies metamorphism in the Sveconorwegian Province of SW Sweden. *Precambrian Res.*

Kilpatrick, J.A. & Ellis, D.J. 1992: C-type magmas: igneous charnockites and their extrusive equivalents. *Trans. Roy. Soc. Edinburg: Earth Sciences, 83, 155-164.*

Knorn, H. & Krause, H. 1977: Die verbandsverhältnisse Südlich von Tellnes in Zentralteil des Åna-Sira-Massivs (Südnorwegen). *Norsk Geol. Tidsskr. 57*, 85-95.

Knudsen, T.-L. 1996: Petrology and geothermobarometry of granulite facies metapelites from the Hisøy–Torungen area, south Norway: new data on the Sveconorwegian P–T–t path of the Bamble sector. *J. Metamorphic Geol. 14*, 267–287.

Knudsen, T.-L. & Andersen, T. 1999: Petrology and geochemistry of the Tromøy gneiss complex, South Norway, an alleged example of Proterozoic depleted lower continental crust. *J. Petrol. 40*, 909–933.

Knudsen, T.-L., Andersen, T., Whitehouse, M. J., & Vestin, J. 1997: Detrital zircon ages from southern Norway - implications for the Proterozoic evolution of the southwestern Baltic Shield. *Contrib. Mineral. Petrol. 130*, 47–58.

Kolker, A. & Lindsley, D.H. 1989: Geochemical evolution of the Maloin Ranch pluton, Laramie Anorthosite Complex, Wyoming: petrology and mixing relations. *Amer. Mineral. 74*, 307-324.

Krause, H., Gierth, E. & Schott, W. 1985: Fe-Ti deposits in the South Rogaland igneous complex, especially in the Anorthosite-massif of Åna-Sira. *Norges Geol. Unders. 402*, 25-37**.**

Krause, H. & Pape, H. 1975: Mikroskopische Untersuchung der Minerallvergesellschaftung in Erz und Nebengestein der Ilmenitlagerstätte Storgangen (Süd-Norwegen). *Norsk Geol. Tidsskr. 55*, 387-422**.**

Krause, H. & Pedall, G. 1980: Fe-Ti mineralizations in the Åna-Sira anorthosite, Southern Norway. *In*: Siivola, J. (ed) *Metallogeny of the Baltic Shield.* Geol. Surv. Finland, 307, 56-83.

Krause, H. & Zeino-Mahmalat, R. 1970: Untersuchungen an Erz und Nebengestein der Grube Blåfjell in SW-Norwegen. *Norsk Geol. Tidsskr. 50*, 45-88**.**

Kullerud, K., Rolfsen, R., Bjørlykke, A., Hagen, R. & Tønnesen, H. in prep: Geochemical and mineralogical variations of the Tellnes ilmenite ore deposit, southwest Norway.

Kullerud, L. & Machado, N. 1991: End of a controversy: U–Pb geochronological evidence for significant Grenvillian activity in the Bamble area, Norway. *Terra Abstracts, supplement to Terra Nova 3*, 504.

Lambert, J.M. 1998: *Contribution à l'étude structurale, pétrographique et géochimique du massif anorthositique d'Egersund-Ogna (Norvège méridionale) et des gisements de Fer-Titane associés du Liåsen.* Unpub. Licence Thesis, University of Liège.

Lamb, R. C., Smalley, P. C., & Field, D. 1986: P-T conditions for the Arendal granulites, southern Norway: implications for the roles of P, T and CO2 in deep crustal LILE-depletion. *J. Metamorphic Geol. 4*, 143–160.

Larsen, T.R. 1931: Homse nikkel og kobbergrube. Rapport av cand. min. Chr. Otterbech 1871 og 1903. *NGU report 1442*, 3 p.

Larson, S. Å., Cornell, D. H., & Armstrong, R. A. 1999: Emplacement ages and metamorphic overprinting of granitoids in the Sveconorwegian Province in Värmland, Sweden - an ion probe study. *Norsk Geol. Tidsskr. 79*, 87–96.

Liégeois, J.-P. & Black, R. 1987: Alkaline magmatism subsequent to collision in the Pan-African belt of the Adrar des Iforas. *In*: Fitton, J.G. & Upton, B.G.J. (ed) *Alkaline Igneous rock.* Geological Soc. Special publication, 30, 381-401.

Liégeois, J.P., Navez, J., Hertogen, J. & Black, R. 1998: Contrasting origin of post-collisional high-K calc-alkaline and shoshonitic versus alkaline and peralkaline granitoids. The use of the sliding normalization. *Lithos 45*, 1-28**.**

Lindsley, D.H. & Andersen, D.J. 1983: A two-pyroxene thermometer. *Proc. 13th Lunar Planet. Sci. Conf., part 2, J. Geophys. Res. 88, supplement*, A887-A906**.**

Lindsley, R.F. & Frost, B.R. 1992: Equilibria amonf Fe-Ti oxides, pyroxenes, olivine, and quartz: Part I. Theory. *Amer. Miner. 77*, 987-1003**.**

Longhi, J., Fram, M.S., Vander Auwera, J. & Montieth, J.N. 1993: Pressure effects, kinetics, and rheology of anorthositic and related magmas. *Amer. Mineral. 78*, 1016-1030**.**

Longhi, J., Vander Auwera, J., Fram, M. & Duchesne, J.C. 1999: Some phase equilibrium constraints on the origin of Proterozoic (Massif) anorthosites and related rocks. *J. Petrol. 40*, 339-362**.**

Maijer, C. 1987: The metamorphic envelope of the Rogaland intrusive complex. *In*: Maijer, C. & Padget, P. (ed) *The geology of southernmost Norway: a guidebook.* Norges geol. Unders., Special publication, 1, 68-72.

Maijer, C. & Padget, P. 1987: The geology of southernmost Norway. An excursion guide. *Norg. Geol. Unders. Spec. Public. 1*, 109 p.

Maijer C. & Verschure R. H. (1998) Petrology and isotope geology of the Hunnedalen monzonoritic dyke swarm, SW Norway: a possible late expression of Egersund anorthosite magmatism. *Norges Geol. Unders. Bulletin 434*, 83–107.

Maniar, P.D. & Piccoli, P.M. 1989: Tectonic discrimination of granitoids. *Geol. Soc. Amer. Bull. 101*, 635-643.

Maquil, R. 1979: Preliminary investigation on giant orthopyroxenes with plagioclase exsolution lamellae from the Egersund-Ogna anorthositic massif (SW Norway). *Progress in experimental petrol.: 4th Report 1975-1978. NERC Publ. Ser. D* 144-146.

Maquil, R. 1980: Field relations of the Egersund-Ogna anorthosite. *Colloquium on high-grade metamorphic Precambrian and its intrusive masses (abstract)* , Utrecht.

Maquil, R. & Duchesne, J.C. 1984: Géothermométrie par les pyroxènes et mise en place du massif anorthositique d'Egersund-Ogna (Rogaland, Norvège méridionale). *Ann. Soc. Géol. Belg. 107*, 27-49.

Maquil, R., Roelandts, I., Hertogen, J. & Duchesne, J.C. 1980: Ortopyroxènes géants et plagioclases associés dans l'anorthosites d'Egersund-Ogna (SW Norvège).*8e réunion annuelle des Sciences de la Terre, Marseille* , 238.

Martignole, J. 1996: Tectonic setting of anorthositic complexes of the Grenville Province, Canada. *In*: Demaiffe, D. (ed) *Petrology and geochemistry of magmatic suites of rocks in the continental and oceanic crusts. A volume dedicated to Jean Michot.* ULB-MRAC, Brussels, 3-18.

Martignole, J. & Schrijver, K. 1970: Tectonic significance and evolution of the Morin anorthosite, Grenville Province, Quebec. *Bull. Geol. Soc. Finland 42*, 165-209.

Martignole, J. & Sisi, J.C. 1981: Cordierite-garnet-H_2O equilibrium: a geological thermometer, barometer and water fugacity indicator. *Contrib. Mineral. Petrol. 77*, 38-46.

McBirney, A.R., Baker, B.H. & Nilson, R.H. 1985: Liquid fractionation. Part I: Basic principles and experimental simulations. *J. Volcan. Geotherm. Res. 24*, 1-24.

Menuge, J.F. 1988: The petrogenesis of massif anorthosites: a Nd and Sr isotopic investigation of the Proterozoic of Rogaland/Vest-Agder, SW Norway. *Contrib. Mineral. Petrol. 98*, 363-373.

Michot, J. 1957a: Un nouveau type d'assocoation anorthosito-noritique dans la catazone norvégiene. *Ann. Soc. Géol. Belg. 80*, 449-461.

Michot, J. 1961a: The anorthositic complex of Haaland-Helleren. *Norsk Geol. Tidsskr. 41*, 157-172.

Michot, J. 1961b: Le massif complexe anorthosito-leuconoritique de Haaland-Helleren et la palingenèse basique. *Acad. Roy. Belg., Bull. Cl. Sci, Mémoires, Coll. in-4°, 2e série XV,*, 1-95.

Michot, J. & Michot, P. 1969: The problem of anorthosites: the South Rogaland igneous complex, southern Norway. *In*: Isachsen, Y.W. (ed) *Origin of anorthosite and related rocks.* New York State Museum Science Service Mem., 18, 399-410.

Michot, P. 1955a: Anorthosites et anorthosites. *Acad. Roy. Belg. Bull. Cl. Sci. Série 5 41*, 275-294.

Michot, P. 1955b: L'anatexie leuconoritique. *Acad. Roy. Belg. Bull. Cl. Sci., Série 5 41*, 374-385.

Michot, P. 1956a: Les gisements de minerais noirs de la région d'Egersund. *Ann. Soc. Géol. Belg. 79*, 183-202.

Michot, P. 1956b: Structures tectoniques dans la catazone norvégienne. *Acad. Roy. Belg. Bull. Cl. Sci., Série 5 42*, 209-227.

Michot, P. 1957b: Constitution d'un dôme de gneiss coiffé en milieu catazonal profond. *Acad. Roy. Belg. Bull. Cl. Sci,.Série 5 43*, 23-44.

Michot, P. 1960: La géologie de la catazone: le problème des anorthosites, la palingenèse basique et la tectonique catazonale dans le rogaland méridional (Norvège méridionale). *Norges geol. Unders. 212g*, 1-54.

Michot, P. 1965: Le magma plagioclasique. *Geol. Rundschau 54*, 956-976.

Mitchell, J.N., Scoates, J.S. & Frost, C.D. 1995: High-Al gabbros in the Laramie Anorthosite complex, Wyoming: implications for the composition of melts parental to Proterozoic anorthosite. *Contrib. Miner. Petrol. 119*, 166-180.

Mitchell, J.N., Scoates, J.S., Frost, C.D. & Kolker, A. 1996: The geochemical evolution o anorthosite residual magmas in the Laramie Anorthosite Complex, Wyoming. *J. Petrology 37*, 637-660.

Möller, C. 1998: Decompressed eclogites in the Sveconorwegian (-Grenvillian) orogen of SW Sweden: petrology and tectonic implications. *J. Metamorphic Geol. 16*, 641–656.

Möller, C. 1999: Sapphirine in SW Sweden: a record of Sveconorwegian (-Grenvillian) late-orogenic tectonic exhumation. *J. Metamorphic Geol. 17*, 127–141.

Morse, S.A. 1982: A partisan review of Proterozoic anorthosites. *Amer. Mineral. 67*, 1087-1100.

Newton, R.C. & Haselton, H.T. 1980: Thermodynamics of the Garnet-Plagioclase- Al_2SiO_5 - Quartz geobarometer. *In*: Newton, R.C., Navrotsky, A. & Wood, B.J. (ed) *Thermodynamics of Minerals and Melts, Advances in Physical Geochemistry,* Springer, Heidelberg, 1, 131-149.

Nielsen, F.M., Campbell, I.H., McCulloch, M. & Wilson, J.R. 1996: A strontium isotopic investigation of the Bjerkreim-Sokndal layered intrusion, southwest Norway. *J. Petrology 37*, 171-193.

Nielsen, F.M. & Wilson, J.R. 1991: Crystallization processes in the Bjerkreim-Sokndal layered intrusion, south Norway: evidence from the boundary between two macrocyclic units. *Contrib. Mineral. Petrol. 107*, 403-414.

Nijland, T. G. & Maijer, C. 1993: The regional amphibolite to granulite facies transition at Arendal, Norway: evidence for a thermal dome. *Neues Jahrbuch für Mineralogie, Abhandlungen 165*(2), 191–221.

Nordgulen, Ø., Tucker, R. D., Sundvoll, B., Solli, A., Nissen, A. L., Zwaan, K. B., Birkeland, A., & Sigmond, E. M. O. 1997: Palaeo- to Mesoproterozoic intrusive rocks in the area between Numedal and Mjøsa, SE Norway (extended abstract). *Copena Conference Trondheim*, 69–70.

Owens, B.E., Rockow, M.W., Icenhower, J.P. & Dymek, R.F. 1993: Jotunites from the Grenville Province, Quebec: petrological characteristics and implications for massif anorthosite petrogenesis. *Lithos 30*, 57-80.

Page, L. M., Möller, C., & Johansson, L. 1996: 40Ar/39Ar geochronology across the Mylonite Zone and the Southwestern Granulite Province in the Sveconorwegian Orogen of S Sweden. *Precambrian Res. 79*, 239–259.

Paludan, J., Hansen, U.B. & Olesen, N.Ø. 1994: Structural evolution of the Precambrian Bjerkreim-Sokndal intrusion, South Norway. *Norsk Geolog. Tidsskr. 74*, 185-198.

Park, R. G., Åhäll, K.-I., & Boland, M. P. 1991: The Sveconorwegian shear-zone network of SW Sweden in relation to mid-Proterozoic plate movements. *Precambrian Res. 49*, 245–260.

Pasteels, P., Demaiffe, D. & Michot, J. 1979: U-Pb and Rb-Sr geochronology of the eastern part of the south Rogaland igneous colmplex, southern Norway. *Lithos 12*, 199-208.

Pasteels, P., Michot, J. & Lavreau, J. 1970: Le complexe éruptif du Rogaland méridional (Norvège). Signification pétrogénétique de la farsundite et de la mangérite quartzitique des unités orientales; arguments géochronologiques et isotopiques. *Ann. soc. géol. Belg. 93*, 453-476.

Pasteels P. & Michot J. (1975) Geochronologic investigation of the metamorphic terrain of southwestern Norway. *Norsk Geol. Tidsskrift 55*, 111–134.

Pedersen, S. & Konnerup-Madsen, J. 2000: Geology of the Setesdalen area, South Norway: implications for the Sveconorwegian evolution of South Norway. *Bull. Geol. Soc. Denmark 46*, 181–201.

Philpotts, A.R. 1981: A model for the generation of massif-type anorthosites. *Can. Mineral. 19*, 233-253.

Piron, J.M. 1981: *Etude pétrologique et géochimique de la lentille de Koldal (Rogaland, Norvège méridionale)*. Unpub. Licence Thesis, University of Liège.

Poorter, R.P.E. 1972: Paleomagnetism of the Rogaland Precambrian (southwestern Norway). *Phys. Earth Planet. Interiors 5*, 167-176**.**

Priem, H.N.A. & Verschure, R.H. 1982: Review of the isotope geochronology of the high-grade metamorphic Precambrian of SW Norway. *Geol. Rundschau 71*, 81-84**.**

Ramdohr, P. 1960: Die Erzmineralien und ihre Verwachsungen (3rd edition). Akad.Verlag, Berlin, 1089 p.

Richter, S. 1943: Das Nickelmagnetkiesvorkommen Homsevand bei Egersund. *NGU report 822*, 2 p.

Rietmeijer, F.J.M. 1979: Pyroxenes from iron-rich igneous rocks in Rogaland, SW Norway. *Geol. Ultrajectina 21*, 341 p.

Rivers, T. & Corrigan, D. 2000: Convergent margin on southeastern Laurentia during the Mesoproterozoic: tectonic implications. *Can. J. Earth Sci. 37*, 359–383.

Rivers, T., Martignole, J., Gower, C. F., & Davidson, A. 1989: New tectonic divisions of the Grenville Province, southeast Canadian Shield. *Tectonics 8*, 63–84.

Roberts, M.P. & Clemens, J.D. 1993: Origin of high-potassium, calc- alkaline, I-type granitoids. *Geology 21*, 825-828**.**

Robins, B., Tumyr, O., Tysseland, M. & Garmann, L.B. 1997: The Bjerkreim-Sokndal Layered Intrusion, Rogaland, S.W. Norway: Evidence from marginal rocks for a jotunite parent magma. *Lithos 39*, 121-133**.**

Roelandts, I. & Duchesne, J.C. 1979: Rare-earth elements in apatite from layered norites and iron-titanium oxide ore-bodies related to anorthosites (Rogaland, S.W. Norway). *In*: Ahrens, L.H. (ed) *Origin and distribution of the elements.* Pergamon, New-York, 199-212.

Roelandts, I., Robaye, G., Weber, G., Delbrouck, J.M. & Duchesne, J.C. 1987: Determination of fluorine by proton induced gamma ray emission (PIGE) spectrometry in igneous and metamorphic charnockitic rocks from Rogaland (S.W. Norway). *J. Radioanalytic. Nucl. Chem. 112*, 453-460**.**

Romer, R. L. & Smeds, S.-A. 1996: U–Pb columbite ages of pegmatites from Sveconorwegian terranes in southwestern Sweden. *Precambrian Res. 76*, 15–30.

Rudnick, R.L. & Fountain, D.M. 1995: Nature and composition of the continental crust: a lower crustal perspective. *Rev. Geophys. 33*, 267-309**.**

Sawyer, E.W. 1991: Disequilibrium melting and the rate of melt-residuum separation during migmatization of mafic rocks from the Grenville Front, Quebec. *J. Petrology 32*, 701-738**.**

Schärer, U., Wilmart, E. & Duchesne, J.C. 1996: The short duration and anorogenic character of anorthosite magmatism: U-Pb dating of the Rogaland complex, Norway. *Earth Planet. Sci. Lett. 139*, 335-350**.**

Schiellerup, H., Lambert, D.D., Larsen, R.B., Nilsson, L.-P., Duchesne, J.C., Robins, B. & Prestvik, T. in prep: Sulfide deposits related to the Proterozoic Rogaland anorthosite province, South Norway: Implications for sulfide ore genesis and massif-type anorthosite magmatism.

Schiellerup, H., Lambert, D.D., Prestvik, T., Robins, B., McBride, J.S. & Larsen, R.B. 2000: Re-Os isotopic evidence for a lower crustal origin of massif-type anorthosites. *Nature 405*, 781-784**.**

Sellevoll, M.A. & Aalstad, I. 1971: Magnetic measurements and seismic profiling in the Skagerrak. *Mar. Geophys. Res. 1*, 284-302**.**

Sigmond, E. M. O. 1978: Beskrivelse til det berggrunnsgeologiske kartbladet Sauda 1:250000. *Norges Geol. Unders. Bull. 341*, 1–94.

Sigmond, E.M.O. 1997: The Precambrian geology of Central Southern Norway (abstract). *COPENA conference,* Trondheim.

Sigmond, H. 1985: The Mandal-Ustaoset line, a newly discovered major fault zone in South Norway. *In*: Tobi, A.C. & Touret, J.L.R. (ed) *The deep Proterozoic crust in the North Atlantic Provinces.* NATO Adv. Stud. Inst., Reidel, Dordrecht, C158, 323-332.

Smethurst, M.A., Olesen, O. & Håbrekke, H. 1994: An aeromagnetic compilation over mainland Norway. *12*, 203-210**.**

Smithson, S.B. & Ramberg, I.B. 1979: Gravity interpretation of the Egersund anorthosite complex, Norway: its petrological and geothermal significance. *Geol Soc. Amer. Bull., Part I 90*, 199-204**.**

Söderlund, U. 1996: Conventional U–Pb dating versus single-grain Pb evaporation dating of complex zircons from a pegmatite in the high-grade gneisses of southwestern Sweden. *Lithos 38*, 93–105.

Söderlund, U., Jarl, L.-G., Persson, P.-O., Stephens, M. B., & Wahlgren, C.-H. 1999: Protolith ages and timing of deformation in the eastern, marginal part of the Sveconorwegian orogen, southwestern Sweden. *Precambrian Res. 94*, 29–48.

Stadheim, J. 1968: Stadheims dagbok (Ueland v/ Ogna og Tunggårdsbakken) 1938. *NGU report 2757*, 3 p.

Stephens, M. B., Wahlgren, C. H., Weijermars, R., & Cruden, A. R. 1996: Left lateral transpressive deformation and its tectonic implications, Sveconorwegian Orogen, Baltic Shield, Southwestern Sweden. *Precambrian Res. 79*, 261–279.

Swanberg, C.A., Chessman, M.D. & Simmons, G. 1974: Heat flow-heat generation studies in Norway. *Tectonophysics 23*, 31-48**.**

Tegner, C., Meyer, G.B., Schiellerup, H., Robins, B. & Wilson, J.R. 2000: Crustal assimilation and fractional crystallisation (AFC) of basalt r-values from Norwegian layered intrusions (abstract), AGU Fall Meeting. *American Geophysical Union Eos Transactions 81*, 1357**.**

Thompson, A.B. 1976: Mineral reactions in pelitic rocks: II. Calculation of some P-T-X(Fe,Mg) phase relations. *Amer. J. Sci. 276*, 425-454**.**

Tobi, A.C., Hermans, G.A.E.M., Maijer, C. & Jansen, J.B.H. 1985: Metamorphic zoning in the high - grade Proterozoic of Rogaland-Vest Agder, SW Norway. *In*: Tobi, A.C. & Touret, J.L.R. (ed) *The deep Proterozoic crust in the North Atlantic Provinces.* NATO Adv. Sci. Inst. Ser., Reidel, Dordrecht, C158, 477-497.

Touret, J. L. 1971: Le facies granulite en Norvège méridionale. 1. Les associations minéralogiques. *Lithos 4*, 239–249.

Van den Kerkhof, A.M., Touret, J.L.R., Maijer, C. & Jansen, J.B.H. 1991: Retrograde methane-dominated fluid inclusions from high-temperature granulites of Rogaland, southwestern Norway. *Geochim. Cosmochim. Acta 55*, 2533-2544**.**

Vander Auwera, J. 1993: Diffusion controlled growth of pyroxene-bearing margins on amphibolite bands in the granulite facies of Rogaland (Southwestern Norway): implications for granulite formation. *Contrib. Miner. Petrol. 114*, 203-220**.**

Vander Auwera, J., Liégeois, J.P., Demaiffe, D., Bolle, O., Bogaerts, M. & Duchesne, J.C. 2001: Two distinct post-collisional magmatic suites in the Sveconorwegian of Southern Norway: consequences for the evolution of the Proterozoic continental lithosphere (abstract) EUG XI, Strasbourg.

Vander Auwera, J. & Duchesne, J.C. 1996: Petrology and geochemistry of the noritic Hogstad layered body (Rogaland, SW Norway): implications for the nature of the andesine anorthosite parent magma. *In*: Demaiffe, D. (ed) *Petrology and geochemistry of magmatic suites of rocks in the continental and oceanic crust.* ULB-MRAC, Brussels, 111-128.

Vander Auwera, J., Liégeois, J.P., Demaiffe, D., Wilmart, E. & Duchesne, J.C. 1999: Variability of plutonism related to the Mandal-Ustaoset line (Southern Norway): AMCG and granitoid suites. *Journal of Conference Abstract 4*, 686**.**

Vander Auwera, J. & Longhi, J. 1994: Experimental study of a jotunite (hypersthene monzodiorite): constraints on the parent magma composition and crystallization conditions (P, T, fO_2) of the Bjerkreim-Sokndal layered intrusion. *Contrib. Miner. Petrol. 118*, 60-78.

Vander Auwera, J., Longhi, J. & Duchesne, J.C. 1998: A liquid line of descent of the jotunite (hypersthene monzodiorite) suite. *J. Petrol. 39*, 439-468.

Vander Auwera, J., Longhi, J. & Duchesne, J.C. 2000: The effect of pressure on DSr (plag/melt) and DCr (opx/melt): implications for anorthosite petrogenesis. *Earth Planet. Sci. Lett. 178*, 303-314.

Verschure R. H., Andriessen P. A. M., Boelrijk N. A. M., Hebeda E. H., Maijer C., Priem H. N. A., & Verdurmen E. A. T. (1980) On the thermal stability of Rb–Sr and K–Ar biotite systems: evidence from coexisting Sveconorwegian (ca 870 Ma) and Caledonian (ca 400 Ma) biotites in SW Norway. *Contrib. Mineral. Petrology 74*, 245–252.

Versteeve, A.J. 1975: Isotope geochronology in the high-grade metamorphic Precambrian of southwestern Norway. *Norges geol. unders. 318*, 1-50.

Vogt, J.H.L. 1893: Bildung von Erzlagerstätten durch differentiations process in basichen Eruptivmagma. *Z. für prakt. Geol,* 4-11.

Weis, D. & Demaiffe, D. 1983: Pb isotope geochemistry of a massif-type anorthositic-charnockitic body: the Hidra massif (Rogaland, S.W. Norway). *Geochim. Cosmochim. Acta 47*, 1405-1413.

Wells, P. 1977: Pyroxene thermometry in simple and complex systems. *Contrib. Mineral. Petrol. 62*, 129-139.

Wendlandt, R.F. 1981: Influence of CO_2 on melting of model granulite facies assemblages: a model for the genesis of charnockites. *Amer. Mineral. 66*, 1164-1174.

Walderhaug H. J., Torsvik T. H., Eide E. A., Sundvoll B., & Bingen B. (1999) Geochronology and palaeomagnetism of the Hunnedalen dykes, SW Norway: implications for the Sveconorwegian apparent polar wander loop. *Earth and Planetary Science Letters 169*, 71–83.

Wiebe, R.A. 1979: Fractionation and liquid immiscibility in an anorthositic pluton of the Nain complex, Labrador. *J. Petrol. 20*, 239-269.

Wiebe, R.A. 1984: Commingling of magmas in the Bjerkrem-Sogndal lopolith (Southwest Norway): evidence for the compositions of residual liquids. *Lithos 17*, 171-188.

Wiebe, R.A. 1992: Proterozoic anorthosite complexes. *In*: Condie, K.C. (ed) *Proterozoic crustal evolution (Development in Precambrian Research vol. 10).* Elsevier, Amsterdam, 215-262.

Wielens, J.B.W., Andriessen, P.A.M., Boelrijk, N.A.I.M., Hebeda, E.H., Priem, H.N.A., Verdurmen, E.A.T. & Verschure, R.H. 1980: Isotope geochronology in the high-grade metamorphic Precambrian of Southwestern Norway: new data and reinterpretations. *Norges geol. unders. 359*, 1-30.

Wilmart, E. 1982: *Série supracrustale, granito-gneiss et charnockites de l'enveloppe métamorphique du massif anorthositique d'Åna-Sira (Rogaland, Norvège méridionale).* Unpub. Licence Thesis, University of Liège.

Wilmart, E. 1988: Etude géochimique des charnockites du Rogaland. *Mém. Sc. Terre Univ. Curie, Paris 88-20*, 1-341.

Wilmart, E., Clocchiatti, R., Duchesne, J.C. & Touret, J.L.R. 1991: Fluid inclusions in charnockitic rocks from the Bjerkreim-Sokndal massif (Rogaland, Southwestern Norway): fluid origin and in situ evolution. *Contrib. Mineral. Petrol. 108*, 453-468.

Wilmart, E., Demaiffe, D. & Duchesne, J.C. 1989: Geochemical constraints on the genesis of the Tellnes ilmenite deposit (S.W. Norway). *Econ. Geol. 84*, 1047-1056.

Wilmart, E. & Duchesne, J.C. 1987: Geothermobarometry of igneous and metamorphic rocks around the Ana-Sira anorthosite massif: implications for the depth of emplacement of the South Norwegian anorthosites. *Norsk Geol. Tidssk. 67*, 185-196.

Wilson, J.R., Pedersen, S., Berthelsen, C.R. & Jakobsen, B.M. 1977: New light on the Precambrian Holum granite. *Norsk Geol. Tidsskr. 57*, 347-360**.**

Wilson, J.R., Robins, B., Nielsen, F., Duchesne, J.C. & Vander Auwera, J. 1996: The Bjerkreim-Sokndal layered intrusion, Southwest Norway. *In*: Cawthorn, R.G. (ed) *Layered Intrusions.* Elsevier, Amsterdam, 231-256.

Wood, B.J. & Banno, S. 1973: Garnet-orthopyroxene and orthopyroxene-clinopyroxene relationships in simple and complex systems. *Contrib. Mineral. Petrol. 42*, 109-124**.**

Zhou, X.Q., Bingen, B., Demaiffe, D., Hertogen, J., Liégeois, J.P. & Weis, D. 1995: The 1160 Ma old Hidderskog meta-charnockite: implications of this A-type pluton for the Sveconorwegian belt in Vest Agder (S.W. Norway). *Lithos 36*, 51-66**.**